Lehrstuhl für Biologische Chemie

der Technischen Universität München

Structural Requirements for Activation and Membrane Binding of Human µ-Calpain

Amaury Ernesto Fernández-Montalván

Vollständiger Abdruck der von dem Wissenschaftszentrum Weihenstephan für Ernährung, Landnutzung und Umwelt der Technischen Universität München zur Erlangung des akademischen Grades eines

Doktors der Naturwissenschaften

genehmigten Dissertation.

Vorsitzender:	Univ.-Prof. Dr. Dieter Langosch
Prüfer der Dissertation:	1. Univ.-Prof. Dr. Arne Skerra
	2. Univ.-Prof. Dr. Werner Machleidt

Die Dissertation wurde am *30.08.2004* bei der Technischen Universität München eingereicht und durch das Wissenschaftszentrum Weihenstephan für Ernährung, Landnutzung und Umwelt am *27.10.2004* angenommen.

A mis padres

Acknowledgements

I would like to express my deepest gratitude to the following persons:

Prof. Dr. Werner Machleidt, who believed in the feasibility of the project since its conception and offered his laboratory facilities for the accomplishment of the experimental work. This thesis would not have been finished without his bright supervision and fruitful discussions. Many thanks for the insightful reading of the manuscript and -last but not least- for letting me enjoy an unlimited creative freedom during the past four years.

Prof. Dr. Arne Skerra on the Chair for Biological Chemistry of the Technical University of Munich, for the serious and objective mentorship of this thesis.

Prof. Dr. Emeritus Hans Fritz for allowing me to work in his Department, for his engagement in difficult times and for his wise counselling ever.

Prof. Dr. Marianne Jochum, who continued to support this project after taking over the Department's leadership and stimulated my further development as a scientist.

Dr. Irmgard Machleidt, whose expertise in enzyme kinetics and biophysical characterization of proteins was of invaluable help during the different stages of this work. Besides her competent advice on experimental issues, she provided lots of motivation and affective support.

Prof. Dr. Wolfram Bode at the Max Planck Institute for Biochemistry: being the initiator of the "electrostatic switch" hypothesis he maintained a sustained interest in the progress of the project, helped with stimulating discussions and provided finnancial support for its completion.

The assistance of the laboratory technicians Heide Hinz and Rita Zauner was essential for the performance of the experiments presented here. I benefited greatly from their accurate bench work and learned to cherish them as wonderful human beings.

Contents

A. Summary

A.1. Deutsch

Die Calpaine (EC 3.2.22.17) sind intrazelluläre Cysteinproteasen, deren Enzymaktivität in einzigartiger Weise Ca^{2+}-abhängig ist. Mitglieder der Calpain-Superfamile kommen in niederen Organismen, Pflanzen und Wirbellosen bis hin zu den Säugetieren vor. Ihre Funktionen stehen im Zusammenhang mit dem Umbau des Cytoskeletts, mit der Signaltransduktion, der Regulation des Zellzyklus und mit Reaktionswegen des Zelltods. Am besten charakterisiert sind die µ- und m-Isoformen, jeweils heterodimere Enzyme, die in fast allen Säugetiergeweben exprimiert und die *in vitro* durch Ca^{2+}-Konzentrationen von 3-50 µM bzw. 0,4-0,8 mM aktiviert werden. Sie werden endogen in Ca^{2+}-abhängiger Weise gehemmt durch Calpastatin, einen weiteren gut bekannten Akteur des Calpain-Systems.

µ-Calpain und m-Calpain bestehen aus jeweils unterschiedlichen, aber homologen großen (L-) Untereinheiten (80 kDa), welche die Papain-ähnliche katalytische Domäne (II) enthalten, und aus einer identischen kleinen (S-) Untereinheit (28 kDa). Jede der beiden Untereinheiten enthält eine C-terminale Calmodulin-ähnliche Domäne (IV bzw. VI) mit 5 "EF-Händen", die potenzielle Ca^{2+}-Bindungsstellen tragen. Vor der Domäne VI liegt ein Glycin-reiches, hydrophobes Segment (Domäne V); eine "C2-ähnliche" Domäne (III) befindet sich zwischen Domäne IV und dem Protease-Kern der L-Untereinheit. Moderate Sequenzunterschiede der großen Untereinheiten der beiden Isoformen (55-65 % Sequenz-homologie) führen zu dem beträchtlichen Unterschied der *in vitro* für die Enzymaktivität benötigten Ca^{2+}-Konzentrationen. Für beide Isoformen liegen diese Konzentrationen dennoch weit über den in lebenden Zellen verfügbaren Ca^{2+}-Spiegeln (50-300 nM). Durch die in Gegenwart von Ca^{2+} ablaufende autoproteolytische Prozessierung der Calpaine wird ihre Ca^{2+}-Sensitivität erhöht. Darüber hinaus wurden Interaktionen mit Substraten, Aktivatorproteinen und/oder Membranphospholipiden, aber auch Phosphorylierungen durch Proteinkinasen als mögliche Faktoren für die Absenkung des Ca^{2+}-Bedarfs bis in den nanomolaren Bereich der intrazellulären Konzentrationen vorgeschlagen.

Die in dieser Arbeit vorgestellten Experimente basieren auf den Kristallstrukturen des Ca^{2+}-freien m-Calpains der Ratte und des Menschen, die im Winter 1999-2000 von zwei getrennten Gruppen veröffentlicht wurden. Diese Untersuchungen erklärten die Inaktivität der Calpaine in Abwesenheit von Ca^{2+} und warfen neue Fragen zum Mechanismus der Aktivierung durch Ca^{2+}-Ionen auf. Eines der fesselndsten Probleme ist die mögliche Rolle der Domäne III beim Aktivierungsprozess, weil diese Domäne eine zentrale Position in der Raumstruktur des Moleküls einnimmt und zahlreiche Interaktionen mit anderen Domänen eingeht. Ein hervorstechendes Merkmal der Domäne III ist ihre sog. "saure Schleife", ein Abschnitt von aufeinander folgenden Asp- oder Glu-Resten, die Salzbrücken und/oder schwächere elektrostatische Interaktionen mit basischen Lys- oder Arg-Resten eingehen, die auf der katalytischen Subdomäne IIb und in anderen Teilen der Domäne III liegen. Es wird vermutet, dass die "saure Schleife" Teil des Mechanismus eines "elektrostatischen Schalters" ist, der die Fusion der Subdomänen IIa und IIb kontrolliert. Das Aufbrechen der elektrostatischen Wechselwirkungen durch Ca^{2+} und/oder Membranphospholipide würde die

Zugspannung auf die Subdomäne IIb lockern und eine Annäherung der beiden Subdomänen erlauben. Die Unterschiede im elektrostatischen Potential der "sauren Schleifen" und ihrer Interaktionspartner könnten auch den unterschiedlichen Ca^{2+}-Bedarf für die Aktivierung von µ-Calpain, m-Calpain sowie der Muskel-spezifischen Isoform p94 erklären.

Um die Rolle dieses Strukturmotivs bei der Aktivierung der Calpaine zu untersuchen, wurde eine Reihe von Mutanten des µ-Calpains hergestellt, in denen Asp- und Glu-Reste der "sauren Schleife" systematisch durch Alanin ersetzt wurden (sog. "Ala-Scan"). Komplette heterodimere µ-Calpaine mit diesen Mutationen wurden mit Hilfe des Baculovirus-Systems in Insektenzellen exprimiert, und zwar sowohl als aktive Enzyme als auch als inaktive Cys115Ala-Mutanten. Durch Messung (i) der Enzymaktivität der aktiven Varianten und (ii) der initialen Konformationsänderungen der inaktiven Mutanten bei verschiedenen Ca^{2+}-Konzentrationen mittels Fluoreszenzspektroskopie wurde der Ca^{2+}-Bedarf für den Aktivierungsprozess mit und ohne gleichzeitige Autoproteolyse bestimmt. In beiden Fällen führte die Unterbrechung einzelner Interaktionen der "sauren Schleife" zu einer erheblichen (bis zu siebenfachen) Verminderung der für die Aktivierung benötigten Ca^{2+}-Konzentrationen und diese Verminderung korreliert mit der auf Grund der Ladungsabstände vorhergesagten Stärke der elektrostatischen Wechselwirkungen. Ausgehend von diesen Befunden wurde ein hypothetisches Modell für die Rolle der "sauren Schleife" und der gesamten Domäne III bei der Calpain-Aktivierung vorgeschlagen.

Parallel dazu wurde untersucht, in welcher Weise die autoproteolytische Abspaltung der Domäne V der S-Untereinheit die Calpain-Aktivierung beeinflusst, indem die gleichen Methoden auf eine Mutante mit deletierter Domäne V angewandt wurden. Wiederum konnten eine Abnahme des Ca^{2+}-Bedarfs für Aktivität und Konformationsänderungen gemessen werden, ähnlich wie sie nach Autoproteolyse der "Anker"-Domäne I der L-Untereinheit berichtet worden war. Diese Ergebnisse eröffnen einen neuen Aspekt der Regulation der Calpain-Aktivierung durch Autolyse. Die vermutete Aktivierung der Calpaine über ihre Interaktion mit Membranphospholipiden wurde an den oben beschriebenen heterodimeren Varianten und an der isolierten S-Untereinheit mit Hilfe von Fluoreszenz-Resonanz-Energie-Transfer (FRET)- und Oberflächen-Plasmon-Resonanz (BIAcore)-Techniken überprüft. Es stellte sich heraus, dass µ-Calpain in Ca^{2+}-abhängiger Weise mit nanomolaren Affinitäten an Membranen bindet. Die zur Membranbindung benötigte Ca^{2+}-Konzentration ist jedoch ähnlich der für Konformationsänderungen und Aktivierung erforderlichen Konzentrationen. Das spricht dafür, dass die Membranbindung eher eine Folge der Calpain-Aktivierung und nicht ihre Voraussetzung ist. Die ca. 10-fach reduzierte Liposomen-Affinität der Domäne-V-Deletionsmutante bestätigte die vorgeschlagene Rolle dieses Motivs bei der Assoziation mit Phospholipiden. Mutationen in der Domäne III beeinflussten den K_d-Wert der Membranbindung nicht, was auf funktionelle Unterschiede zwischen der Domäne III der Calpaine und den topologisch verwandten Ca^{2+}- und Phospholipid-bindenden C2-Domänen anderer Proteine hindeutet. Ausgehend von der Ca^{2+}-Abhängigkeit der Interaktionen und dem Fehlen einer Selektivität des Calpains für spezifische Phospholipid-Zusammensetzungen oder –Kopfgruppen wurde ein Membranbindungs-Mechanismus über die Ca^{2+}-induzierte Freilegung hydrophober Regionen des Proteins vorgeschlagen.

A.2. English

Calpains (EC 3.4.22.17) are intracellular cysteine proteinases showing a unique dependency on Ca^{2+} for enzymatic activity. Members of the calpain superfamily have been found from lower organisms, plants and invertebrates through mammals. Their functions are related with cytoskeleton remodelling, signal transduction, cell cycle regulation and cell death pathways. The best characterized calpains are the µ- and m-isoforms, heterodimeric enzymes expressed in most mammalian tissues and activated *in vitro* by Ca^{2+} concentrations of 3-50 µM and 0.4-0.8 mM, respectively. They are endogenously inhibited in a Ca^{2+}-dependent fashion and with nanomolar K_i values by calpastatin, another well known player in the calpain system.

µ-Calpain and m-calpain are composed of distinct but homologous large (L) subunits (80 kDa) harbouring the papain-resembling catalytic domain (II) and a common small (S) subunit (28 kDa). Each subunit contains a C-terminal calmodulin-like domain (IV or VI, respectively) with 5 EF-hands representing potential Ca^{2+}-binding sites. Domain VI is preceded by a Gly-rich hydrophobic segment (domain V), and a "C2-like" domain (III) is located between domain IV and the protease core in the L-subunit. The moderate sequence differences between the large subunits of both isoforms (55-65% sequence homology) are responsible for the major difference in the Ca^{2+} concentrations required for activity *in vitro*. For both isoforms these Ca^{2+} requirements are far above the Ca^{2+} levels available in living cells (50-300 nM). Ca^{2+}-induced autoproteolytic processing increases the Ca^{2+} sensitivity of the calpains. Moreover, interactions with substrates, activator proteins and/or membrane phospholipids as well as phosphorylation by protein kinases have been suggested as factors lowering the Ca^{2+}-requirement to the intracellular nanomolar range.

The experiments presented in this work are largely based on the crystal structures of Ca^{2+}-free rat and human m-calpain published in winter 1999-2000 by two different groups. These studies explained the inactivity of calpain in the absence of Ca^{2+} and raised several new questions about the mechanism of activation by Ca^{2+} ions. One of the most exciting issues was the possible role of domain III in this process owing to its central position in the three-dimensional structure of the molecule and the numerous interactions it makes with the other domains. A striking feature of domain III is its so-called "acidic loop", a stretch of consecutive Asp and Glu residues forming salt bridges and/or weaker electrostatic interactions with basic Lys or Arg residues located in the catalytic subdomain IIb and in other parts of domain III. It was proposed that the acidic loop is part of an "electrostatic switch" mechanism controlling the fusion of subdomains IIa and IIb. Disruption of the electrostatic interactions by Ca^{2+} and/or membrane phospholipids would relieve the tension on subdomain IIb and allow the subdomains to approach one another. Differences in the electrostatic potential of the acidic loops and their basic interaction partners could also explain the

different Ca^{2+}-requirement for the activation of μ-calpain, m-calpain as well as the muscle-specific isoform p94.

In order to analyze the role of this structural motif in the activation of the calpains a series of mutants of μ-calpain were prepared in which Asp- and Glu- residues of the "acidic loop" were systematically replaced by alanine ("Ala-scan"). Complete heterodimeric μ-calpains containing these mutations were expressed with the baculovirus system in insect cells, both as active enzymes and as inactive active-site Cys115Ala mutants. By measuring (1) the enzymatic activity of the active variants and (2) the initial conformational changes of the inactive mutants at different Ca^{2+} concentrations using fluorescence spectroscopy, the Ca^{2+} requirement for the activation process with and without concomitant autoproteolysis was evaluated. In both cases disruption of single acidic loop interactions led to a significantly (up to 7-fold) reduced Ca^{2+} requirement for activation, and this reduction correlates with the strength of electrostatic interactions predicted from charge distances. Based on these findings, a hypothetical model for the role of the acidic loop and of whole domain III in calpain activation was proposed.

Concomitantly, it was investigated how autoproteolytic removal of domain V of the S-subunit affects calpain activation by applying the same methodology to a domain V deletion mutant. Again a decrease in the Ca^{2+} requirement for activity and conformational changes was measured, as reported previously after autoproteolysis of the "anchor" domain I in the L-subunit. These results reveal a novel aspect in the regulation of calpain activity by autolysis.

The putative activation of the calpains upon interaction with membrane phospholipids was tested in the heterodimeric variants described above and in the S-subunit alone using fluorescence resonance energy transfer (FRET) and surface plasmon resonance (BIAcore) technologies. It was found that μ-calpain associates with membranes in a Ca^{2+}-dependent fashion with nanomolar affinities. However, the Ca^{2+} concentration needed for membrane binding is similar to the Ca^{2+} requirement for conformational changes and activation, suggesting that membrane binding is rather a consequence and not a premise for calpain activation. A ~10 fold reduction of the affinity for liposomes in the domain V deletion mutant confirmed the proposed role of this motif in the association with phospholipids. Mutations in domain III did not affect the K_d for membrane binding, indicating functional differences between domain III of the calpains and the topologically related Ca^{2+}- and phospholipid-binding C2 domains of other proteins. Based on the Ca^{2+} dependency of the interaction and the lack of selectivity of calpain for specific phospholipid compositions or headgroups a membrane binding mechanism by Ca^{2+}-induced exposure of hydrophobic regions of the protein was proposed.

B. Introduction

The history and evolution of enzymology are closely linked to the discoveries in the field of proteases. In fact the term "diastase" -coined by Jean-François Persoz and Anselm Payen in 1833 to describe the amylase enzyme complex isolated from barley malt- was replaced in 1876 by the word "enzyme" in the same paper in which the German physiologist Wilhem Kühne introduced the name "trypsin" to designate a substance able to digest proteins in pancreatic juice (Kühne, 1876). That pioneer work marked the begin of the research on an amazing new class of biological catalysts which continued with the isolation, purification and structural characterization at the atomic level of the proteases present in that digestive juice and many other proteolytic enzymes from a variety of human fluids and tissues, as well as animals, plants and micro-organisms (see (Barrett *et al.,* 1998) for a comprehensive treatise on peptidases). As a consequence of the impressive body of knowledge accumulated on structural features, catalysis and inhibition mechanisms of proteases, most biochemistry textbooks published nowadays use them to illustrate how enzymes work.

Proteases (also known as peptidases or peptide hydrolases) promote the cleavage of peptide bonds by hydrolysis. They are classified upon the position of the peptide bond they cleave in the target protein into exopeptidases (which cleave amino acids from the N- or C-terminus of target proteins) or endopeptidases (proteinases) (Figure 1). A further organization in four major classes according to the catalytic mechanism was introduced by Hartley in 1960. This classification was formalized in the late 1970s by Alan Barret (Barrett, 1979), who also allocated the proteases in evolutionary families according to their amino acid sequences and grouped some of these families in distantly related "clans" (Rawlings and Barrett, 1993).

Since proteases were originally identified as protein-degrading enzymes in digestive juice or tissue homogenates, it was thought for a long time that their function was to completely "destroy" proteins. The understanding of zymogens and the elucidation of the blood-clotting cascades in the 1960s and 1970s indicated, however, that specific, limited proteolysis is an important general biological mechanism. The current view sees proteases playing pivotal roles in many biological processes such as fertilization, development, morphogenesis, cell signalling, transcriptional control, blood coagulation, cell division, migration, growth, apoptosis and the activation of cytokines and growth factors. The fact that approximately 2 % of human genes encode proteolytic enzymes underlines the importance of proteolysis (Saklatvala *et al.,* 2003).

Peptidases (or proteases) EC 3.4.-.-

Exopeptidases EC 3.4.11-19.-   Endopeptidases (or proteinases) EC 3.4.21-99.-

3.4.11 Aminopeptidases   3.4.21 Serine proteinases

3.4.13 Dipeptidases   3.4.22 Cysteine proteinases

3.4.14 Dipeptidyl-peptidases and tripeptidyl   3.4.23 Aspartic proteinases
peptidases

3.4.15 Peptidyl-dipeptidases   3.4.24 Metallo proteinases

3.4.16 Serine-type carboxypeptidases   3.4.99 Proteinases of unknown mechanism

3.4.17 Metallocarboxypeptidases

3.4.18 Cysteine-type carboxypeptidases

3.4.19 Omegapeptidases

Figure 1. Global classification of proteases (peptidases) according to the position of the cleavage sites
(exo- and endopeptidases) and their catalytic mechanism. Enzyme nomenclature numbers are
specified for each class and subclass as recommended by the IUBMB
(http://www.chem.qmul.ac.uk/iubmb/enzyme/).

Due to their irreversibility (a major difference to other posttranslational modifications)
proteolytic processes are strictly regulated under physiological conditions. In fact, most
proteases are synthesized as inactive zymogens which become activated by limited
proteolysis and/or structural rearrangements upon binding of cofactors or removal of
inhibitors in response to specific signals. The existence of these natural inhibitors, some of
which specifically bind to their target proteases, represents a further strategy to manage with
undesired proteolytic activity. In addition, confining proteolysis to restricted conditions (i.e.
pH) and/or precisely defined cell compartments (i.e. lysosomes), environments (i.e. the
ECM), tissues or body fluids constitutes an efficient way to achieve this control. Deregulation
of proteolysis in organisms has been shown to be deleterious: abnormal development and a
large number of diseases are attributed to aberrant activities of proteases. Many pathogenic
organisms (multi- and unicellular parasites, fungi, bacteria and viruses) depend on proteases
or protease inhibitors to successfully infect their hosts and replicate. For all these reasons,
proteases are interesting targets for the therapy of diseases. The successful story of captopril
and derived ACE inhibitors since the late 1970s for the treatment of hypertension and the

more recent use of the HIV protease inhibitors as part of an effective management of AIDS support this statement. Such achievements place the understanding of how proteolytic activity is physiologically regulated in the focus of several scientific disciplines. This work deals with the regulation of the activity of calpain, a Ca^{2+} dependent cysteine protease.

B.1. Cysteine proteases

Peptidases with a catalytic dyad containing cysteine and histidine are grouped as cysteine proteases (also known as sulfhydryl or thiol proteases) (Figure 2). The requirement of a third residue (Asn in most cases, X in Figure 2) for activity is still discussed. At least seven different evolutionary origins have been attributed to these enzymes. They have been consequently grouped into seven clans, subdivided in over forty families (Barret, 2001). The largest (and perhaps the most important) clan (CA) includes the proteases with structural homology to papain. Despite substantial differences in the overall structures throughout the families, the two-domain fold of the catalytic unit with the active site located in a groove inbetween (Kamphuis *et al.,* 1984) (Figure 2) is conserved in all members of the clan.

Papain-like lysosomal cathepsins (family C1) are the best characterized proteins of the clan CA with 9 crystal structures of 11 human enzymes currently known (cathepsins B, C, F, H, L, K, O, S, V, X and W). Analysis of several knock out mice indicates the importance of cathepsins in physiological and pathological processes and their suitability as therapeutical targets (Turk *et al.,* 2003). The discovery of the genes responsible for programmed cell death (apoptosis) in the nematode C. elegans (Ellis and Horvitz, 1986) led to the identification in humans of the cysteine-dependent aspartate-specific proteases (caspases, clan CD, family C14). This family of thiol proteases has received a great deal of attention due to their crucial role in the differentiation and development of multicellular organisms (see (Hengartner, 2000; Danial and Korsmeyer, 2004) for reviews).

Other cysteine proteases from different organisms are gaining in importance due to their physio/pathological relevance and/or their unique structural features. Among them, the gingipains (clan CD, family C25) are the weapons used by the bacteria Porphyromonas gingivalis to dismantle the cellular immunity of the host, thereby causing inflammation and
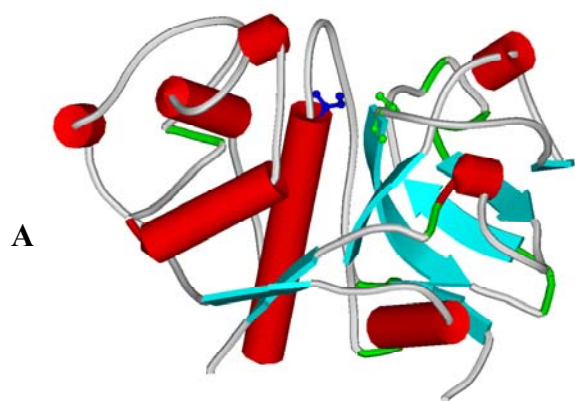
Figure 2. Structure and catalytic mechanism of papain-like cysteine proteases.

A: Schematic representation of the 3D structure of papain (PDB code 9PAP). The fold of proteases of the clan CA is characterized by a left (L) domain whose main feature is a central α-helix. Active site Cys (blue) is placed in top of this helix. The right domain forms a kind of β-barrel and includes short α-helical motifs. The active site His (green) is located in this R domain.
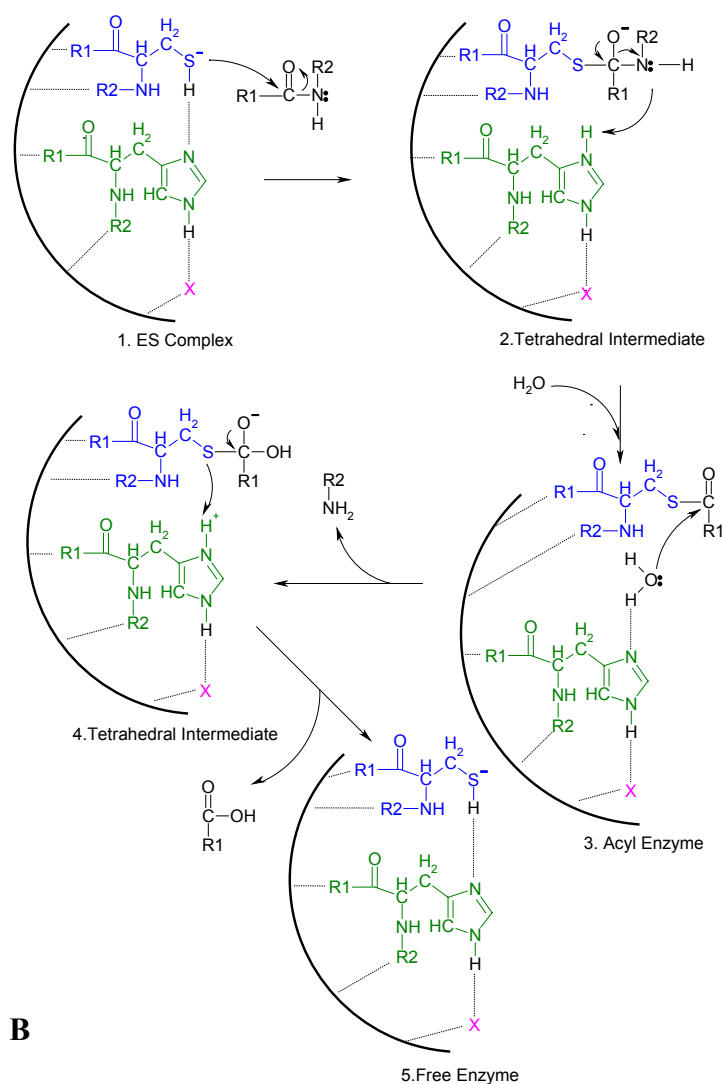
B: General catalytic mechanism of thiol-proteases. The hydrogen bonding between the imidazol and sulfhydryl groups of the catalytic His and Cys residues enhance the nucleophile character of the Cys and facilitate the attack to the substrate peptide bond. Through the formation of tetrahedral intermediates, the interactions between the different residues of the active site are stabilized and the hydrolysis of the peptide bond and release of the reaction products are favoured. X is Asn in papain.

chronic periodontitis lesions (Travis *et al.,* 2000). Separins (clan CD, family C50) play a crucial role in cell division by cleaving cohesin, a protein that keep the sister chromatides together (Uhlmann, 2003). From the evolutionary point of view, the viral picornains, from picornaviruses (clan PA) are of great interest. Their fold is similar to trypsin and chymotrypsin, suggesting that one of these viruses long ago acquired a serine peptidase gene from a eukaryotic host and mutated the active site serine to cysteine in order to evade endogenous serine protease inhibitors of the host (Barrett and Rawlings, 2001).

B.2. Calcium and Ca^{2+}-binding proteins: Properties and biological functions

In vertebrates calcium (in a form of $CaSO_4$) is the most important (and specific) compound of bones. Besides giving strength to the skeleton, calcium is required for physiological funtions as important as muscle contraction and blood clotting. Within the cell, Ca^{2+} ions are the most universal and versatile second messengers. Their entrance into the cytoplasm -either through receptor operated channels (ROCs) or voltage-operated channels (VOCs) at the cell membrane or from internal stores by means of the IP_3 receptors (IP_3Rs) and ryanodine receptors (RyRs) in the sarcoplasmic/endoplasmic reticulum- can trigger diverse life or death signals. Processes that depend on Ca^{2+} signals include fertilization, axis formation, cell differentiation, proliferation, transcriptional activation and apoptosis (Berridge *et al.,* 2000). In order to initiate such a variety of responses, Ca^{2+} signals must be tightly regulated in time, space and amplitude. Mutations causing drastic functional changes in intracellular Ca^{2+} homeostasis are most likely not compatible with life. Abnormalities in one of the various proteins involved in intracellular Ca^{2+} regulation, which in vitro seem only to induce trivial alterations in the function of the protein, often lead ot a plethora of diseases (Missiaen *et al.,* 2000).

The effects of calcium as an intracellular second messenger are mediated by its interaction with calcium binding proteins (CaBPs) (Figure 3). Generally, Ca^{2+} binding to the apo-protein induces a conformational change which is transduced either into (1) a direct cellular response (i.e. muscle contraction and cell motility), (2) binding to interaction partners followed by modification of them (like calmodulin does) or (3) translocation of the target proteins to membranes or specific organelles where they become active. In some cases, no conformational changes but a modification of the electrostatic properties of the region where calcium binds is sufficient to achieve an effect.
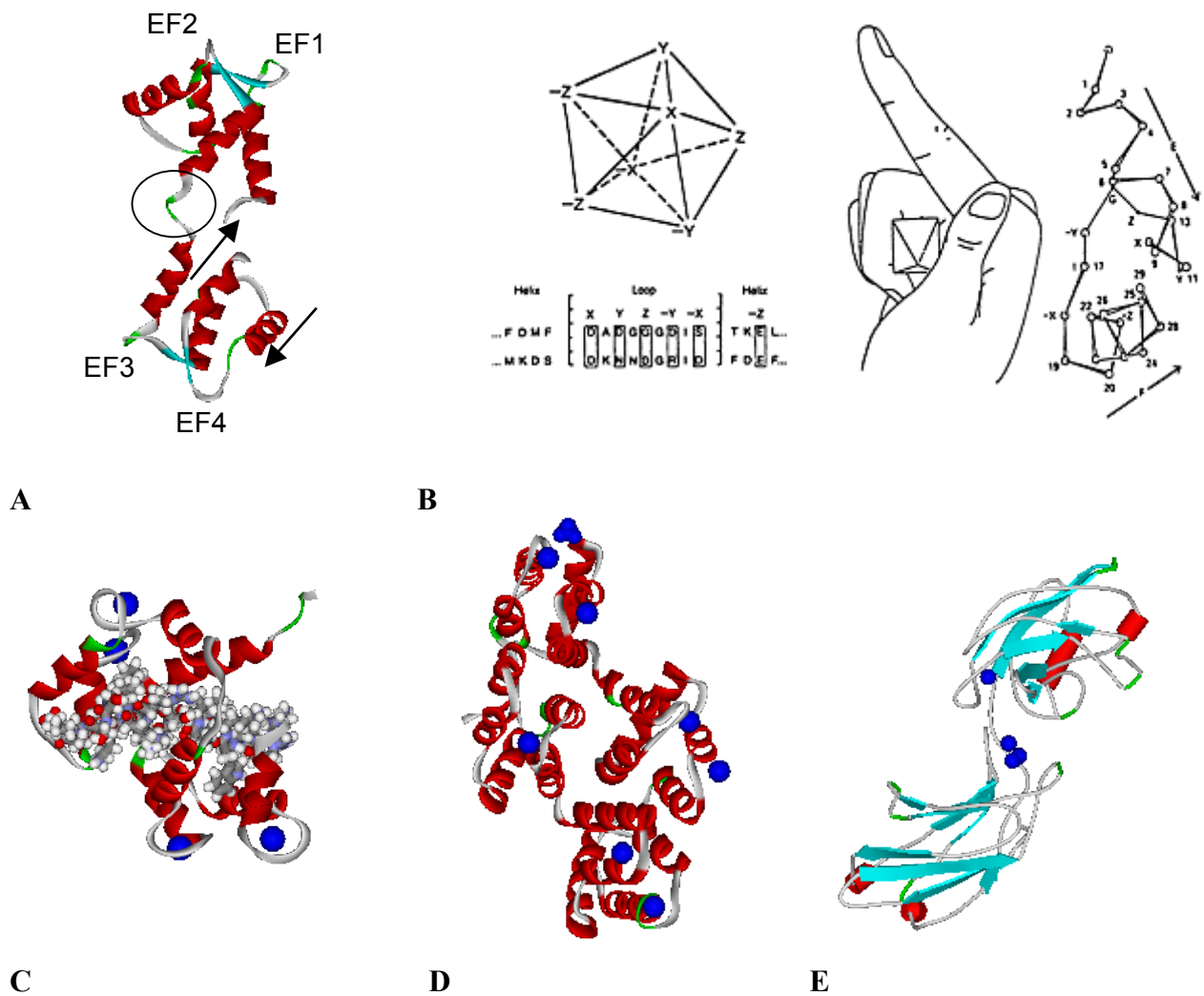
Figure 3. Structural features of some Ca^{2+} binding proteins.

A: Solid ribbon representation of "apo" calmodulin (PDB code 1CFC). Calmodulin is a two-domain protein with two EF-hands in each domain. Ca^{2+} binding induces a bending of the domains about the interdomain flexible loop enclosed here in a circle. The arrows represent the direction of the incoming and outgoing helices.

B: Original representation of an EF-hand by R. H. Kretsinger (1973).The binding of calcium is described by a right hand with the helices represented by the stretched index-finger (incoming helix) and the thumb (outgoing helix), with the rest of the fingers curved to illustrate the calcium binding loop. Letters E and F were used to describe the incoming and outgoing helices respectively in parvalbumin, the first protein in which the motif was identified.

C: Ribbon plot of Ca^{2+}-bound calmodulin in complex with a myosin light chain kinase (MLCK) peptide (PDB code 2BBM). Comparison with A reveals the conformational changes originated by the nucleation of 4 Ca^{2+} ions by the EF-hands.

D: AnnexinV(PDB 2RAN) shows calcium binding structures resembling EF-hands.

E: In the case of synaptotagmin (PDB 1DQV, here in a schematic representation), calcium binds to the loops between the β-strands at one extreme of the C2A and C2B domains. Coloring is according to secondary structure: helices are red, beta sheets cyan, turns green, and coils are grey.

The best characterized group of CaBPs is the calmodulin superfamily with more than 200 members containing the high-affinity calcium-binding EF-hand motif (Lewit-Bentley

and Rety, 2000; Haeseleer *et al.,* 2002). This group includes calmodulin, TnC, the S100-proteins, and parvalbumin among others. A cannonical EF- hand structure consists of a ~10 residue α-helix, a ~10-residue loop, and another approximately 10 residues long α-helix (Figure 3, A-C). The Ca atoms are accomodated by the loops through coordination with five O atoms from five loop residues side chains. Calmodulin and many other proteins contain four EF-hands. A new subfamily of EF-hand proteins with a fifth non-typical EF-hands has been described recently and named penta EF-hand (PEF) proteins (Maki *et al.,* 2002). Another important group of CaBPs is the annexin protein family (Gerke and Moss, 2002), macromolecules which interact with phospholipids (cellular membranes in particular) in a calcium-dependent manner. These proteins contain internally conserved regions that are responsible for calcium binding and which might be described as mutated EF-hand structures (Figure 3, D).

In recent years a new type of CaBPs has been identified within a growing number of signaling proteins. They share a topologically similar motif named C2 domain (second conserved domain of protein kinase C). In many of these proteins, Ca^{2+} binding to the C2 motif is required for translocation to cellular membranes or oligomerization. Besides the PKC isoforms, other prominent members of this family are the phospholipases A, C and D, synaptotagmin (Syt) (Figure 3, E) and the IP_3 phosphatase PTEN. The fold of these C2 domains is a β- sandwich with eigth antiparallel strands which serves as a scaffold for variable surface loops (Rizo and Sudhof, 1998; Jimenez *et al.,* 2003). In the X-ray structures determined to date, two or three Ca^{2+} ions have been detected in associaton with these interconecting loops. The effect of Ca^{2+} binding to this region is either the induction of conformational changes leading to the exposure of hydrophobic residues or the modification of the electrostatic charge properties of the protein. In both cases membrane binding can be achieved by (1) hydrophobic interactions with the apolar moiety of the phospholipids, (2) electrostatic interaction with the head groups or (3) specific recognition of a special head group (e.g. of second messengers like DAG or PIP_2) (Cho, 2001; Nalefski *et al.,* 2001). These C2 motifs are functionally but not structurally related with the C2 domains of the coagulation factors V and XIII (Fuentes-Prior *et al.,* 2002). Nature managed to build more than one Ca^{2+} binding unit in many proteins. Syt for example, contains two C2 domains, phospholipase C is equipped with one EF-hand and one C2 domain, and the calpains contain one or two PEF domains and one "C2-like" domain.

B.3. Calpains: Calcium-dependent cysteine proteases

The first report about a neutral Ca^{2+} activated proteinase (CANP) isolated from the soluble fraction of rat brain appeared back in 1964 (Guroff, 1964). The same year an independent group communicated the identification of a *kinase activating factor* (KAF) in skeletal muscle (Meyer *et al.,* 1964). This factor was isolated four years later by the same group and classified as a Ca^{2+}-dependent protease (Huston and Krebs, 1968). Other laboratories continued to rediscover this enzyme and new names were given to it such as *calcium activated sarcoplasmic factor* (CaSF) (Busch *et al.,* 1972) and *protein kinase C-activating factor* (Taka *et al.,* 1977), until it was purifed to homogeneity and characterized in 1976 and 1978 by two different groups (Dayton *et al.,* 1976; Ishiura *et al.,* 1978). The complete nucleotide sequence of a CANP and its derived primary structure was revealed after the cloning in 1984 of the cDNA of a chicken isoform nowadays known as µ/m-calpain (Ohno *et al.,* 1984). Several cDNA of calpains from different organisms have been cloned since then (see (Goll *et al.,* 2003) for a review) The names CANP and calpain (coined from **cal**cium dependent pa***pain***-like cysteine protease, (Murachi *et al.,* 1980), were unified as "calpain" in 1990s (Suzuki, 1991). The current definition describes calpains as a family of Ca^{2+}-dependent cysteine proteases (clan CA, family C2 in Barret and Rawlings' classification) including typical and atypical homologues (Goll *et al.,* 2003). A further classification proposed by Sorimachi (Sorimachi *et al.,* 1994) divides the calpains into ubiquitous and tissue-specific isoforms. This classification, frequently found in the literature of the past years, is nowadays being reconsidered (Farkas *et al.,* 2003).

The typical calpains share two common features: they have a papain-like protease domain and a calmodulin like penta EF-hand (PEF) domain. Atypical calpains lack the PEF domain. Some members of both groups do not have the catalytical His, Cys and Asn residues and should be therefore inactive. Calpain genes have been found in a variety of organisms from bacteria to humans (14 genes found in the human genome (Dear and Boehm, 2001), yet only a few of them have been well characterized at the protein level. Calpains have been implicated in a variety of physiological processes including the remodeling of cytoskeletal attachments to the plasma membrane during cell fusion and cell motility (Glading *et al.,* 2002; Goll *et al.,* 2003), proteolytic modification of molecules in signal transduction pathways (Santella *et al.,* 1998; Sato and Kawashima, 2001; Goll *et al.,* 2003), degradation of enzymes controlling progression through the cell cycle (Santella *et al.,* 1998; Goll *et al.,* 2003),

regulation of gene expression (Yajima and Kawashima, 2002; Goll *et al.*, 2003), substrate degradation in some apoptotic pathways (Wang, 2000; Goll *et al.*, 2003) and an involvement in long term potentiation (Tomimatsu *et al.*, 2002; Goll *et al.*, 2003). The functions of calpains might not be restricted to their proteolytic activity. This idea is supported by the fact that some members of the family lack the catalytic residues and by the presence of other functional domains in the calpain structure.

The phenotypes of the available calpain knock-out mice are contradictory and reveal the complexity of the physiological roles played by the calpain system. *Capn4*-deficient mice lacking the small subunit, in which the activity of μ- and m-calpain was completely abolished, died at early embryonic stages (Arthur *et al.*, 2000; Zimmerman *et al.*, 2000). Disruption of the μ-calpain large subunit alone, however, resulted in viable and fertile mice displaying a significant reduction of platelet aggregation but normal bleeding times (Azam *et al.*, 2001). Conversely, *Capn2* $^{-/-}$ mice lacking the large subunit of m-calpain were not viable, suggesting an essential role of m-calpain in embryonal development (Goll *et al.*, 2003).

The involvement of the calpain system in some pathological conditions was first demonstrated by the linkage of disruptions in the calpain 3a gene to the limb girdle muscular dystrophy type 2A (LGMD2A) (Richard *et al.*, 1995). Knock-out and transgenic mice lacking calpain 3 (p94) or expressing different splice variants of it or an active site-mutated protein were viable and fertile, but the *Capn3* $^{-/-}$ mice showed a mild progressive muscular dystrophy that affects a specific group of muscles (Richard *et al.*, 2000). Mutations in intron 3 of the *Capn10* gene have been repeatedly associated with increased incidence of type 2 diabetes in some populations (Horikawa *et al.*, 2000; Goll *et al.*, 2003). Pancreatic β-cells in *Capn10 -/-* knock-out mice were recently shown to have an impaired response to several apoptotic stimuli (Johnson *et al.*, 2004). Downregulation of the *Capn9* gene is associated with human gastric cancer and *in vitro* induced tumorigensis in NIH3T3 cells (Yoshikawa *et al.*, 2000; Goll *et al.*, 2003). In addition to these genetic diseases, an involvement of calpain has been implicated in a series of Ca^{2+} homeostasis-linked pathologies like Alzheimer's disease, cataract formation, muscular dystrophies, myocardial infarcts, multiple sclerosis (MS) (demyelination), neuronal ischemia (stroke), obsessive-compulsive disorders and traumatic spinal cord (brain) injury (Huang and Wang, 2001; Goll *et al.*, 2003). The participation of the calpains in such a variety of diseases explains the growing interest in their characterization at the molecular level.

As mentioned above, only a few calpains have been isolated and/or recombinatly expressed and thoroughly characterized. Among them, the ubiquitous μ- and m-calpains, herein after referred to as "canonical calpains", have been studied extensively. These enzymes owe their names to the range of Ca^{2+} concentrations at which they are activated *in vitro* (3-50 μM for μ-calpain and 0.4-0.8 mM for m-calpain). They are heterodimers consisting of a 55-65 % homologous but distinct large 80 kDa catalytic subunit (80K- or L-subunit) and a common

A

B
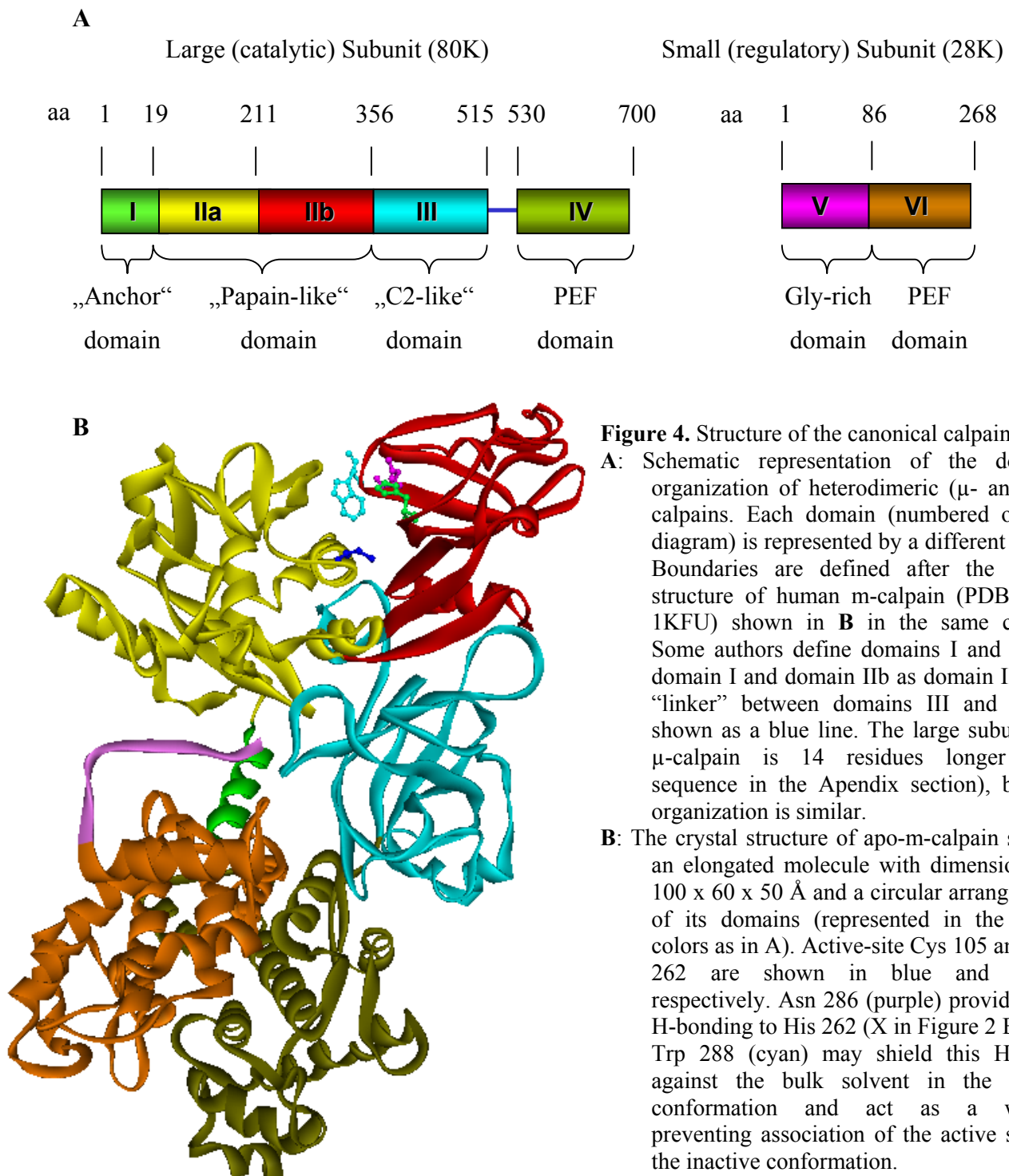
Figure 4. Structure of the canonical calpains

A: Schematic representation of the domain organization of heterodimeric (μ- and m-) calpains. Each domain (numbered on the diagram) is represented by a different color. Boundaries are defined after the X-ray structure of human m-calpain (PDB code 1KFU) shown in **B** in the same colors. Some authors define domains I and IIa as domain I and domain IIb as domain II. The "linker" between domains III and IV is shown as a blue line. The large subunit of μ-calpain is 14 residues longer (see sequence in the Apendix section), but its organization is similar.

B: The crystal structure of apo-m-calpain shows an elongated molecule with dimensions of 100 x 60 x 50 Å and a circular arrangement of its domains (represented in the same colors as in A). Active-site Cys 105 and His 262 are shown in blue and green respectively. Asn 286 (purple) provides the H-bonding to His 262 (X in Figure 2 B) and Trp 288 (cyan) may shield this H-bond against the bulk solvent in the active conformation and act as a wedge preventing association of the active site in the inactive conformation.

small 28 kDa regulatory subunit (30K-, 28K- or S-subunit). Sequence analysis and later elucidation of the X-ray structures of Ca^{2+}-free rat (Hosfield *et al.,* 1999) and human (Strobl *et al.,* 2000) m-calpain revealed that the large subunit is organized in four domains, I to IV (Figure 4).

The NH_2-terminal domain I is a short peptide with no similarity to proteins other than calpains, and is deeply anchored in domain VI. The catalytic domain II is similar to papain. A close look to its structure explains the inactivity of calpain in the absence of calcium: The active site is disrupted because the catalytic Cys105 S_γ and His262 N_δ are 10.5 Å appart. A 5° rotation and 1-2 Å translation of subdomains IIa and IIb relative to each other would be necessary to reduce this distance to 3.7 Å and allow productive binding of peptide substrates. The third domain has no sequence homology with any other known protein, but is topologically related to the C2 domains described in section B.3. An interesting structural feature of this domain is the presence of two separate clusters of basic and acidic residues respectively placed on two solvent exposed loops (see Figure 6, A). These "basic" and "acidic" loops make important contacts with the catalytic domain and are thought to influence the activity and Ca^{2+} dependency of the enzyme as well as its interactions with membrane phospolipids (Strobl *et al.,* 2000; Tompa *et al.,* 2001). Domain IV is a typical member of the penta EF-hand subfamily of CaBPs with four typical EF-hand motifs and an atypical fifth Ca^{2+} binding site. It associates with domain VI of the S-subunit, providing the basis for the heterodimeric nature of the canonical calpains. Domain VI is also a PEF protein with 24-44% identity and 51-54% similarity to domain IV of µ- or m-calpain. The 28K subunit NH_2-terminal domain V is composed of long polyglycine stretches and predominantly hydrophobic residues. Remotely related sequences have been described for other PEF proteins (Maki *et al.,* 2002), but the high content (40 %) of Gly residues is unique. The first 85 residues of domain V were not represented by a clear electron density in the crystal structure. Domain V has been implicated in the association of calpain with membrane phospholipids (Imajoh *et al.,* 1986; Arthur and Crawford, 1996).

The canonical calpains are tigthtly inhibited (Ki < 3 nM) in a calcium-dependent fashion by their endogenous inhibitor calpastatin, another well characterized player of the calpain system (Goll *et al.,* 2003). Full-length calpastatin is a random-coiled polypeptide composed of six domains, termed XL, L and 1 to 4, which inhibits exclusively calpain and no other protease so far tested. The molecular masses predicted from the amino acid sequences vary among the different isoforms between 46 and 84 kDa. However, the calpastatins migrate at quite different apparent molecular weights in SDS-PAGE due to their random-coiled

structure. Splice variants with shorter NH$_2$-termini (domain XL region) have been found in different tissues. The XL and L domains alone have no inhibitory activity. Domains 1 to 4 are repetitive sequences which are individually able to inhibit calpain, albeit with different potency (domain I > domain IV > domain III > domain IV) (Maki *et al.,* 1987). Each domain comprises three subdomains, A, B and C, coded by three exons of the gene. Only subdomain B inhibits calpain reversibly, whereas the non-inhibitory subdomains A and C bind to domains IV and VI of calpain, respectively. A synthetic 27 aa peptide representing subdomain B is used as an effective and highly selective inhibitor of μ- and m-calpain in experimental studies (Gil-Parrado *et al.,* 2003). Although the inhibition of calpain by calpastatin has been extensively characterized *in vitro*, the molecular mechanism and the physiological regulation of this process are still not completely understood. A growing number of studies with cultured cells indicate, however, that regulated expression, subcellular localization and phosphorylation of calpastatin are essential for the control of calpain activity within the cell.

B.4. Current standard of knowledge and aims of this work

Understanding how the calpains are activated by calcium has been an unsolved puzzle for many years. When the primary structure of the enzyme was elucidated in the 1980s and the calmodulin-like domains were identified, it seemed obvious that this process would involve a conformational change upon Ca^{2+} binding to the EF-hands (Croall and DeMartino, 1991), as observed as in the case of calmodulin. However, the determination of the crystal structures of a Ca^{2+} bound dimer of domain VI (Blanchard *et al.,* 1997; Lin *et al.,* 1997), and of Ca^{2+}-free rat and human m-calpains (Hosfield *et al.,* 1999; Strobl *et al.,* 2000), revealed that, unlike the effect of Ca^{2+}-binding to calmodulin, the conformational change induced by Ca^{2+} binding to the PEF domains of calpain is expected to be very small (Figure 5). Thus it is difficult to figure out how this small structural rearrangements upon Ca^{2+} binding to domains IV and VI would bring about the extensive conformational change required for the assembly of the protease domain.

At this point, new hypotheses emerged trying to explain the Ca^{2+}-dependent activation of calpain. Hosfield and colleagues (Hosfield *et al.,* 1999) postulated that domain III and the extended segment connecting it to the calmodulin-like domain IV (shown in blue in Figures 4, A and 14, A) might serve as an "intramolecular signal transducer" amplifying the small conformational changes generated by Ca^{2+}-binding to the calmodulin-like domains. This

"lever" function is reminiscent of the myosin head where small structual changes associated with binding of ATP are amplified throug the "stalk" of the myosin head to produce a movement of ~ 10 nm relative to the actin filament (Goll *et al.,* 2003).

A   **B**
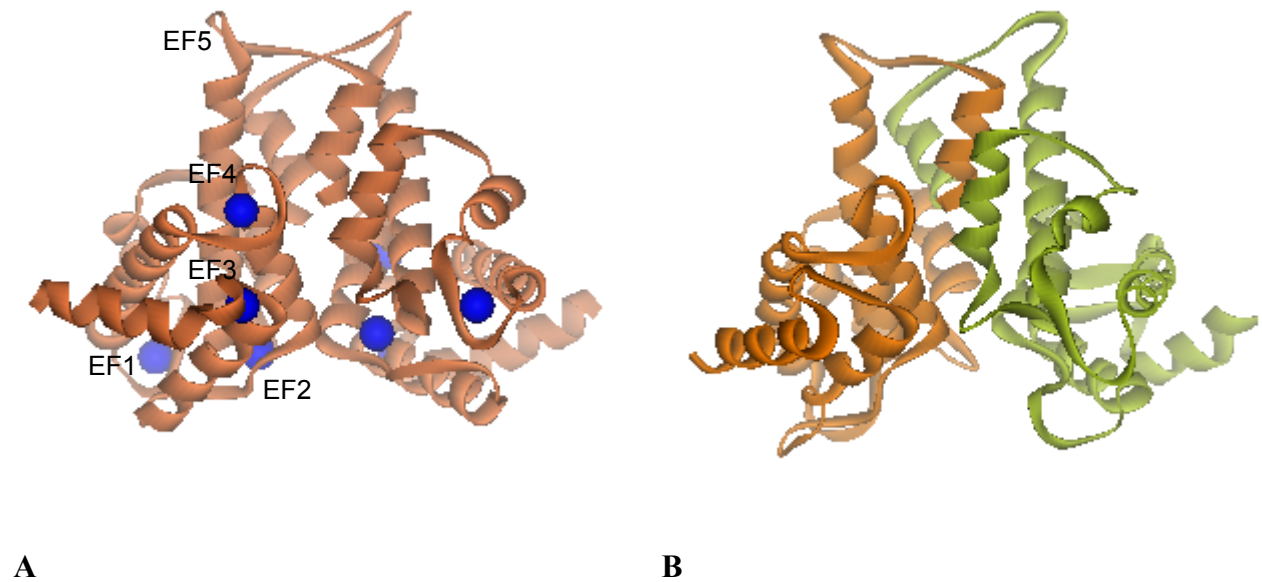
Figure 5. Effect of Ca^{2+}-binding to the calmodulin-like domains of calpain. **A**: Ribbon plot of a domain VI dimer crystallized in the presence of high Ca^{2+} concentrations (PDB code 1DVI). EF-5 does not bind Ca^{2+}, but is involved in forming the interface between the two monomers in the homodimer. Comparison of this structure with the structure of domains IV and VI of "apo"- m-calpain (panel **B**) reveals that only very small Ca^{2+}-induced conformational changes can be expected in these PEF domains.

B.4.1. Objective 1: Test the "electrostatic switch" hypothesis

A second proposal by Strobl (Strobl *et al.,* 2000) associated the activation of calpain with an electrostatic switch operated by the binding of Ca^{2+} and/or membrane phospholipids to the "acidic loop", a cluster of acidic residues placed in a solvent-exposed loop of domain III (Figure 6, A). These authors postulated that Ca^{2+}-binding to the acidic residues would disrupt the multiple electrostatic contacts at the interface of the acidic loop with the protease subdomain IIb. This would allow the latter to freely rotate by 50° and translate by 12 Å toward subdomain IIa, thereby accomplishing the assembly of the active site. This simple mechanism would also explain the differences in Ca^{2+} requirement for activity between
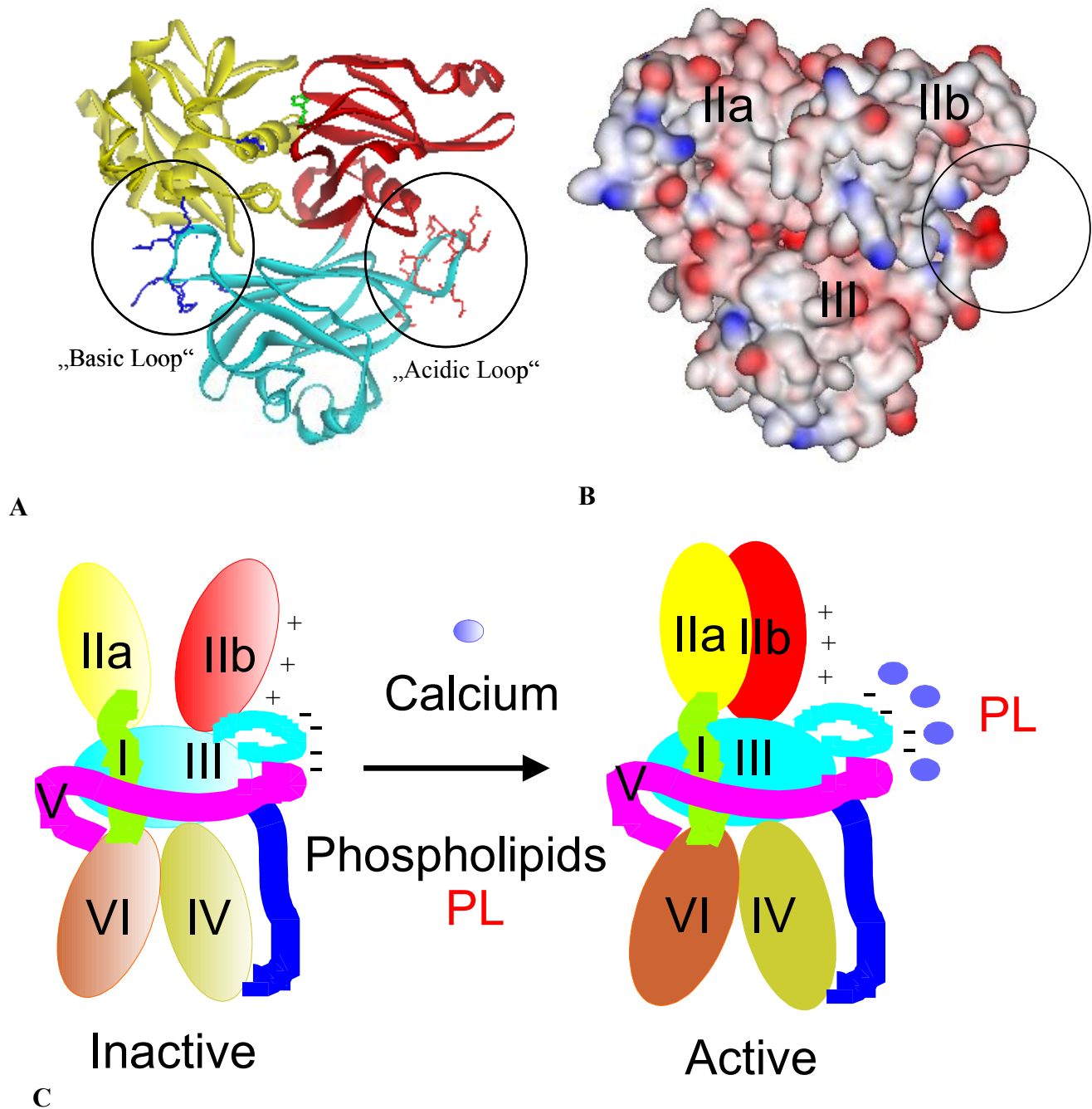
Figure 6. Putative "electrostatic switch activation mechanism" of calpain.

A: Ribbon plot of m-calpain domains II and III showing the solvent-exposed basic and acidic loops in domain III. Domains IIa, IIb and III as well as the catalytic dyad residues were colored as in Figure 4. Basic and acidic residues on the loops are shown as blue and red sticks respectively.

B: Electrostatic surface representation of m-calpain domains III and III showing charge density at the interface between domain IIb and domain III acidic loop (enclosed in a circle).

C: Schematic representation of the electrostatic switch proposed by Strobl (2000) (adapted from Reverter *et al.,* 2001). Disruption of the attractive forces between domain III acidic loop and subdomain IIb allows the movement of the latter toward domain IIa and the assembly of the active site.

μ-calpain, m-calpain, and p94. m-Calpain makes more contacts with subdomain IIb than μ-calpain and therefore would need more Ca^{2+} ions to disrupt the electrostatic interactions whereas p94 –which has been reported to be active in the presence of EDTA- is expected to make less interface contacts due to the lack of basic residues corresponding to Lys-354, Lys-355 and Lys-357 (m-calpain). This hypothesis was supported by the finding that μ- and m-calpain constructs lacking domain III had an increased Ca^{2+} requirement for activity (Vilei *et al.,* 1997).

Evidently the elucidation of the X-ray structure of a Ca^{2+}-bound full-length heterodimeric calpain would be the best way to understand the activation of the calpains by calcium. Yet, attempts to crystallize the m-isoform in the presence of Ca^{2+} failed due to massive aggregation and dissociation of the subunits (Pal *et al.,* 2001). Similar difficulties were encountered in crystallization experiments with the μ-isoform, even in the presence of EDTA (Reverter, unpublished results). Because of these persistent technical hindrances, mutagenesis of the putative Ca^{2+}-binding sites followed by biochemical characterization of the mutants and crystallization of separate domains in the presence of Ca^{2+} became the methods of choice to study the activation of the calpains.

By the time the apo-m-calpain structure was published, our laboratory had suceeded in expressing both active heterodimeric human μ-calpain and a non-autolyzing active-site mutant in insect cells using the baculovirus expression system (Pfeiler, 2001). Purification of the active μ-calpain turned to be troublesome and inefficient as reported by other groups (Elce, 1999). The active-site mutant, however, was easily isolated in large amounts by one-step purfication on a calpastatin BC-peptide affinity column. Based on these possibilities, **the first aim of this work was to test the electrostatic switch hypothesis by producing a series of mutants of μ-calpain in which the individual residues of the acidic loop were replaced by alanine. These mutants should be characterized by their Ca^{2+} requirement for activation and by their phospholipid binding properties.**

As this experimental work was in progress**,** several research papers concerning calpain activation were published by other laboratories (Hosfield *et al.,* 2001; Moldoveanu *et al.,* 2001; Nakagawa *et al.,* 2001; Dainese *et al.,* 2002; Dutt *et al.,* 2002; Moldoveanu *et al.,* 2002; Moldoveanu *et al.,* 2003; Pal *et al.,* 2003; Smith *et al.,* 2003; Alexa *et al.,* 2004; Farkas *et al.,* 2004; Moldoveanu *et al.,* 2004). Our results will be analyzed in the light of the newest knowledge in the Discussion chapter.

B.4.2. Objective 2: Investigate the role of domain V in activation

Answering the questions concerning calpain activation by calcium at the molecular level is by no means the solution of the riddle: even more difficult to understand is how the cell bridges the gap between the Ca^{2+} requirements of the native calpains *in vitro* and the actual concentrations of calcium in the cytosol ($\leq 1\mu M$). This paradox has early stimulated the search for factors which would decrease the Ca^{2+} requirement *in vitro* to the physiological levels. One of the first observations concerning this topic was that autolytical processing of the calpain subunits (Figure 7) resulted in a decreased Ca^{2+} concentration required for activity (Suzuki *et al.,* 1981; Hathaway *et al.,* 1982; DeMartino *et al.,* 1986; Edmunds *et al.,* 1991; Zimmerman and Schlaepfer 1991; Brown and Crawford, 1993; Baki *et al.,* 1996; Elce *et al.,* 1997; Farkas *et al.,* 2004). The responsibility of autolytic processing of the large subunit at its NH_2-terminus for this decrease has been well documented (Imajoh *et al.,* 1986; Brown and Crawford, 1993; Elce *et al.,* 1997; Farkas *et al.,* 2004). The X-ray structures showed that domain I is not a classical zymogen pro-peptide blocking the active site cleft, but is buried in domain VI. It has been proposed that Ca^{2+} binding to domain VI would disrupt a salt bridge between Lys-7 of the L-subunit and Asp-154 of the S-subunit (Asp-154 is part of EF2 of domain VI) facilitating the liberation and possible unfolding of this peptide followed by autocatalytic cleavage. Release of the N-terminal helix might relieve tension between domain VI and domain IIa, alleviating the approach of the latter to domain IIb and formation of a productive catalytic domain.

It has been shown that domain V of the small subunit is removed early in the autolytic degradation process by cleavage before Ala-92 (reviewed in Croall and DeMartino, 1992 and Goll *et al*, 2003) (Figure 7). Presumably due to its extensive structural flexibility, the position of this domain, as well as its interactions within the intact molecule are not resolved in the crystallographic m-calpain structure. Moreover, few has been published about the impact of its autoprotolytic removal on calpain activation (DeMartino *et al.,* 1986). Therefore, **the second aim of this work was to investigate the effect of domain V on the Ca^{2+} requirement for the activation of µ-calpain.**

To address this question experimentally seemed attractive, because methods had been established in this laboratory that allowed the expression in insect cells of the full-length small subunit (28K) as a single molecule as well as part of a µ-calpain heterodimer (Pfeiler, 2001). Additionally, a truncated small subunit lacking domain V (21K) had been expressed and isolated from *E. coli* (Gollmitzer, 1999; Diaz *et al.,* 2001). One objective of this thesis
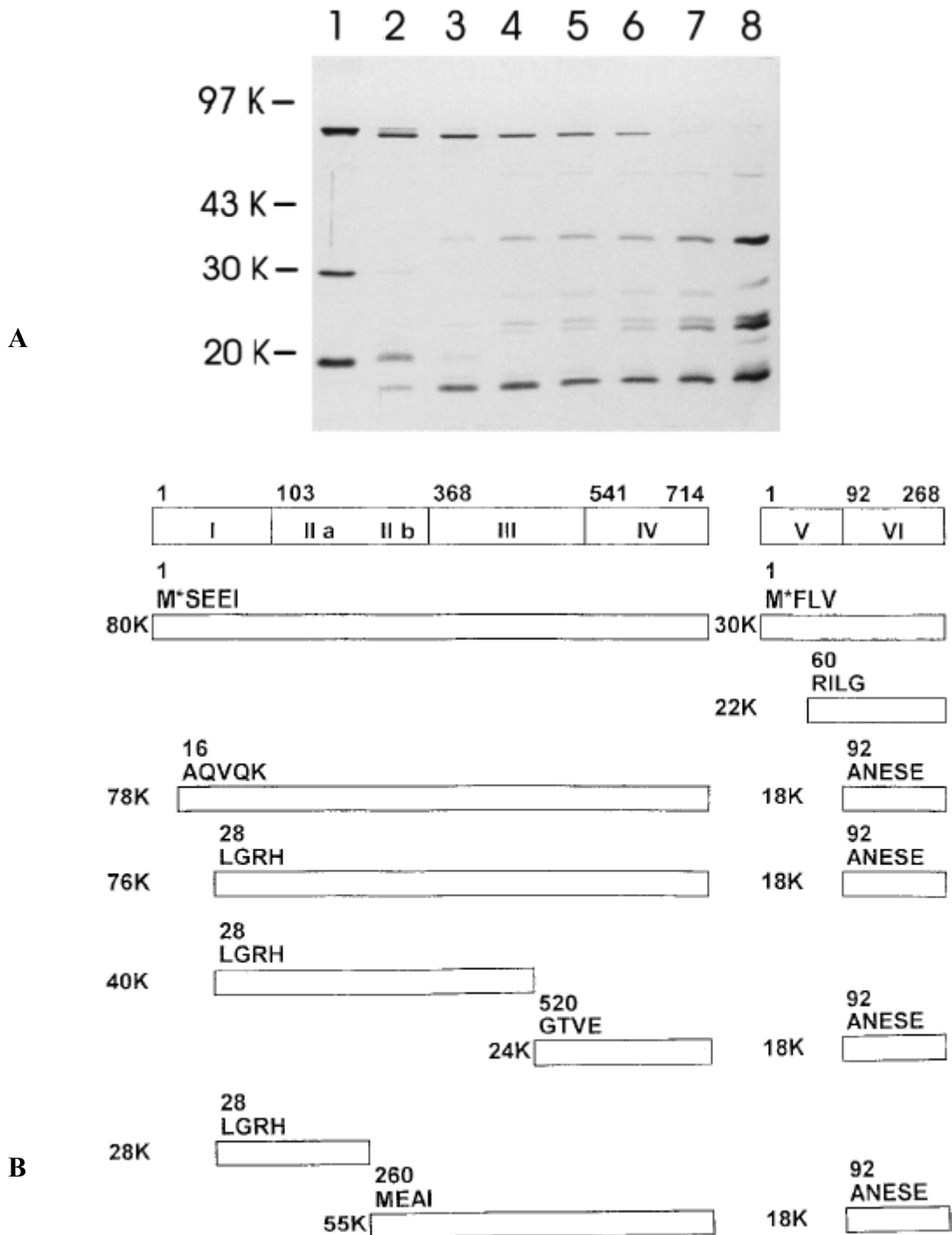
Figure 7. The autoproteolytic degradation of µ-calpain in the presence of calcium. (Taken from Gabrijelcic-Geiger *et al.,* 2001).

A: *In vitro* autolysis of human erythrocyte µ-calpain followed by SDS-PAGE. Lane 1, purified µ-calpain after storage for 2 weeks at – 80 °C; lanes 2 – 8, autolytic fragments 0 min (2), 1 min (3), 5 min (4), 15 min (5), 30 min (6), 60 min (7) and 120 min (8) after addition of 0.5 mM free Ca2+ (final concentration) to purified µ-calpain (27.5 µg) in 50 mM Tris-HCl, pH 7.5, 100 mM NaCl and 1 mM DTT at room temperature. After the indicated time intervals aliquots were taken (1.1 µg), EDTA was added (25 mM final concentration) and the material was applied to the gel.

B: Scheme of observed autolysis fragments of purified µ-calpain after calcium activation. Cleavage points are identified by their N-terminal sequences.

was to express also a heterodimer containing this truncated small subunit (80K/21K heterodimer) in insect cells using the baculovirus system and to compare its Ca^{2+} sensitivity with that of the full-length heterodimer.

B.4.3. Objective 3: Evaluate the contributions of domain III and V to phospholipid binding of µ-calpain

Besides autoproteolysis, a second factor that has been suggested to to decrease the threshold of Ca^{2+} sensitivity is the interaction of the calpains with membrane phospholipids. Several laboratories have reported a reduction of the Ca^{2+} requirement for autolysis and substrate processing of the calpains *in vitro* when incubated with phospholipids of diverse compositions (Coolican and Hathaway, 1984; Pontremoli *et al.,* 1985; Chakrabarti *et al.,* 1990; Saido *et al.,* 1992; Arthur and Crawford, 1996; Chakrabarti *et al.,* 1996). In living cells, immunofluorescence staining studies, immunogold electron microscopy and subcellular fractionation studies have shown that calpains are localized exclusively in the cytoplasm with a rather wide distribution. Some of these studies (including one published by our group (Gil-Parrado *et al.,* 2003) showed that upon a specific signal (mostly involving a calcium influx), an important part of calpain is relocated to the cell periphery (Goll *et al.,* 2003). Based on these *in vitro* and *in situ* observations, it has been postulated that calpain is activated at the cell membranes (Mellgren, 1987; Suzuki *et al.,* 1987; Kawasaki and Kawashima, 1996; Molinari and Carafoli, 1997; Suzuki and Sorimachi, 1998). Early works pointed to the hydrophobic Gly-rich domain V as the mediator of the interactions of calpain with membranes (Imajoh *et al.,* 1986). In addition to the polyglycine stretches, a specific GTAMRILGGVI sequence in this domain seems to be implicated in the association with membranes (Crawford *et al.,* 1990; Arthur and Crawford, 1996; Daman *et al.,* 2001; Brandenburg *et al.,* 2002). The identification of domain III as a C2-like structure suggested the existence of a second phospholipid binding region in this domain which was recently shown to interact with calcium and liposomes *in vitro* (Tompa *et al.,* 2001) and with cellular mebranes *in situ* (Gil-Parrado *et al.,* 2003). Given the existence of two possible membrane binding sites, **the elucidation of the individual contributions of domains III and V to phospholipid binding of heterodimeric µ-calpain was the third aim of this work**.

To address these questions, it was planned to compare phospholipid binding of the full-length 80K/28K-heterodimer, its acidic loop mutants (see B.4.1), and the truncated

80K/21K heterodimer (see B.4.2). FRET and surface plasmon resonance techniques should be established in the laboratory and applied to analyze the interactions of the calpains with fluorescence-labeled or immobilized liposomes of various composition.

B.4.4. Objective 4: Study the Ca^{2+} response of fluorescent calpain mutants in living cells

Building upon the obtained *in vitro* results, **the fourth aim of this work was to study the effect of the introduced mutations on the localization and Ca^{2+}-induced translocation of the calpain variants in living cells.** For this investigation it was planned to construct fluorescent fusion proteins of the large subunit of wild type and mutated calpains with EYFP and to overexpress them transiently and/or permanently in mammalian cell lines. Similar studies with calpain subunits and separate domains overexpressed in mammalian cells had been performed in the group before (Gil-Parrado et al., 2003).

C. Materials and Methods

C.1. Materials

C.1.1. Equipment

Balances
Analytic Balance, A 120 S (mg range)   Sartorius, Göttingen
Analytic Balance, Mettler (mg range)   E. Mettler, Zurich
Technical Balance, MA AF200 (g-Kg range)   Sartorius, Göttingen
Centrifuges:
Kontron, Centrikon H-401   Kontron Instruments, Eching
(with rotors A6.9 and 8.24)
Heraeus, Varifuge 3.0 R   Heraeus Sepatech, München
Heraeus, Varifuge 3.2 RS   Heraeus Sepatech, München
Heraeus, Sepatech Biofuge *primo*   Heraeus Sepatech, München
Heraeus, Sepatech Biofuge 15   Heraeus Sepatech, München
Eppendorf 3200, spin down centrifuge   Eppendorf-Netheler-Hinz, Hamburg
Cuvette centrifuge, Hellma Rotto-vette 310   Bachofer, Reutlingen
Clean benches:
BDK 7419, Mod. UVF 6.18S   BDK, Sonnenbühl-Genkingen
Clean Air type DLF 460   Clean Air, Göttingen
Herasafe type HS12   Heraeus Instruments, München
Chromatographic systems:
Peristaltic pump Minipuls 3   Gilson (Abimed), München
Fraction collector Probentisch 5122   Eppendorf, Hamburg
UV recorder 2138 Uvicord S   LKB, Freiburg
Recorder Tarkan 600   W + W electronics, Basel; CH
Deep freezing refrigerator:
Colora UF 85-300S (-80 ^{o}C)   Colora, Lorch
Gas phase aminoacid sequencer:
Mod. 473A   Applied Biosystems, Weiterstadt
Horizontal DNA electrophoresis chambers:
HE 33 mini submarine unit   Hoefer, Heidelberg
HE 99X max submarine unit   Hoefer, Heidelberg

Ice machine:
AF-10   Scotsman, Frimont, Italy
Incubators:
B30 and BE30   Memmert, Schwabach
Forma Scientific Model 3682   Forma Scientific, OH, USA
Innova 4230   New Brunswick Scientific, Nürtingen
Heraeus BK 600   Heraeus Instruments, München
Gel imaging system:
Image Master® VDS   Pharmacia, Freiburg
Liquid nitrogen tank

Cryo 4000   MVE Cryosystems, MN, USA
Lyophilizer:
Alpha I-6 Vacuum pump type DUO 004B with   Heraeus-Christ, Osterode
Speed Vac Concentrator   Bachofer, Reutlingen

Magnetic stirrers:
Ika-Combimag RCO   Janke & Kunkel, Staufen
Ikamag RET, thermostatted stirrer   Janke & Kunkel, Staufen
Mechanical shakers:
Vortex Genie 2   Scientific Industries, NY, USA
Microscopes:
Leitz Periplan   Leitz, Wetzlar
Olympus IX 50-S8F   Olympus, Feldkirchen-Westerham
Axiovert 200M/510META   Carl Zeiss, Jena
Microwave oven:
R-6270   Sharp, Osaka, Japan
Orbital shakers:
Infors TU and TR150
with air stream incubator covers Infors ITE   Infors AG, Bottmingen, CH
PCR thermal cyclers:
Gene Amp 2400   Perkin Elmer, Langen
Primus 25   MWG Biotech,
pH-meters:
Type 114D with   WTW, Weilheim
pH electrodes   Ingold, Steibach-Taunus
Power supplies:
EPS 500/400   Pharmacia, Freiburg
Mighty Slim™   Hoefer, Heidelberg
Protein transfer apparatus:
MilliBlot™-SDE System   Millipore, Eschborn
Sonifiers
Elma® Laboson 200 (bath sonifier)   Hans Schmidbauer KG, Singen
Branson Sonifier 250 (microtip sonifier)   Branson, Danbury, CT, USA
Spectrophotometers:
LKB Ulstrospec III   Pharmacia, Freiburg

Spectrofluorimeters:
Kontron SFM-25   Kontron Instruments, Eching
Spex Fluoromax®   SPEX Industries Inc, Edison, NJ, USA
HTS-700   Perkin Elmer, Langen
UV transiluminator:
302 nm   Bachofer, Reutlingen
Vertical protein electrophoresis system:
Mighty Small II   Hoefer, Heidelberg
Water deionization system:
Membrapure   MembraPURE, Bodenheim
Water baths:
Memmert   Memmert, Schwabach
Haake   Haake Gebrüder, Berlin

C.1.2. Chemicals and Materials

All chemicals (quality "p.a.") used in this work are listed below.

General chemicals

-1,4-dithiothreitol (DTT)	Sigma, Deisenhofen
-acetic acid	Merck, Darmstadt
-acriylamide:bisacrylamide (37,1:1) sol.	Serva, Heidelberg
-Brij-35	Sigma, Deisenhofen
-Triton X-100	Sigma, Deisenhofen
-bromophenol blue	Serva, Heidelberg
-chloroform	Sigma, Deisenhofen
-chlorhydric acid	Merck, Darmstadt
-coomassie brilliant blue R250 and G250	Serva, Heidelberg
-dimethyl sulfoxide (DMSO)	Sigma, Deisenhofen
-ethanol	Merck, Darmstadt
-ethidium bromide	Serva, Heidelberg
-glycerol	Serva, Heidelberg
-Hepes	Sigma, Deisenhofen
-isopropanol	Baker Chemikalien, Gross-Gerau
-methanol	Merck, Darmstadt
-SDS	Serva, Heidelberg
-sodium hydroxide	Merck, Darmstadt
-ß-mercaptoethanol	Sigma, Deisenhofen
-Tris base	Sigma, Deisenhofen
-TNS	Molecular Probes (MoBiTec), Göttingen
-PG, PS, PC, PE, PI, Cholesterol, PIP and PIP_2	Avanti Polar Lipids, Alabaster, AL, USA
-dansyl DHPE	Molecular Probes (MoBiTec), Göttingen
-boric acid	Sigma, Deisenhofen
-natrium chloride	Sigma, Deisenhofen

Chemicals and materials for protein chemistry techniques

-NHS activated Sepharose 4B	Pharmacia, Freiburg
-Ni-NTA Sepharose	Qiagen, Hilden
-5 ml laboratory (empty) columns for affinity chromatography	MoBiTec, Göttingen
-See Blue™ pre-stained protein ladder for SDS-PAGE	Invitrogen, Groningen, The Netherlands
-Bench Mark™ protein ladder for SDS-PAGE	Invitrogen, Groningen, The Netherlands
-nitrocellulose membrane BA 85 (0,45 μm)	Schleicher and Schuell, Kassel
-Slide-A-Lyzer™ dialysis cassettes	Pierce, Rockford, IL, USA
-Immobilon™-P PVDF membrane	Millipore, Eschborn
-Kodax BioMax, Cassette	Kodak, Rochester, NY, USA
-Kodax BioMax, 18 x 24 films	Kodak, Rochester, NY, USA

-Gelatine   Merck, Darmstadt
-Supersignal   West   Pico   chemiluminscent Pierce, Rockford, IL, USA
substrate

Chemicals and materials for the molecular biology techniques

-restriction endonucleases   Roche Molecular Biochemicals, Manheim
-IPTG   Roche Molecular Biochemicals, Manheim
-agarose, Nusieve   FMC, Biozym, Hameln
-agarose, Seakem GTG   FMC, Biozym, Hameln
-DNA molecular length markers   Roche Molecular Biochemicals, Manheim
-Qiagen, plasmid purification kits   Qiagen, Hilden
(maxi, midi and miniprep)
-Qiagen gel extraction kit   Qiagen, Hilden
-DNA sequencing kit   Applied Biosystems, Weiterstadt
-ATP   Sigma, Deisenhofen
-dNTPs   Pharmacia, Freiburg
-Quick Change™ Site Directed Mutagenesis Kit   Stratagene, Amsterdam, The Netherlands
-ampicillin Na-salt   Roche Molecular Biochemicals, Manheim
-kanamycin   Roche Molecular Biochemicals, Manheim

Chemicals and materials for the microbiological techniques

-bacto agar   Difco, Augsburg
-bacto yeast extract   Difco, Augsburg
-bacto tryptone   Difco, Augsburg
-bacto peptone   Difco, Augsburg
-culture flasks 1,8 l (Fernbach)   Wagner and Munz, München
-culture flasks (Erlenmeyer)   Wagner and Munz, München
-Petri dishes polystyrol 9 cm (sterilized)   Sarstedt, Nümbrecht
-Cryo tubes 1,8 ml (sterilized)   Nunc, Wiesbaden-Biebrich

Chemicals and materials for the insect and mammalian cell culture

-Fetal Calf Serum   Gibco BRL, Paisley, Scotland
-Fugene™6   Roche Molecular Biochemicals, Manheim
-Geneticin (G-418)   Roche Molecular Biochemicals, Manheim
-Gentamicin   Roche Molecular Biochemicals, Manheim
-L-Glutamine 200 mM   Gibco BRL, Paisley, Scotland
-PBS (10x Solution)   Gibco BRL, Paisley, Scotland
-Penicillin-Streptomycin   Gibco BRL, Paisley, Scotland
(10000 IU/mL-10000 µg/mL)
-Pluronic   Sigma, Deisenhofen
-Roswell Park Memorial Institute Media 1640   Gibco BRL, Paisley, Scotland
 (RPMI 1640) with 2 mM L-Glutamine
-SF-900 II Insect Cells Medium (Serum free)   Gibco BRL, Paisley, Scotland

-Sodium Pyruvate 100 mM   Gibco BRL, Paisley, Scotland
-Sterilized tissue culture flasks   Nunc, Wiesbaden-Biebrich
-Sterilized tissue culture plates   Nunc, Wiesbaden-Biebrich
-Sterilized tissue culture multiwell plates   Nunc, Wiesbaden-Biebrich
-Sterilized cell scrapers   Nunc, Wiesbaden-Biebrich
-Sterilized cryo-tubes   Nunc, Wiesbaden-Biebrich
-Sterilized serological pippetes   Sarstedt, Nümbrecht
-Sterilized pipete tipps   Biozym, Oldendorf
-MD-System object slides   Madaus Diagnostik, Köln
-TNM-FH Insect Cells Medium (with Serum)   Pharmingen, Heidelberg
-Trypan blue 0.4 % Solution   Bio Whittaker, Cambridge, UK
-Trypsin-EDTA (10x Solution)   Gibco BRL, Paisley, Scotland

Miscellaneous

-1.5 and 2.5 mL reaction tubes   Eppendorf, Hamburg
-13 and 50 mL "Falcon" centrifuge tubes   Sarstedt, Nümbrecht
-membrane filter 0.2 and 0.45 µM   Millipore, Eschborn
-Gilson pipete tips   Abimed, München

Oligonucleotides used as primers for PCR identification of recombinant baculoviruses

Polyhedrin Forward   5'-AAATGATAACCATCTCGC-3'
Polyhedrin Reverse   5'-GTCCAAGTTTCCCTG-3'c

Oligonucleotides used as primers for PCR-based site directed mutagenesis of µ-calpain

Mutant D402A Forward   5'-CAAGATCCGGCTGGCTGAGACGGATGAC -3'
Mutant D402A Reverse   5'-GTCATCCGTCTCAGCCAGCCGGATCTTG-3'
Mutant E403A Forward   5'-GATCCGGCTGGATGCGACGGATGACCC-3'
Mutant E403A Reverse   5'-GGGTCATCCGTCGCATCCAGCCGGATC-3'
Mutant D405A Forward   5'-GCTGGATGAGACGGCTGACCCGGACGACTACG-3'
Mutant D405A Reverse   5'-CGTAGTCGTCCGGGTCAGCCGTCTCATCCAGC-3'
Mutant D406A Forward   5'-GGATGAGACGGATGCCCCGGACGACTACG-3'
Mutant D406A Reverse   5'-CGTAGTCGTCCGGGGCATCCGTCTCATCC-3'
Mutant D408A Forward   5'-GATGAGACGGATGACCCGGCCGACTACGGGGAC-3'
Mutant D408A Reverse   5'-GTCCCCGTAGTCGGCCGGGTCATCCGTCTCATC-3'
Mutant D409A Forward   5'-CGGATGACCCGGACGCCTACGGGGACC-3'
Mutant D409A Reverse   5'-GGTCCCCGTAGGCGTCCGGGTCATCCG-3'
Mutant D412A Forward   5'-CGGACGACTACGGGGCCCGCGAGTCAGG-3
Mutant D412A Reverse   5'-CCTGACTCGCGGGCCCCGTAGTCGTCCG-3'
Mutant E414A Forward   5'-CGACTACGGGGACCGCGCGTCAGGCTGC-3'
Mutant E414A Reverse   5'-GCAGCCTGACGCGCGGTCCCCGTAGTCG-3'

Oligonucleotides used as primers for DNA sequencing

Sequencing of 80K subunit
For-161   5'-CCGGAATTCCCTATAAATATGTCGGAGGAGATCATC-3'
For-421   5'-CCGGAATTCCCTATAAATCCCACGGAACTGCTGTC-3'
For-421-syn   5'-CCGACCGAACTGCTGAGC-3'
For-760   5'-CAGCTACGAGGCCCTGTC-3'
For-1099   5'-AGTGGAACAACGTGGACCC-3'
For-1416   5'-CGTGCTCGCCCTTATGC-3'
For-1740   5'-GATCCAGGCCAATCTCC-3'
For-1989   5'-GAGTTCAACATCCTGTGGAACC-3'
Rev-405   5'-TGACAGCAGTTCCGTGGG-3'
Rev-405-syn   5'-GCTCAGCAGTTCGGTCGG-3'
Rev-765   5'-CCCTCTGAGGTGCTGCC-3'
Rev-1124   5'-CGCGGATCCTCATTAGACCCGGAGCTGGTCCCG-3'
Rev-1504   5'-AAGTGTACGGCCGGCTGG-3'
Rev-1894   5'-CACGACTCTAGGCTGAAG-3'
Rev-2285   5'-CGCGGATCCTCATTATGCAAACATGGTCAGC-3'
Sequencing of 28K/21K subunit
30K-For-1   5'-GCCTGGGAAATGTGCTTG-3'
30K-For-2   5'-CCCACGCACACATTACTCC-3'
30K-Rev-3   5'-GATCGGTCAGTGTCGAACTG-3'
30K-Rev-4   5'-CAAGAGATTTGAAGGCACGG-3'

Escherichia coli strains

TOP 10 (Invitrogen): F - *mcr*A _(*mrr-hsd*RMS-*mcr*BC) _80*lac*Z_M15 _*lac*X74 *deo*R *rec*A1 *ara*D139 _(*ara-leu*)7697 *gal*U *gal*K *rps*L (Str R) *end*A1 *nup*G

XL-10 Gold (Stratagene): Tet *Δ(mcrA)183 Δ(mcr CB-hsdSMR-mrr)173 endA1 sup E44 thi-1 recA1 gyrA96 relA1 lac* Hte [F′*proAB lacl^q ZΔM15* Tn10 (Tet[R]) Amy Cam[R]][a] Chloramphenicol resistant (Cam[R]) at concentrations of <40 µg/ml, but chloramphenicol sensitive (Cam[S]) at concentrations of 100 µg/ml.

B834(DE3) (Novagen)**:** F - ompT hsdS B (r B - m B -) gal dcm met

Insect cell lines

The invertebrate cell line *Sf21*, from the fall army worm *Spodoptera frugiperda* was used in this work for the heterologous expression of recombinant proteins. This cell line was established from ovarian tissues of *S. frugiperda* larvae and is commonly used as host cell line

in the baculovirus protein expression system due to its sensibility to infection by the *Autgrapha californica* nuclear polyhedrosis virus (AcNPV).

Mammalian cell lines

N-terminal EYFP-μ-calpain 80K chimeras were expressed in the human large cell lung carcinoma cell line (*LCLC 103H*) (Bepler *et al.,* 1988). This cell line was established from the pleural effusion of a 61-year-old man with large cell lung carcinoma with giant cells who had received chemo- and radiotherapy. *LCLC 103H* cells have been described to be PAS negative, to exhibit remarkable stroma formation and to overexpress the proto-oncogene c-myc. Due to their giant size, these cells are suitable for *in vivo* localization experiments.

Plasmid vectors for gene cloning

pVL1392

The pVL1392 baculovirus transfer vector is a derivative of the plasmid pVL941 (Luckow and Summers, 1989). It contains the complete polyhedrin gene locus including flanking regions of AcNPV cloned into the pUC8 vector, but it lacks part of the polyhedrin gene coding region. A MCS region has been inserted 36 nucleotides downstream of the ATG polyhedrin start codon, which has been changed into an ATT, therefore the insert of choice must provide its own ATG start signal at the 5' end of the gene. The distance between the cloning site and the transcription start should not be longer than 100 nucleotides, otherwise the protein expression will be poor.
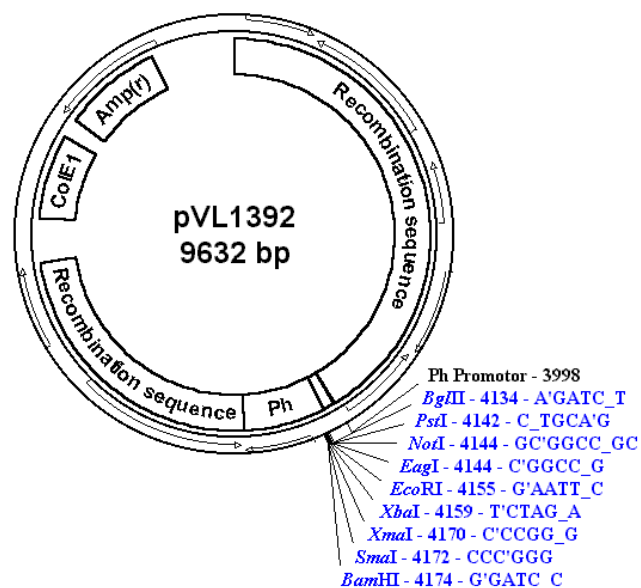
Figure 8. Baculovirus transfer vector pVL1392 The complete polyhedrin gene locus was cloned into pUC8 with the origin of replication of (Col E1) and the ampicillin resistance gene (Amp(r)). A multiple cloning site (enzymes in blue) was inserted 36 nucleotides downstream of the ATG polyhedrin start codon. The polyhedrin promotor region (Ph Promotor) regulates the expression of the gene of interest.

pEYFP-C1

pEYFP-C1 (Clontech) encodes an enhanced yellow-green variant of the *Aequorea victoria* green fluorescent protein (GFP). The EYFP gene contains the four amino acid substitutions previously published as GFP-10C (Ormö *et al.,* 1996): Ser-65 to Gly; Val-68 to Leu; Ser-72 to Ala; and Thr-203 to Tyr. The fluorescence excitation maximum of EYFP is 513 nm; the emission spectrum has a peak at 527 nm (in the yellow-green region). When excited at 513-nm, the emission coefficient of EYFP is 36,500 cm^{-1} M^{-1} and the fluorescent quantum yield is 0.63 (Ormö *et al.,* 1996), resulting in a bright fluorescent signal. In addition to the chromophore mutations, EYFP contains >190 silent mutations that create an open reading frame comprised almost entirely of preferred human codons (Haas *et al.,* 1996). Furthermore, upstream sequences flanking EYFP have been converted to a Kozak consensus translation initiation site (Kozak, 1987). These changes increase the translational efficiency of the EYFP mRNA and consequently the expression of EYFP in mammalian and plant cells. The MCS in pEYFP-C1 is between the EYFP coding sequence and the stop codon. Genes cloned into the MCS will be expressed as fusions to the C-terminus of EYFP if they are in the same reading frame as EYFP and there are no intervening in-frame stop codons. EYFP with a

C-terminal fusion moiety retains the fluorescent properties of the native protein and thus can be used to localize fusion proteins in vivo. The vector contains an SV40 origin for replication and a neomycin resistance (Neo(r)) gene for selection (using G418) in eukaryotic cells. A bacterial promoter (P) upstream of Neo(r) expresses kanamycin resistance in *E. coli*. The vector backbone also provides a pUC19 origin of replication for propagation in *E. coli* and an f1 origin for single-stranded DNA production.
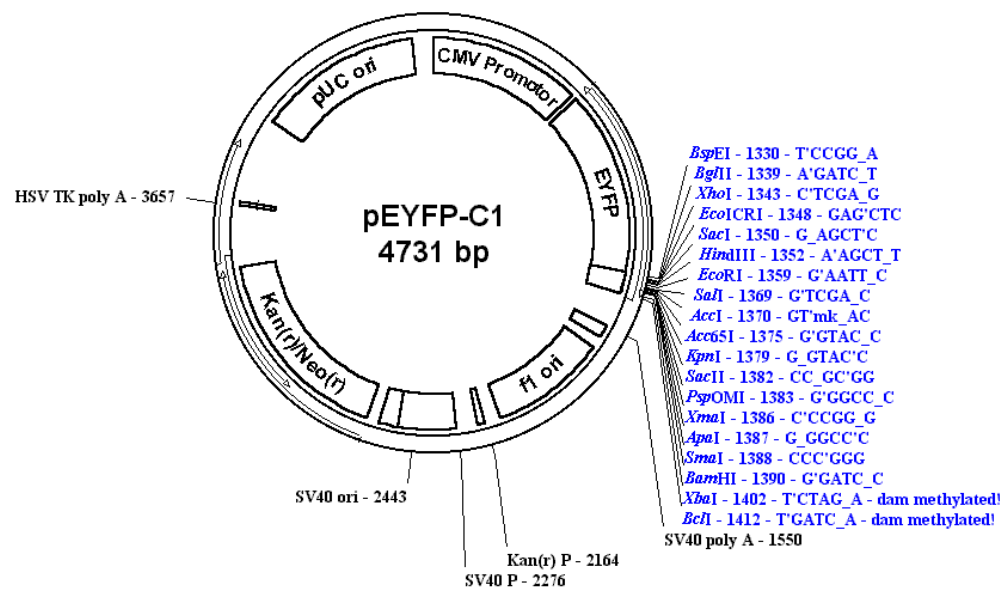
Figure 9. Expression vector pEYFP-C1. Enzymes from the multiple cloning site are listed in blue. SV40 poly A is the polyadenilation site of SV40 viurs. SV40 P serves as promotor for the mammalian expression of the Neo (r) gene. HSV TK poly A. More details about the vector features are given in the text.

Plasmid templates for PCR and subcloning

pVL1392-syn80K (C115A) (Pfeiler D, PhD thesis)

In this baculovirus transfer vector was inserted (*EcoRI*/*BamHI*) a semi-synthetic gene coding for the 80K subunit of μ-calpain in which the active site Cys 115 residue was converted to Ala using cassette mutagenesis. These mutation allows the expression in the baculovirus system of an inactive, non self-autolyzing μ-calpain. The encoded protein was C-terminally His$_6$ tagged. This vector served as template for PCR based mutagenesis of μ-calpain domain III.
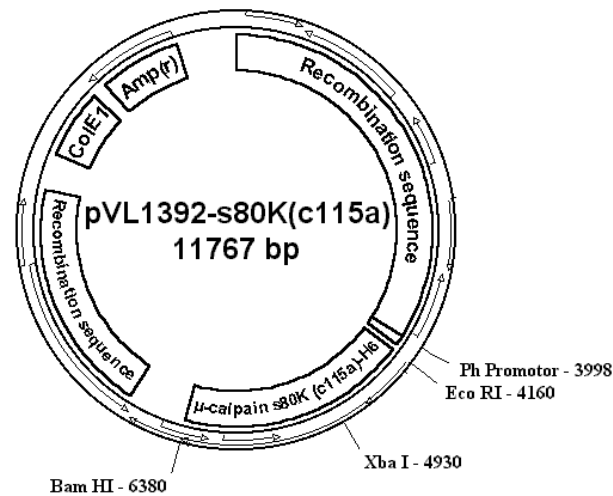
Figure 10. Baculovirus transfer vector pVL1392-s80K(C115A)-His$_6$. The 80K semisynthetic gene was cloned using the EcoRI and BamHI sites from the MCS. The ATG from the calpain gene is ~68 nucleotides downstream the polyhedrin (Ph) promotor, allowing good expression levels of the recombinant protein. More details are given in the text.

pUC18-syn 80K (Gil-Parrado S, PhD thesis)

pUC18 (Vieira and Messing, 1991) vector is a small, high copy number, plasmid, 2686 bp in length. This plasmid contains: (1) the pMB1 replicon rep responsible for the replication of plasmid (source - plasmid pBR322). The high copy number of pUC plasmids is a result of the lack of the rop gene and a single point mutation in rep of pMB1; (2) bla gene, coding for beta-lactamase that confers resistance to ampicillin (source – plasmid pBR322). It differs from that of pBR322 by two point mutations; (3) region of *E. coli* operon lac containing CAP protein binding site, promoter Plac, lac repressor binding site and 5'-terminal part of the lacZ gene encoding the N-terminal fragment of beta-galactosidase (source – M13mp18/19). This fragment, whose synthesis can be induced by IPTG, is capable of intra-allelic (alfa) complementation with a defective form of beta-galactosidase encoded by host (mutation lacZDM15). In the presence of IPTG, bacteria synthesize both fragments of the enzyme and form blue colonies on media with X-Gal. Insertion of DNA into the MCS located within the lacZ gene (codons 6-7 of lacZ are replaced by MCS) inactivates the N-terminal fragment of beta-galactosidase and abolishes alfa-complementation. Bacteria carrying recombinant plasmids therefore give rise to white colonies. A semi-synthetic gene encoding for the 80K subunit of human μ-calpain was cloned in this vector by Shirley Gil-Parrado. The

introduction of several unique restriction sites in the region of domain I and domain II allows cassette mutagenesis of the protease domain. This plasmid was used as template for the construction of active 80K domain III mutants.
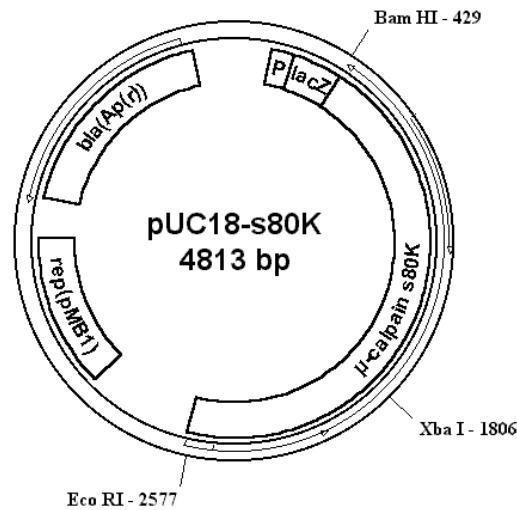
Figure 11. Cloning vector pUC18-s80K. The semisynthetic μ-calpain gene was cloned using the EcoRI and BamHI sites from the MCS of pUC18. The 80K gene interrupts the lac Z gene, and allows the differentiation of this plasmid from parental pUC18 on a X-Gal plate. See the text for more details.

Plasmid vectors for protein expression

pET-22b(+)-21K and pET-22b(+)-BC-calpastatin (Pfeiler D, PhD thesis)

The pET System (Novagen) is a powerful system for cloning and expression of recombinant proteins in *E. coli*. Target genes are cloned in pET plasmids under control of strong bacteriophage T7 transcription and (optionally) translation signals; expression is induced by providing a source of T7 RNA polymerase in the host cell. In addition, expression levels can be regulated by controlling the concentration of inducer. Recombinant protein expression may be initiated either by infecting the host with **l** CE6, a phage that carries the T7 RNA polymerase gene under the control of the **l** *p* L and *p* I promoters, or by transferring the plasmid into an expression host containing a chromosomal copy of the T7 RNA polymerase gene under *lacUV5* control. In the second case, expression is induced by the addition of IPTG to the bacterial culture. The pET-22b(+) vector carries an N-terminal pelB signal sequence (pectate lyase from *Ewinia carotovora*) for potential periplasmic localization, plus optional C-

terminal His$_6$ Tag sequence. Using a *NdeI* restriction site to clone gene inserts allows alternative cytoplasmatic expression of recombinant proteins. The truncated small subunit of calpain (21K) and the BC peptide of calpastatin domain I were cloned for cytoplasmatic expression in this vector by Dietmar Pfeiler using *NdeI* and *BamHI* restriction sites. A His$_6$ tag was attached for easy isolation using Ni-NTA chromatography. The plasmid pET-22b(+)-21K was also used as template for subcloning of the 21K subunit in pVL1392.
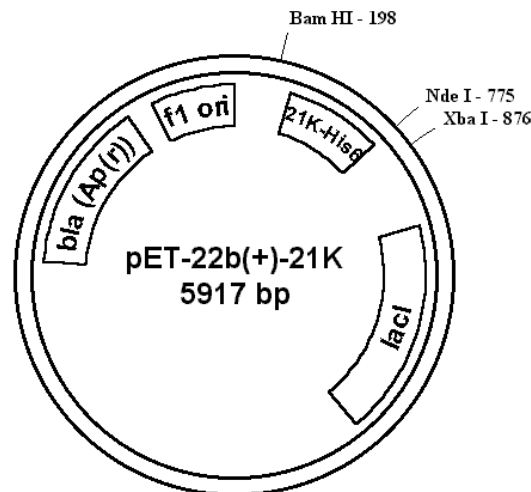
Figure 12. Expression vector pET-22b(+)-21K His$_6$. The 21K gene was cloned using NdeI and BamHI restriction sites from the MCS in order to ensure cytoplasmatic expression. Other features are described in the text.

pECFP-Membrane Marker

pECFP-Mem (Clontech) encodes a fusion protein consisting of the N-terminal 20 amino acids of neuromodulin, also called GAP-43 (Skene, 1989), and a cyan fluorescent variant of the enhanced green fluorescent protein (EGFP). The neuromodulin fragment contains a signal for posttranslational palmitoylation of cysteines 3 and 4 that targets ECFP to cellular membranes. The ECFP gene contains amino acid substitutions that give ECFP fluorescence excitation (major peak at 433 nm and a minor peak at 453 nm) and emission (major peak at 475 nm and a minor peak at 501 nm) spectra similar to other cyan emission
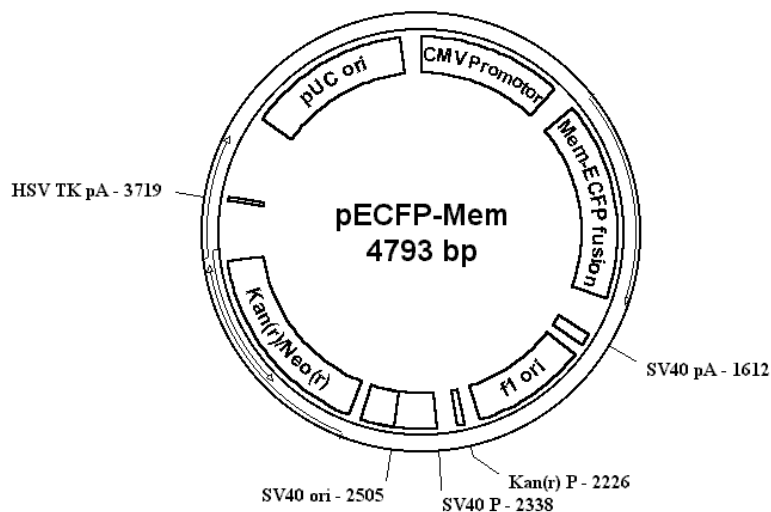
Figure 13. Expression vector pECFP-Mem. The neuromodulin fragment was attached to the N-terminus of ECFP. SV40 poly A is the polyadenilation site of SV40 viurs. SV40 P serves as promotor for the mammalian expression of the Neo (r) gene. HSV TK poly A. More details about the vector features are given in the text.

variants (Heim and Tsien, 1996; Heim *et al.,* 1994). These substitutions also enhance the brightness and solubility of the protein (Heim and Tsien, 1996, Cormack *et al.,* 1996 and Heim *et al.,* 1995). In addition to the chromophore mutations, ECFP contains over 190 silent mutations that create an open reading frame comprised almost entirely of preferred human codons (Yang *et al.,* 1996; Haas *et al.,* 1996). Furthermore, upstream sequences flanking the ECFP-Mem fusion protein have been converted to a Kozak consensus translation initiation site. These changes increase the translational efficiency of the fusion protein and consequently its expression in mammalian cells. Expression of ECFP-Mem is driven by the immediate early promoter of CMV (P CMV IE). The vector contains an SV40 origin of replication and a neomycin resistance (Neo(r)) gene for selection in mammalian cells. A bacterial promoter upstream of this cassette (P) expresses kanamycin resistance in *E. coli*. The vector backbone also provides a pUC19 origin of replication for propagation in *E. coli* and an f1 origin for single-stranded DNA production.

Viral vectors

BaculoGold™ linearized baculovirus DNA

This is a modified *Autographa californica* nuclear polyhedrosis virus (AcNPV) which contains a lethal deletion and does not code for viable virus. Co-transfection of the BaculoGold™ DNA with a complementing baculovirus transfer vector rescues the lethal deletion by homologous recombination. Since only the recombinant BaculoGold™ produces viable virus, recombination frequencies exceed 99%. The flanking sequences of the complementing vector's promoter region must be derived from the polyhedrin locus of the AcNPV wild-type DNA. p10 locus derived vectors will not recover the lethal deletion of BaculoGold™. Furthermore, not all polyhedrin derived vectors are compatible with BaculoGold™. The lethal deletion spans 1.7 kb downstream of the polyhedrin gene. Small streamlined vectors may not contain the entire region and will not rescue the lethal deletion.

C.2. Methods

C.2.1. Microbiological and cell culture methods

Most microbiological methods presented in this work were performed as described by Sambrook (1989). Methods regarding insect cell culture and baculovirus expression system were taken from Richardson (1996). Culture of human cells was performed mostly after Celis (1997). Literature references will be given for methods taken from another source.

C.2.1.1. Culture of *E. coli* strains

Growth media

All bacterial growth media mentioned below were adjusted to pH 7.5 with NaOH and sterilized by autoclaving during 20 min at a pressure of 1.2×10^5 Pa and a temperature of 121 $^{\circ}$C. Temperature-unstable solutions were sterile-filtered through a 0.2 μm pore membrane and

added to the broth once it was cooled to ≤50 ^{o}C. For the preparation of solid culture plates, liquid media were complemented with 15 g/l agar before autoclaving.

Luria Bertani Medium (LB):	10 g/l Bacto-tryptone
	5 g/l Bacto-yeast extract
	10 g/l NaCl
2xYT Medium (dYT):	16 g/l Bacto-tryptone
	10 g/l Bacto-yeast extract
	5 g/l NaCl
SOC Medium:	20 g/l Bacto-tryptone
	10 g/l Bacto-yeast extract
	0.5 g/l NaCl
	1.2 g/l $MgSO_4$
	0.95 g/l $MgCl_2$
	20 g/l D(+)-glucose
NYZ$^+$ Medium:	10 g/l NZ amine (casein hydrolysate)
	5 g/l yeast extract
	5 g/l NaCl
	12.5 mM $MgCl_2$
	12.5 mM $MgSO_4$
	20 mM D(+) glucose

Antibiotics

200 mg/ml Ampicillin stocks were prepared in 70 % ethanol and stored at -20 ^{o}C for no longer than 2 months. Stock solutions containing precipitates were discarded.200 mg/ml Kanamycin stocks were prepared in sterile H_2O and stored at -20 ^{o}C for no longer than 2 months. Antibiotics were diluted into the broth at room temperature to a final concentration of 200 µg/ml.

Storage of E. coli strains

For short term storage (up to 4 weeks), bacterial strains were streaked on LB-agar plates containing antibiotics. In order to preserve strains for longer periods of time, 3 ml cultures were inoculated from single colonies and grown overnight in the presence of antibiotics. After supplementing the cultures with glycerol to a final concentration of 15 % (v/v), 1 ml aliquots (glycerol stocks) were prepared and immediately placed at -80 $^{\circ}$C. Each new strain was numbered and its features were recorded in the laboratory strain catalogue.

Inoculation and growth of E. coli cultures

For plasmid isolation, culture flasks containing LB medium supplemented with 200 µg/ml antibiotics were inoculated by picking a single colony of the recombinant strain from a freshly streaked plate or by taking a small volume out of a glycerol stock. Cultures were grown overnight at 37 $^{\circ}$C with shaking at 200 rpm. The next day, cells were pelleted at 5000 rpm for 10 min at 4 $^{\circ}$C and DNA was isolated using the methods described in C.2.2.1

Heterologous gene expression by recombinant E. coli strains

For protein expression, glycerol stocks of the recombinant strains were used to inoculate culture flasks containing 200 ml 2xYT medium supplemented with 200 µg/ml ampicillin. After overnight incubation at 37 $^{\circ}$C and 120 rpm shaking, cells were pelleted (10 min, 5000 rpm, 4 $^{\circ}$C) and resuspended in 200 ml 2xYT medium. 10 ml of the resuspended cells were used to inoculate 1 liter of 2xYT medium supplemented with 500 µg/ml ampicillin. These new inoculum was incubated (37 $^{\circ}$C) with shaking (200 rpm) until they reached the log-growth phase. To monitor cell growth, OD_{600nm} was measured every 20 min. An OD_{600nm} between 0.2 and 0.6 was an indicator of logarithmic growth. At this point, cells were pelleted (10 min, 5000 rpm, 4 $^{\circ}$C) and resuspended in the same volume of 2xYT containing 500 µg/ml ampicillin and 1 mM IPTG. Cells were then further incubated for 3 hours at room temperature with 200 rpm shaking. Finally the culture was centrifuged (10 min, 5000 rpm, 4 $^{\circ}$C) and cells were either lysed or stored at –80 $^{\circ}$C.

C.2.1.2. Culture of insect cells

Spodoptera frugiperda (*Sf*) cells grow well both as monolayers attached to a surface or in suspension. For routine maintenance of the cells, as well as for transfection, virus amplification and analytic expression experiments, we used adherent cultures. Suspension cultures were set for preparative expression of recombinant proteins.

Growth media

Adherent cells were cultured in TNM-FH medium (Pharmingen Ltd.). This medium is a fully supplemented Grace's medium including trace metals, lactalbumin hydrolysate, yeastolate, 10 % heat inactivated FBS, and gentamycin (50 µg/ml). Suspension cultures were fed with a mixture of 50 % TNM-FH medium and 50 % SF-900 II medium. SF-900 II (Gibco BRL) is a patent protected variation of the classic serum free Grace's medium. Medium for suspension cultures was additionally supplemented with 0.1 % Pluronic F-68.

Freezing of insect cells

Sf21 cells in log phase were detached from an almost confluent 15 cm plate ($\sim$2.9 x 10^7 cells). After centrifugation for 10 min at 1000 g, the pellet was resuspended in 1.5 ml of freezing medium (90 % TNM-FH, 10 % DMSO) and transferred to cryovial. Cells were then placed for 1 hour at -20 ^{o}C; overnight at -80 ^{o}C and finally in a liquid nitrogen tank.

Thawing of insect cells

Cryovials containing frozen cells were quickly thawed in a water bath at 37 ^{o}C. The cell suspension was then transferred to a 15 cm culture dish containing 30 ml of prewarmed (27 ^{o}C) TNM-FH medium. After 30-45 min, medium containing non viable cells was removed and replaced with fresh medium.

Counting of cells

Inscect cells are similar in size to leucocytes. That is why the cell density in adherent and suspension cultures can be determined using standard clinical diagnostic methods. Normally a special urine diagnostic object slide purchased from Madaus AG was filled up with some drops of a 1/40 dilution from either the resuspended cells or the suspension culture. The slide was observed under a Leitz, Periplan phase contrast microscope using a 10X ocular and a 40X objective and the number of living cells in fourty 0.3 mm x 0.3 mm small squares was determined. This number was finally corrected in a conversion table provided by the object slide manufacturer to a cell density as follows:

(X cells/40 squares) x 5 = cell number in 5 squares = Y cells/µl in the conversion table

Y cells/µl x 40 (dilution factor) x suspension volumen (in µl) = number of cells

Handling and maintenance of adherent cultures

Adherent cells were cultured in 15 cm dishes with TNM-FH medium. After reaching confluency (~ 48 hours) they were subcultured at a dilution of 1:3. To detach cells, medium was removed and plates were tapped until cells started to roll down the culture dish. At this point, fresh medium was added and cells were pipeted up and down at least three times. Resuspended cells were then transferred either to other plates or to a suspension culture flask.

Handling and maintenance of suspension cultures

Suspension cultures were set in 150 ml and 500 ml Nalgene filter flasks. To start a suspension culture, at least five confluent 15 cm plates were detached, centrifuged 10 min at 1000 g in 50 ml Falcon tubes and resuspended in 50 ml medium. Cells were then transferred to a 150 ml flask and placed in a shaking incubator (27 $^{\circ}$C, 120 rpm). Good aeration of the culture was assured by loosening the bottle cap. Every 48 hours cells were counted and subcultured when required (concentration $\geq 2.0 \times 10^6$ cells/ml). In this case, cells were centrifuged and resuspended in a new volume of medium to a concentration between 1.0-1.5 x 10^6 cells/ml.

Generation of recombinant baculoviruses by cotransfection

In order to create recombinant baculoviruses coding for the proteins of our interest, the recombinant transfer plasmids bearing the gene to be expressed and the BaculoGold™ linearized viral DNA (Pharmingen Ltd.) were introduced simultaneously into *Sf21* insect cells. For these purposes a liposome-mediated transfection reagent (Cellfectin™, Gibco BRL) was used due to its high efficiency and reproducibility.

For one transfection, 2 x 10^6 cells were seeded on a 60 mm cell culture dish and allowed to fully attach to the bottom of it forming a monolayer for 15 min at least. Once the cells attached to the culture dish, medium was removed and replaced with 2 ml fresh serum free medium. In the meantime the following transfection mixture was set up:

- 3 µg of recombinant transfer plasmid
- 0.5 µg of BaculoGold™ DNA
- 1 ml SF 900 II Insect Medium (Gibco BRL) (serum free medium)
- 20 µl Cellfectin™ liposomes

The vial containing the mixture was briefly flicked and incubated for 15 min at RT. After this step, medium was removed again from the dishes and the transfection mix was added dropwise to the cells. In order to avoid drying, 1 ml of serum free medium was additionally added and culture dishes were wrapped in Parafilm. The dishes were then incubated 4 hours at RT on a slow speed rocking platform. Following the incubation period, 2 ml of complete TNM-FH medium were added to each dish and cells were incubated for at least 5 days in a 27 °C incubator. Normally after 5 days we were able to see the typical signs of viral infection (Luckow and Summers, 1989). On the 7th day, medium was spun down (1000 rpm, 10 min) and recombinant baculoviruses were harvested by sterile filtration of the supernatants. The resultant virus stock stored at 4 °C and used for subsequent identification and amplification of the recombinant baculoviruses.

Identification of recombinant baculoviruses via PCR

The success of the cotransfection experiment was always confirmed by the PCR method reported by Malitscheck and Schartl (1991). Viral DNA was isolated from the culture supernatant using a kit purchased from Talent Ltd, and following the instructions provided by the manufacturer . After an initial step in which virus DNA was extracted with thioisocyanate, DNA was purified from the medium by specific binding to a ion exchange resin. Finally the bound DNA was eluted with H_2O at 70 ^oC. After determining the DNA concentration (C.2.2.6) a PCR reaction was set up as follows:

- X µl (100 ng) template viral DNA
- 5 µl (100 pmol) Polyhedrin Forward Primer (C.1.2)
- 5 µl (100 pmol) Polyhedrin Reverse Primer (C.1.2)
- 1µl (1.25 mM final concentration of each) 100x dNTPs
- 0.5 µl (2.5 Units) Taq Polymerase
- X µl H_2O up to 100 µl

As positive and negative controls, the transfer vector bearing the 80K gene and the empty vector were used as templates. In some experiments, wild type virus or a control virus stock coding for the Xyl E protein (Pharmingen) served as additional controls. The amplification of the DNA was performed using the following cycling parameters:

Step	No. of cycles	Time	Temperature
1	1	5 min	94 ^oC
2	30	1 min	94 ^oC
		1 min	55 ^oC
		1 min*	72 ^oC
3	1	2 min	72 ^oC
4	1	∞	4 ^oC

*For DNA fragments larger than 2000 base pairs this step was prolonged to 2 min.

The resulting PCR products were finally analyzed by agarose gel electrophoresis (C.2.2.3).

Virus amplification

For protein expression in preparative scale, large virus stocks were prepared from the initial virus supernatant in 4 amplification rounds. The normal procedure consisted on seeding 2×10^7 cells on a 150 mm culture dish and infecting them with a multiplicity of infection (defined as the number of viral particles per insect cell) ≤ 1. After 5-6 days, virus was harvested from the medium supernatant and used for the next amplification round. Care was taken not to use MOIs larger than 1, in order to ensure passaging of a clonal virus population and prevent the appearance of deletions and/or mutations in the virus DNA.

Titration of recombinant virus by plaque assay

The concentration of infectious virus particles in a virus stock (titer) was estimated by means of a plaque assay. In this assay, cell monolayers are infected with a low ratio of virus, such that only isolated cells become infected. An overlay of agarose keeps the cells stable and limits the spread of virus. When each infected cell produces virus and eventually lyses, only the immediate neighboring cells become infected. Each group of infected cells is referred to a plaque. After several infection cycles, the infected cells in the center of the plaques begin to lyse, and the light passing through the plaques refracts differently from the light passing through healthy cells. In this way, plaques can be identified either by naked eye-examination of the culture dish or by observation under the microscope. Staining of plates with neutral red would also identify plaques as a clear spot in the red-stained uninfected cells. First, healthy insect cells were seeded on a 10 cm plate, at a concentration of 7×10^6 cells/plate. After allowing cells to attach firmly to the plate (10 min at least), medium was replaced with fresh TNM-FH. Immediately thereafter, 100 µl virus inoculum was added to the plate. Normally we prepared 3 different dilutions of the viral stock: 10^{-3}, 10^{-4} and 10^{-5}. Plates were gently rocked to distribute virus over the whole surface and incubated for 1 hour at 27 ^{o}C to permit viral infection of the cells. During this incubation, 0.8-1.0 % agarose was prepared by diluting Agarplaque Plus^{TM} agarose in a half volume of serum free medium (2 % agarose), heating it in a microwave oven and adding the second half of TNF-FH medium once the temperature of the melted agarose reached 45 ^{o}C. Following the incubation, cells were overlaid with the agarose solution and incubated for 10 days at 27 ^{o}C. The plates were then stained with 0.03 % neutral red and further incubated for 24 hours. To count the plaques, plates were inverted on a

dark background and illuminated with a strong light source from the side. Virus titer was calculated as follows:

Titer (pfu/ml) = (No. of plaques / 0.1 ml) x dilution factor

Storage of virus particles

Supernatants containing baculovirus particles were stored at 4 ^{o}C for periods up to 6 months and frozen at –80 ^{o}C for longer periods of time.

Infection of cells and expression of heterologous proteins

To produce heterologous proteins in insect cells, suspension cultures were grown until they reached a cell number $\geq$ 1.0 x 10^{8} in 100-150 ml cultures. After replacing the medium and adjusting the cell density to ~ 1.0 x 10^{6} cells/ml, suspension cultures were infected with recombinant baculoviruses at a multiplicity of infection (MOI) of 1. In the case of heterodimeric µ-calpain variants, each of both recombinant viruses coding for the large and the small subunit were added with a MOI of 1. Cultures were then returned to the incubator and incubated (27 ^{o}C) with shaking (120 rpm) for 72 hours. Finally, the cells were pelleted (1000 g, 10 min) and lysed. Analytical expressions were performed in 70 % confluent multi-well plates or 15 cm culture dishes following the same principle.

C.2.1.3. Culture of mammalian cells

Growth media

For routine culture of *LCLC 103H* cells, RPMI 1640 medium was supplemented with 10 % heat inactivated-fetal calf serum; L-Glutamine and antibiotics. A 500 ml growth medium bottle was prepared as follows:

440 ml RPMI 1640 Medium
50 ml FCS

5 ml Glutamine

5 ml Penicillin-Streptomycin

Selection media

Selection of EYFP-μ-calpain positive cell lines was achieved by supplementing the growth medium with 800 μg/ml Geneticin (G-418).

Maintenance media

Stable clones were maintained in growth medium containing 100 μg/ml Geneticin (G-418).

Freezing media

One volume of freezing medium was composed of 50 % RPMI 1640 medium, 30 % of FCS and 20 % of DMSO.

Additional solutions

PBS

Phosphate buffer saline was prepared in sterile water from a 10x concentrated solution purchased from Gibco-BRL. The composition of the 1x solution was as follows:

13.7 mM NaCl

2.7 mM KCl

80.9 mM Na_2HPO_4

1.5 mM KH_2PO_4, pH 7.4 (HCl)

Trypsin-EDTA

1x trypsin-EDTA solution was prepared in PBS from a 10x concentrated solution purchased from Gibco-BRL

Trypan blue

Trypan blue was prepared 0.2 % in PBS.

Thawing of mammalian cells

Freezing vials were taken from the liquid nitrogen tank and transported in dry ice to the cell culture room. Immediately thereafter they were constantly agitated in a water bath previously set at 37 ^{o}C, rinsed with 70 % ethanol and placed into the sterile bench. Cells were dispensed in a Falcon tube containing 10 ml pre-warmed growth medium and centrifuged for 10' at 200 g. Pelleted cells were resuspendend in fresh medium and plated in a T25 ml tissue culture flask. Medium was changed once after 12 to 24 hours.

Handling and maintenance of mammalian cells

Under the following conditions, *LCLC 103H* cells grow well as adherent monolayers, with a doubling time between 18 and 24 hours:

Temperature: 37 ^{o}C
Concentration of CO_2: 5 %
Humidity: 90 %
The cells were subcultured twice a week, at a dilution of 1:3.

Trypsination

In order to split or freeze the cells, medium was removed from the dish or flask and cells were washed twice with pre-warmed PBS. Subsequently, a volume of 37 ^{o}C trypsin-EDTA enough to cover the growth surface was added, and cells were placed for ~5' in the incubator (37 ^{o}C, 5 % CO_2, 90 % humidity). After incubation, the flasks or dishes were tapped laterally and the cells were resuspended in the desired volume of pre-warmed growth medium.

Counting of cells

The cell number was determined by mixing an aliquot of resuspended cells with trypan blue to an end concentration of 0.18 % of the stain. Dilution of the cells was optimized to achieve a concentration of 10-50 cells/square in a Neubauer hemocytometer (0.1 µl). After covering the chamber with a damped coverslip and checking for the appearance of Newton rings, 10 µl of the mix were applied and the hemocytometer was placed under the microscope. After focusing, only non-stained cells were counted in each square. The total number of cells was calculated as follows:

# of cells/ml of cell suspension = Total # of cells/# of squares x 10^4 x dilution factor

Freezing of cells

Cells from a healthy log-phase culture were centrifuged for 5' at 200 g. The cell pellet was resuspended in freezing medium by pipeting the suspension up and down at a concentration of at least 2 x 10^6 cells/ml. 1.8 ml aliquots were dispensed into freezing vials and placed overnight at –70 $^{\circ}$C in an isopropanol bath purchased from Nunc. The next day, frozen cells were transferred to a cryo-box and placed in the liquid nitrogen tank.

Transfection of mammalian cells

Preparation of cells for transfection

The day prior to transfection, cells that had been regularly passaged were plated on a 6-well tissue culture plate at a concentration of 1-3 x 10^5 cells/ml. After incubation overnight the cells were at 50-80 % confluency and transfection was performed.

Transfection of *LCLC 103H* with FuGENE 6™

Before transfection, growth medium was changed and reagent mix was prepared as follows:

For one 35 mm well

2 µg Plasmid DNA

5 µl FuGENE 6™

x µl Serum free medium up to 100 µl

The mix was prepared as recommended by the reagent's manufacturer: First, medium was added to a sterile Eppendorf tube and then FuGENE 6™ was pippeted directly into the medium. This mixture was pre-incubated for at least 15' at RT and then was transferred to a second tube containing the plasmid DNA. The reagent mix was then added dropwise to the cells in a circular manner to allow even distribution. The wells were swirled and then returned to the incubator. After 24 hours the expression of recombinant proteins could be monitored by observation at the fluorescence microscope and western blot analysis.

Establishment of stable cell lines

To create cell lines expressing EYFP-µ-calpain variants, transfected cells were transferred from the 35 mm well to a 15 cm culture dish one day after transfection. The next day, culture medium was supplemented with 800 µg/ml Geneticin (G-418) and cells were kept under antibiotic pressure for two weeks with one medium change after the first week. A control plate containing non transfected cells served as negative control. Normally 14 days selection were enough to kill all non resistant cells, including the negative control. In this time resistant cells formed clones which were easily identified by observation under the fluorescence microscope. The best 12 clones (selected by their size, isolation from other clones and fluorescence intensity) were picked and transferred to a 24-well culture plate. After reaching confluence they were transferred successively to a 6-well plate, a T25 flask and finally to a T75 flask. During this time, cells were always kept in medium containing 100 µg/ml G-418. Cells from a confluent T75 flask were frozen as described before.

C.2.1.4. Light and confocal microscopy

Insect cells were routinely observed under a Leitz Periplan phase contrast microscope. In the case of *LCLC 103H* cells, light and fluorescence microscopy were performed in an Olympus IX 50-S8F phase contrast microscope equipped with a fluorescent light source and a set of fluorescence filters suited for the observation of EGFP, EYFP and ECFP. Confocal images were acquired in the laboratory of PD Dr. Ralph Gräf (Adof Butenandt Institut für Zellbiologie, LMU, Munich) on an Axiovert 200M/510META laser scanning system

equipped with a 63×/1.4 lens. Images were taken at a frame rate of 2/s and a resolution of 512 × 256 pixels using the standard filter settings for EGFP, EYFP and ECFP provided by the manufacturer. Finally the pictures were processed with the LSM software from Carl Zeiss and transferred to Adobe Photoshop (Adobe Systems Inc.).

C.2.2. Molecular biology methods

The methods presented in this section were mostly performed as described by Sambrook (1989). Literature references will be given for methods taken from another source.

C.2.2.1. Plasmid preparation from *E. coli*

For analytical and preparative purposes, plasmid DNA was prepared using the DNA purification kits from QIAGEN, which are based on a modified alkaline lysis procedure (Birnboim and Doly, 1979). Briefly described, the bacterial cells are pelleted, resuspended in a buffer containing RNAse A and lysed with a basic solution. After neutralization, the chromosomal DNA is discarded by filtration (Midi and Maxi) or centrifugation (Mini) and the soluble plasmid DNA is selectively bound to an anion exchange or to a hydrophobic resin, which is washed twice in order to eliminate contaminant proteins, RNA and low molecular weight impurities. Elution from the columns is achieved by addition of high salt concentration buffer in the case of the anion exchange resin or just by addition of water in the case of the hydrophobic resin. The Midi and Maxi kits precipitate the plasmid DNA by the addition of 3.5 volumes of isopropanol. After washing with 70 % ethanol and drying the pellet, the plasmid DNA is resuspended in sterile water or EB buffer (10 mM Tris/HCl, pH 8.5). The following table describes the kits used for different applications.

Table 1. Overview of the DNA purification kits used in this work

Scale	Purpose	Kit	Principle	Vol. of culture∗	Yield (µg DNA)
Analytical	• Screening of recombinant DNA by restriction endonuclease analysis • DNA sequencing	QIAprep Spin Miniprep Kit	hydrophobic interactions	5 ml	5-10
Preparative	• Digestion of vectors and insert DNA with restricton endonucleases for subsequent ligation • DNA sequencing	QIAfilter Midiprep (QIAGEN-tip 100)	Anion exchange	25 ml	50-100
Preparative	• Transfection of insect and mammalian cells	QIAfilter Maxiprep (QIAGEN-tip 500)	Anion exchange	100 ml	250-500

∗ Volume of culture for high copy plasmids.

C.2.2.2. DNA cleavage with restriction endonucleases

Digestion of DNA with specific endonucleases was performed in order to linearize plasmids and/or liberate fragments of defined sizes. The final aim was either to screen for recombinant plasmids or to subclone specific DNA sequences. The resulting fragments were analyzed by agarose gel electrophoresis (C.2.2.3) and purified from the gel if required (C.2.2.4). Reaction buffers and additives were always provided with the enzymes. For each single or double restriction enzyme digests, optimal buffer conditions were chosen according to manufacturer's information. For analytical purposes 1-2 µg of DNA were digested at 37 ^{o}C for about 2 h and for preparative purposes 5-10 µg of plasmid DNA were digested for 4-16 h.

C.2.2.3. Agarose gel electrophoresis

The homogeneity and the correct size of the plasmid DNA and DNA fragments were analyzed by submerged horizontal gel electrophoresis in 1-2 % agarose gels (Sealey PG, 1982). For preparation of the gels TAE buffer (40 mM Tris, 20 mM acetate; 2 mM EDTA, pH 8.3) was added to the corresponding amount of agarose and solubilization performed by

heating 3 min at 600 W in a microwave oven. Seakem® high melting temperature agarose was used for analytical purposes and Nusieve® low melting temperature agarose for preparative gels. Ethidium bromide was added to a final concentration of 1 μg/ml for visualization of the DNA under UV light. The running buffer was also TAE. Electrophoretic separation was achieved by constant currents at 5-7 V/cm for about 1-3 h. A marker mixture (30 % w/v glycerol, 0.25 % (w/v) bromophenol blue, 0.25 % xylencyanol FF and 0.25 % (w/v) orange G) was added to the samples (ratio 1:10) before loading the gel in order to control the separation during the run. The gels were observed on a UV transilluminator (302 nm) and the size of the fragments was determined by comparing their mobility with the DNA standards.

C.2.2.4. Extraction of DNA fragments from agarose gels

After separation of the DNA fragments by agarose gel electrophoresis, the band corresponding to the fragment of interest was cut off the gel with a sterile scalpel and the DNA was isolated using the QIAquick gel extraction kit of QIAGEN. Due to the low melting point of the agarose Nusieve®, solubilization of the gel slice containing the DNA fragment was achieved by addition of the buffer QX1 in the amounts indicated by the manufacturer and incubation with constant shaking at 50 ^{o}C for 10 min. The DNA fragment was selectively bound to a silica-gel resin in the presence of a high concentration of chaotropic salts (QX1). Salts were quantitatively washed out by the ethanol containing buffer PE. After removal of residual PE buffer, DNA was eluted under low salt concentrations and basic conditions (EB buffer).

C.2.2.5. DNA precipitation

Based on the fact that DNA precipitates in high percentage alcohol solutions in the presence of sodium acetate, ammonium sulphate or even sodium chloride, alcohol precipitation (Sambrook *et al.,* 1989) was used to desalt or to concentrate the DNA. 2.5 volumes of absolute ethanol or 1 volume of isopropanol were added to the DNA solution, previously mixed with 0.1 volumes of 3 M sodium acetate. The solution was vortexed and centrifuged at 15 000 g for 30 min. Excess of salts in the pellets was removed by washing with 2-3 volumes of 70 % ethanol (v/v). The pellets were resuspended in an appropriate volume of sterile water.

C.2.2.6. Determination of DNA concentration by UV spectroscopy

The concentration of DNA was determined spectroscopically by measuring the absorbance at 260 nm. To calculate the concentration, we used the absorption coefficient of 1 for 50 µg/ml solution of dsDNA (1 cm pathlenght) (Sambrook *et al.,* 1989). The purity of the preparation was estimated by recording an UV absorption spectrum in the range of 200-300 nm and the absorbance ratio A_{260nm}/A_{280nm} was calculated to detect the presence of contaminating proteins. A $A_{260\,nm}/A_{280\,nm}$ between 1.8 and 2.0 was the criteria for a pure DNA preparation.

C.2.2.7. DNA sequencing

Automated chain termination DNA sequencing using fluorescein labelled dideoxynucleotides (Sanger *et al.,* 1977; Ansorge *et al.,* 1988) was performed by Medigenomix (Martinsried, Germany). Sequencing PCRs were performed using the Red Terminator Dye kit of Applied Biosystems following the instructions of the manufacturer. After thermal cycling, DNA was alcohol-precipitated (C.2.2.5) and the products were sent to Medigenomix for subsequent analysis. The composition of a normal sequencing PCR reaction was as follows:

X µl (250-500 ng) plasmid DNA

X µl (2.5-20 pmol) sequencing oligonucleotide primer

4 µl PCR mix (contains *Taq* polymerase, reaction buffer and fluorescein-labeled dNTPs)

X µl sterile H_2O up to 10 µl

Thermal cycling was performed as indicated by the manufacturer.

C.2.2.8. Removal of the 5' –terminal phosphates of the linearized vector DNA

To reduce the religation rate of a linearized vector, its 5'-termini were dephosphorylated by calf intestine phosphatase (CIP) according to the recommendations of the manufacturer. 1 unit of CIP was added to 5-10 pmol of the linearized vector dissolved in the buffer supplied with the enzyme and incubated for 30 min at 37 ^{o}C in a water bath. Thereafter, the CIP was removed by phenol extraction and the dephosphorylated vector was obtained by ethanol precipitation.

C.2.2.9. Ligation of DNA fragments

For the ligation of sticky ends, a 5-100 molar excess of DNA fragment was added to 100 ng of linearized vector in a final volume of 10-20 µl (1-2 units) of T$_4$ DNA ligase as well as ligase buffer were added. For blunt end-ligation, the reaction was supplemented with 5 % PEG 6000. The reaction mixtures were usually incubated 1-16 h at 16 ^{o}C.

C.2.2.10. Transformation of *E. coli* strains

The transformation of *E. coli* strains was performed either by electroporation or by heat shock.

Transformation of E. coli strains by electroporation

Compentent cells for electroporation were prepared by inoculating 5 ml of sterile dYT medium (C.2.2.1) with a single colony of the desired strain. The culture was grown overnight at 37 ^{o}C, and the next day a larger culture was prepared by dilution (1:1000) and grown until OD$_{550 \ nm}$ ~0.8. The cells were then chilled and centrifuged at 4 ^{o}C and 5000 g for 10 min under sterile conditions. The cell pellet was washed twice with chilled sterile water and resuspended in the same volume of 10 % sterile glycerol. Finally 50 µl aliquots were stored at −80 ^{o}C for 3-4 months.

For electroporation, 0.5 ng of plasmid DNA or 1-3 µl of the ligation reaction

mixtures (C.2.2.9) were added to 50 µl competent cells on ice and transferred to the electroporation cuvettes. The electroporation pulse was performed at a voltage 2.5 kV, capacity 25 µF and resistance 200 Ω. Immediately thereafter, 0.5 ml of pre-warmed SOC medium (C.2.1.1) was added and the cells were incubated for 30 to 60 min at 37 ^{o}C with continuous shaking.

Transformation of E. coli strains by heat shock

Competent cells for heat shock transformation were prepared according to Hanahan (1983). Starting from a single colony an overnight culture in dYT was prepared. The next day, cells were diluted 1:100 and grown to a OD$_{550\ nm}$ ~0.3, chilled and centrifuged at 4 ^{o}C and 5000 g for 10 min under sterile conditions. The pelleted cells were resuspended in 1/3 of the initial volume of TFB1 buffer (30 mM potassium acetate, pH 5.8, 50 mM MnCl$_2$, 100 mM RbCl, 10 mM CaCl$_2$, 15 % (w/v) glycerol) and centrifuged again. Finally the pellet was carefully resuspended in 1/12 of the initial volume of TFB2 buffer (10 mM Na-MOPS, pH 6.8, 10 mM RbCl, 75 mM CaCl$_2$, 15 % (w/v) glycerol) and chilled for 15 min. 50 µl aliquots were stored at −80 ^{o}C for 3-4 months.

For heat shock transformation; 0.5 ng of plasmid DNA or 1-3 µl of the ligation reactions were added to the 50 µl competent cells on ice and incubated for 30 min in the presence of 25 mM 2-mercaptoethanol. After incubation, the vials containing the transformation mixtures were heat pulsed in a 42 ^{o}C water bath for 30 seconds and immediately placed for 2 min on ice. Subsequently 0.5 ml of pre-warmed NYZ+ medium (C.2.2.1) were added and the cells were incubated for 30 to 60 min at 37 ^{o}C with continuous shaking.

In both transformation methods, 20-500 µl of the incubation mixture were plated onto agar plates containing either ampicillin or kanamycin (200 µg/ml), and the plates were incubated at 37 ^{o}C overnight. The next day, single colonies were picked and grown analytically for plasmid preparation and restriction analysis to determine the clones containing recombinant plasmids. The transformation efficiency was always monitored by transforming the same amount of competent cells with 10 pg of pUC18 DNA. Efficiency was defined as the number of colony forming units per µg of plasmid and was normally between 10^7 and 10^9 cfu/µg pUC18.

C.2.2.11. Site directed mutagenesis of (C115A) µ-calpain 80K subunit

Specific mutations in µ-calpain were made using the QuickChange™ site directed mutagenesis kit from Stratagene. This protocol allows the generation of point mutations, switching of amino acids and deletions or insertions of single or multiple amino acids in virtually any double stranded plasmid. The method is performed using Pfu*Turbo*® DNA polymerase and a thermal temperature cycler. Pfu*Turbo* DNA polymerase replicates both plasmid strands with 6-fold higher fidelity than *Taq* DNA polymerase and without displacing the mutant oligonucleotide primers. The basic procedure utilizes a supercoiled double-stranded dsDNA vector with an insert of interest and two synthetic oligonucleotide primers containing the desired mutation. The oligonucleotide primers, each complementary to opposite strands of the vector are extended during temperature cycling by using Pfu*Turbo* DNA polymerase. Incorporation of the oligonucleotide primers generates a mutated plasmid containing staggered nicks. Following temperature cycling, the product is treated with *DpnI*. The *DpnI* endonuclease (target sequence: 5'-Gm^{6}ATC-3') is specific for methylated and hemimethylated DNA and is used to digest the parental DNA template and to select for mutation-containing synthesized DNA. DNA isolated from almost all strains is dam methylated and therefore susceptible to *DpnI* digestion. The nicked vector DNA incorporating the desired mutations is then transformed into XL1-Blue supercompetent cells. The small amount of starting DNA template required to perform this method, the high fidelity of the Pfu*Turbo* DNA polymerase, and the low number of thermal cycles all contribute to the high mutation efficiency and decreased potential for random mutations during the reaction.

Primer design

Mutagenic oligonucleotide primers (see C1) were designed according to the rules mentioned below:

1. Both mutagenic primers must contain the desired mutation and anneal to the same sequence on opposite strands of the plasmid

2. Primers should be between 25 and 45 bases in length, and the melting temperature (Tm) of the primers should be greater than or equal to 78 °C. The following formula is commonly used for estimating the Tm of primers:

Tm = 81.5 + 0.41(% GC) – 675/N - % mismatch

For calcultating Tm:

- N is the primer length in bases

- Values for % GC and % mismatch are whole numbers

Tm's of the primers designed to introduce insertions or deletions were calculated with the following modified version of the above formula:

Tm = 81.5 + 0.41(% GC) – 675/N,

where N does not include the bases which are being inserted or deleted.

3   The desired mutation (deletion or insertion) should be in the middle of the primer with ~10-15 bases of correct sequence on both sides.

4   The primers optimally should have a minimum GC content of 40 % and should terminate in one or more C or G bases

5   Primers need not be 5' phoshporylated but must be purified either by fast polynuclotide liquid chromatography (FPLC) or by polyacrylamide gel electrophoresis (PAGE). Failure to purify the primers results in a significant decrease in mutation efficiency.

6   It is important to keep primer concentration in excess. For optimization of the method, it is recommended to vary the amount of template while keeping the concentration of the primer constantly in excess.

In addition to these considerations, the cloning and primer design software SE Central was used to analyze the quality of the primers. Both synthesis and PAGE purification of oligonucleotide primers were performed by Roth.

Mutagenesis PCR

For the mutagenesis PCR the baculovirus transfer vector pVL-1392 containing the cysteine 115 to alanine mutated semisynthetic gene of human μ-calpain large subunit (80K) was used as a plasmid template. This construct was created by Dietmar Pfeiler in his PhD work and had been already employed with success to generate recombinant virus coding the 80K polypeptide. In a thin wall PCR tube the following reagents were pipeted:

5 μl of 10x reaction buffer

1 μl of dsDNA template (pVL-1392-80K 10 ng/μl)

X μl (125 ng) of oligonucleotide primer #1 (forward)

X µl (125 ng) of oligonucleotide primer #2 (reverse)

1 µl of dNTP mix

Double-distilled water (ddH$_2$O) to a final volume of 50 µl

A control reaction was set as indicated in the kit:

5 µl of 10x reaction buffer

2 µl (10 ng) of pWhitescript 4.5-kb control plasmid (5 ng/µl)

1.25 µl (125 ng) of oligonucleotide control primer #1 [34-mer (100 ng/µl)]

1.25 µl (125 ng) of oligonucleotide control primer #2 [34-mer (100 ng/µl)]

1 µl of dNTP mix

ddH$_2$O to a final volume of 50 µl

The pWhitescript 4.5-kb control plasmid contains a stop codon (TAA) at the position where a glutamine codon (CAA) would normally appear in the ß-galactosidase gene of the pBluescript® II SK(-) phagemid (corresponding to amino acid 9 of the protein). XL1-Blue supercompetent cells appear white on LB-ampicillin agar plates containing IPTG and X-gal, because ß-galactosidase activity has been obliterated. The oligonucleotide control primers create a point mutation that reverts the T residue of the stop codon (TAA) in the ß-galactosidase gene encoded on the pWhitescript 4.5-kb control template to the C residue to produce a glutamine codon (Gln, <u>C</u>AA). Following transformation, colonies can be screened for the ß-galactosidase (ß-gal$^+$) (blue) phenotype.

Temperature cycling

The cycling parameters recommended by the manufacturer of the kit were applied to our particular case. The PCR program used is described below:

Segment	Cycles	Temperature	Time
1	1	95 °C	30 seconds
2	16	95 °C	30 seconds
		55 °C	1 minute
		68 °C	24 minutes

After temperature cycling, 1 µl (10 units) of *DpnI* was added to each PCR reaction vial. The mix was then incubated at 37 °C for 1 h in order to digest methylated DNA. Finally 2 µl of each reaction were used to transform competent *E. coli* as described in C.2.2.10

C.2.2.12. Construction of active µ-calpain 80K domain III acidic loop mutants

In order to generate active µ-calpain acidic loop mutants, the C115A mutation introduced by D. Pfeiler in the semisynthetic µ-calpain 80K gene by means of cassette mutagenesis was reverted using a cassette exchange. Synthetic cassettes 1 and 2 (coding for domains I and II) from the inactive mutants in pVL-1392 were removed via *EcoRI*/*XbaI* restriction (C.2.2.2) and separated by means of agarose gel electrophoresis (C.2.2.3). Simultaneously, the same procedure was applied to the active semi-synthetic µ-calpain 80K gene cloned in pUC-18. The remaining vectors containing the acidic loop mutated domain III and domain IV in one hand and the synthetic gene fragment coding for active domains I and II in the other hand were purified from the agarose gel (C.2.2.4) and ligated (C.2.2.9). The resulting constructs (pVL-1392-active 80K) were sequenced in order to confirm the replacement Ala $\rightarrow$ Cys at position 115.

C.2.2.13. Construction of the transfer vector for expression of the N-terminal truncated calpain small subunit (21K) in insect cells

For expression of a domain V deletion mutant in insect cells using the baculovirus expression system, the 21K subunit was subcloned from the *E. coli* expression vector pET-22b(+) (C.1.2) into pVL 1392. Restriction sites *BamHI* and *XbaI* were available in the multiple cloning site (MCS) of both vectors. First, preparative digestions (C.2.2.2) of pET-22b(+)-21K and pVL1392 were performed using the aforementioned endonucleases. Afterwards both insert and linearized vector were isolated and purified (C.2.2.3 and C.2.2.4). The DNA fragments were then ligated (C.2.2.9), and *E. coli* was transformed with the ligation products. The recombinant plasmids were analyzed by digestion with *BamHI*/*XbaI* and by sequencing of the 5' and 3' ends of the inserted gene with the polyhedrin forward and reverse oligonucleotide primers (C.1.2).

C.2.2.14. Construction of the vectors for the expression of µ-calpain 80K domain III mutants as EYFP fusion proteins in mammalian cells

For the intracellular localization studies of the µ-calpain 80K domain III mutants, a N-terminal fusion protein with EYFP (enhanced yellow fluorescent protein) was created by subcloning these mutants into the vector pEYFP-C1. Restriction sites *EcoRI* and *BamHI* were available in the MCS of both vectors, but the subcloning altered the reading frame of the fusion protein and introduced a stop codon downstream from the starting ATG of µ-calpain 80K gene. In order to eliminate the shift, plasmids were digested with *HindIII* in a unique site upstream of the *EcoRI* site. The generated sticky ends were subsequently polished by incubation with *Pfu* Polymerase and dNTPs for 15 min at 72 ^{o}C. The reaction products were blunt ligated as described (C.2.2.9) and the ligation reactions were used to transform competent *E. coli* cells. The described procedure not only corrected the frame shift, but also substituted the *HindIII* restriction site by a *NheI* one. This feature allowed fast screening for the positive recombinant plasmids by means of (*NheI*) restriction analysis (C.2.2.2).

C.2.3. Protein chemical and biochemical methods

C.2.3.1. Separation methods

C.2.3.1.1. Extraction of soluble proteins from *E. coli* cells

E. coli cell extracts were prepared using the BugBuster™ Protein Extraction Reagent from Novagen in combination with the endonuclease Benzonase. The BugBuster reagent is a detergent-based buffer able to disrupt cells in a non-mechanical fashion. Benzonase is a genetically engineered endonuclease from *Serratia marcescens* (Eaves and Jeffries, 1963; Nestle and Roberts, 1969) which promiscuously attacks and effectively degrades all forms of DNA and RNA over a wide range of operating conditions (Benzonase Brochure (1999), Code No. W 220911, Merck KGaA, Darmstadt, Germany). The enzyme prefers GC-rich regions in dsDNA while avoiding d(A)/d(T)-tracts. Cell lysis was performed as recommended by the manufacturer. Briefly, cell pellets (C.2.2.1) were weighted and 5 ml of BugBuster were added per gram of cell paste. The pellets were then resuspended by vortexing or pipeting and 10 µl 100 fold concentrated protease inhibitor cocktail (100 mM AEBSF, 80 µM Aprotinin from

bovine lung, 5 mM Bestatin, 1.5 mM E-64, 2 mM Leupeptin and 1 mM Pepstatin A) were added per ml suspension. At this point 1 µl (25 units) of Benzonase were added per 1 ml of BugBuster reagent and the cell suspension was incubated for 20 min on a rotating mixer at slow setting. This step allowed lysis of the cells and eliminated the viscosity of the lysates. Finally, the insoluble cell debris were removed by centrifugation at 16 000 g for 20 min at 4 ^{o}C. The supernatant was transferred to a fresh tube and either immediately loaded onto the affinity column or stored at –20 ^{o}C.

C.2.3.1.2. Extraction of soluble proteins from insect cells

Soluble proteins from the cytosol of *Sf21* insect cells were extracted in a lysis buffer containing 50 mM Tris/HCl, pH 7.5, 100 mM NaCl, 5 mM ß-mercaptoethanol, 2.5 mM EGTA, 2 % glycerol and 1 % Triton X-100. Prior to lysis, additional 2 mM PMSF, 1 µM Pepstatin A, 1 mM Pefabloc and 30 µM E-64 in case of the C115A mutated variants were added to the buffer. To lyse the cells, cell pellet (C.2.1.2) was resuspended by pipeting in cold lysis buffer with inhibitors (20 ml buffer per 10^8 cells). The cell suspension was then transferred to a Potter homogenizer and lysed on ice with 10 or more strokes. The lysate was finally cleared by centrifugation at 13000 g, 30 min , 4 ^{o}C. The supernatant was transferred to a fresh tube, placed on ice and immediately loaded onto the affinity column. For analytic applications, the homogenates were alternatively stored at –80 ^{o}C.

C.2.3.1.3. Extraction of soluble proteins from mammalian cells

Cytoplasmic cell lysates of *LCLC 103H* were prepared in a hypotonic buffer containing 20 mM HEPES, pH 7.5, 10 mM KCl, 1.5 mM $MgCl_2$, 1 mM EGTA, 1 mM EDTA and fresh added inhibitor cocktail described in (C.2.3.1.1). After removing culture medium, cells were washed once with PBS and either trypsinyzed (C.2.1.3) or scrapped using a cell scrapper. Cells were then centrifuged (500 g, 10 min, 4 ^{o}C) and consecutively washed with RPMI 1640 medium and PBS. The pelleted cells were resuspended in ice cold buffer and sonicated in 3 cycles of 10 seconds each, using the lowest energy and with 30 second intervals. Disrupted cells were centrifuged (13000 g, 30 min, 4 ^{o}C) and supernatants were stored at –20 ^{o}C.

C.2.3.1.4. Affinity chromatography on Ni-NTA Sepharose

C-terminal His$_6$-tagged calpastatin BC peptide and truncated calpain small subunit (21K) were isolated on Ni-NTA Sepharose (Qiagen) columns. The two step procedure was the same for both proteins with only minor differences in the buffers selected. The composition of the buffers was:

Protein	Binding buffer	Elution buffer
calpastatin BC-peptide	50 mM Tris/HCl, pH 8.0 2 mM 2-mercaptoethanol 0.5 M NaCl 2 % glycerol 5 mM imidazol	25 mM Tris/HCl, pH 8.0 2 mM 2-mercaptoethanol 0.5 M NaCl 250 mM imidazol
calpain 21K subunit	20 mM Tris/HCl, pH 8.0 2 mM 2-mercaptoethanol 0.5 M NaCl 5 mM imidazol	20 mM Tris/HCl, pH 8.0 2 mM 2-mercaptoethanol 0.5 M NaCl 250 mM imidazol

First the columns were equilibrated with the binding buffer, and the cell lysates were loaded. The columns were then washed with 10 volumes of binding buffer and finally the bound proteins were eluted with 250 mM imidazol: Eluted proteins were collected in 0.5 ml fractions. The chromatography was performed at RT, normal pressure and a flow rate of 1 ml/min.

C.2.3.1.5. Immobilization of Calpastatin BC peptide on NHS-activated Sepharose

Calpastatin BC peptide was immobilized on NHS-activated Sepharose (Pharmacia) following the recommendations of the manufacturer. First, bacterially expressed BC peptide was isolated on a Ni-NTA column (C.2.3.1.4) and dialyzed (C.2.3.1.7) against the coupling buffer (0.2 mM NaHCO$_3$, pH 8.3, 0.5 M NaCl). The matrix (provided in 50 % ethanol) was dried on a suction filter and washed 10-15 times with 1 mM HCl before being resuspended in an equal volume of coupling buffer. At this point, the calpastatin BC peptide and the matrix were mixed at a ratio of 5 mg protein/ml of dry gel with constant agitation for 3 hours at RT. In the next step, the gel was washed twice with TBS (10 mM Tris/HCl, pH 7.4, 137 mM NaCl), resuspended in blocking buffer (0.5 M ethanolamine/HCl, pH 8.3, 0.5 M NaCl) and incubated for 2 hours with constant agitation at RT to saturate all free –NH$_2$ groups. This blocking step was followed by abundant washing with 0.1 M Na-Acetate, pH4.0, 0.5 M NaCl and finally with TBS. The matrix was preserved in 50 % ethanol at 4 °C.

C.2.3.1.6. Affinity chromatography on BC-calpastatin Sepharose

This method, first reported by Anagli *et al.,* (1996) is based on Ca^{2+}-dependent binding of heterodimeric µ- and m-calpains to their endogenous inhibitor calpastatin. Specific binding to the affinity matrix takes place in the presence of calcium and elution requires a Ca^{2+} chelating agent. Calpain variants were purified on separate columns following the same protocol. Prior to immobilization, the columns were equilibrated with 20 volumes of buffer 1 (see below) and 1 M $CaCl_2$ was added to the cell lysates (C.2.3.1.2) to a final concentration of 2 mM. Loading of (ice cold) lysates onto the columns was followed by washing with buffer 1 until a stable baseline was reached. Proteins were finally eluted with buffer 2 and collected in 0.5 ml fractions. All chromatographic steps were performed at RT, normal pressure and a flow rate of 1 ml/min. Peak fractions (normally 3-5 per run) were shortly spun down to eliminate calpain aggregates. The buffers used are listed below:

Buffer 1(binding):   50 mM Tris/HCl,pH7.5, 100 mM NaCl, 5 mM 2-mercaptoethanol, 2 % (w/v) glycerol, 0.015 % BRIJ-35, 2 mM $CaCl_2$

Buffer 2 (elution):   50 mM Tris/HCl,pH7.5 100 mM NaCl, 5 mM 2-mercaptoethanol, 2 % (w/v) glycerol, 0.015 % BRIJ 35, 2.5 mM EGTA

C.2.3.1.7. Dialysis

Desalting and buffer changing of protein solutions were achieved by dialyzing the sample in Slide a Lyzer dialysis cassettes (Pierce). Depending on the volumes to be dialyzed, 0.5-3.0 ml or 3.0-15.0 ml cassettes with 10 kDa exclusion limit were used. Dialysis were always performed in two rounds of at least 2 hours each, in 0.5-2.0 liter of buffer per round.

C.2.3.2. Identification and quantification methods

C.2.3.2.1. UV absorption spectra

In order to estimate the quality and quantity of purified proteins, UV spectra of them were recorded in the range of 250 nm-350 nm. The molar extinction coefficient of each

protein -calculated by the method of Pace (1995)- and the absorbance at 280 nm (OD_{280nm}) were used to calculate the protein concentration.

C.2.3.2.2. BCA method for determination of protein concentration

The concentration of heterogeneous protein solutions was estimated using the bicinchoninic acid method (BCA). This procedure –introduced by Smith (1985)- improves the Biuret reaction (reduction of Cu^{2+} to Cu^+ by peptidic bonds of proteins) by chelating the Cu^+ ions with the BCA reagent. The complex formed is stable, water soluble and has an absorbance maximum at 562 nm. A kit containing reagents and bovine serum albumin standards was purchased from Pierce and a microplate assay was performed following the instructions of the manufacturer.

C.2.3.2.3. Electrophoresis of proteins on SDS-polyacrylamide gels (SDS-PAGE)

Electrophoretical separation of proteins was achieved with the discontinuous method of Laemmli (1970). It consists of two gel layers of different composition. The upper stacking gel is a low percentage polyacrylamide (PAG) with pH 6.8 where the proteins are concentrated and the lower separation gel is cast at a higher percentage of polyacrylamide with pH 8.8, where the proteins are separated. The polyacrylamide content in the separation gel can be distributed homogeneously or in gradients. Adding SDS to both gels ensures that all proteins are denatured and negatively charged, so that the separation only depends on their molecular mass. The buffers used are listed below:

Running buffer: 25 mM Tris, 192 mM glycine, 0.1 % (w/v) SDS
Sample buffer (4X):   250 mM Tris/HCl, pH 6.8, 4 % (w/v) SDS, 20 % (w/v) glycerol,
                      1/1000 (v/v) saturated bromophenol blue solution, 10 % (w/v) DTT

Depending on the size of the analyzed proteins 7 % and 12.5 % PAG homogeneous separation gels were used, while the stacking gels were always cast at 3 % PAG. Before loading onto the gel, the samples were mixed with sample buffer in a 4:1 ratio and heated for 5 min at 90 ^{o}C. The electrophoresis was performed at a constant power of 150 V during 70 min. The proteins were visualized by staining for 30 min with Coomassie blue (Schägger and von Jagow, 1987) and destaining with 10 % (v/v) acetic acid.

C.2.3.2.4. Casein zymography

This method, described by Raser (1995) served to evaluate qualitatively the activity of μ-calpain variants. As in the Laemmli procedure, two gel layers were cast: a 3 % PAG stacking gel with pH 6.8 and a 10 % PAG separation gel with pH 8.8. Contrarily to SDS-PAGE, zymography gels and buffers were devoid of detergent (native gels), in order to preserve enzyme structure and function. In addition, casein 0.2 % (w/v) was used as embedded substrate in the separation gel. In this case, the samples were not heated before loading, and electrophoresis were run at constant 125 V during 3 hours on an ice bad. After separation, gels were washed 2 x 30 min in calcium containing activation buffer and incubated overnight in the same buffer in order to ensure casein degradation by μ-calpain. The next day, gels were fixed with 30 % (v/v) ethanol, 10 % (v/v) acetic acid, stained with Coomassie blue and destained with 10 % (v/v) acetic acid. The buffers used are listed below:

Running buffer.   25 mM Tris, pH 8.3 192 mM glycine, 1 mM EGTA, 1 mM DTT

Sample buffer: 150 mM Tris/HCl, pH 6.8, 20 % (w/v) glycerol, 0.004 % bromophenol
                       blue solution, 2 mM ß-ME

Activation buffer: 20 mM, Tris/HCl, pH 7.5, 10 mM DTT, 10 mM $CaCl_2$

C.2.3.2.5. Transfer of proteins from gels to nitrocellulose membranes

For immunological detection with specific antibodies, proteins were transferred onto a nitrocellulose membrane after electrophoretic separation. This was performed using the semi-dry electrotransfer procedure described by Gershoni and Palade (1983). First, one nitrocellulose membrane and 20 Whatman No. 1 filters were cut to the size of the gel to be blotted and soaked in transblot buffer (50 mM Tris, 40 mM glycine, 0.13 mM SDS, 20 % (v/v) methanol). After separation, the gel was shortly incubated in the same buffer and the following transfer sandwich was set:

Anode (+)

10 Whatman filters

Nitrocellulose membrane

SDS-polyacrylamide gel

10 Whatman filters

Cathode (-)

After excluding gas bubbles from the sandwich, proteins were blotted during 2 hours at a constant current of 70 mA/gel. In the final step, the free binding sites of the nitrocellulose were blocked by 9 x 20 min incubation with NET-gelatin buffer (0.25 % (w/v) gelatin in NET buffer (see below)).

C.2.3.2.6. Transfer of proteins from gels to PVDF membranes

Proteins to be N-terminally sequenced were transferred to a PVDF membrane using the same semi-dry blotting apparatus but different transfer buffers. In this case, the first 10 Whatman filters were incubated in an anode buffer (50 mM $NaHBO_3$, pH 9.0, 20 % (v/v) ethanol) and the second stack of filters was incubated in a cathode buffer (50 mM $NaHBO_3$, pH 9.0, 5 % (v/v) ethanol). The PVDF membrane was incubated in methanol. The protein transfer was achieved in 2 hours at 70 mA/gel. Blotted proteins were visualized with Coomassie staining.

C.2.3.2.7. Immunoprinting of blotted proteins

Gelatin blocked nitrocellulose membranes were incubated at 4 ^{o}C overnight with the primary antibody (table 5). The next day, membranes were washed 3 x 20 min with NET buffer (50 mM Tris/HCl, pH 7.5, 150 mM NaCl, 5 mM EDTA, 0.05 % (v/v) Triton X-100) and incubated for 2 hours at RT with the secondary antibody (Table 2).

After this step, membranes were washed again (3 x 20 min with NET buffer) and prepared for signal development with a luminescence based procedure. Incubation with the developing reagents and exposure on the autoradiography films were performed as recommended by the kit manufacturer (Pierce). Exposed films were finally developed in a photography dark room using chemicals and procedures from Kodak.

C.2.3.2.8. N-terminal sequence analysis

This technique was used to determine the purity of the isolated recombinant proteins and to characterize cleavage sites in limited proteolysis experiments. For this purpose the protein sample was immobilized onto a PVDF membrane and subjected to Edman degradation (Edman P, 1967) coupled to RP-HPLC in an automated procedure described by Hewick (1981). This work was performed on a gas phase Sequenator 473 from Applied Biosystems

Table 2. Overview of the antibodies used in this work

Primary antibodies	Origin	Availability	Working Dilution[*]
Anti μ-calpain 80K	Mouse, monoclonal	Alexis, #804-051-R100	1:500
Anti-Calpain Small Subunit	Mouse, monoclonal	Chemicon, #MAB 3083	1:1000
Anti-μ-calpain heterodimer	Rabbit, polyclonal	Dr. D. Grabijelcic-Geiger, LMU München	1:200
Anti-GFP	Rabbit, polyclonal	PD Dr. J Faix, LMU München	1:2000
Secondary antibodies	Origin	Availability	Working Dilution[*]
Anti-mouse Ig G, HRP-linked	Goat, polyclonal	Cell Signaling Technology, #7076	1:10000
Anti-rabbit Ig G, HRP-linked	Goat, polyclonal	Cell Signaling Technology, #7074	1:10000

*Antibodies were diluted in NET-Gelatin buffer

by Reinhard Mentele at the Max-Planck-Institute for Biochemistry.

C.2.3.3. Kinetic assays and molecular interaction analysis

C.2.3.3.1. Preparation of lipid vesicles

Liposomes were prepared following the instructions provided by Avanti Polar Lipids (www.avantilipids.com). In other cases, specific references will be given.

Preparation of large multilamellar vesicles (LMV's)

To prepare LMV's, lipids provided as a powder were resuspended in chloroform at a concentration of 1 g/l. The resulting organic solution was aliquoted in glass vials and the organic solvent was evaporated using a dry nitrogen stream. The lipid film produced by evaporating the chloroform was then hydrated in the same volume of an aqueous buffer CB1 (see Table 3). In some experiments, this CB2 (Table 3) was used as hydration buffer. After

this step, the resuspended lipids were vortexed vigorously for 30-60 min until a cloudy emulsion was formed.

Table 3. Buffers used for kinetic assays and molecular interaction analysis of μ-calpain

Buffer name	Composition
Calpain buffer 1 (CB1)	50 mM Tris/HCl, pH 7.5, 0.1 mM EGTA and 5 mM ß-ME
Calpain buffer 2 (CB2)	CB1 + 200 mM NaCl
Calpain buffer 3 (CB3)	10 mM Tris/HCl, pH 7.5 and 150 mM NaCl
Calpain buffer 4 (CB4)	50 mM Tris/HCl, pH 7.5 and 100 mM NaCl

Preparation of small unilamellar vesicles (SUV's)

Prior to preparation of SUV's, lipids in solid state (powder) were resuspended with chloroform to yield a concentration of 20 mM. Aliquots of these stock solutions were stored at –20 $^{\circ}$C until final use. To prepare SUV's of different lipid compositions, various 20 mM lipid stocks were mixed at proper ratios and diluted with chloroform to a final concentration of 10 mM total lipid. These mixtures were distributed in 0.2 ml aliquots into glass vials. At this point, the chloroform was evaporated using a dry nitrogen stream and the lipids were further desiccated for 1 hour on Na-Al silicate beads using a vacuum pump. The resulting lipid film was then resuspended by vortexing in the same volume of buffer CB3 (Table 3) and the hydrated LMV's formed were downsized to SUV's by extrusion. For this purpose, the liposome emulsion was loaded on one of the two syringes of a LiposoFast™ mini-extruder equipped with a 50 nm filter and passed back and forth about 20 times. SUV's of equal size were collected from the second syringe and stored at 4 $^{\circ}$C.

Preparation of dansyl-labeled SUV's

Preparation of dansyl-DHPE labeled liposomes was carried out as reported by Nalefsky (2002). First, a 10 mM chloroform solution of dansyl-DHPE was prepared and added at a concentration of 5 % (mol/mol) to the different lipid mixtures. Finally, the SUV's wereprepared as described above. The composition of the liposome preparations used in this work is listed in Table 4.

Table 4. Overview of the liposome vesicles used in this work

Vesicle Type	Size	Composition	Ratio (mol/mol) (%)	Aqueous calpain buffers	Application
LMV	Heterogeneous	PC	100	CB1	Differential sedimentation
LMV	Heterogeneous	PG	100	CB1	Differential sedimentation
LMV	Heterogeneous	PS	100	CB1	Differential sedimentation
SUV	50 nm	PC	100	CB3	SPR
SUV	50 nm	PC/PE	60:40	CB3	SPR
SUV	50 nm	PC/PS	60:40	CB3	SPR
SUV	50 nm	PC/PG	60:40	CB3	SPR
SUV	50 nm	PC/PE/PS	60:20:20	CB3	SPR
SUV	50 nm	PC/PE/PS/PI	60:20:18:2	CB3	SPR
SUV	50 nm	PC/PE/PS/PIP	60:20:18:2	CB3	SPR
SUV	50 nm	PC/PE/PS/PIP_2	60:20:18:2	CB3	SPR
SUV	50 nm	PC/PE/PS/PI/ Cholesterol*	12:35:22:9:22	CB3	SPR
SUV	50 nm	PC/PE/PS/PI/ Cholesterol[+]	61:21:4:7:7	CB3	SPR
SUV	50 nm	PC/PE/ dansyl-DHPE	57.5:37.5:5	CB1/CB2	Protein-Membrane FRET
SUV	50 nm	PC/PS/ dansyl-DHPE	57.5:37.5:5	CB1/CB2	Protein-Membrane FRET
SUV	50 nm	PC/PG/ dansyl-DHPE	57.5:37.5:5	CB1/CB2	Protein-Membrane FRET
SUV	50 nm	PC/PI/ dansyl-DHPE	57.5:37.5:5	CB1/CB2	Protein-Membrane FRET
SUV	50 nm	PC/ dansyl-DHPE	95:5	CB1/CB2	Protein-Membrane FRET

*Plasma membrane mimick   [+]Nuclear membrane mimick

C.2.3.3.2. Differential sedimentation of lipid-protein complexes

A simple assay to asses Ca^{2+}-dependent interaction of μ-calpain with artificial lipid vesicles was derived from the methods described by Fukuda (2002) and Perisic (1999). In 1.5 ml Eppendorf reaction vials, sufficient μ-calpain to be visualized on a SDS-polyacrylamide gel (2-5 μg) were incubated together with 4X (w/w) LMV's (80-200 μg) during 30 min at RT with constant shaking. All reactions were performed in CB1 buffer in a final volume of 500 μl. The reaction mixtures were supplemented with either 1 mm $CaCl_2$ or 1 mm $MgCl_2$. The effect of ionic strength was also investigated by adding 1 M NaCl to some reaction mixtures.

After incubation, the samples were spun down at 12000 rpm for 15 min at RT and the pellets were resuspended in 16 µl Laemmli sample buffer. After heating the samples for 5 min at 90 ^{o}C, they were loaded on 12.5 % polyacrylamide gels and run as described in C.2.3.2.3. Differences in the intensity of protein bands were analyzed by means of the Scion Image scanning densitometry software.

C.2.3.3.3. Autoproteolytic digestion of calpain

The "autolysis" pattern of C115A inactive mutant µ-calpain variants was investigated by incubating these proteins with active µ-calpain isolated from human erythrocytes (Hitomi *et al.,* 1998). In a typical assay 18-36 µg of inactive µ-calpain were mixed with 1/10 of erythrocyte µ-calpain (molar ratio of 10:1) in a final volume of 110 µl. The reaction buffers were CB1 and CB2 (C.2.3.3.1, Table 3). Reactions were started by adding 100 mM CaCl$_2$ to a final concentration of 1 mM followed by short vortexing. Nine 12 µl-aliquots were taken at different times between 0 min and 90 min and mixed immediately with 1 µl 100 mM EDTA. These samples were finally heated 5 min at 90 ^{o}C and loaded on a 12.5 % SDS gel for PAGE analysis.

C.2.3.3.4. Chymotryptic digestion of calpain

In order to determine possible structural differences between inactive µ-calpain and its domain III acidic loop variants, limited proteolysis with chymotrypsin was performed as described by Moldoveanu (2000) and Thompson (2003) A typical assay contained 18-36 µg of inactive µ-calpain and 1/100 of chymotrypsin (molar ratio of 100:1) in a volume of 110 µl. The reaction buffers were CB1 and CB2 (C.2.3.3.1, Table 3), supplemented with either 1 mM CaCl$_2$ or 1 mM Mg Cl$_2$. Reaction was started by adding chymotrpsin and vortexing for a few seconds. Nine aliquots of 12 µl were taken at different times (between 0 min and 90 min) and mixed with 4 µl 4X Laemmli sample buffer. After heating for 5 min at 90 ^{o}C, the samples were analyzed on 12.5 % SDS polyacrylamide gels.

C.2.3.3.5. Calpain activity assay

Calpain activity was measured in CB4 (C.2.3.3.1, Table 3) complemented straight before use with 1 mM DTT , Suc-LY-AMC (500 µM, stock 50 mM in DMSO) and CaCl$_2$ (0

– 1000 μM free, additional 50 - 100 μM to neutralize EGTA from lysate buffer) in a total volume of 500 μl. Temperature of the assay was 12 °C to slow down autolysis. Cuvettes were prethermostatted 15 min before adding 10 – 20 μl of insect cell lysate freshly thawed. After mixing AMC release for four cuvettes in parallel was followed in a Kontron SFM-25 fluorimeter (excitation 380 nm, emission 460 mm) which was calibrated with AMC and data were digitally collected in a PC by a selfprogrammed software (Machleidt *et al.,* 1993). After 20-30 min 100 nM of recombinant calpastatin domain 1 was added and AMC release followed for further 15 min. Calpain activity was calculated from the total initital rate (0.5 -10 min) by subtracting the residual enzymatic activity which was not inhibited by calpastatin: $v = v_{initial} - v_{residual}$. Obtained rates (nM x min^{-1}) and the corresponding free Ca^{2+} concentration (μM) were fitted by nonlinear regression analysis to the Hill equation:

$$y = v_{max} \left[x^n / (x^n + [Ca^{2+}]_{0.5}^n) \right]$$

v_{max} : Maximum rate by Ca^{2+} saturation

$[Ca^{2+}]_{0.5}$: Ca^{2+} concentration for half-maximal enzymatic calpain activity

n   : Hill coefficent
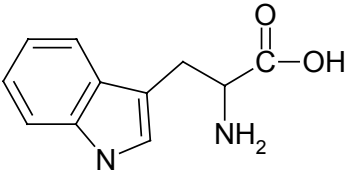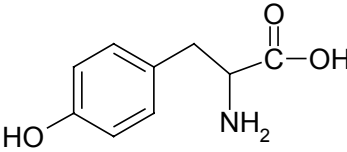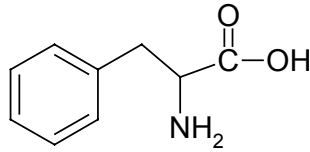
x   : Free Ca^{2+} concentration (μM)

y   : $v_{initial} - v_{residual}$ (nM x min^{-1})

C.2.3.3.6. Tryptophan intrinsic fluorescence

Proteins contain three aromatic amino acid residues which may contribute to their ultraviolet fluorescence: tryptophan (Trp), tyrosine (Tyr) and phenylalanine (Phe) (Table 5). In experimental situations it has been demonstrated that upon excitation at 280 nm, the fluorescence emission of most native proteins is dominated by the tryptophan fluorescence, with a minor contribution of tyrosine. Furthermore, only the tryptophan emission maximum is highly sensitive to the solvent polarity, as well as to specific interactions between the solvent and the indole ring. So the emission maxima of proteins vary with the location of the Trp residues. When tryptophan residues are shielded from the aqueous phase a blue shift in the emission maximum is observed. The exposure of Trp residues to the solvent is characterized by a red shift. This properties can be used to characterize structural rearrangements in a protein from simple conformational changes to denaturation. It is also a method to evaluate the association of proteins with substrates, inhibitors or other molecules (Lakowicz, 1983).

Table 5. Aromatic residues involved in protein fluorescence shown from left to rigth in descending order of contribution

Aminoacid	Tryptophan (Trp)	Tyrosine (Tyr)	Phenylalanine (Phe)
Formula			
Excitation maximum	$\lambda_{ex}^{max} = 280$ nm	$\lambda_{ex}^{max} = 278$ nm	$\lambda_{ex}^{max} = 256$ nm
Emission maximum	$\lambda_{em}^{max} = 348$ nm	$\lambda_{em}^{max} = 303$ nm	$\lambda_{em}^{max} = 282$ nm

The intrinsic Trp fluorescence of inactive μ-calpain variants was measured at different concentrations of $CaCl_2$ in order to evaluate the Ca^{2+}-induced conformational changes (Zimmerman and Schlaepfer, 1988; Hong *et al.,* 1990). Measurements were performed in a Spex FluoroMax fluorescence spectrophotometer equipped with a thermostatted cuvette holder using a stirrer-adapted 4 ml quartz cuvette (Hellma). The data acquisition settings were:

Temperature   : 22 ^{o}C
Excitation wavelength   : 280 nm
Emission wavelength   : 340 nm
Integration time   : 30 seconds
Slits (excitation and emission)   : 1 nm
Photomultiplier voltage   : 950 V

In a preliminary experiment, emission spectra were recorded between 300 nm and 360 nm at varying Ca^{2+} concentrations. Once the maximum emission wavelength was established, small quantities (< 1 % of the total volume) of $CaCl_2$ stock solutions (0.03-0.5 mM) were added to the permanently stirred reaction every two minutes and fluorescence intensity was recorded after 1.5 min incubation. The reaction buffers were CB1 and CB2 (C.2.3.3.1, Table 3) and the protein concentration was 0.1 μM in a volume of 3 ml In the first injection, the 0.1 μM EGTA present in CB was compensated with the same quantity of Ca^{2+} ions. In the following steps additive quantities ranging between 0 mM and 2 mM Ca^{2+} were administered

to the reaction. The same measurement performed using water or $MgCl_2$ instead of $CaCl_2$ served as control experiments.

The collected fluorescence intensity data were plotted against the Ca^{2+} concentrations and fitted using the modified Hill equation:

$$y = F_0 + F_m [x^n / (x^n + [Ca^{2+}]_{0.5}{}^n)]$$

F_0 : Fluorescence without Ca^{2+} (0 μM)

F_m : Maximum fluorescence change by Ca^{2+} saturation

$[Ca^{2+}]_{0.5}$: Ca^{2+} concentration at which half-maximal fluorescence changes were observed

n   : Hill coefficent

x   : Free Ca^{2+} concentration

y   : Fraction of maximum fluorescence at the concentration x

C.2.3.3.7. TNS fluorescence

2-p toluidinylnaphthalene-6-sulfonic acid (2,6 TNS or TNS), together with 1-anilino-8-naphthalene-sulfonic acid (1,8 ANS or ANS) and similar derivatives, are frequently used as noncovalent labels for proteins and membranes. These compounds have proved to be sensitive probes for partially folded intermediates in protein folding pathways. They are also useful in the study of conformational changes induced by interactions with other proteins, lipid membranes, nucleic acids or allosteric effectors. These amphiphilic dyes are essentially nonfluorescent in water, but are highly fluorescent when dissolved in nonpolar solvents or when bound to macromolecules.
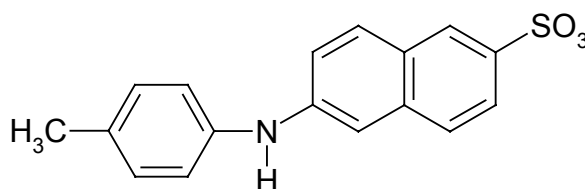
TNS

Consequently the basis of the aforementioned applications is the strong fluorescence enhancement exhibited by them when their exposure to water is lowered. Ca^{2+}-induced conformational changes have been investigated in several proteins (calpains among them)

using this method (Tanaka and Hidaka, 1980; Hong *et al.,* 1990; Arthur and Elce, 2000). In most of the experiments, a typical increase in the fluorescence intensity upon Ca^{2+} binding is observed due the exposure of hydrophobic core regions of the protein that are inaccessible to the dye in the Ca^{2+}-free form.

The Ca^{2+}-dependent fluorescence changes of TNS-labelled C115A inactive μ-calpain acidic loop mutants was monitored in a Spex FluoroMax fluorescence spectrophotometer equipped with a thermostatted cuvette holder using a stirrer-adapted 4 ml quartz cuvette (Hellma). The data acquisition settings were:

Temperature	: 22 ^{o}C
Excitation wavelength	: 320 nm
Emission wavelength	: 435 nm
Integration time	: 30 seconds
Slits (excitation and emission)	: 1 nm
Photomultiplier voltage	: 950 V

In a similar experimental setup as described above but with 1.2 μM TNS in the reaction mix, the emission spectra at different Ca^{2+} concentration were first recorded between 400 nm and 550 nm in order to find the maximum emission wavelength. Following these preliminary measurements, TNS fluorescence intensity changes at different Ca^{2+} concentrations were recorded with the same conditions and controls described in C.2.3.3.6. Collected fluorescence intensity data were plotted against the Ca^{2+} concentrations and fitted using the Hill equation (C.2.3.3.6).

C.2.3.3.8. Right angle light scattering

The theory of light scattering -first described in the 19th century by Lord Rayleigh (John William Strutt)- and its extensions (Rayleigh-Gans-Debye theory) describe the scattering of the incident light by very small molecules (compared to the wavelength of the light) and larger macromolecules in solution. In a typical Rayleigh scattering experiment, a well collimated, single frequency polarized light beam (e.g. from a laser) is used to illuminate a solution containing a suspension of the macromolecules of interest. The electric field of the polarized light beam is generally produced perpendicular to the plane in which the intensity and angular dependence of the subsequently scattered light is to be measured. The intensity

carries information about the molar mass, while the angular dependence carries information about the size of the macromolecule. The direct proportionality between the light scattered by a molecule and its molecular mass makes light scattering a powerful technique for monitoring the presence and formation of aggregates.

Right angle light scattering by C115A µ-calpain variants was measured as described by Pal for rat m-calpain (Pal *et al.,* 2001) using a Spex FluoroMax fluorescence spectrophotometer equipped with a thermostatted cuvette holder using a stirrer-adapted 4 ml quartz cuvette (Hellma). The data acquisition settings were:

Temperature   : 22 ^{o}C
Excitation wavelength   : 320 nm
Emission wavelength   : 320 nm
Integration time   : 30 seconds
Slits (excitation and emission)   : 1 nm
Photomultiplier voltage   : 950 V

Two types of experiments were conducted under the same conditions mentioned previously (0.1 µM protein in 3 ml CB1). First, a time-course of the scattering intensity was recorded during 30 min at different concentrations of NaCl and adding $CaCl_2$ and EDTA after 10 min and 20 min respectively. In a second assay the Ca^{2+}-dependent increase of the scattering intensity was recorded as described in C.2.3.3.6. The collected scattering intensity data were plotted against the Ca^{2+} concentrations and fitted using the modified Hill equation (C.2.3.3.6).

C.2.3.3.9. Liposome binding assay

The binding of µ-calpain variants to artificial lipid vesicles was measured by means of the <u>f</u>luorescence <u>r</u>esonance <u>e</u>nergy <u>t</u>ransfer (FRET) effect. This phenomenon arises from the nonradiative transfer of energy from a fluorescent donor to an acceptor molecule (Wu and Brand, 1994). FRET requires overlap between donor emission and acceptor absorbance spectra and is exquisitely sensitive to the distance between donor and acceptor. The efficiency of FRET (E) is given by the equation:

$$E = R_0^6 / R^6 + R_0^6$$

where R is the distance between the donor and acceptor and R_0 is the characteristic donor-acceptor distance resulting in half maximal FRET. Typical R_0 values are on the order of 10-50 Å, which enables FRET to be useful for many biochemical applications. A standard FRET assay for docking proteins (Nalefski and Falke, 2002) to phospholipid membranes utilizes one or more intrinsic tryptophans in the protein as the fluorescence donor (λ_{em}^{max} = 320 to 350 nm) and N-(5-dimethylaminonaphthalene-1- sulfonyl) (Dansyl) groups covalently attached to the head group of phospholipids as the fluorescence acceptor (λ_{ex}^{max} = ~ 330 nm). The R_0 value of 21 Å (Wu and Brand, 1994) for this pair guarantees that FRET is only observed when the protein is docked to the membrane and not when free in solution. The existence of 16 Trp residues in µ-calpain 80K subunit and 3 Trp residues in the 28K subunit, makes this assay useful for the investigation of calpain membrane binding phenomenon. Liposomes containing 5 % of 1,2-dihexadecanoyl-sn- glycero-3-phosphoethanolamine, triethyl-
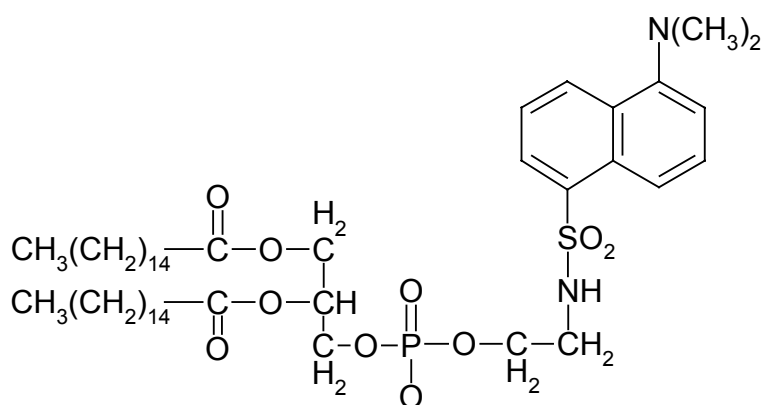
Dansyl-DHPE

ammonium salt (dansyl DHPE) as fluorescent probe were prepared as described in C.2.3.3.1. In a typical experiment, 10 µM liposomes were mixed with 0.1 µM protein in a final volume of 3 ml. Assays were performed in CB buffers (C.2.3.3.1, Table 3). After recording the emission of the liposomes (blank), protein was added and the fluorescence intensity monitored in the presence and absence of Ca^{2+}. In a first approach, fluorescence spectra in the range between 400 nm and 540 nm were recorded. Afterwards, a Ca^{2+} titration was performed as described in C.2.3.3.6. Measurements were conducted in a Spex FluoroMax fluorescence spectrophotometer equipped with a thermostatted cuvette holder using a stirrer-adapted 4 ml quartz cuvette (Hellma). The data acquisition settings were:

Temperature   : 22 ^{o}C

| Excitation wavelength	: 280 nm
Emission wavelength	: 510 nm
Integration time	: 30 seconds
Slits (excitation and emission)	: 4 nm (ex) and 8 nm (em)
Photomultiplier voltage	: 650 V

The collected Dansyl fluorescence intensity data were plotted against the Ca^{2+} concentrations and fitted to the modified Hill equation (C.2.3.3.6).

C.2.3.3.10. Biomolecular interaction analysis using the BIAcore technology

Real time biomolecular interaction analysis (BIA) was used in order to gain more insight in the binding of μ-calpain to artificial membranes. The BIA method is based on the surface plasmon resonance (SPR), an optical phenomenon ocurring at an interface between two transparent media of different refractive index (i.e. glass and water). Under these conditions, light coming from the side of higher refractive index is partly reflected and partly refracted. Above a certain critical angle of incidence, no light is refracted across the interface, and total internal reflection is observed. While incident light is totally reflected the electromagnetic field component penetrates a short (tens of nanometers) distance into a medium of a lower refractive index creating an exponentially detenuating evanescent wave. If the interface between the media is coated with a thin layer of metal (gold), and light is monochromatic and p-polarized, the intensity of the reflected light is reduced at a specific incident angle producing a sharp shadow (called surface plasmon resonance) due to the resonance energy transfer between evanescent wave and surface plasmons. The resonance conditions are influenced by the material adsorbed onto the thin metal film. Satisfactory linear relationship is found between resonance energy and mass concentration of biochemically relevant molecules such as proteins, sugars and DNA. The SPR signal which is expressed in resonance units (RU) is therefore a measure of mass concentration at the sensor chip surface. This means that the analyte and ligand association and dissociation can be observed and ultimately rate constants as well as equilibrium constants can be calculated.

The light source for SPR is a high efficiency near-infrared light emitting diode which has a fixed range of incident angles. The SPR response is monitored by a fixed array of light sensitive diodes covering the whole wedge of reflected light. The angle at which minimum reflection occurs is detected and converted to resonance units. The SPR angle depends on

several factors, most notably the refractive index into which the evanescent wave propagates on the non-illuminated side of the surface. In addition the other parameters are the wavelength of the incident light and the properties of the metal film.

A typical experiment consisted of four phases: 1) immobilization of the ligand, 2) analyte association, 3) analyte dissociation and 4) regeneration.

1) Capture of liposomes:

Phospholipid vesicles were captured on a Pioneer L1 sensor chip (Biacore) as follows:

Using CB3 (C.2.3.3.1, Table 3) as running buffer and at a flow rate of 2 µl/min, the chip surface was first washed by a 5 minute injection of 40 mM N-octyl-β-D-gluocopyranoside (nonionic detergent). In the following step, the prepared liposomes (C.2.3.3.1) previously diluted to a concentration of 0.2 mM in running buffer were injected during 15 minutes. Finally the flow rate was increased to 100 µl/min and short pulse (2 min) of 100 mM NaOH was used to remove any loose lipids which may not be attached to the hydrophobic surface. This procedure was performed separately with different vesicles for every four flow cells in the sensor chip. Each capturing experiment was saved as an independent sensorgram reflecting the immobilization process. These sensorgrams were useful for monitoring the changes in binding capacity of the sensor chip with increasing number of runs. The following phases (2-4) were recorded in a separate sensorgram.

2) Analyte association:

Upon capturing liposome mixtures on the sensor chip two different types of experiments were performed on the immobilized bilayers.

Evaluation of Ca^{2+} requirement for membrane association:

Using CB3 as running buffer, constant calpain quantities (~ 50 mM for the C115A inactive heterodimers and ~ 200 nM for the small subunit variants) were injected at varying Ca^{2+} concentrations (0-10 mM).

Evaluation of association/dissociation rates

These parameters were determined in running buffer CB3 supplemented with 1 mM $CaCl_2$. Varying concentrations (0-200 nM) of the inactive C115A heterodimeric µ-calpain and small subunit variants in a constant Ca^{2+} concentration (1 mM) were injected.

In both cases 80 µl of 100-200 nM µ-calpain at a Ca^{2+} concentration of 1 mM was injected to the lipid monolayer prior to injection of the different samples, to block possible residues of

unspecific binding. Proteins were mixed with the required volume of a $CaCl_2$ stock solution shortly before injection to avoid aggregation and precipitation effects. The volume of sample injected was always 80 µl and the rate 20 µl/min.

3) Analyte dissociation:

Once samples were injected, running buffer was pumped during 8-12 minutes in order to allow dissociation of the sample. The flow rate was kept at 20 µl/min.

4) Surface regeneration:

The lipid monlayer was regenerated at a flow rate of 100 µl/min by injecting 50 µl of 10 mM Tris-HCl pH 7.5, 100 mM EDTA and 50 µl 100 mM NaOH consecutively.

Once the optimum assay conditions were established, all steps described above were performed in automated modus.

For the first type of measurement (Ca^{2+} requirement) only the increase in the relative response (RUs) during the association phase was analyzed. Non saturation conditions were chosen where RU values raised almost linearly with time. This parameter was plotted against the Ca^{2+} concentration and the $[Ca^{2+}]_{0.5}$ was calculated using the modified Hill equation

$$y = R_0 + R_m [x^n / (x^n + [Ca^{2+}]_{0.5}{}^n)]$$

where

F_0 : Response without Ca^{2+} (0 µM)

F_m : Maximum Response by Ca^{2+} saturation

$[Ca^{2+}]_{0.5}$: Ca^{2+} concentration at which half-maximal response change was observed

n   : Hill coefficent

x   : Free Ca^{2+} concentration

y   : Response at the concentration x

The binding kinetics in the second type of experiment was evaluated using the 1:1 Langmuir association and 1:1 Langmuir dissociation models (separate *ka/kd*) (BIAevaluation 3.0 Software Handbook, 1997).

1:1 Langmuir association:

$$R = R_{eq}(1-e^{-(k_aC+k_d)(t-t_0)}) + RI$$

where

$$R_{eq} = (k_aC / k_aC + k_d) R_{max}$$

k_a : Association rate constant ($M^{-1}s^{-1}$)

R_{max} : Maximum analyte binding capacity (RU)

C   : Analyte concentration (M)

t_0 : Injection start time (s)

k_d : Dissociation rate constant (s^{-1})

RI   : Bulk refractive index contribution (RU)

R_{eq} : Steady state binding level

1:1 Langmuir dissociation:

$$R = R_0 e^{-k_d(t-t_0)} + Offset$$

k_d : Dissociation rate constant (s^{-1})

R_0 : Response at start of fitted data (RU)

t_0 : Time at start of fitted data (s)

Offset : Response at infinite time (RU)

K_D was calculated from the obtained velocity constants as:

$$K_D = k_d / k_a (M)$$

C.2.4. Bioinformatic Tools

Oligonucleotide primer design for PCR applications was accomplished using Clone Manager Professional Suite from Scientific & Educational Software. Vector maps were prepared with pDRAW32, a freeware available in the world wide web. Densitometry of Coomassie stained SDS gels was performed using the software Scion Image, from the NIH public domain. Chemical structures were drawn with help of the free version of Isis Draw

software from MDL®. Sequence alignments were performed with Clustal-W, from the Expasy Molecular Biology Server (Gasteiger *et al.,* 2003). The tridimensional structure of human μ-calpain was modelled on the coordinates of human m-calpain (PDB code 1KFU) and rat μ-like calpain (PDB code 1QXP) using the automated comparative modelling server SWISS MODEL (Schwede *et al.,* 2003). Structures were visualized with Viewer Lite 5.0 from Accelrys Inc. Curve fitting was performed using Origin® version 6.0 from Microcal Software Inc.

D. Results

D.1. Modelling of human μ-calpain and analysis of the electrostatic interactions of domain III acidic loop residues

Human μ-calpain was modeled on the coordinates of human m-calpain (PDB code 1KFU) (Figure 14). The sequence identity of both isoforms is 60.5 % and the similarity over 90 %. The overall structure around the acidic loop region was similar to that from m-calpain, as expected from sequence alignment. We measured the distances between the acidic loop residues and all basic residues within a radius of ~ 30 Å. The results of this analysis are presented in Table 6.

A   **B**
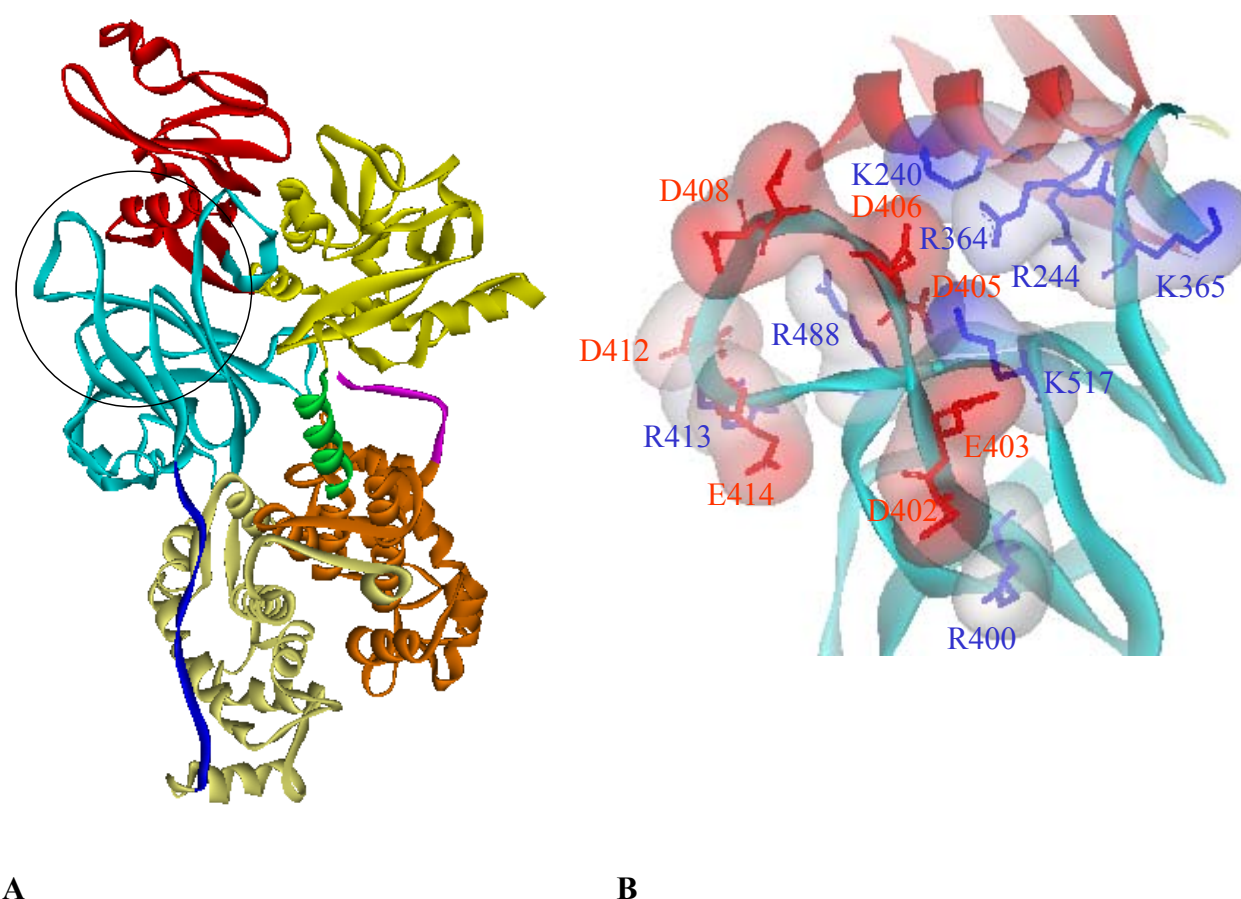
Figure 14. A: Ribbon diagram showing the model of human μ-calpain. Note that the structure was rotated ~180° on its vertical axis with respect to the structure of m-calpain shown in Figure 4. Domains were colored as previously indicated in that figure. **B**: Ribbon diagram showing the electrostatic surfaces at the interface region between domains IIb and III in the μ-calpain model (enclosed in a circle in **A**). Acidic and basic residues involved in electrostatic interactions in this region (see Table 6) are shown in red and blue respectively.

Residues D402, E403, D405, D406, D407, D408, D412 and E414 from the acidic loop make important contacts with residues K240, R244, R364, K365, R400, R413, R488 and K517. Taking into account that the strength of Coulombic interactions is inversely proportional to the square of the distance between two oppositely charged groups ($F = q_1q_2 / r^2D$) and that the optimum distance for an electrostatic attraction is ~ 2.8 Å, we were able to predict the importance of the individual loop residues in a putative electrostatic switch activation mechanism. Distances between all ion pairs in the analyzed region are longer than 4 Å and therefore out of range for the formation of salt bridges (Kumar and Nussinov, 2002). The strongest interactions of the acidic loop with basic residues in subdomain IIb (K240, R244, R364 and K365) were made by aminoacids D405 and D406. Within domain III, the predominant electrostatic contacts detected within a distance of 6 Å were D402 with R400, E403 with K517, D405 with R488 and K517, D406 with K517 and D412 with R413.

Table 6. Distances in Å between the acidic residues in the acidic loop of domain III mutated in this work and their putative basic interaction partners in subdomain IIb and domain III.

DIIb and DIII basic residues	Mutated residues in DIII acidic loop						
	D402	E403	D405	D406	D408	D412	E414
K240	20.27	15.12	8.19	8.17	9.72	17.12	18.46
R244	17.56	12.75	8.68	11.47	17.32	21.01	20.05
R364	16.63	10.63	7.27	6.43	12.49	20.15	18.56
K365	22.13	16.49	17.33	16.66	23.28	30.56	28.15
R400	5.16	11.07	16.13	19.37	25.55	23.51	14.97
R413	19.32	21.03	14.25	20.56	20.72	4.62	9.30
R488	16.04	14.18	5.65	10.80	11.53	8.52	9.86
K517	11.43	5.75	5.10	5.00	12.27	18.27	14.23

D.2. Expression of μ-calpain (C115A) domain III acidic loop mutants using the baculovirus expression system

Attempts to express catalytically active μ-calpain have not been as succesful as expression of m-calpain (Goll *et al.,* 2003). It has been difficult to repeat the early studies reporting that catalytically active μ-calpain could be obtained from either *E. coli* (Vilei *et al.,*

1997) or baculovirus (Meyer *et al.,* 1996) expression systems. When expressed in *E. coli,* μ-calpain is deposited in inclusion bodies and only very low yields of catalytically active enzyme are obtained. Similar low yields of proteolytically active μ-calpain have been gained whith the baculovirus system (Elce, 1999). The expression of enzyme with the active site Cys-115 mutated to Ser in insect cells (Hitomi *et al.,* 1998) avoided autolytical self-destruction during the purification process, thereby improving the expression yields. A protocol established by Pfeiler (2001) for the expression and isolation of active site Cys-115 mutated to Ala μ-calpain in insect cells allowed us to perform the first functional study of this enzyme by means of site-directed mutagenesis.

D.2.1. Construction of the transfer vectors

An Ala scan of the acidic loop of μ-calpain domain III was performed using the Quick Change™ site directed mutagenesis kit from Stratagene (C.2.2.11). The baculovirus transfer vector pVL1392-syn80K(C115A)-His$_6$ (Pfeiler, 2001) encoding the large subunit of human μ-calpain was used as template for the mutagenesis PCR. The mutations introduced in the region of the acidic loop are represented in Figure 15. Eight primer pairs were designed to

```
aa  →  398 399 400 401 402 403 404 405 406 407 408 409 410 411 412 413 414 415 416 417

WT    5'- c  aag atc cgg ctg gat gag acg gat gac ccg gac gac tac ggg gac cgc gag tca ggc tgc -3'
             K   I   R   L   D   E   T   D   D   P   D   D   Y   G   D   R   E   S   G   C

D402A 5'- c  aag atc cgg ctg gct gag acg gat gac ccg gac gac tac ggg gac cgc gag tca ggc tgc -3'
             K   I   R   L   A   E   T   D   D   P   D   D   Y   G   D   R   E   S   G   C

E403A 5'- c  aag atc cgg ctg gat gcg acg gat gac ccg gac gac tac ggg gac cgc gag tca ggc tgc -3'
             K   I   R   L   D   A   T   D   D   P   D   D   Y   G   D   R   E   S   G   C

D405A 5'- c  aag atc cgg ctg gat gag acg gct gac ccg gac gac tac ggg gac cgc gag tca ggc tgc -3'
             K   I   R   L   D   E   T   A   D   P   D   D   Y   G   D   R   E   S   G   C

D406A 5'- c  aag atc cgg ctg gat gag acg gat gcc ccg gac gac tac ggg gac cgc gag tca ggc tgc -3'
             K   I   R   L   D   E   T   D   A   P   D   D   Y   G   D   R   E   S   G   C

D408A 5'- c  aag atc cgg ctg gat gag acg gat gac ccg gcc gac tac ggg gac cgc gag tca ggc tgc -3'
             K   I   R   L   D   E   T   D   D   P   A   D   Y   G   D   R   E   S   G   C

D409A 5'- c  aag atc cgg ctg gat gag acg gat gac ccg gac gcc tac ggg gac cgc gag tca ggc tgc -3'
             K   I   R   L   D   E   T   D   D   P   D   A   Y   G   D   R   E   S   G   C

D412A 5'- c  aag atc cgg ctg gat gag acg gat gac ccg gac gac tac ggg gcc cgc gag tca ggc tgc -3'
             K   I   R   L   D   E   T   D   D   P   D   D   Y   G   A   R   E   S   G   C

E414A 5'- c  aag atc cgg ctg gat gag acg gat gac ccg gac gac tac ggg gac cgc gcg tca ggc tgc -3'
             K   I   R   L   D   E   T   D   D   P   D   D   Y   G   D   R   A   S   G   C
```

Figure 15. Schematic representation of the gene region in human μ-calpain coding for the acidic loop in domain III (top) and the amino acid sequence derived from it (second line). Sequences of the forward primers designed for mutagenesis are shown in cursive. The desired aminoacid substitutions (with the exception of D409A) could be generated with the Quick Change™ site directed mutagenesis method.

change each of the acidic amino acids in the loop of domain III. The base mispairment was kept = 1 for all mutagenic primers. As described in C.2.2.11 the PCR products were digested with *DpnI* and the digests were transformed in competent *E. coli*. With the exception of the mutant D409A, transformants were obtained from all PCR reactions after 1-3 trials. Plasmid DNA from the transformant colonies was isolated using the mini-prep method described in C.2.2.1 and further analyzed by restriction analysis and agarose gel electrophoresis. This first analysis indicated that the template plasmids were amplified completely by the *Pfu* polymerase (Figure 16). In the next step, transformants were sequenced using the complete set of μ-calpain sequencing primers (C.1.2). After analyzing 1-5 different clones for each mutant, a transformant was found with the expected sequence.
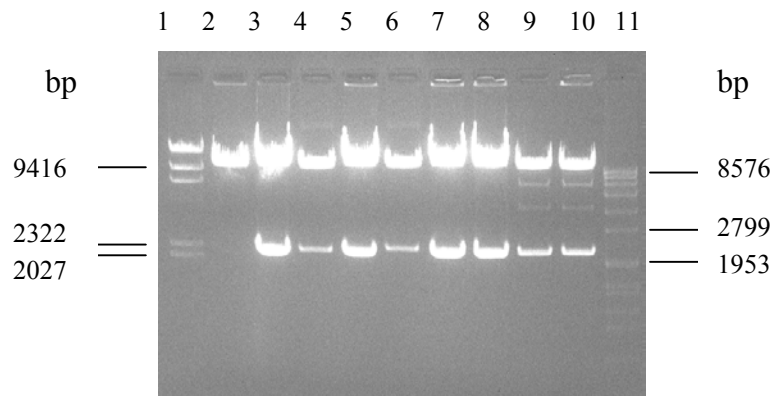
Figure 16. 1% Agarose gel showing 2 μg of pVL1392-syn 80K (C115A) domain III acidic loop mutants digested with 10 units of *EcoRI* and *BamHI*. As positive controls were used the template plasmid pVL1392-syn80K(C115A)-His$_6$ and the empty pVL1392 vector (lanes **2** and **3**). Mutants D402A, E403A, D405A, D406A, D408A, D412A and E414A are shown in lanes **4** to **10**. Roche DNA lenght markers II and VII are represented in lanes **1** and **11**.

D.2.2. Generation and identification of recombinant baculoviruses

Plasmid DNA from positive clones was isolated using a maxi-prep kit (C.2.2.1) and used for cotransfection of *Sf21* insect cells with linearized BaculoGold™ virus DNA (C.2.1.2). Recombinant baculoviruses were harvested (C.2.1.2) and their DNA was isolated (C.2.1.2). This DNA was used as template in a PCR for the identification of recombinant baculoviruses (C.2.1.2). A band of about 2.2 kb was amplified using the polyhedrin primers which recognize the flanking regions of the inserted gene (Figure 17). The same results were obtained using specific primers for μ-calpain 80K (data not shown). This experiment

corroborated that no wild type virus was present in the viral stock (the typical band for wild type AcPNV is about 0.7 kb) and only recombinant baculoviruses were produced by homologous recombination during cotransfection. Thanks to this high recombination efficiency it was not necessary to purify the viral stocks by plaque assay. They were instead amplified in four serial passages (C.2.1.2) in order to obtain larger stocks for protein expression. The titer of the final virus stock was determined by plaque assay (C.2.1.2). Figure 18 show as example the results of one
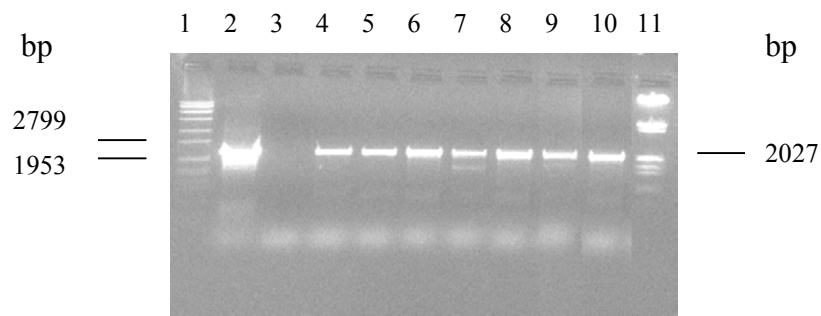
Figure 17. 1% Agarose gel showing the identification of recombinant µ-calpain 80K mutants baculoviruses by PCR amplification. Transfer vector pVL1392-syn80K (C115A)-His$_6$ served as positive control (lane **2**). Empty pVL1392 vector was used as negative control (lane **3**). Baculoviruses coding for Mutants D402A, E403A, D405A, D406A, D408A, D412A and E414A are shown in lanes **4** to **10**. Roche DNA leght markers VII and III were loaded on lanes **1** and **11**.
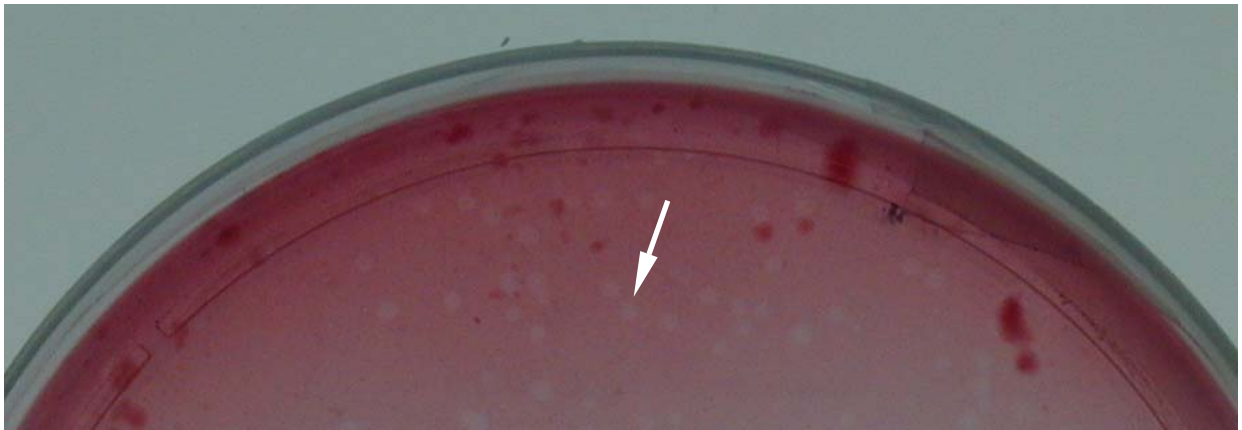
Figure 18. Section from a plaque assay corresponding to the fourth amplification of D406A mutant recombinant baculovirus in a 10^{-4} dilution. Plaques are visualized as clear spots (example pointed by the arrow) in the neutral red-stained background. In each experiment three different dilutions of the viral stock were analyzed and the resulting titers were averaged. In this example the titer of the stock was 1.3×10^7 pfu/ml.

these analyses. The virus titer for all mutants ranged in repeated experiments between 1-2 x 10^7 pfu/ml. Such titers proved to be sufficient for expression experiments. Stocks were finally sterile filtered and stored at 4 °C until use in expression experiments. The final confirmation about the capability of generated recombinant baculoviruses to express heterologous proteins was provided by an analytical expression experiment. 70 % confluent six-well culture plates were co-infected with two viruses, one coding for the large subunit and one for the small subunit of μ-calpain at a multiplicity of infection (MOI) of 1 and lysed 3 days after infection. The lysates were run on a 12.5 % SDS-PAGE and the separated proteins were blotted onto a nitrocellulose membrane. Immunoprinting of this membrane with a polyclonal antibody specific for both subunits of human μ-calpain (Gabrijelcic-Geiger *et al.,* 2001) variants showed two major recognition bands corresponding to the 80K and the 28K subunits (see Figure 19).
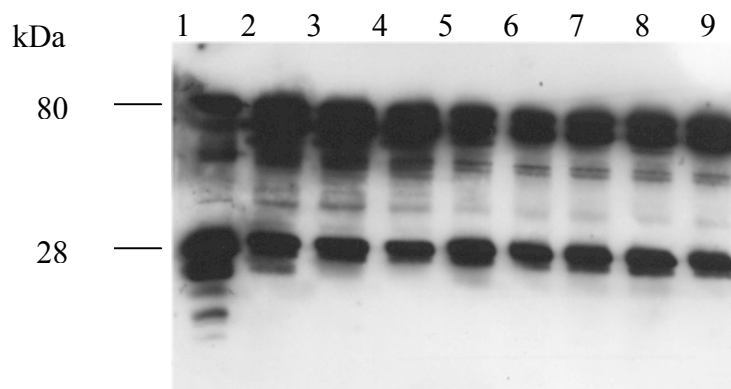
Figure 19. Western Blot analysis of the expression of μ-calpain (C115A) acidic loop variants in insect cells. As positive control, **1** μg of purified μ-calpain (C115A) was run on lane (Pfeiler D, 2001). Lanes **2** to **9**: cell lysates from Sf 21 cells infected with μ-calpain (C115A) wild type and mutants D402A, E403A, D405A, D406A, D408A, D412A and E414A

D.2.3. Expression and purification of the mutants

μ-Calpain (C115A) and the generated domain III mutants were expressed in *Sf21* insect cells following the protocol established by Pfeiler (2001) (C.2.1.2). Two different recombinant baculoviruses coding for the 80K subunit and for the 28K subunit were used to infect the insect cells with a MOI of 1. 72 hours post infection the cells were harvested and lysed as described (C.2.3.1.2).

Preparation of affinity columns

BC-peptide harbouring the two subdomains B and C of the specific calpain inhibitor calpastatin was cloned in the expression vector in pET22-b(+) by Pfeiler (2001). The expression in *E. coli* and the isolation on Ni-NTA columns was performed as described in C.2.3.1.4. ~ 35 mg of recombinant protein were isolated from 1 L *E. coli* culture. Figure 20 shows the results of the expression procedure. The peak fractions were collected, dialyzed against coupling buffer and immobilized on NHS-activated sepharose as described in C.2.3.1.5. Several 5 ml columns were packed with the prepared material and stored at 4 $^{\circ}$C until use.
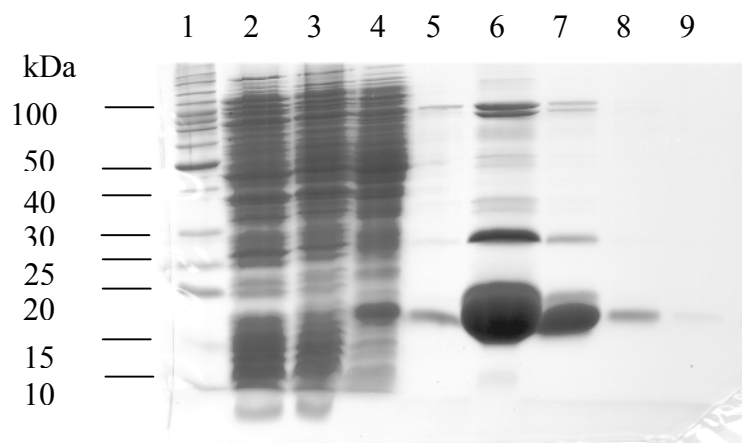
Figure 20. 12.5 % SDS-PAGE of different stages of expression and purification of calpastatin BC peptide. Lane **1**: Invitrogen's Bench Mark™ molecular weight markers. Lane **2**: soluble proteins from ~2.0 x 10^8 *E. coli* cells before induction with IPTG. Lane **3**: soluble proteins from the same quantity of cells after 2 hours induction. Lane **4**: Bug-Buster bacterial cell lysate. Lanes **5** to **9**: elution fractions (4, 6, 9, 12 and 15) of the affinity chromatography on Ni-NTA.

Affinity chromatography on BC-calpastatin sepharose column.

Lysates from *Sf21* cells infected with different baculoviruses were loaded on separate affinity columns. The Ca^{2+}/EGTA dependent binding/elution procedure (Figure 21) was successful for all variants (Figure 22). Normally ~5 mg of μ-calpain were isolated from ~1.0 x 10^8 infected *Sf21* cells in a 150 ml culture
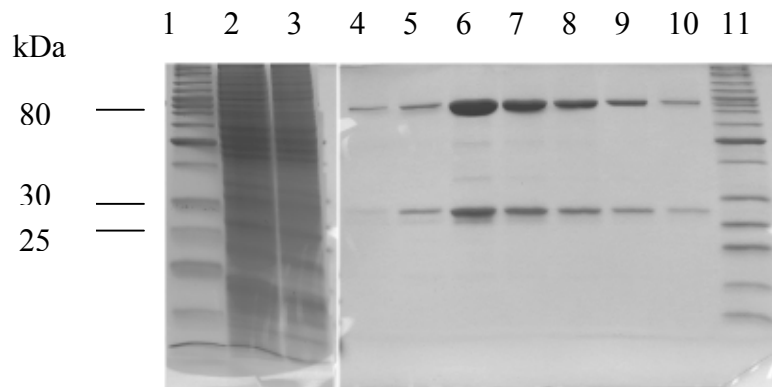
Figure 21. 12.5 % SDS-PAGE showing the isolation of μ-calpain (C115A) on a BC-calpastatin affinity column. Invitrogen's Bench Mark™ molecular weight markers were loaded on lanes **1** and **11**.The cell lysate loaded on the column is represented in lane **2**. The flow through containing unbound proteins is shown in lane **3**. In the next lanes (**4-10**) appear the elution fractions 3 to 9 consecutively.
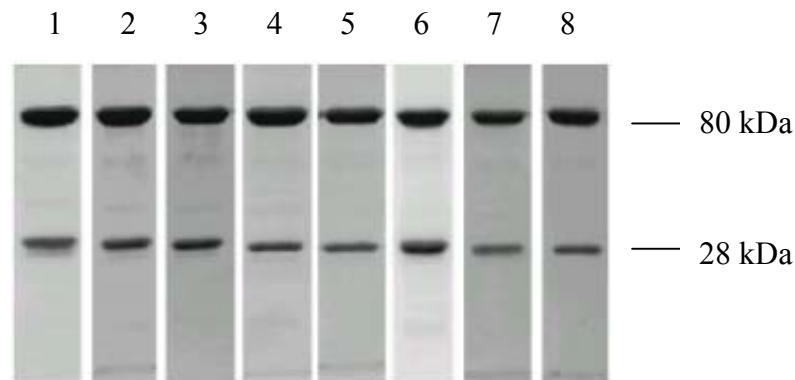
Figure 22. 12.5 % SDS-PAGE analysis of the μ-calpain (C115A) acidic loop variants in insect cells eluted from a calpastatin affinity column. Lanes **1** to **8** represent μ-calpain (C115A) wild type and mutants D402A, E403A, D405A, D406A, D408A, D412A and E414A respectively**.**

D.2.4. Validation of the mutants

N-terminal sequence analysis

The purity of the recombinant proteins was corroborated by N-terminal sequence analysis (C.2.3.2.8). From ~ 250 pmol protein only of a putative AcPNV DNA helicase (Kamita and Maeda, 1997) was detected as the major contaminant (~ 10 pmol) co-eluting

with the expressed variants. N-termini of both the large and small calpain subunits were blocked for sequencing. Such posttranslational modification of μ-calpain when expressed in insect cells had been already described by Pfeiler (2001).

Proteolysis by native μ-calpain

Purified active site mutated μ-calpain variants were -as expected- unable to autolyze in the presence of Ca^{2+} (data not shown). However, when incubated with native μ-calpain isolated from human erythrocytes in a molar ratio of 10:1, they showed the same autolysis pattern reported for μ-calpain (Gabrijelcic-Geiger *et al.,* 2001). Three major bands were detected after 90 min incubation (Figure 23): a 76 kDa and a 38 kDa band derived from the 80K subunit with identical N-terminal sequence [28]LGRH, and a 18 kDa band from the 28K subunit with N-terminal sequence [92]ANESE.
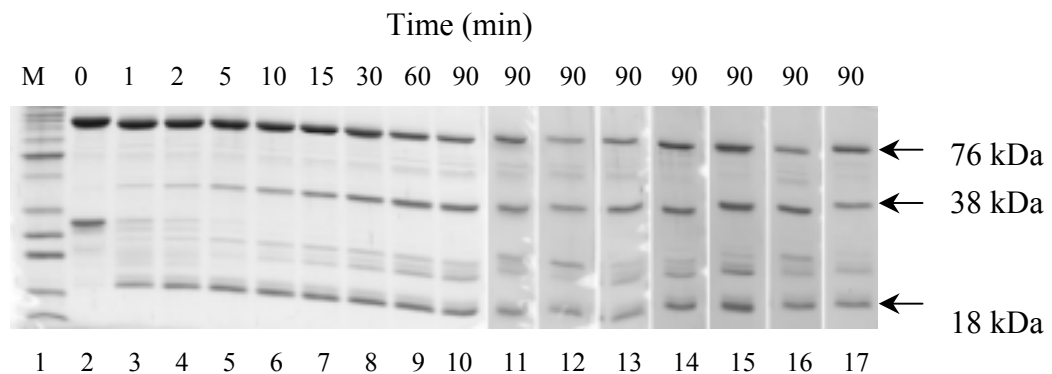
Figure 23. 12.5 % SDS-PAGE of the proteolysis of active site mutated human μ-calpain by native μ-calpain from human erythrocytes. Lane **1**: Invitrogen's Bench Mark™ protein ladder (M). Lanes **2** to **10**: Wild type proteolysis products taken at different incubation times. Lanes **11** to **17**: Mutants D402A, E403A, D405A, D406A, D408A, D412A and E414A after 90 min digestion. Main autolysis products are pinpointed with arrows (right).

Aggregation

A tendency to form small soluble and large insoluble protein aggregates in the presence of calcium has been described for native μ-calpain (Dainese *et al.,* 2002) and recombinant m-calpain (Pal *et al.,* 2001). Massive protein precipitation during Ca^{2+}-dependent elution from the affinity column was also observed in the purification process of our recombinant μ-calpain variants. We characterized the formation of small soluble aggregates

by these variants using the right angle light scattering methodology employed by Pal (2001). In preliminary experiments it was determined that 1 mM CaCl$_2$ promoted the aggregation of our recombinant calpain variants as in the cases of recombinant m-calpain (Pal, Elce *et al.,* 2001) and native μ-calpain (Dainese, 2002) (Figure 24). As described by Pal, formation of soluble aggregates was reversible either by adding 1 mM EDTA or by increasing the ionic strength (Figure 24). The influence of ionic strength on the Ca^{2+}-dependent formation of large insoluble aggregates was investigated by means of a pull down experiment. Equal quantities of recombinant μ-calpain were incubated 30 min at room temperature with 1 mM CaCl$_2$ and different concentrations of NaCl. After 15 min centrifugation at 12000 rpm, the pellets were dissolved in 16 μl Laemmli sample buffer and loaded on a SDS-PAGE. The results (Figure 25) evidenced that formation of large insoluble aggregates is independent from the concentration of NaCl and suggested that rigth angle light scattering was only able to detect small soluble aggregates. Ca^{2+} requirements for the formation of these small aggregates could be determined thanks to the correlation observed between [Ca^{2+}] and scattered light intensity (Figures 24 and 29).
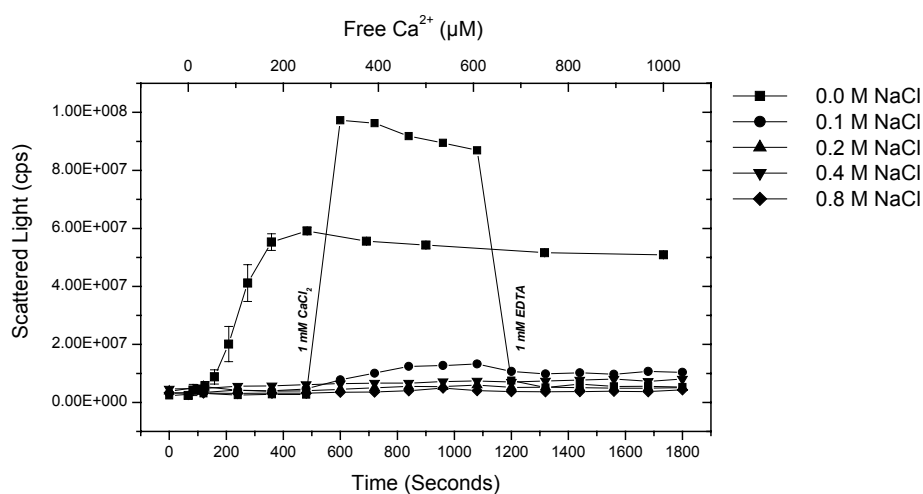
Figure 24. Effect of Ca^{2+} and ionic strength in the formation of μ-calpain aggregates. Time course curves represent the scattered light during 30' by 0.1 μM μ-calpain (C115A) at different concentrations of NaCl (see color legend). CaCl$_2$ (1 mM) was added to the solution after 10' and chelated with 1 mM EDTA after 20'. In a separate experiment the scattered light was measured at increasing concentrations of CaCl$_2$ by 0 mM NaCl (saturation curve, upper abscissa).
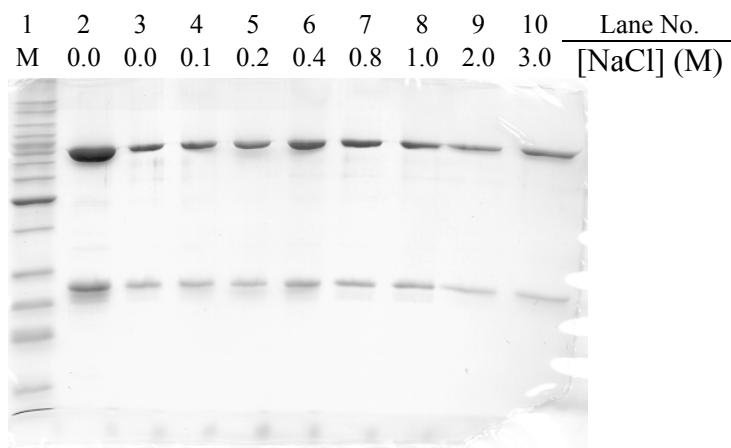
Figure 25. 12.5 % SDS-PAGE showing the effect of ionic strength in the Ca^{2+}-dependent formation of large μ-calpain insoluble aggregates. Lane **1**: Invitrogen's Bench Mark™ molecular weight markers (M). Lane **2**: 5 μg of control μ-calpain without $CaCl_2$. Lanes **3** to **10**: 5 μg of μ-calpain incubated during 30' with 1 mM $CaCl_2$ at different concentrations of NaCl. After 15' centrifugation at 12000 rpm, the pellets were dissolved in Laemmli sample buffer and loaded on the gel.

D.3. Functional characterization of μ-calpain domain III acidic loop mutants

D.3.1. Study of Ca^{2+}-induced conformational changes

Limited proteolysis with chymotrypsin

Proteolysis of inactive calpains by digestive proteases has been assayed in order to track Ca^{2+}-induced conformational changes (Moldoveanu *et al.,* 2001 and Thompson *et al.,* 2003). We used this method to characterize the nature of the Ca^{2+}-induced structural rearrangements by DIII mutants. For this purpose the inactive variants were incubated with chymotrypsin in a molar ratio of 100:1 in the presence of either 1 mM $CaCl_2$ or 1 mM $MgCl_2$. Contrarily to the results reported by Moldoveanu (2001) and Thompson (2003), the presence of Ca^{2+} did not considerably accelerate the rate of degradation of inactive μ-calpain variants. This contradiction was probably originated by the different calpain:chymotrypsin molar ratio used (100:1) in our experiments in comparison to the 10:1 used by Moldoveanu and 25:1 used by Thompson. The proteolytic degradation patterns of the samples after 90 min in the
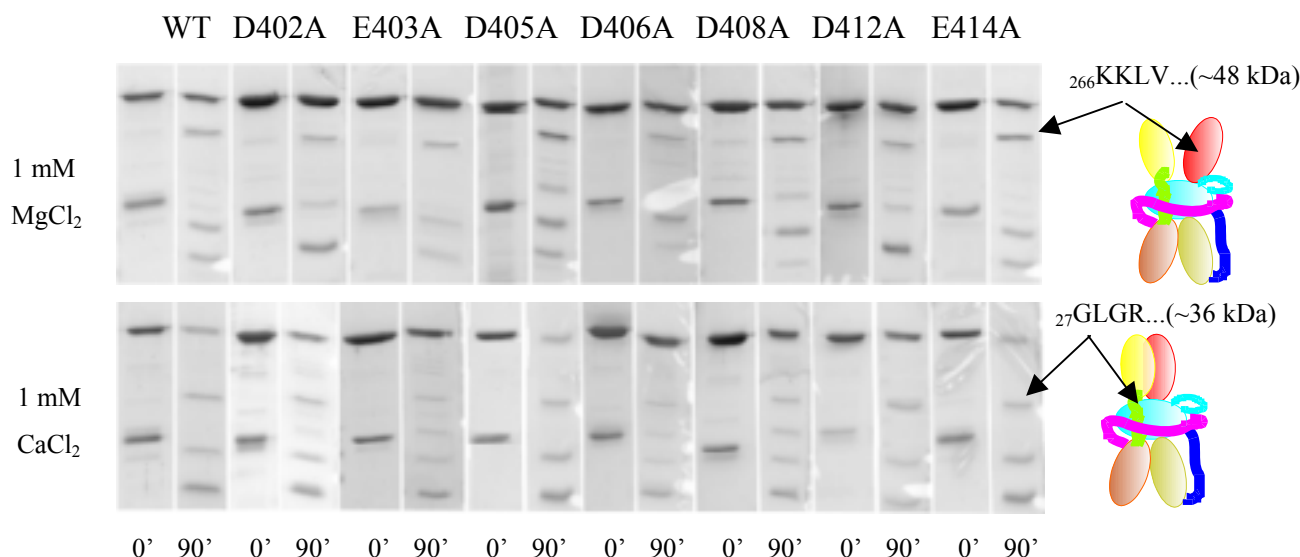
Figure 26. 12.5 % SDS-PAGE analysis of the chymotryptic proteolysis of C115A active site mutated human μ-calpain variants in the presence of 1 mM $MgCl_2$ or 1 mM $CaCl_2$. Samples taken before addition of chymotrypsin (0') and after 90 min digestion. Most notorious proteolytic products seen on the gels are pinpointed with arrows indicating the position of the cleavage in the calpain molecule. Calpain domains are coloured in the accompanying cartoon as in Figure 6.

presence of Ca^{2+} were different from those corresponding to the samples incubated with Mg^{2+} (Figure 26). In the presence of Mg^{2+} the main digestion product was a 48 kDa fragment with N-terminal sequence ^{266}KKLV. This cleavage site in the protease domain (see model in Figure 26) was protected in the presence of Ca^{2+}, where a 36 kDa fragment with N-terminal sequence ^{27}GLGR was the most important band observed. Our results were consistent with the findings of Moldoveanu for m-calpain and indicated that the main conformational change induced by Ca^{2+} was the assembly of the protease domain.

Tryptophan intrinsic fluorescence

With this classic method we started to investigate the conformational changes in domain III variants. Initial measurements were performed in CB1 (without NaCl) buffer and the results obtained were not reproducible probably because scattering effects originated by the formation of protein aggregates affected the collection of fluorescence data. When assayed in buffer CB2 (containing 200 mM NaCl), a more stable signal was recorded (Figure 27) and the fluorescence changes at varying Ca^{2+} concentrations were monitored as described in C.2.3.3.6. With this method, a small difference in the $[Ca^{2+}]_{0.5}$ value could be already observed between the wild type and the mutant D405A (Table 7). This result was an initial suggestion that the acidic residues of the loop were involved in Ca^{2+}-dependent

conformational changes. The role of these residues was further investigated using a more powerful technique like the TNS fluorescence (C.2.3.3.7).
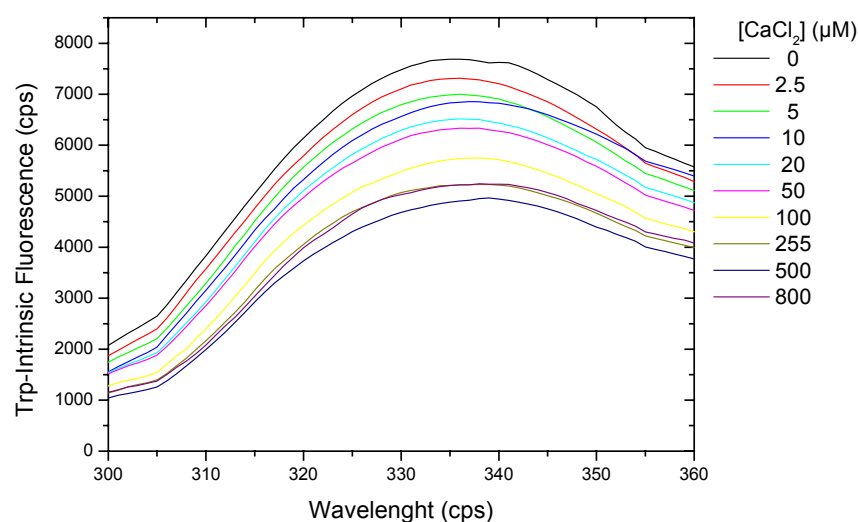
A
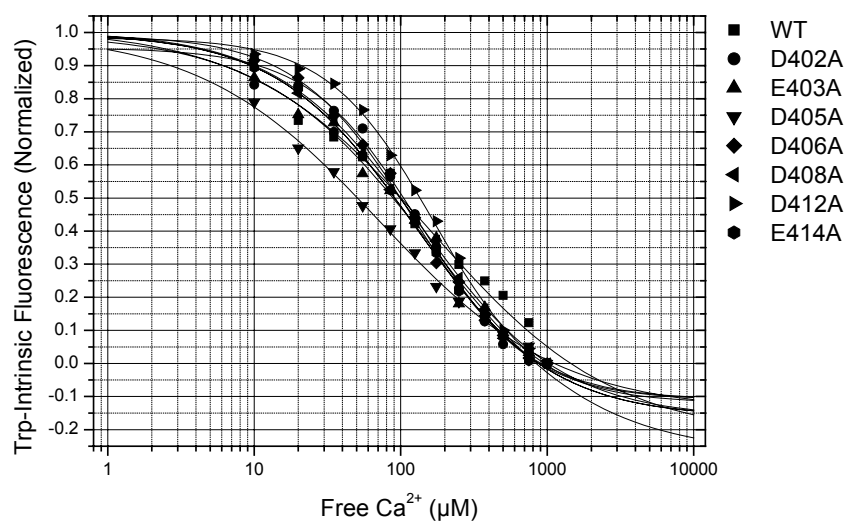
B

Figure 27. Study of Ca^{2+} induced conformational changes in recombinant heterodimeric μ-calpain (C115A) wild type and domain III acidic loop mutants by Trp intrinsic fluorescence. Panel **A** represents the emission fluorescence spectra of 0.1 μM μ-calpain (C115A) excited at 280 nm with different Ca^{2+} concentrations in buffer CB2. Panel **B** shows the corresponding semi-logarithmic plots of the normalized emission fluorescences at 340 nm against the increasing Ca^{2+} concentrations for the wild type and the acidic loop mutants. Each point represents the average of three independent measurements. Fitting of these plots to the modified Hill equation described in (C.2.3.3.6) yielded the $[Ca^{2+}]_{0.5}$ values presented in Table 7.

Table 7. Half-maximal Ca^{2+} concentrations ($[Ca^{2+}]_{0.5}$) required for Trp intrinsic fluorescence changes in µ-calpain (C115A) wild type and its domain III acidic loop variants

Variant	In CB2 (50 mM Tris, 200 mM NaCl)	
	$[Ca^{2+}]_{0.5}$ (µM)	Hill coefficient
WT	139.0 ± 18.0	0.7 ± 0.1
D402A	135.3 ± 15.5	1.1 ± 0.1
E403A	157.9 ± 59.5	0.8 ± 0.1
D405A	81.3 ± 9.3	0.7 ± 0.0
D406A	121.1 ± 7.5	1.1 ± 0.1
D408A	135.0 ± 8.1	0.9 ± 0.0
D412A	166.0 ± 11.0	1.2 ± 0.1
E414A	123.8 ± 8.8	0.9 ± 0.0

TNS fluorescence

Due to the fluorescence properties of TNS, this method constitutes a much more sensitive alternative to the Trp intrinsic fluorescence for the study of conformational changes in proteins. Therefore the role of the domain III acidic loop in the Ca^{2+} induced conformational changes was further investigated by creating TNS-µ-calpain (C115A) complexes and monitoring the TNS fluorescence changes at increasing Ca^{2+} concentrations (C.2.3.3.7). Reproducible fluorescence spectra were recorded using buffers with and without NaCl (Figure 28, A). The logarithmic plot of the emission fluorescence values against the different Ca^{2+} concentrations followed by fitting to the modified Hill equation yielded a sigmoidal curve (Figure 28, B) and the $[Ca^{2+}]_{0.5}$ values derived from them revealed significant differences among the variants when assayed in buffer lacking NaCl and almost no differences when assayed in a buffer containing 200 mM NaCl (Table 8) These results were further evidence for the involvement of the domain III acidic loop in conformational changes required for activation of the enzyme.
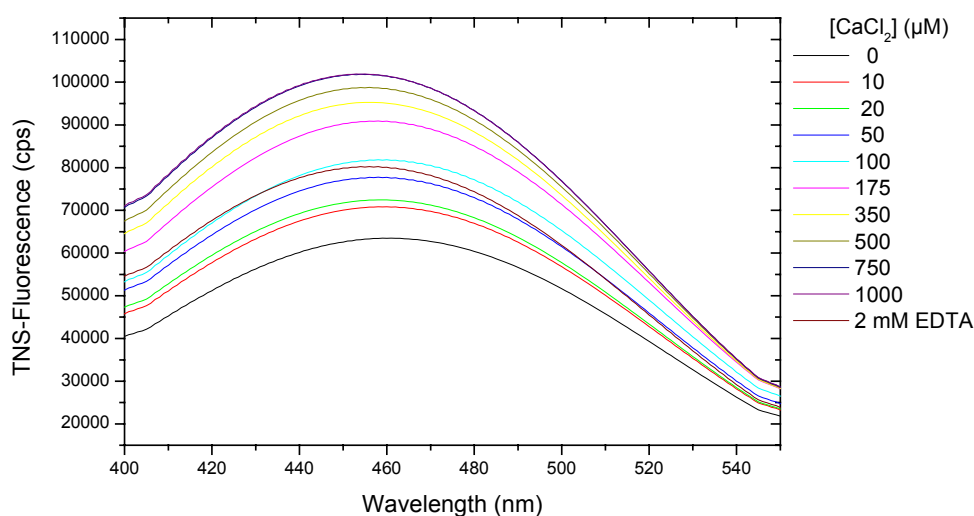
A
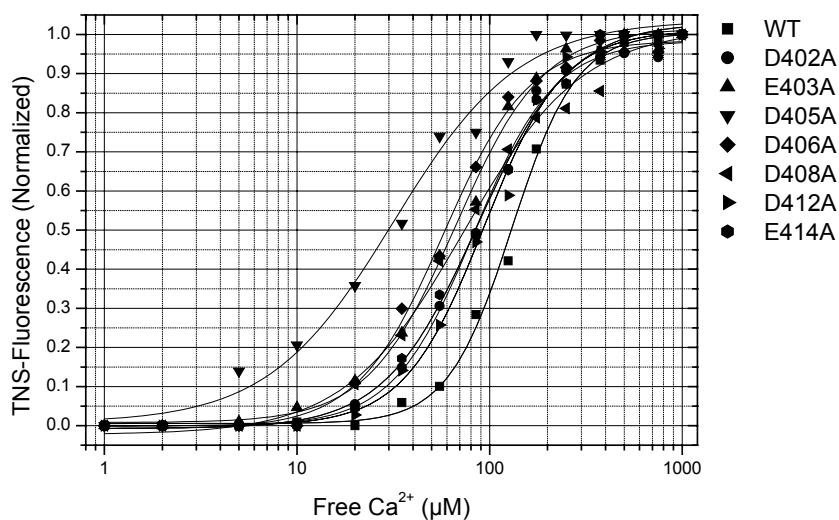
B

Figure 28. Study of Ca^{2+}-induced conformational changes in recombinant µ-calpain (C115A) by TNS fluorescence. Panel **A** represents the emission fluorescence spectra of 0.1 µM µ-calpain (C115A) excited at 320 nm at increasing Ca^{2+} concentrations in buffer CB1. Panel **B** shows the corresponding semi-logarithmic plots of the average normalized maximum emission fluorescences at 435 nm against the increasing Ca^{2+} concentrations for the (C115A) wild type and the (C115A) acidic loop mutants. Each point represents the average of three independent measurements. Fitting of these plots to the modified Hill equation described in (C.2.3.3.6) yielded the $[Ca^{2+}]_{0.5}$ values presented in Table 8.

Table 8. Half-maximal Ca^{2+} concentrations ($[Ca^{2+}]_{0.5}$) required for TNS fluorescence changes in μ-calpain (C115A) wild type and its domain III acidic loop variants

Variant	In CB1 (50mM Tris)		In CB2 (50mM Tris, 200mM NaCl)	
	$[Ca^{2+}]_{0.5}$ (μM)	Hill coefficient	$[Ca^{2+}]_{0.5}$ (μM)	Hill coefficient
WT	130.6 ± 3.8	2.6 ± 0.2	154 ± 10	1.8 ± 0.2
D402A	82.8 ± 2.7	2.1 ± 0.1	140 ± 6	1.4 ± 0.1
E403A	66.7 ± 2.5	1.9 ± 0.1	133 ± 14	1.4 ± 0.2
D405A	31.7 ± 3.0	1.3 ± 0.2	132 ± 9	1.6 ± 0.2
D406A	57.7 ± 2.1	2.0 ± 0.1	174 ± 26	1.2 ± 0.2
D408A	73.5 ± 5.6	1.4 ± 0.1	176 ± 13	1.8 ± 0.2
D412A	93.0 ± 4.1	2.1 ± 0.2	145 ± 17	1.5 ± 0.3
D414A	86.5 ± 3.1	1.8 ± 0.1	144 ± 20	1.3 ± 0.3

Light Scattering

Ca^{2+}-dependent calpain aggregation has been postulated to be the consequence of conformational changes leading to exposure of hydrophobic regions (Pal *et al.,* 2001). Following this idea, we reasoned that measuring the formation of aggregates at increasing Ca^{2+} concentrations constitutes an indirect method to monitor conformational changes in μ-calpain (C115A). First it was demonstrated that the formation of large soluble aggregates measured with the right angle light scattering technique is strictly Ca^{2+}-dependent and reversible by EDTA and $[NaCl] \geq 100$ mM. This observation was followed by experiments in which the scattered light was measured at increasing Ca^{2+} concentrations until saturation was reached. Logarithmic plotting of the values obtained and fitting to the modified Hill equation (Figure 29) allowed to determine half-maximal Ca^{2+} concentrations for changes in the scattered light intensity ($[Ca^{2+}]_{0.5}$). As it had been previously observed with the TNS fluorescence method, domain III acidic loop mutants showed substantial differences in $[Ca^{2+}]_{0.5}$ when compared to the wild type (Table 9). The $[Ca^{2+}]_{0.5}$ values were surprisingly 2-3 fold lower than those determined by TNS fluorescence.
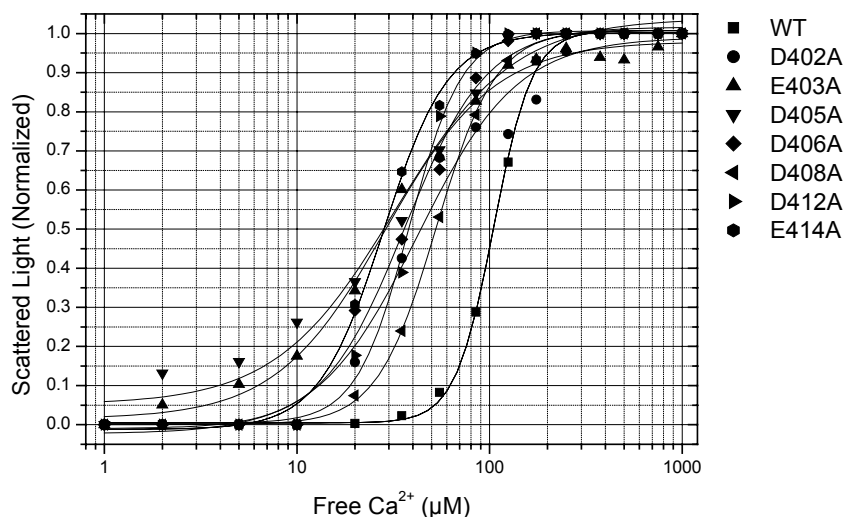
Figure 29. Semi-logarithmic plot of the average normalized Ca^{2+}-dependent changes in the 320 nm light scattered by 0.1 μM recombinant μ-calpain (C115A) wild type and acidic loop mutants. Each point represents the average of three independent measurements. Fitting of these plots to the modified Hill equation described in (C.2.3.3.7) yielded the $[Ca^{2+}]_{0.5}$ values presented in Table 9.

Table 9. Half-maximal Ca^{2+} concentrations ($[Ca^{2+}]_{0.5}$) required for scattered light changes in μ-calpain (C115A) wild type and its domain III acidic loop variants

Variant	In CB1 (50 mM Tris)	
	$[Ca^{2+}]_{0.5}$ (μM)	Hill coefficient
WT	105.2 ± 1.1	4.3 ± 0.2
D402A	42.3 ± 4.0	1.7 ± 0.2
E403A	28.7 ± 1.6	1.5 ± 0.1
D405A	32.1 ± 3.4	1.4 ± 0.2
D406A	36.3 ± 1.9	2.0 ± 0.2
D408A	52.8 ± 0.6	2.8 ± 0.1
D412A	38.3 ± 1.0	3.2 ± 0.2
E414A	28.1 ± 0.8	2.6 ± 0.2

D.3.2. Study of membrane binding

Sedimentation of protein-liposome complexes

This technique (C.2.3.3.2), commonly used for the study of membrane docking of C2 domains (Perisic *et al.,* 1999; Fukuda *et al.,* 2002), served to estimate qualitatively the phospholipid binding of our purified μ-calpain variants. Due to relatively low centrifugation

speeds, the presence of protein in the pellets (Figure 30, A) can only be attributed to aggregation or binding to phospholipid vesicles which are known to sediment at low speeds. Even when the aggregation phenomenon greatly interfered in the observations, an increase of the quantity of protein pelleted in the presence of $CaCl_2$ and lipid vesicles could be measured via densitometry (Figure 30, B). Interestingly this membrane binding was strictly Ca^{2+}-dependent, because Mg^{2+} did not produce the same effect. As reported for some C2 domains (Perisic *et al.,* 1999), membrane docking was prevented by high ionic strengths. Using this method it was not possible to establish significant differences between the membrane binding levels of the wild type and the domain III acidic loop mutants. Comparison of binding to PC, PG and PS liposomes did not show any special preference of µ-calpain (C115A) for one of these phospholipids.
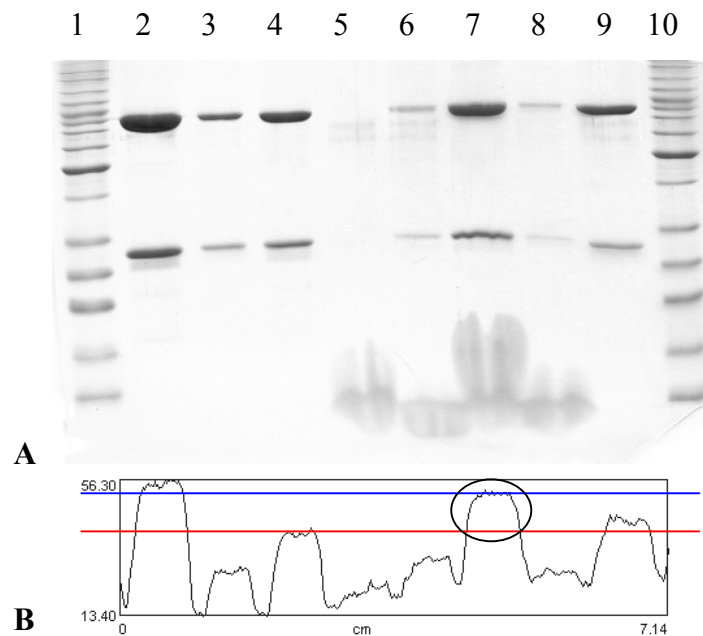
Figure 30. Panel A: 12.5 % SDS-PAGE showing differential sedimentation of recombinant µ-calpain (C115A) and PC large multilamellar vesicles. With the exception of markers and controls, all the samples shown are centrifugation (15 min, 12000 rpm) pellets after 30 min incubation at RT: Lanes **1** and **10**: Invitrogen's Bench Mark™ protein ladder. Lane **2**: 5 µg control µ-calpain (C115A). Lane **3**: pellet from 5 µg µ-calpain (C115A). Lane **4**: pellet from 5 µg µ-calpain (C115A) incubated with 1 mM $CaCl_2$. Lane **5**: pellet from 200 µg PC LMVs. Lane **6**: pellet from 5 µg µ-calpain (C115A) incubated with 200 µg PC LMVs. Lane **7**: pellet from 5 µg µ-calpain (C115A) incubated with 1 mM $CaCl_2$ and 200 µg PC LMVs. Lane **8**: pellet from 5 µg µ-calpain (C115A) incubated with 1 mM $MgCl_2$ and 200 µg PC LMVs. Lane **9**: pellet from 5 µg µ-calpain (C115A) incubated with 1 mM $MgCl_2$ and 200 µg PC LMVs in a buffer containing 1 M NaCl. Panel B shows the densitometry plot from lanes **2** to **9**. The red line indicates the fraction of protein pelleted due to Ca^{2+}-induced aggregation effects (lane **4**) whereas the blue line shows the protein pelleted in the presence of Ca^{2+} and phospholipids (lane **7**). The circle indicates the fraction from the total amount of µ-calpain (C115A) (lane **2**) which interacts with phospholipids in a Ca^{2+}-dependent fashion.

Protein to membrane FRET

Sedimentation assays roughly suggested the ability of μ-calpain to bind to phospholipids, but did not reveal the molecular mechanisms of this phenomenon. In order to gain more insight in how μ-calpain binds to biological membranes and to test the postulated role of the domain III acidic loop in this mechanism we used a more accurate fluorescence-based technique. Its principle was to measure the energy transfer between the Trp residues of the protein and Dansyl labeled lipids embedded in small unilamellar vesicles of different composition (C.2.3.3.1). The results obtained confirmed the observation that μ-calpain binds lipid vesicles in a Ca^{2+}-dependent manner. Spectra showing a clear increase in the lipid binding of μ-calpain in the presence of $CaCl_2$ were recorded using vesicles composed by PC:PG (Figure 31, A), PC:PE, PC:PS, PC:PI and PC alone (data not shown). Measuring the energy transferred from μ-calpain to the dansyl-labeled vesicles at different Ca^{2+} concentrations (Figure 31, B), logarithmic plotting and fitting to the modified Hill equation described in C.2.3.6, allowed to calculate the calcium concentrations required for half-maximal lipid binding (Table 10). Surprisingly domain III acidic loop mutants behaved similarly as they did in the conformational changes studies. These results suggested that membrane binding of μ-calpain to lipid vesicles also requires structural rearrangements in the molecule and that domain III with its acidic loop is involved in this process. Unfortunately due to the high quantities of protein required, it was not possible to study the affinity of μ-calpain for this vesicles and calculate affinity constants. This aspect was later investigated using BIAcore technology.

Table 10. Half-maximal Ca^{2+} concentrations ($[Ca^{2+}]_{0.5}$) required for protein to membrane FRET changes in μ-calpain (C115A) wild type and its domain III acidic loop variants

Variant	$[Ca^{2+}]_{0.5}$ (μM) In CB1 (50 mM Tris)	Hill coefficient
WT	97.1 ± 1.5	2.8 ± 0.1
D402A	50.9 ± 1.5	2.2 ± 0.1
E403A	29.4 ± 2.5	1.9 ± 0.3
D405A	41.5 ± 0.6	2.8 ± 0.1
D406A	43.8 ± 1.2	2.5 ± 0.2
D408A	58.1 ± 2.1	2.5 ± 0.2
D412A	58.1 ± 2.6	2.5 ± 0.3
E414A	50.1 ± 2.1	2.1 ± 0.2

A

B
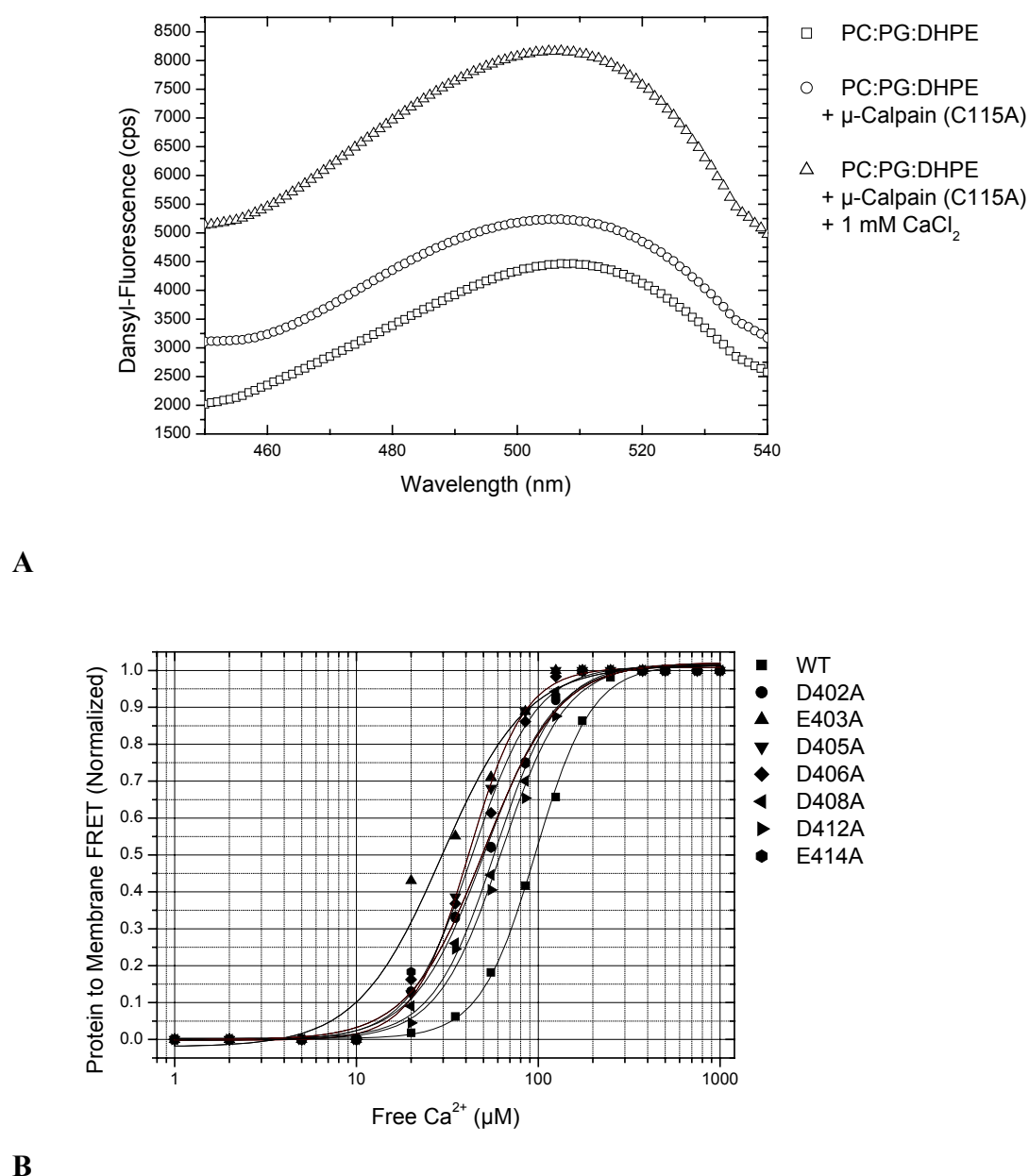
Figure 31. Study of Ca^{2+}-dependent interaction of μ-calpain with dansyl-labeled liposomes. **A**: Spectra showing the fluorescence energy transfer from the Trp residues present in 0.1 μM μ-calpain (C115A) to dansyl groups of 10 μM PC:PG:Dansyl-DHPE vesicles in the abscence and presence of 1 mM $CaCl_2$. Labeled liposomes have a well defined emission spectrum with λmax (em) ~ 510 nm when excited at 280 nm (squares). The incorporation of μ-calpain to the cuvette (circles) is characterized by a small change in the dansyl fluorescence. The addition of 1 mM $CaCl_2$ to the reaction yields an increase in the dansyl fluorescence originated by Ca^{2+}-dependent membrane binding (triangles). Panel **B** shows the semi-logarithmic plots of the average normalized maximum Trp fluorescence transferred to the dansyl labeled liposomes against increasing Ca^{2+} concentrations for the wild type and the acidic loop mutants. Each point represents the average of three independent measurements. Fitting of these plots to the modified Hill equation described in (C.2.3.3.6) (continuous line) yielded the $[Ca^{2+}]_{0.5}$ values presented in Table 10.

SPR measurements

The use of the surface plasmon resonance technology allowed a better characterization of *in vitro* membrane binding of μ-calpain. First we confirmed the Ca^{2+} dependency of the binding in an experiment in which at increasing Ca^{2+} concentrations a constant quantity of enzyme was passed over the liposomes immobilized on the L1-chip. As illustrated in Figure 32, A, there was a Ca^{2+}-dependent increase of the binding of μ-calpain to liposome vesicles. Obtained response units were plotted in a semi-logarithmical representation as a function of the Ca^{2+} concentrations and fitted to the modified Hill equation. This allowed us to determine the $[Ca^{2+}]_{0.5}$ values for the membrane binding of the heterodimeric wild type μ-calpain and the acidic loop mutant D405A. The Ca^{2+} requirements (shown in Table 11) confirmed the results obtained with the FRET measurements. Interestingly these $[Ca^{2+}]_{0.5}$ values remained unaltered as vesicles of diverse composition were tested, indicating that the phospholipid headgroup has no influence on the Ca^{2+} requirement for membrane binding. The same observation was made when the binding to nuclear envelope and plasma membrane mimicking vesicles was analyzed. In a second set of experiments the affinity for various immobilized vesicles was determined by injecting varying concentrations of protein at a constant Ca^{2+} concentration of 1 mM. A rapid association rate in the order of 10^5 $M^{-1}s^{-1}$ was measured with a slow dissociation rate (10^{-4} s^{-1}), indicating a relatively high affinity in the low nanomolar range. Table 12 shows the rate constants and the K_D values calculated using the Langmuir 1:1 model for the heterodimeric wild type μ-calpain (C115A) and the acidic loop D405A mutant. Interestingly the latter mutation in the acidic loop of domain III did not modify the affinity of μ-calpain for the artificial membranes. Among the different phospholipid compositions studied, no preference for a specific headgroup or vesicle composition was observed.

A

B
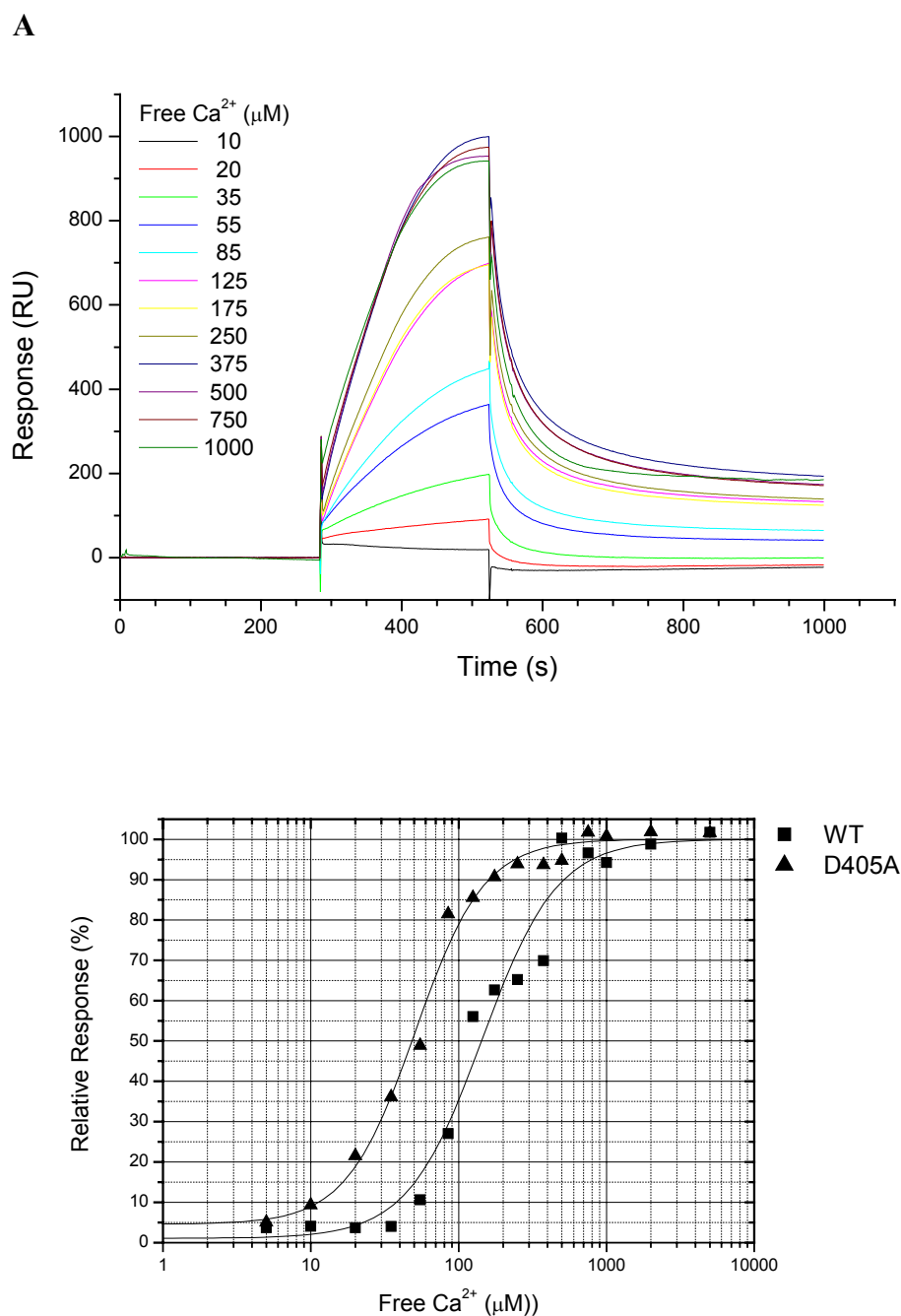
Figure 32. SPR measurement of Ca^{2+}-dependent association of heterodimeric μ-calpain (C115A) with immobilized liposomes. **A**: Overlay plots of original BIAcore sensorgrams ("bulk" effect from buffer not substracted) corresponding to the addition of 50 nM wild type enzyme at different Ca^{2+} concentrations to plasma membrane mimicking liposome vesicles coated onto the L1-chip. **B**: Semi-logarithmic plot of the relative response changes against the Ca^{2+} concentrations corresponding to the wild type and the D405A mutant (measured with PC:PE vesicles). Each point represents the average of three independent measurements. Fitting to the modified Hill equation (sigmoidal line) yielded $[Ca^{2+}]_{0.5}$ values of 145 ± 17.9 and 51± 3.3 μM respectively.

Table 11. Half-maximal Ca^{2+} concentrations ($[Ca^{2+}]_{0.5}$) required for the binding of μ-calpain (C115A) wild type and mutant D405A to immobilized liposome vesicles determined by SPR analysis.

Analyte (Variant)	Ligand (Lipid Vesicle)	$[Ca^{2+}]_{0.5}$ (μM)	Hill coefficient
WT 80K28K	PC/PE 60:40	125 ± 19.0	1.7 ± 0.39
	PC/PS 60:40	117 ± 17.4	1.76 ± 0.39
	PC/PG 60:40	135 ± 19.6	1.6 ± 0.32
	PC 100	106 ± 16.1	1.9 ± 0.47
	PC/PE/PS 60:20:20	111 ± 5.7	2.3 ± 0.24
	PC/PE/PS/PI 60:20:18:2	115 ± 6.3	2.3 ± 0.25
	PC/PE/PS/PIP 60:20:18:2	109 ± 5.7	2.2 ± 0.23
	PC/PE/PS/PIP$_2$ 60:20:18:2	108 ± 5.3	2.2 ± 0.21
	Plasma membrane-like	99 ± 2.5	2.2 ± 0.21
	Nuclear membrane-like	111 ± 8.8	1.8 ± 0.07
D405A 80K28K	PC/PE 60:40	51 ± 3.3	1.9 ± 0.21
	PC/PS 60:40	46 ± 6.0	1.7 ± 0.21
	PC/PG 60:40	47 ± 10.3	1.5 ± 0.21
	PC 100	41 ± 16.1	1.8 ± 0.14
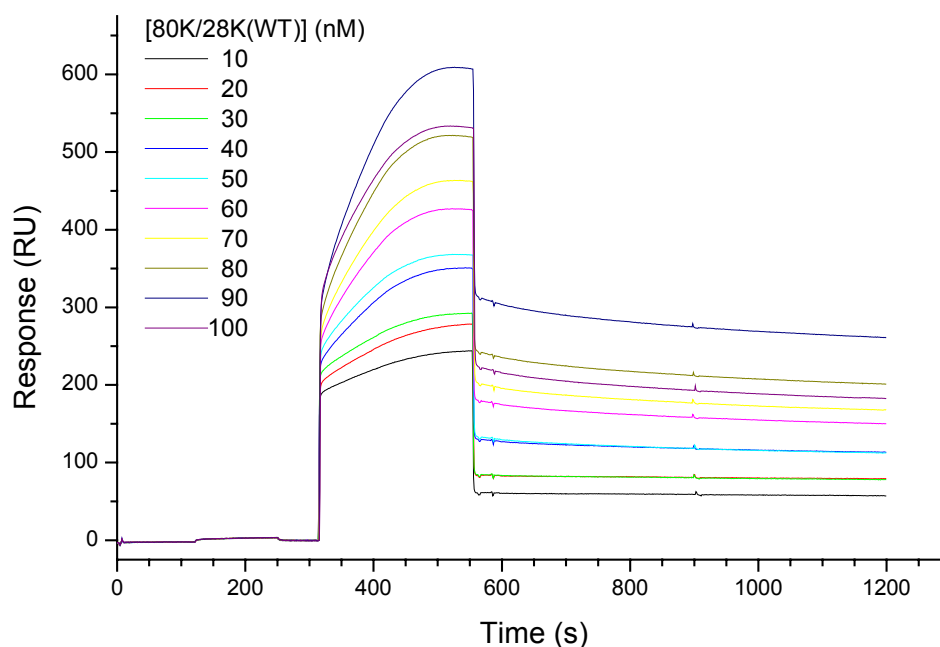
Figure 33. SPR study of the binding kinetics of heterodimeric μ-calpain (C115A) to immobilized liposomes: Overlay plots of original BIAcore sensorgrams ("bulk" effect from buffer not substracted) corresponding to the addition of increasing concentrations of μ-calpain (C115A) at a Ca^{2+} concentration of 1 mM to plasma membrane mimicking liposome vesicles coated onto the L1-chip. Rate constants were calculated with the BIAcore evaluation program as described in C.2.3.3.10. Results are shown in table 12.

Table 12. Phospholipid binding parameters of μ-calpain wild type and domain III mutant D405A determined by SPR analysis.

Analyte (Variant)	Ligand (Lipid Vesicle)	k_a ($M^{-1}s^{-1}$)	k_d (s^{-1})	K_D (nM)
WT 80K28K	PC/PE 60:40	$(1.4 \pm 0.3) \times 10^5$	$(3.8 \pm 1.0) \times 10^{-4}$	2.7 ± 0.92
	PC/PS 60:40	$(1.2 \pm 0.1) \times 10^5$	$(2.8 \pm 0.2) \times 10^{-4}$	2.3 ± 0.25
	PC/PG 60:40	$(1.4 \pm 0.2) \times 10^5$	$(4.5 \pm 0.5) \times 10^{-4}$	3.2 ± 0.58
	PC 100	$(1.6 \pm 0.1) \times 10^5$	$(4.0 \pm 0.5) \times 10^{-4}$	2.5 ± 0.35
	PC/PE/PS 60:20:20	$(1.8 \pm 0.17) \times 10^5$	$(4.1 \pm 0.63) \times 10^{-4}$	2.3 ± 0.41
	PC/PE/PS/PI 60:20:18:2	$(1.5 \pm 0.22) \times 10^5$	$(3.0 \pm 0.57) \times 10^{-4}$	2.0 ± 0.48
	PC/PE/PS/PIP 60:20:18:2	$(1.6 \pm 0.24) \times 10^5$	$(3.9 \pm 0.98) \times 10^{-4}$	2.4 ± 0.70
	PC/PE/PS/PIP$_2$ 60:20:18:2	$(1.6 \pm 0.22) \times 10^5$	$(4.2 \pm 1.10) \times 10^{-4}$	2.6 ± 0.77
	Plasma membrane-like	$(1.5 \pm 0.17) \times 10^5$	$(2.2 \pm 0.03) \times 10^{-4}$	1.3 ± 0.15
	Nuclear membrane-like	$(1.6 \pm 0.21) \times 10^5$	$(2.7 \pm 0.25) \times 10^{-4}$	1.7 ± 0.27
D405A 80K28K	PC/PE 60:40	$(1.1 \pm 0.1) \times 10^5$	$(3.0 \pm 0.6) \times 10^{-4}$	2.7 ± 0.59
	PC/PS 60:40	$(1.1 \pm 0.03) \times 10^5$	$(2.7 \pm 0.8) \times 10^{-4}$	2.5 ± 0.74
	PC/PG 60:40	$(1.0 \pm 0.1) \times 10^5$	$(3.3 \pm 0.8) \times 10^{-4}$	3.3 ± 0.87
	PC 100	$(1.1 \pm 0.03) \times 10^5$	$(4.2 \pm 0.7) \times 10^{-4}$	3.8 ± 0.64

D.4. Expression of active μ-calpain domain III acidic loop mutants using the baculovirus expression system

In order to test the Ca^{2+} requirement for enzymatic activity of the domain III acidic loop mutants it was necessary to revert the inactivating mutation of Cys 115 to Ala in their protease domains. This was achieved by exchanging the synthetic cassette coding for domains

I and II from the variants with the corresponding DNA fragment from the original semi-synthetic μ-calpain gene (Gil-Parrado, 2001).

D.4.1. Construction of the transfer vectors

The creation of the new baculovirus transfer vectors bearing the domain III acidic loop mutated active μ-calpains required digestion of the semi-synthetic human μ-calpain gene cloned in pUC18 (Gil-Parrado, 2001) and the acidic loop mutated μ-calpains in pVL1392 and ligation of the DNAs as previously described (C.2.2.12.). Unique sites *EcoRI* and *XbaI* were selected and the fragment swapping was successfully finished by ligation of the excised protease domain fragment into the open vectors (Figure 34). Restriction analysis (Figure 34) and DNA sequencing corroborated the intact reading frame as well as the restitution of the active site Cys.

D.4.2. Generation and identification of recombinant baculoviruses

The generation and identification of recombinant baculoviruses coding for the active μ-calpain variants was performed using the same methods employed for the original mutants with identical results. Cotransfection of the created transfer vectors with BaculoGold™ virus DNA rendered recombinant baculoviruses bearing the μ-calpain large subunit gene. As well as for the original mutants, the DNA fragment corresponding to the 80K subunit was PCR-amplified from viral DNA preparations using both the polyhedrin primers and specific 80K primers (Figure 35). The recombinant baculoviruses were amplified in four rounds as described and the virus stocks with titers ranging between 1 and 2 x 10^7 pfu/ml were stored at 4 ^{o}C until use for protein production.
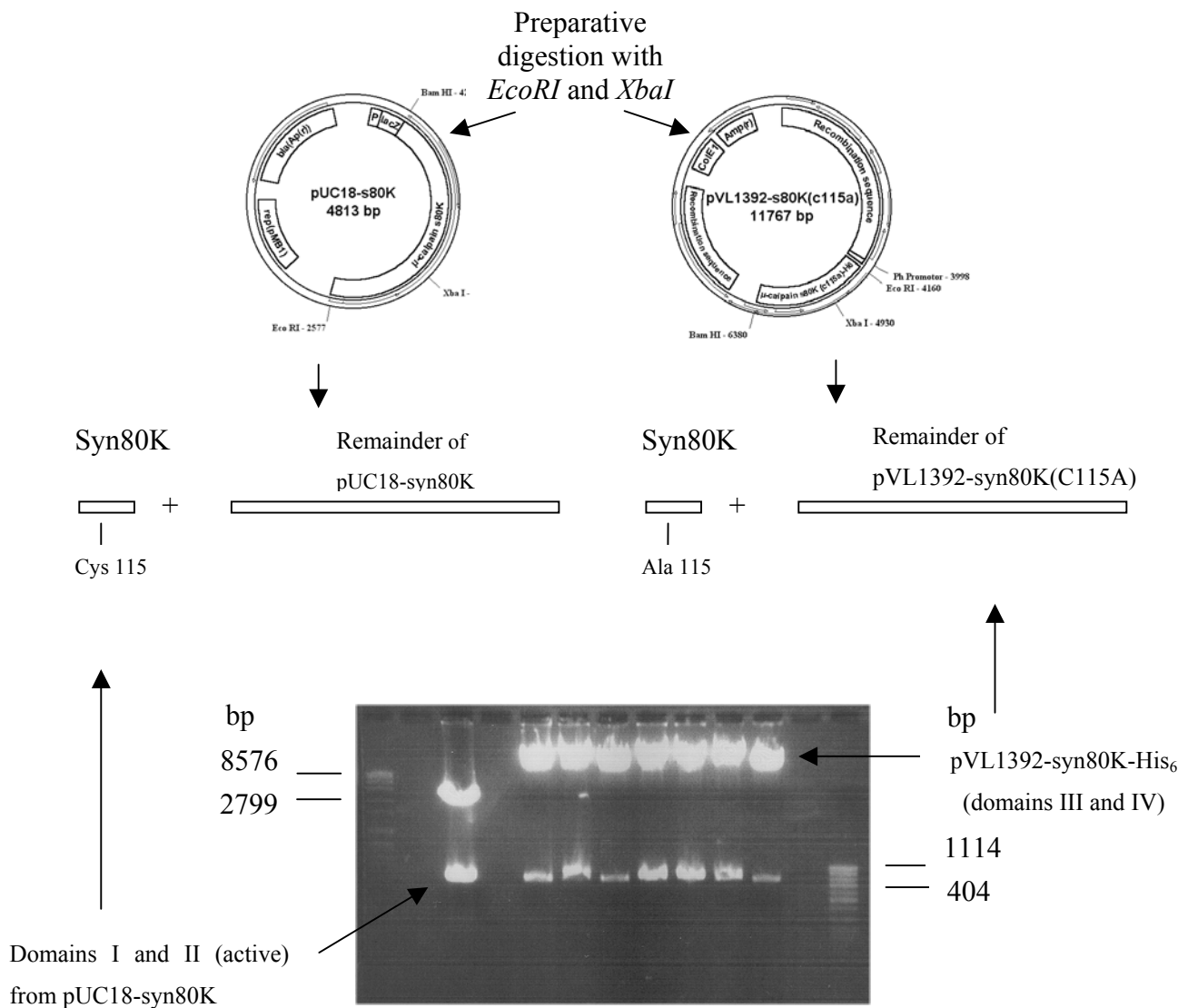
Figure 34. Schematic representation of the generation of active μ-calpain variants. Synthetic cassettes coding for domains I and II were excised from pUC18-syn80K and pVL 1392-syn80K (C115A)-His₆ vectors by digestion with Eco R/*XbaI*. The 2% agarose gel electrophoresis shows the separation of the resulting DNA fragments. Lanes **1** and **10** represent the Roche molecular length markers VII and VIII respectively. Lane **2** shows the digested pUC18-syn80K. Lanes **3** to **9** represent digested pVL1392syn80K (C115A)-His₆ vectors coding for the wild type and the mutants D402A, E403A, D405A, D406A, D408A, D412A and E414A. The active cassette (lane **2**, lower band) and the remainder from pVL1392-syn80K (C115A)-His₆ vectors (lanes **3** to **9**, upper bands) were purified from the gel and ligated. The resulting plasmids were similar to the parent but containing a codon for Cys at position 115.
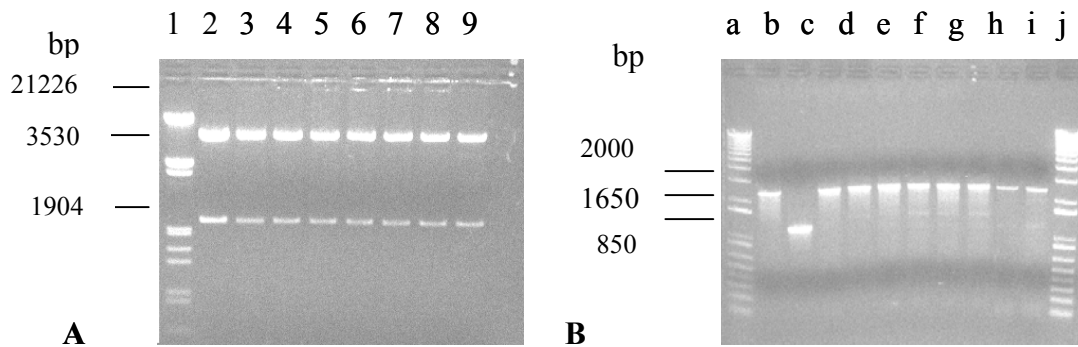
Figure 35. A: 1% Agarose gel showing *EcoRI/BamHI* restriction analysis of the pVL1392syn80K-His$_6$ vector and its domain III acidic loop variants used for the production of recombinant baculoviruses. Lane **1**: Roche molecular length marker III. Lanes **2** to **9**: wild type and mutants D402A, E403A, D405A, D406A, D408A, D412A, E414A. Right panel **B**: 1% agarose gel with the PCR identification of the generated recombinant viruses (lanes **c** to **i**). As controls were set pVL1392syn80K-His$_6$ (lane **b**) and DNA from control virus coding for Xyl E protein (lane **c**). Invitrogen´s 1 kb plus DNA ladder appears on lanes **a** and **j**.

D.4.3. Expression and characterization of the mutants

Due to the reported difficulties to isolate active recombinant µ-calpain (Pfeiler, 2001) preparative scale expression of the active calpain variants was not performed in this work. The active domain III acidic loop mutants as well as the wild type were instead expressed in culture plates at analytic scale. Purification of the recombinant proteins was not attempted, but activity measurements of the cell lysates (C.2.3.3.5) proved to be accurate enough for the functional analysis of the calpain variants. SDS-PAGE of these lysates previously stored for 24 hours at –20 °C followed by immunoprinting with a monoclonal antibody specific for the 80K subunit (Alexis) confirmed the rapid autolytic degradation of the recombinant material.

Nevertheless, the main band observed corresponded to 80 kDa, suggesting that still an important quantity of the expressed protein was intact. This observation was further confirmed by a zymography analysis (Figure 36). Using this technique however, we observed a dramatic degradation of the samples within few weeks (data not shown). The following kinetic experiments were therefore performed with freshly prepared lysates whenever possible. Alternatively, lysates were stored at –80 °C, but no longer than one week.
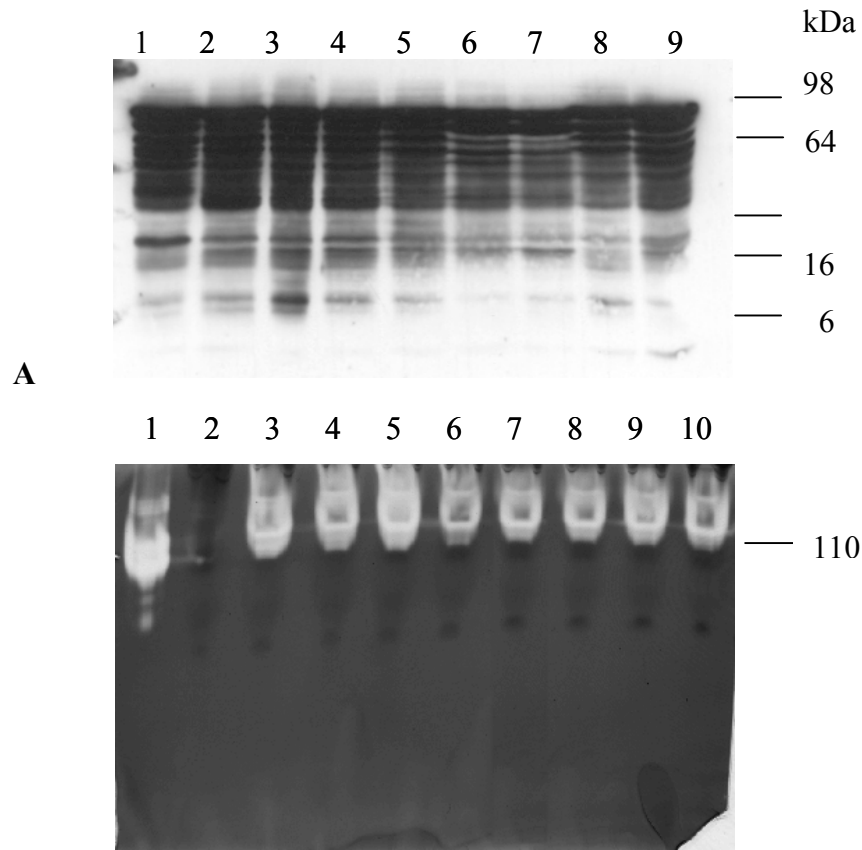
Figure 36. Panel **A**: Western Blot analysis of the cell lysates from *Sf21* cells over-expressing active μ-calpain variants. As positive control, 1 μg of μ-calpain purified from human erythrocytes (Gabrijelcic-Geiger *et al.,* 2001) was loaded in lane **1**. In lanes **2**, **3**, **4**, **5**, **6**, **7**, **8** and **9** appear wild type and mutants D402A, E403A, D405A, D406A, D408A, D412A and E414A respectively. Panel **B** shows a casein zymogram from the same lysates (lanes **3-10**) and positive control (lane **1**). As negative control was used a lysate from uninfected *Sf21* cells (lane **2**).

Analysis of the Ca^{2+} requirement for activity of the acidic loop mutants

Lysates of *Sf21* cells infected with the viruses coding for the wild type μ-calpain and domain III mutants showed a Ca^{2+}-dependent degradation of SLY-AMC not observed in the non infected cells (data not shown). This activity was almost completely inhibited by the addition of recombinant calpastatin domain 1 (Figure 37), supporting that the expressed μ-calpain present in the lysates was the enzyme processing the synthetic substrate. In order to characterize each acidic loop mutant, we collected both the initial rates, $v_{initial}$, (during the first 10 min in Figure 37) and maximum reaction velocities, $v_{maximum}$, (before addition of CD1 in Figure 37) of a series of measurements at different Ca^{2+} concentrations ranging from 0 to 1000 μM and subtracted the residual activity not inhibited by calpastatin. As in the case of the fluorescence measurements, semi-logarithmic plotting of the relative activity against the

corresponding Ca^{2+} concentrations allowed to calculate the [Ca^{2+}]$_{0.5}$ values for activation of the enzyme (Figure 38 and Table 13). A reduction in this parameter in the acidic loop mutants, in the same proportions as for conformational changes, confirmed the involvement of this region in calpain activation. Interestingly the [Ca^{2+}]$_{0.5}$ values of the acidic loop mutants were approximately the same at the beginning and at the end of the activity measurement, whereas the wild type shifted to a lower Ca^{2+} requirement (Table 13). This result indicates that autolytic activation of calpain takes place much faster in the acidic loop mutants and provides additional support for the role of the Ca^{2+}-mediated disruption of the electrostatic interactions at the interface between subdomain IIb and domain III.
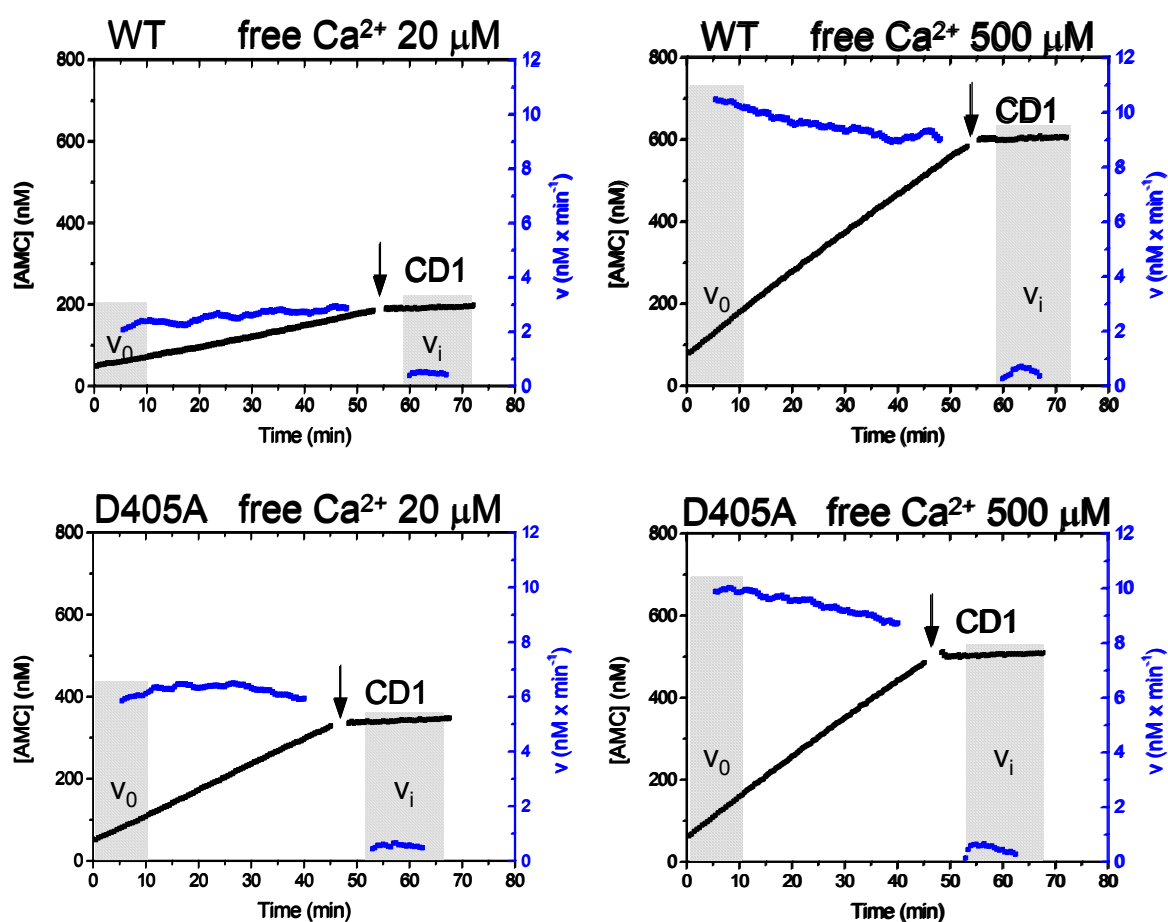
Figure 37. Continuous fluorogenic assays of μ-calpain WT and mutant D405A at 20 μM and 500 μM free calcium concentrations. CD1: addition of recombinant calpastatin domain 1 (100 nM), a specific inhibitor for calpain; v_0: rate (nM x min^{-1}) calculated from the initial 10 min of the assay; v_i: residual rate of non-calpain activity after addition of calpastatin domain 1 (hatched areas).
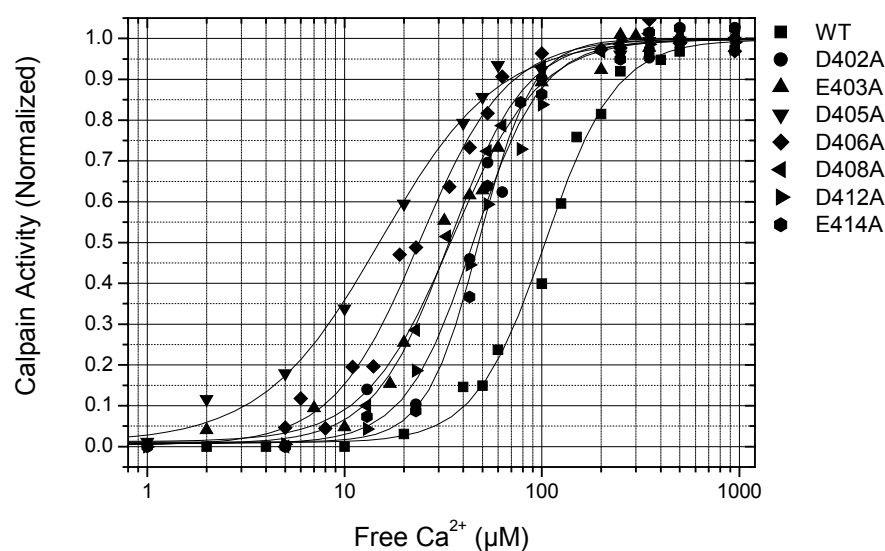
Figure 38. Semi-logarithmic plot of the average normalized Ca^{2+}-dependent calpain activity for wild type and acidic loop mutants. Activity was calculated as the difference $v_o - v_i$ from single experiments at different calcium concentrations and normalized to maximal activity. Each point represents the average of three independent measurements. The calcium concentration for half-maximal activity, $[Ca^{2+}]_{0.5}$, was estimated by non-linear square fitting of these data with the modified Hill equation.

Table 13. Ca^{2+} requirement for half-maximal activity of μ-calpain wild type and acidic loop mutants at initial and maximal rates.

	$v_{initial}$		$v_{maximum}$	
	$[Ca^{2+}]_{0.5}$ (μM)	Hill coefficient	$[Ca^{2+}]_{0.5}$ (μM)	Hill coefficient
WT	104.4 ± 4.9	2.4 ± 0.22	49.5 ± 2.9	2.8 ± 0.45
D402A	44.9 ± 3.4	2.5 ± 0.48	35.7 ± 2.8	2.6 ± 0.45
E403A	34.9 ± 2.0	2.0 ± 0.21	29.2 ± 2.0	1.7 ± 0.19
D405A	15.2 ± 1.1	1.5 ± 0.12	14.6 ± 1.1	1.9 ± 0.25
D406A	24.0 ± 1.5	2.0 ± 0.20	20.0 ± 1.8	1.7 ± 0.22
D408A	34.1 ± 0.9	2.3 ± 0.12	27.7 ± 2.6	2.4 ± 0.41
D412A	46.7 ± 1.1	2.2 ± 0.11	37.7 ± 2.0	2.1 ± 0.21
D414A	48.1 ± 2.0	3.2 ± 0.43	37.5 ± 1.9	3.0 ± 0.38

D.5. Expression of μ-calpain domain V deletion mutant using the baculovirus expression system

Heterodimeric rat m-calpain lacking the glycine-rich domain V from the small subunit has been expressed successfully in *E. coli*. This mutation reportedly improves the expression levels of the enzyme and eliminates the heterogeneity originated by rapid autolysis of the 28K subunit (Elce *et al.,* 1997). In the case of μ-calpain no studies have been published showing the expression of a domain V-truncated heterodimeric enzyme. In the present work, it was attempted for the first time to express and purify recombinant human μ-calpain defective for domain V. The purpose of this mutation was to analyze the putative role of this domain in membrane binding of calpains.

D.5.1. Construction of the transfer vector

Truncated calpain small subunit (21K) was subcloned into the baculovirus transfer vector pVL1392 using available *XbaI* and *BamHI* restriction sites in both donor and acceptor vector. After cutting the DNA fragment coding for the 21K subunit from pET22-b(+)-21K and ligating it in previously digested pVL1392 the resulting recombinant vector was analyzed by restriction analysis and DNA sequencing. Correct restriction pattern and DNA sequencing with polyhedrin primers (C.1.2) confirmed the success of the subcloning procedure. The 21K gene was inserted in frame and the distance between the cloning site and the transcription start was no longer than 100 bp. The generated transfer vector (Figure 39) was prepared with a maxi-prep procedure and used for cotransfection with BaculoGold™ viral DNA.

D.5.2. Generation and identification of recombinant baculoviruses

Recombinant baculoviruses bearing the 21K gene were successfully produced as demonstrated by PCR analysis (data not shown). These viruses were directly amplified without further purification until they reached a titer of 1.2×10^7 pfu/ml in the fourth passage. The final viral stock was used to set an analytical expression in 6-well culture plates. After 72 hours of infection, the expression of the μ-calpain heterodimer lacking domain V (ΔDV) was confirmed by western blot analysis (Figure 40).

1) Cut with *BamHI* and *XbaI*

2) Purification from agarose gel of ~750 bp DNA band corresponding to 21K gene

3) Ligation of 21K gene into open pVL1392

1) Cut with *BamHI* and *XbaI*

2) Purification from agarose gel of 9632 bp band corresponding to the open vector

3) Ligation with 21K DNA from pET-22b(+)-21K
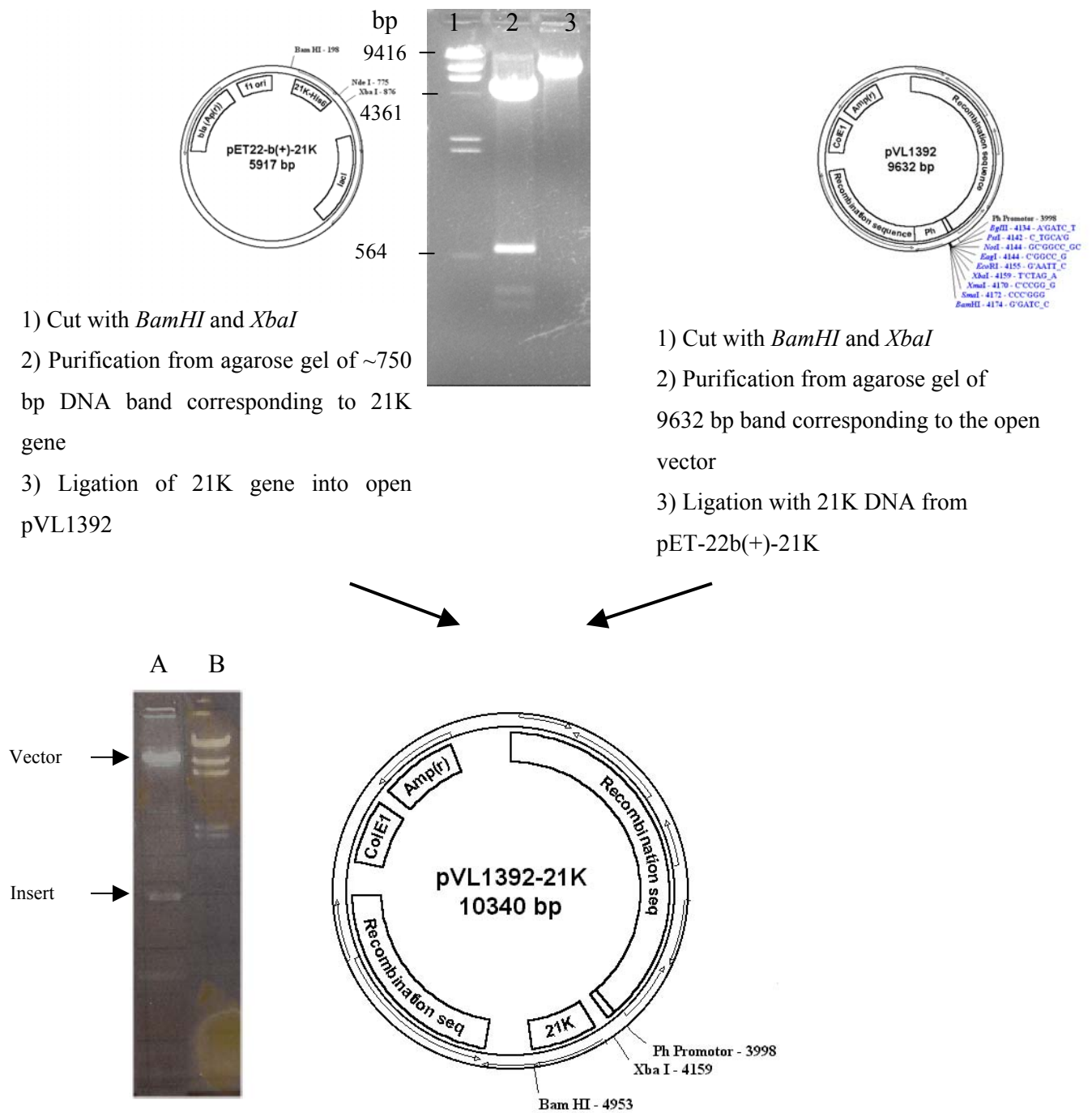
Figure 39. Subcloning of the 21K gene in pVL1392. The donor vector (upper left panel) and acceptor vector (upper right panel) were cut with *BamHI* and *XbaI*. The upper middle panel shows the 1 % agarose gel electrophoresis in which the digested DNA fragments were separated. Roche DNA lenght markers II was loaded in lane **1**. Lane **2** and lane **3** show *BamHI/Xba I* digested pET-22b(+)-21K and pVL1392 plasmids respectively. The fragments corresponding to the 21K DNA and pVL1392 were purified from this gel and ligated. The resulting transfer vector pVL1392-21K is shown in the lower panel. The features corresponding to pVL1392 have been described in the methods section (C.1.2). Truncated calpain small subunit (21K) DNA is inserted within the restriction sites *XbaI* and *BamHI* from the MCS of the vector. The distance between the *XbaI* site and the ATG from 21K is ~ 86 nucleotides, which ensures good expression levels. The accompanying 1% agarose gel (left) shows restriction analysis of the vector with the mentioned enzymes (lane **A**). Bands corresponding to open pVL1392 (vector) and 21K DNA (insert) are highlighted. Roche molecular length marker II appears on lane **B**.
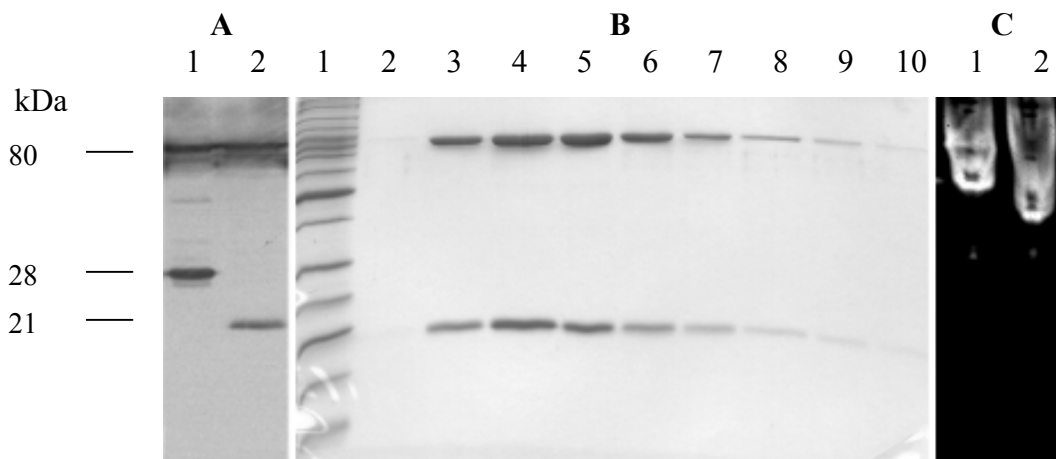
Figure 40. Expression of µ-calpain (C115A) Δ domain V. **A**: Lanes **1** and **2** show the immunoblotting of insect cell lysates over-expressing the wild type µ-calpain (C115A) and the DV deletion mutant respectively. **B**: The elution fractions of the BC-calpastatin affinity chromatography column were visualized on a 12.5 % SDS-PAGE (lanes **2** to **10**). Invitrogen's Bench Mark™ molecular weight markers were loaded in lane **1**. **C**: Casein zymogram showing the active variants of both the wild type µ-calpain (lane **1**) and the DV deletion mutant (lane **2**).

D.5.3. Expression, purification and validation of µ-calpain domain V deletion mutant

Preparative expression and isolation of this mutant was performed under the same conditions used for domain III mutants. The expression yields were 4 fold lower than for the complete heterodimer: averages of 3.5 mg of protein were isolated from ~ 1 x 10^8 infected cells in a 150 ml suspension culture. It was not attempted to improve this yield, because the quantities of protein obtained were still enough for functional analysis. Active ΔDV µ-calpain was expressed by co-infecting *Sf21* cells with the viruses coding for the active 80K subunit and the truncated small subunit respectively. Figure 40 summarizes the expression and purification of both the inactive and active variant as well as the purification of the first one on a BC-calpastatin affinity column.

Autolysis and proteolysis by native µ-calpain

Purified active site mutated heterodimeric µ-calpain (C115A) ΔDV was –as expected- unable to autolyze (data not shown). Nevertheless, when incubated with native µ-calpain

isolated from human erythrocytes the large subunit was degraded to the "classic" autolysis products (data not shown). The truncated small subunit remained resistant to extensive proteolysis by native μ-calpain. These results confirmed the proper folding of the heterodimeric ΔDV variant.

Proteolysis by chymotrypsin

As observed for the full length calpain, there were differences between the chymotryptic degradation patterns in the presence and absence of Ca^{2+} (data not shown). These results are in concordance with those reported by Moldoveanu (2001) in which inactive small subunit truncated m-calpain was differently digested by trypsin and chymotrypsin in a buffer containing $CaCl_2$ or $MgCl_2$.

D.5.4. Functional characterization of μ-calpain domain V deletion mutant

D.5.4.1. Study of Ca^{2+}-induced conformational changes

Tryptophan intrinsic fluorescence

In contradiction to what had been observed with the full length μ-calpain variants, the Trp intrinsic fluorescence of the ΔDV μ-calpain could be measured with accuracy both in the absence and in the presence of NaCl. This fact suggested that the instability of the fluorescence changes recorded in the full length variants was originated by the disordered movement of the glycine-rich domain V. More interesting were the $[Ca^{2+}]_{0.5}$ values determined for this variant (Figure 41 and Table 14). The decrease in the Ca^{2+} requirement for conformational changes to one third of those calculated for the wild type suggested an intrinsic role of domain V in the activation process of μ-calpain.
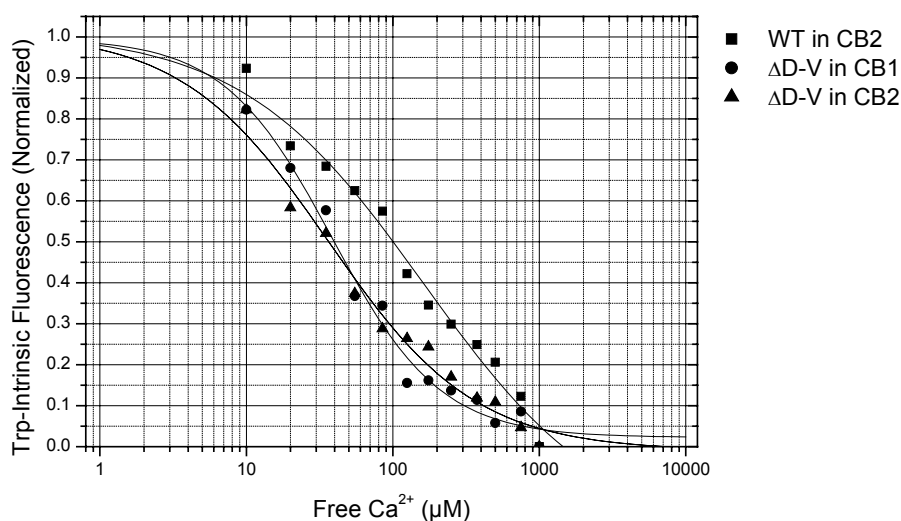
Figure. 41. Semilogarithmic plots of the average normalized emission Trp intrinsic fluorescences against the increasing Ca^{2+} concentrations for the wild type and the domain V deletion mutant. Each point represents the average of three independent measurements. Fitting of these plots to the modified Hill equation described in (C.2.3.3.6) yielded the $[Ca^{2+}]_{0.5}$ values presented in Table 14.

TNS fluorescence

The TNS fluorescence changes of domain V truncated µ-calpain were followed under the same conditions used for the domain III variants. Interestingly the presence of NaCl seemed to reduce the magnitude of the conformational changes: It was impossible to obtain accurate measurements of this parameter in the presence of 200 mM NaCl due to the fact that the dispersion of the data was greater than the fluorescence changes (~50 % standard deviations). In the absence of NaCl however the data obtained were similar to the previously observed with the Trp intrinsic fluorescence method (Figure 42). The Ca^{2+} requirement for conformational changes was ~ 6-fold lower than the one of the full length wild type (Table 14), confirming a role of the domain V in the Ca^{2+}-dependent activation of µ-calpain.
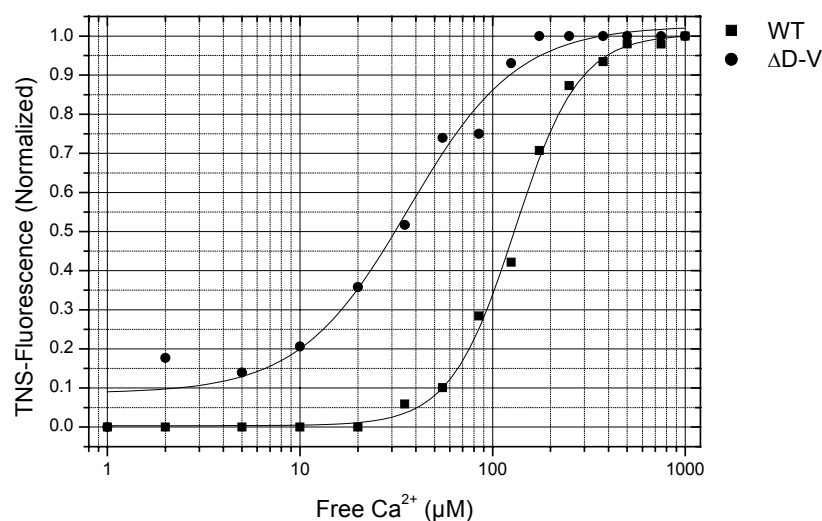
Figure 42. Semi-logarithmic plots of the normalized maximum TNS fluorescences against the increasing Ca^{2+} concentrations for the wild type and the domain V deletion mutant. Each point represents the average of three independent measurements. Fitting of these plots to the modified Hill equation described in (C.2.3.3.6) yielded the $[Ca^{2+}]_{0.5}$ values presented in Table 14.

Light Scattering

The Ca^{2+}-dependent aggregation properties of the μ-calpain lacking domain V were somewhat different from the wild type μ-calpain. The total aggregation of the wild type μ-calpain as measured by right angle light scattering reached values of $\sim 1.0 \times 10^8$ cps (Figure 24) while the maximum value for the same quantity of truncated μ-calpain under the same conditions was $\sim 1.8 \times 10^7$ cps (data not shown). In addition, the $[Ca^{2+}]_{0.5}$ value for half-maximal aggregation was determined to be almost 10-fold lower than the value determined for full length μ-calpain (Figure 43 and Table 14). Assuming aggregation to be the product of calcium driven conformational changes, this result was in agreement with the previous measurements of Trp intrinsic and TNS fluorescence.
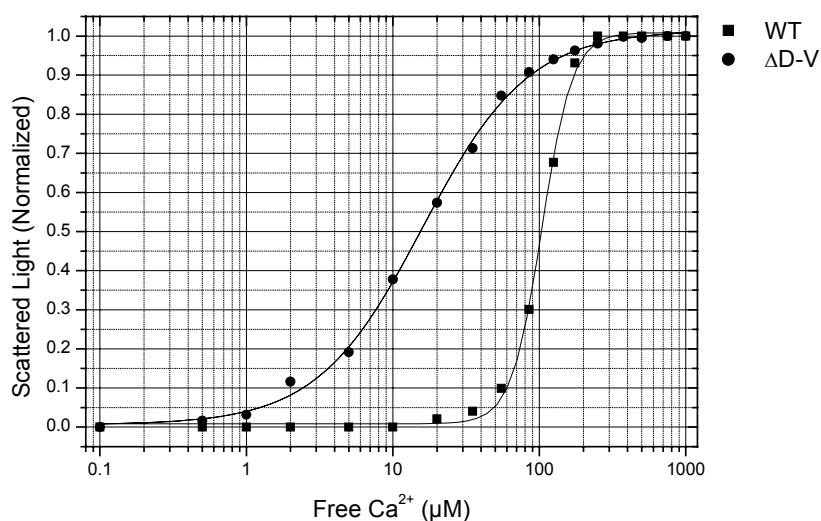
Figure 43. Semi-logarithmic plot of the average normalized Ca^{2+}-dependent changes in the 320 nm light scattered by 0.1 μM recombinant μ-calpain (C115A) wild type and the domain V deletion mutant. Each point represents the average of three independent measurements. Fitting of these plots to the modified Hill equation described in (C.2.3.3.6) yielded the $[Ca^{2+}]_{0.5}$ values presented in Table 14.

Table 14. Half-maximal Ca^{2+} concentrations ($[Ca^{2+}]_{0.5}$) required for Trp intrinsic fluorescence, TNS fluorescence and scattered light changes in heterodimeric μ-calpain (C115A) ΔDV.

	In CB1 (50 mM Tris)		In CB1 (50 mM Tris, 200 mM NaCl)	
	$[Ca^{2+}]_{0.5}$ (μM)	Hill coefficient	$[Ca^{2+}]_{0.5}$ (μM	Hill coefficient
Trp intrinsic fluorescence	38.4 ± 4.5	1.2 ± 0.1	36.2 ± 6.0	0.9 ± 0.1
TNS fluorescence	36.4 ± 3.9	1.5 ± 0.2	n.d.	n.d.
Light Scattering	16.0 ± 0.6	1.2 ± 0.0	n.d	n.d.

D.5.4.2. Analysis of the Ca^{2+} requirement for activity

Sf21 cell lysates containing over-expressed active ΔDV μ-calpain showed Ca^{2+}-dependent hydrolysis of the SLY-AMC substrate. Most of this activity was inhibited by the addition of calpastatin domain 1. As expected from the experiments measuring the

conformational changes in the active site mutant, removal of domain V resulted in a faster activation of the enzyme with decreased Ca^{2+} requirement (Figure 44). The $[Ca^{2+}]_{0.5}$ for activation of the domain V deletion mutant was 13.4 ± 1.6 µM, ~ 8 fold lower than the one of the wild type. The Hill coefficient was 1.7 ± 0.3. This result represented a strong evidence for the involvement of domain V in the activation mechanism of calpain.
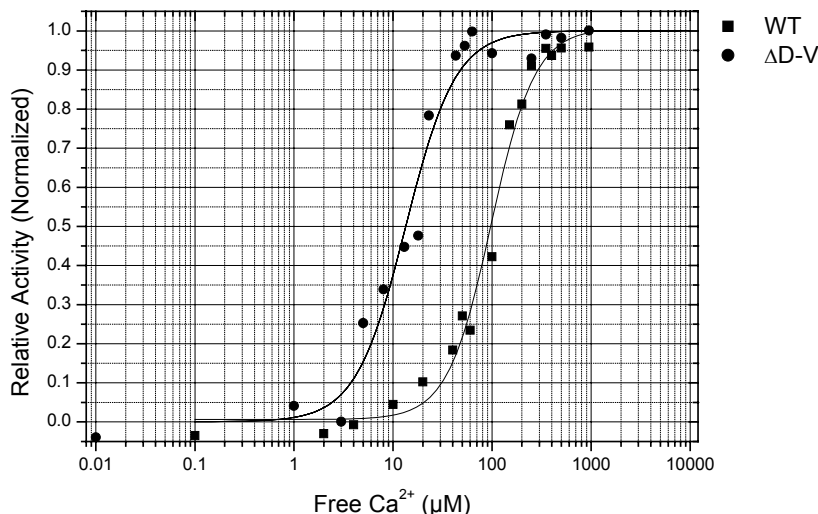
Figure 44. Semi-logarithmic plot of the average normalized Ca^{2+}-dependent calpain activity for wild type and the domain V deletion mutant. Activity was calculated as the difference $v_o - v_i$ from single experiments at different calcium concentrations and normalized to maximal activity (see D.4.3 for details). Each point represents the average of three independent measurements. The calcium concentration for half-maximal activity, $[Ca^{2+}]_{0.5}$, was estimated by non-linear square fitting of these data with the modified Hill equation.

D.5.4.3. Study of membrane binding

Sedimentation of protein-liposome complexes

The use of this technique served again for a qualitative estimation of the binding of the purified domain V truncated µ-calpain to phospholipids (Figure 45). As expected, this variant showed a decrease in vesicle binding compared to the wild type enzyme, assessing the previously reported role of domain V in membrane binding of µ-calpain. Interestingly the membrane binding was not eliminated completely with the deletion of domain V. This observation confirmed the involvement of other domains (e.g. domain III) in the interaction with phospholipids.
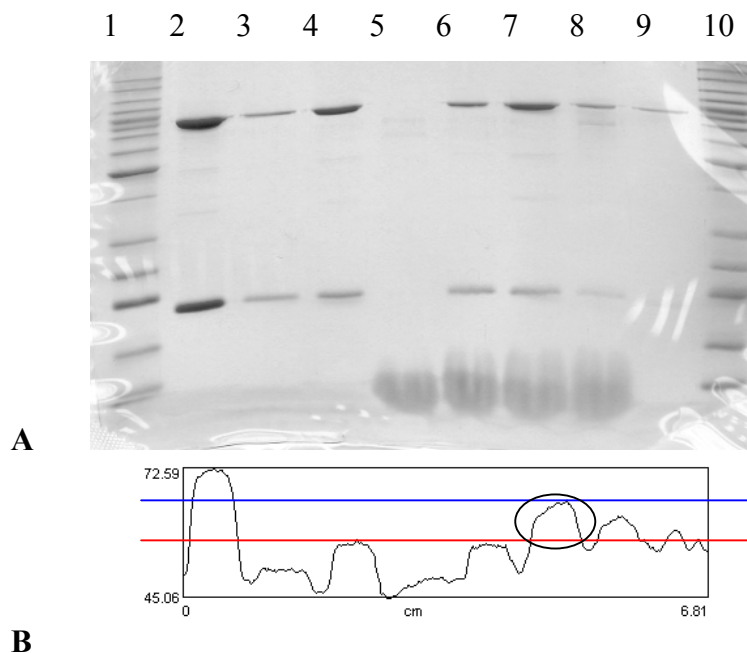
Figure 45. Panel **A**: 12.5 % SDS-PAGE showing differential sedimentation of recombinant μ-calpain (C115A) ΔDV and PC large multilamellar vesicles. With the exception of markers and controls, all the samples shown are centrifugation (15 min, 12000 rpm) pellets after 30 min incubation at RT: Lanes **1** and **10**: Invitrogen's Bench Mark™ protein ladder. Lane **2**: 5 μg control μ-calpain (C115A) ΔDV. Lane **3**: pellet from 5 μg μ-calpain (C115A) ΔDV. Lane **4**: pellet from 5 μg μ-calpain (C115A) ΔDV incubated with 1 mM CaCl$_2$. Lane **5**: pellet from 200 μg PC LMVs. Lane **6**: pellet from 5 μg μ-calpain (C115A) ΔDV incubated with 200 μg PC LMVs. Lane **7**: pellet from 5 μg μ-calpain (C115A) ΔDV incubated with 1 mM CaCl$_2$ and 200 μg PC LMVs. Lane **8**: pellet from 5 μg μ-calpain (C115A) ΔDV incubated with 1 mM MgCl$_2$ and 200 μg PC LMVs. Lane **9**: pellet from 5 μg μ-calpain (C115A) ΔDV incubated with 1 mM MgCl$_2$ and 200 μg PC LMVs in a buffer containing 1 M NaCl. Panel **B** shows the densitometry plot from lanes **2** to **9**. The red line indicates the fraction of protein pelleted due to Ca^{2+}-induced aggregation effects (lane **4**) whereas the blue line shows the protein pelleted in the presence of Ca^{2+} and phospholipids (lane **7**). The circle indicates the fraction from the total amount of μ-calpain (C115A) ΔDV (lane **2**) which interacts with phospholipids in a Ca^{2+}-dependent fashion.

Protein to membrane FRET

The preliminary investigation of binding of domain V truncated μ-calpain to dansyl labeled phospholipids showed that at protein concentrations of 0.1 μM the method was not sensitive enough to study the putative role of DV in the membrane binding. Elimination of the glycine rich domain V resulted in a minimal increase in the fluorescence signal as parameter for Ca^{2+}-dependent binding of truncated μ-calpain to the lipid vesicles composed of PC:PG (Figure 46), PC:PE, PC:PS, PC:PI and PC alone (data not shown). In order to elucidate the

affinity of the truncated μ-calpain for these phoshpolipids as well as the $[Ca^{2+}]_{0.5}$ value for half-maximal membrane binding it was necessary to use SPR measurements.
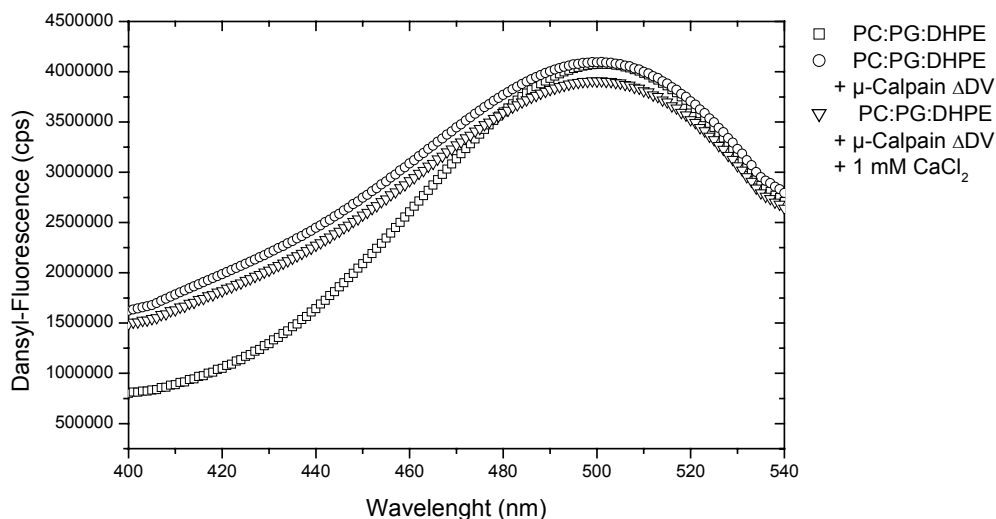
Figure 46. Trp to Dansyl fluorescence energy transfer spectra of μ-calpain lacking domain V and PC:PG:Dansyl-DHPE vesicles in the absence and presence of 1 mM CaCl₂. See Figure 31 for detailed explanation.

SPR measurements

The surface plasmon resonance technique allowed to verify the involvement of regions other than domain V in the association of μ-calpain with membranes observed qualitatively in pull down experiments. Deletion of domain V resulted in ~ 2-fold decrease in Ca^{2+} requirement for membrane binding compared to the full length form (Figure 47 and Table 15). For the activation process this decrease was even ~ 5-fold, suggesting some relationship between the conformational changes leading to activation of calpain and association with membranes. Concerning the binding kinetic measurements, dissociation constants around 25 nM showed that deletion of domain V results in a 10-fold decrease in affinity of the enzyme for phospholipids, indicating the importance of this Gly-rich segment for membrane binding. The contribution of domain III acidic loop to the affinity for phospholipids in the context of a ΔDV heterodimer was tested by producing a D405A variant with a truncated small subunit. SPR measurements using two different vesicle compositions yielded nearly the same K_D values as with the ΔDV mutant, indicating that the acidic loop of domain III does not contribute to the affinity of calpain for membranes.

Figure 47. SPR measurement of Ca^{2+}-dependent association of heterodimeric μ-calpain (C115A) ΔDV with immobilized liposomes.
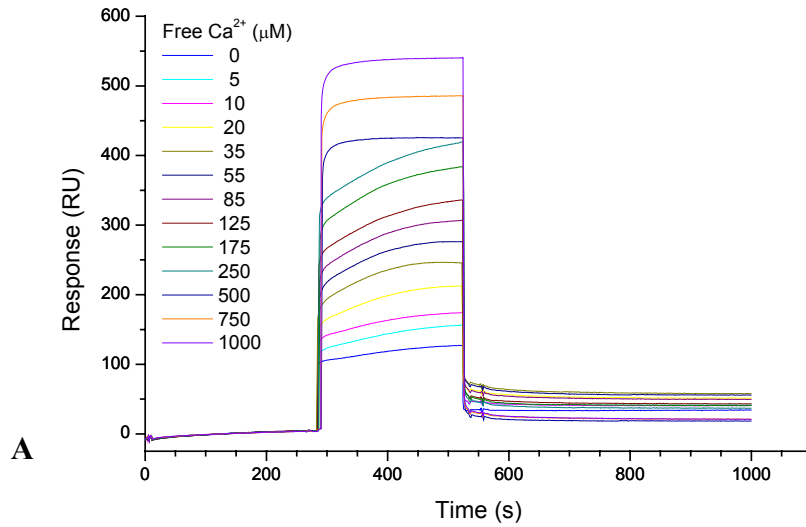
A: Overlay plots of original BIAcore sensorgrams ("bulk" effect from buffer not subtracted) corresponding to the addition of 200 nM enzyme at different Ca^{2+} concentrations to PC:PE liposome vesicles coated onto the L1-chip.
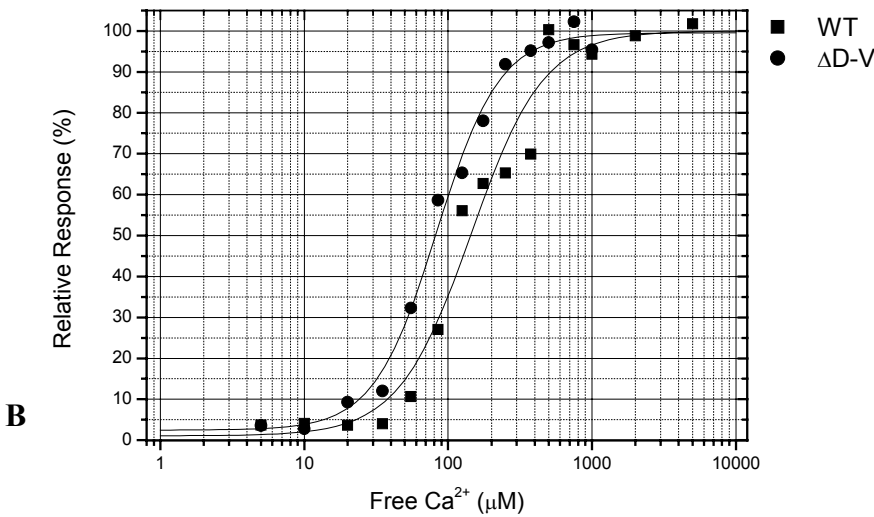
B: Semi-logarithmic plot of the relative response changes against the Ca^{2+} concentrations corresponding to the wild type and the ΔDV mutant (measured with PC:PE vesicles). Each point represents the average of three independent measurements. Fitting to the modified Hill equation (sigmoidal line) yielded the [Ca^{2+}]$_{0.5}$ values presented in Table 15.
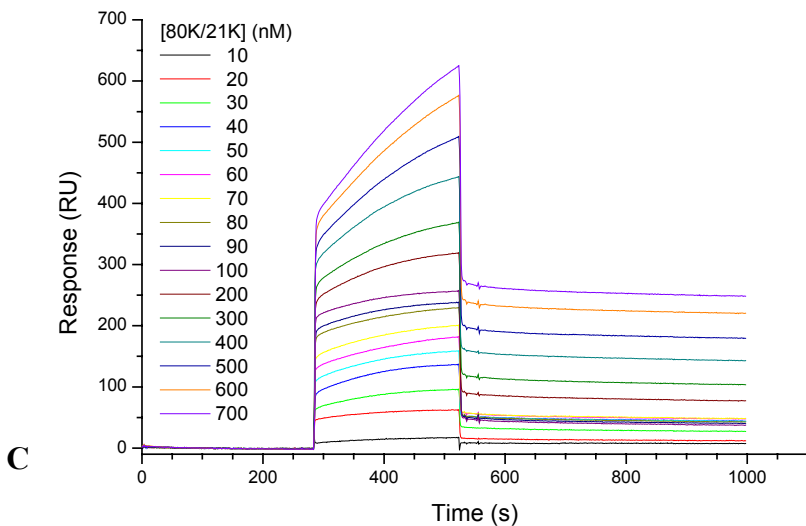
C: Overlay plots of BIAcore sensorgrams corresponding to the addition of increasing concentrations of μ-calpain (C115A) ΔDV at a Ca2+ concentration of 1 mM to plasma PC:PS liposome vesicles coated onto the L1-chip. Rate constants were calculated with the BIAcore evaluation program as described in C.2.3.3.10. Results are shown in Table 15.

Table 15. Ca^{2+} requirement, rate and dissociation constants for phospholipid binding of μ-calpain ΔD-V and domain III mutant D405A ΔD-V determined by SPR analysis.

Analyte (Variant)	Ligand (Vesicle)	$[Ca^{2+}]_{0.5}$	Hill coefficient	k_a ($M^{-1}s^{-1}$) x 10^{-3}	k_d (s^{-1}) x 10^4	K_D (nM)
ΔD-V	PC/PE	75.9 ± 1.8	2.7 ± 0.92	(4.2 ± 1.3)	(1.1 ± 0.3)	26.2 ± 10.8
	PC/PS	55.6 ± 7.4	2.0 ± 0.14	(5.0 ± 1.1)	(1.3 ± 0.4)	26.0 ± 9.8
	PC/PG	nd	nd	(5.3 ± 0.8)	(1.1 ± 0.4)	20.8 ± 8.2
D405A/ ΔD-V	PC/PE	nd	nd	(5.9 ± 1.1)	(1.2 ± 0.4)	20.3 ± 7.8
	PC/PS	nd	nd	(7.3 ± 1.8)	(1.2 ± 0.3)	16.4 ± 5.8

D.6. Expression of calpain 21K and 28K subunits using bacterial and baculovirus expression systems

For a more detailed analysis of domain V's contribution to membrane binding of μ-calpain, we expressed both the full length and the truncated small subunit using a baculovirus expression system for the 28K (Pfeiler, 2001) and an *E. coli* expression system for the truncated variant (Blanchard *et al.,* 1996; Lin *et al.,* 1997 and Pfeiler, 2001).

D.6.1. Expression and purification of the 28K subunit

In order to express the 28K subunit, *Sf21* insect cells were infected with a recombinant baculovirus coding for this protein (Pfeiler, 2001). After 72 hours infection, cell lysates were prepared and loaded onto a calpastatin BC peptide affinity column (Figure 48). Only low μg amounts of protein could be purified from $\sim 1 \times 10^8$ cells in a 150 ml suspension culture. The stability of the isolated protein was affected within few days by aggregation and partial degradation.
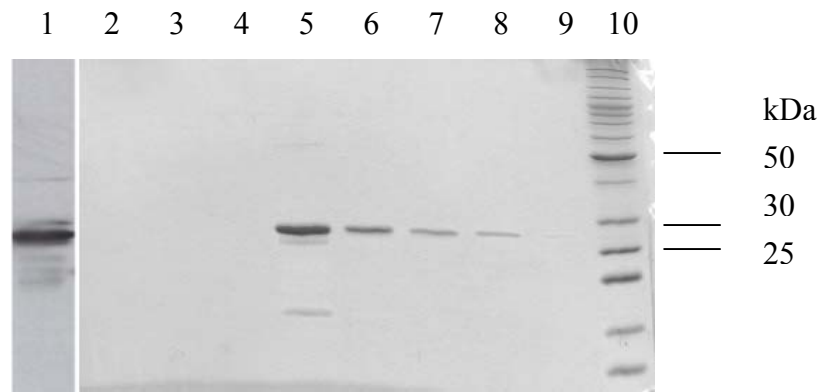
Figure 48. Expression and purification of calpain small subunit (28K) in insect cells. Lane **1** shows immunoprinting of cell lysates from *Sf21* cells expressing the 28K subunit with a monoclonal antibody raised against this protein (Chemicon). In lanes **2** to **9** appear the elution fractions 4 to 17 of the affinity chromatography on a BC-calpastatin column. Lane **10** represent Invitrogen's Bench Mark™ protein ladder.

D.6.2. Functional characterization of the 28K subunit

D.6.2.1. Study of membrane binding

Sedimentation of protein-liposome complexes

This technique was not sensitive enough to distinguish accurately between the aggregation phenomenon and the membrane binding of the 28K subunit (data not shown).

Protein to membrane FRET

Using this method no membrane binding of the 28K subunit was detected (data not shown). Possible explanations are (i) improper positioning of the 3 Trp residues in this subunit, or (ii) too low protein concentrations resulting in a weak FRET signal.

SPR measurements

Surprisingly the full length small subunit associated in a Ca^{2+}-dependent fashion with immobilized phospholipid bilayers with almost the same affinity as the wild type heterodimer did (Figure 49 and Table 16). This result was a strong indication for the role of
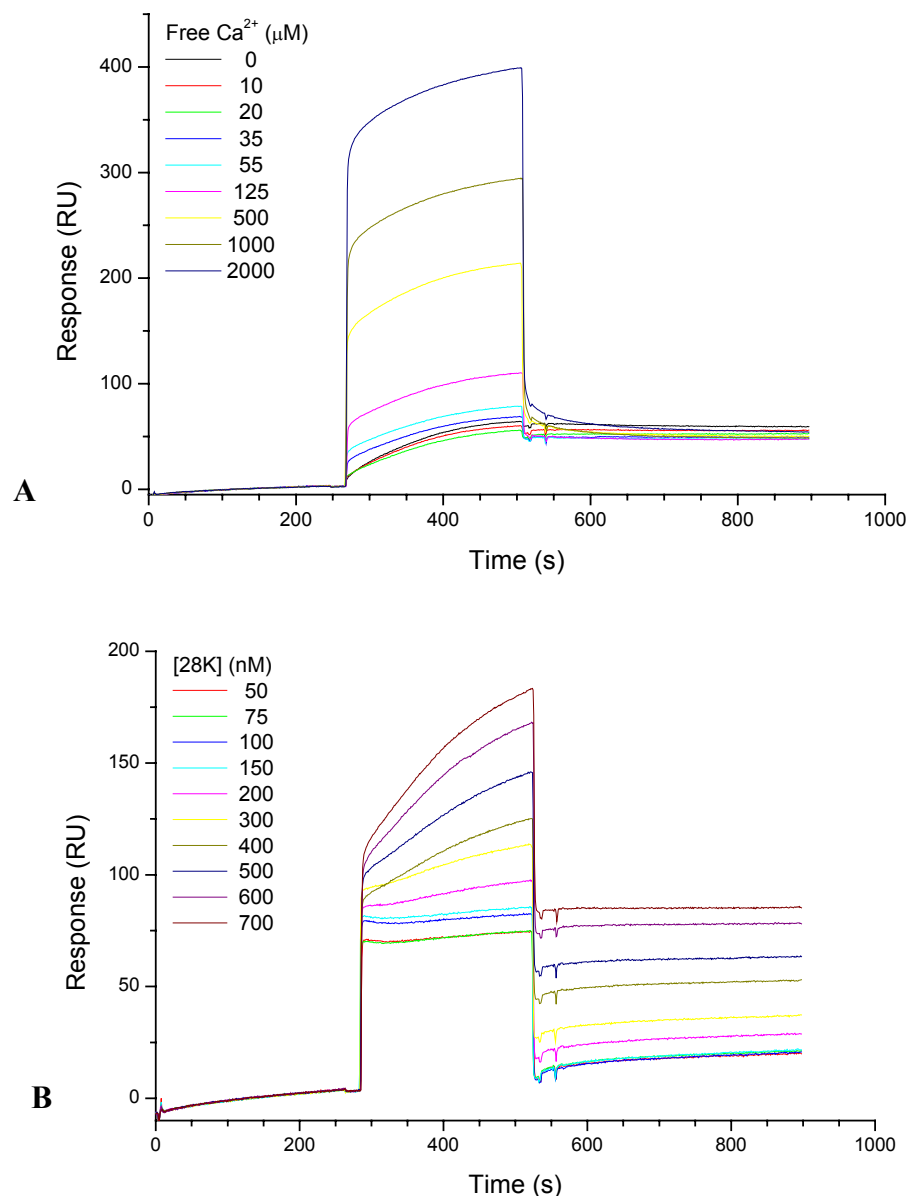
Figure 49. SPR study of the binding kinetics of full length calpain small subunit (28K) to immobilized liposomes.

A: Overlay plots of original BIAcore sensorgrams ("bulk" effect from buffer not subtracted) corresponding to the addition of 400 nM 28K at different Ca^{2+} concentrations to PC:PS liposome vesicles coated onto the L1-chip.

B: Overlay plots of BIAcore sensorgrams corresponding to the addition of increasing concentrations of 28K at a Ca^{2+} concentration of 1 mM to PC:PS liposome vesicles coated onto the L1-chip. Rate constants were calculated with the BIAcore evaluation program as described in C.2.3.3.10. Results are shown in Table 16.

domain V in membrane binding of μ-calpain. Of note, the interaction of the small subunit with the membranes was Ca^{2+}-dependent (data not shown), suggesting that conformational

changes upon Ca^{2+}-binding to the EF-hands in domain VI are required for the interaction with phospholipids.

Table 16. Phospholipid binding parameters of full length calpain small subunit determined by SPR analysis.

Variant	Lipid Vesicle	k_a $(M^{-1}s^{-1})$	k_d (s^{-1})	K_D (nM)
28K	PC/PE 60:40	(2.9 ± 0.2) x 10^4	(1.5 ± 0.4) x 10^{-4}	5.1
	PC/PS 60:40	(2.6 ± 0.5) x 10^4	(1.5 ± 0.5) x 10^{-4}	5.8
	PC/PG 60:40	(2.5 ± 0.4) x 10^4	(1.6 ± 0.4) x 10^{-4}	6.4
	PC 100	(2.1 ± 0.4) x 10^4	(1.4 ± 0.4) x 10^{-4}	6.7

D.6.3. Expression and purification of the 21K subunit

Removal of the first 85 N-terminal aminoacids from calpain small subunit not only increases the bacterial expression levels of recombinant heterodimeric m-calpain (Elce, 1997, Graham-Siegenthaler *et al.,* 1994), but also makes possible the expression of high levels of this (truncated) protein as monomer in *E. coli* (Blanchard *et al.,* 1996; Lin *et al.,* 1997; Pfeiler, 2001). For the expression of the 21K subunit we used B834(DE3) *E. coli* cells transformed with the plasmid pET-22b(+)-21K-His$_6$. The production of recombinant 21K was induced with IPTG and after 2 hours the cells were harvested, lysed and the 21K was purified in one step on a Ni-NTA column (Figure 50). Several mg of 21K could be isolated from 1 L bacterial culture. Recombinant 21K was stable over months and immunreacted with the Chemicon monoclonal antibody raised against the 28K subunit.
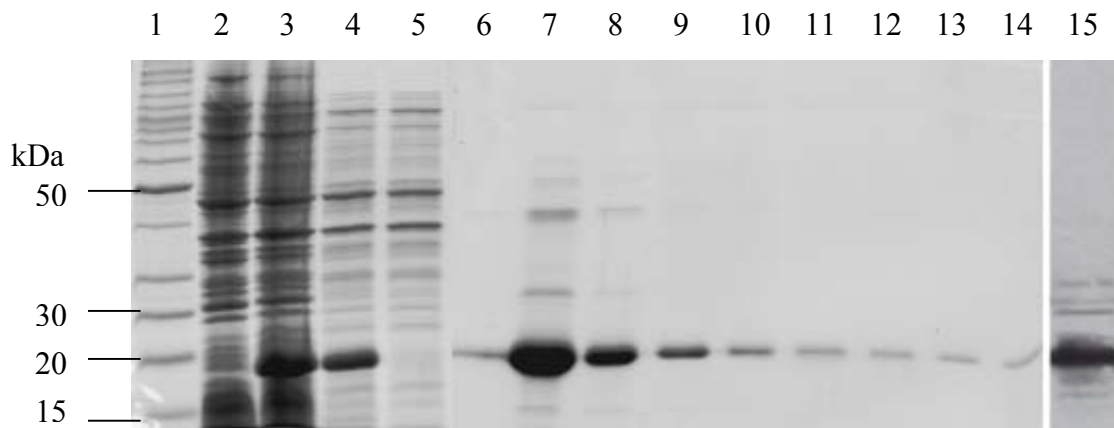
Figure 50. 12.5 % SDS-PAGE of bacterial expression and purification of truncated calpain subunit (21K). Invitrogen's Bench Mark™ molecular weight markers were loaded on lane **1**. Lanes **2** to **4** show soluble proteins from 2 x 10⁸ *E. coli* cells before IPTG induction, 2 hours after induction and after lysis. Flow through from Ni-NTA chromatography appears in lane **5**. Lanes **6** to **14** represent elution fractions 8, 12, 16, 20, 24, 32, 36 and 40 of the affinity column. Lane **15** shows western blot analyis of *E. coli* lysates with a monoclonal antibody against the small subunit.

D.6.4. Functional characterization of the 21K subunit

D.6.4.1. Study of membrane binding

Sedimentation of protein-liposome complexes

The truncated small subunit aggregated weakly in contrast to the full length variant. No membrane binding was detectable in the SDS-PAGE (data not shown). This result suggested that the glycine-rich tail of domain V plays a major role in the formation of aggregates and is responsible for membrane binding of the 28K subunit.

Protein to membrane FRET

In agreement with the results from the sedimentation experiments, the 21K subunit did not show any Ca^{2+} driven binding to the dansyl labeled membranes (data not shown).

SPR measurements

No binding to the immobilized liposome vesicles was observed for the small subunit after removal of domain V: neither in the presence, or absence of calcium (Figure 51). This
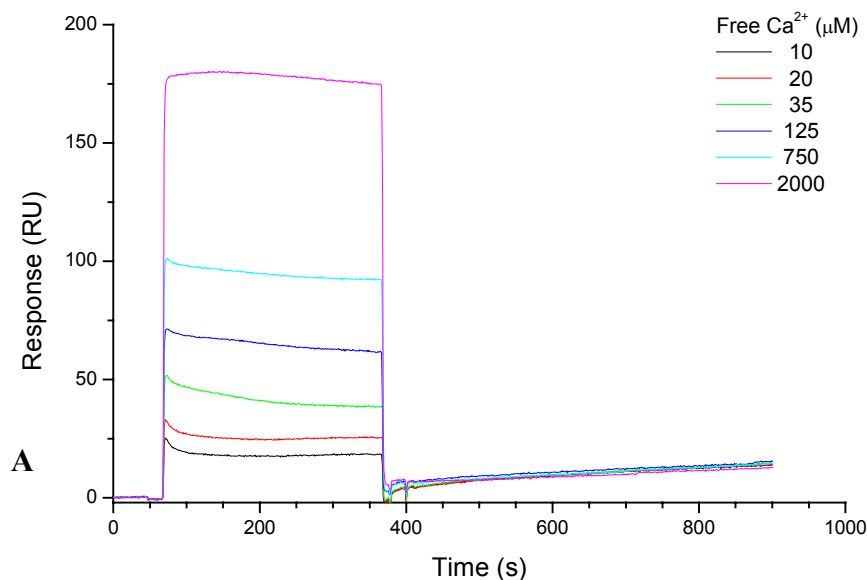
Figure 51. SPR study of the binding kinetics of truncated calpain small subunit (21K) to immobilized liposomes.

A: Overlay plots of original BIAcore sensorgrams ("bulk" effect from buffer not subtracted) corresponding to the addition of 1 μM 21K at different Ca^{2+} concentrations to PC:PS liposome vesicles coated onto the L1-chip.
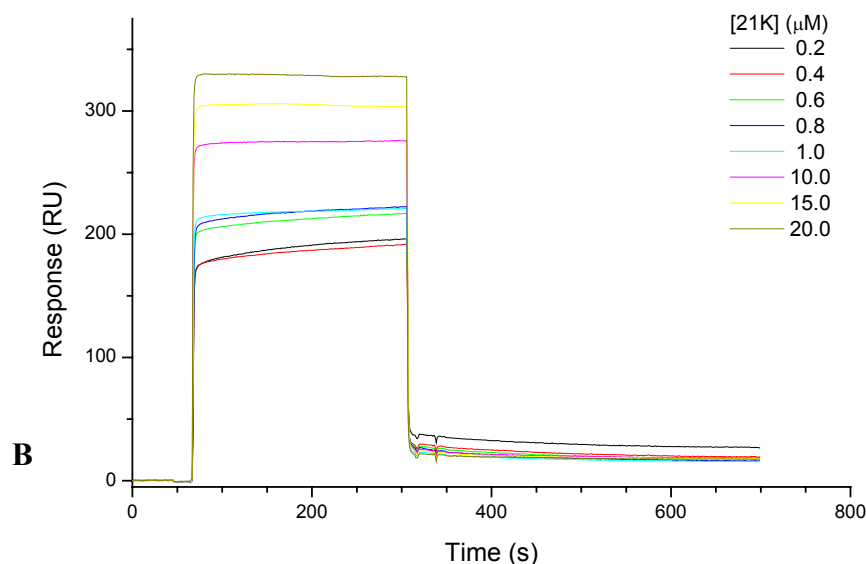
B: Overlay plots of BIAcore sensorgrams corresponding to the addition of increasing concentrations of 21K at a Ca^{2+} concentration of 1 mM to PC:PS liposome vesicles coated onto the L1-chip.

result confirmed the important role of domain V in membrane association and rises questions about the coordinated participation of domains V and VI in this process. Another explanation for the behavior of this variant can be derived from the fact that the truncated small subunit

reportedly dimerizes in solution (Blanchard *et al.,* 1996), thereby hindering association of hydrophobic regions exposed upon Ca^{2+}-binding.

D.7. Expression of EYFP-80K domain III acidic loop mutants in mammalian cells

Expression of chimeras of calpain and fluorescent proteins (EGFP, EYFP and ECFP) was reported for the first time by our laboratory (Gil-Parrado, 2001) and represents a powerful tool to study the cellular localization of this protein (Gil-Parrado *et al.,* 2003). Based on these previous results, we decided to create a tool kit to study the membrane targeting of domain III acidic loop variants *in vivo*.

D.7.1. Construction of expression vectors

In order to generate vectors for the expression of the EYFP-syn80K (C115A)-His$_6$ chimeras, the 80K variants were subcloned from pVL1392-syn80K (C115A)-His$_6$ (Figure 52, I) into the pEYFP-C1 vector (Figure 52, II). For this purpose, the syn80K (C115A)-His$_6$ gene and its variants were excised in a preparative digestion with *EcoRI* and *BamHI* from pVL1392. The same procedure was applied to pEYFP-C1. Inserts and vector were separated, purified and ligated to generate new expression vectors (Figure 521, III). Restriction analysis of these plasmids was positive (data not shown), but DNA sequencing detected the introduction of a stop codon in the 80K moiety of the fusion protein. The effect of this mutation was assessed by transient expression of the chimeras and western blotting of the cell lysates. Fluorescence intensities similar to control cells expressing only EYFP and a band corresponding to a protein much smaller than the expected 116 kDa of the fusion protein confirmed the interrupted transcription of the chimeras (data not shown). In order to overcome this problem a procedure based on *Pfu* polymerase treatment was employed (C.2.2.14). The vectors were all cut with *HindIII* (Figure 52, IV: lanes B to I) and treated with *Pfu* polymerase. They were then blunt ligated and competent *E. coli* cells were transformed. The resulting vectors isolated from transformant colonies (Figure 52, V) were not sensitive anymore to digestion with *HindIII* and had instead a new recognition sequence for *NheI*. Restriction analysis confirmed the success of this strategy (Figure 52, VI and VII).
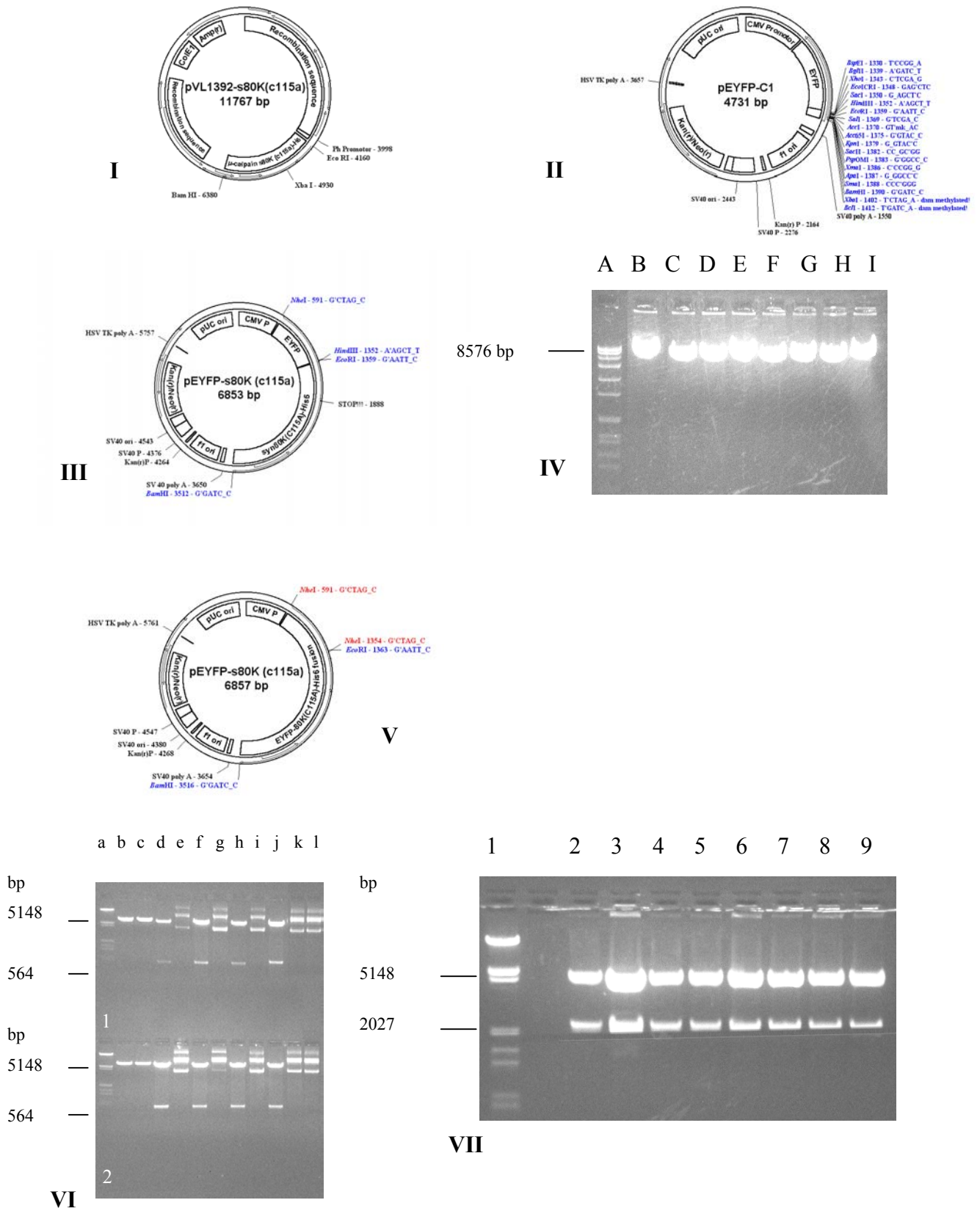
Figure 52. Construction of pEYFP-C1-syn80K (C115A)-His$_6$ plasmid. Panel I: pVL1392-syn80K (C115A)-His$_6$ plasmid. Panel II: Empty pEYFP-C1 vector. Panel III: First pEYFP-C1-syn80K (C115A)-His$_6$ plasmid created by *EcoRI/BamHI* (out of frame) subcloning of the 80K (C115A)-His$_6$ gene. Panel IV: Lane **A**: Roche molecular length marker VII: Lanes **B** to **I**: Out of frame

His$_6$ gene. Panel IV: Lane **A**: Roche molecular length marker VII: Lanes **B** to **I**: Out of frame pEYFP-C1-EYFP-syn80K (C115A)-His$_6$ plasmids digested with *HindIII*. Panel V: In frame pEYFP-C1-EYFP-syn80K (C115A)-His$_6$ plasmid after *HindIII* digestion, *Pfu* polishing and but ligation. Panel VI Lanes **1a** and **2a**: Roche molecular length marker III. Lanes **1b** and **2b**: Out of frame pEYFP-C1-syn80K (C115A)-His$_6$ vector digested with *NheI*. Lanes **1c** and **2c**: Out of frame pEYFP-C1-syn80K (C115A)-His$_6$ vector digested with *HindIII*. Lanes **1d**, **1f**, **1h**, **1j**, **2d**, **2f**, **2h** and **2j**: In frame pEYFP-C1- syn80K (C115A)-His$_6$ wild type and mutants D402A, E403A, D405A, D406A, D408A, D412A, E414A digested with *NheI*. Lanes **1e**, **1g**, **1i**, **1k**, **2e**, **2g**, **2i** and **2k**: In frame pEYFP-C1-syn80K (C115A)-His$_6$ wild type and mutants D402A, E403A, D405A, D406A, D408A, D412A, E414A digested with *HindIII*. Lanes **1l** and **2l**: non digested in frame pEYFP-C1-syn80K (C115A)-His$_6$. Panel VII: Restriction analysis of pEYFP-C1- syn80K (C115A)-His$_6$ and mutants D402A, E403A, D405A, D406A, D408A, D412A, E414A with *EcoRI* and *BamHI* (lanes **2** to **9**). Lane **1** represents Roche molecular length marker III.

D.7.2. Generation and characterization of cell lines overexpressing EYFP-80K domain III acidic loop mutants

The constructed plasmids were used to transfect *LCLC 103H* cells both stably and transiently. First, a transient transfection was performed with the aim of confirming the expression of chimeras by fluorescence microscopy and western blot. Two days after transfection a yellow fluorescence less intense than the control cells expressing EYFP alone was detected in all culture dishes transfected. These cells were lysed (C2.3.1.3) and the cell lysates were subjected to western blot analysis. Immunoprinting with three different antibodies yielded similar results: A ~ 116 kDa (36 kDa EYFP + 80 kDa μ-calpain large subunit) band was detected by a polyclonal antibody anti μ-calpain and a monoclonal anti μ-calpain 80K subunit (Figure 53, A and B). Using both antibodies endogenous calpain and its degradation products could be detected. Intriguingly, the polyclonal antibody also recognized proteins over 110 kDa. Detection with a highly specific anti GFP antibody which recognizes all GFP variations showed a convincing ~ 116 kDa band, which could only be explained by the existence of a EYFP-80K fusion protein in the lysates (Figure 53, C).These results served as basis to create stable cell lines over-expressing the chimeras (C.2.1.3). The resulting lines (Figure 53, D) conserved both morphology and doubling time of the parent cell line. They grew well under low antibiotic pressure (100 μg/ml G-418). After a maximum of three passages, cells were frozen and stored in liquid nitrogen until use in localization experiments.
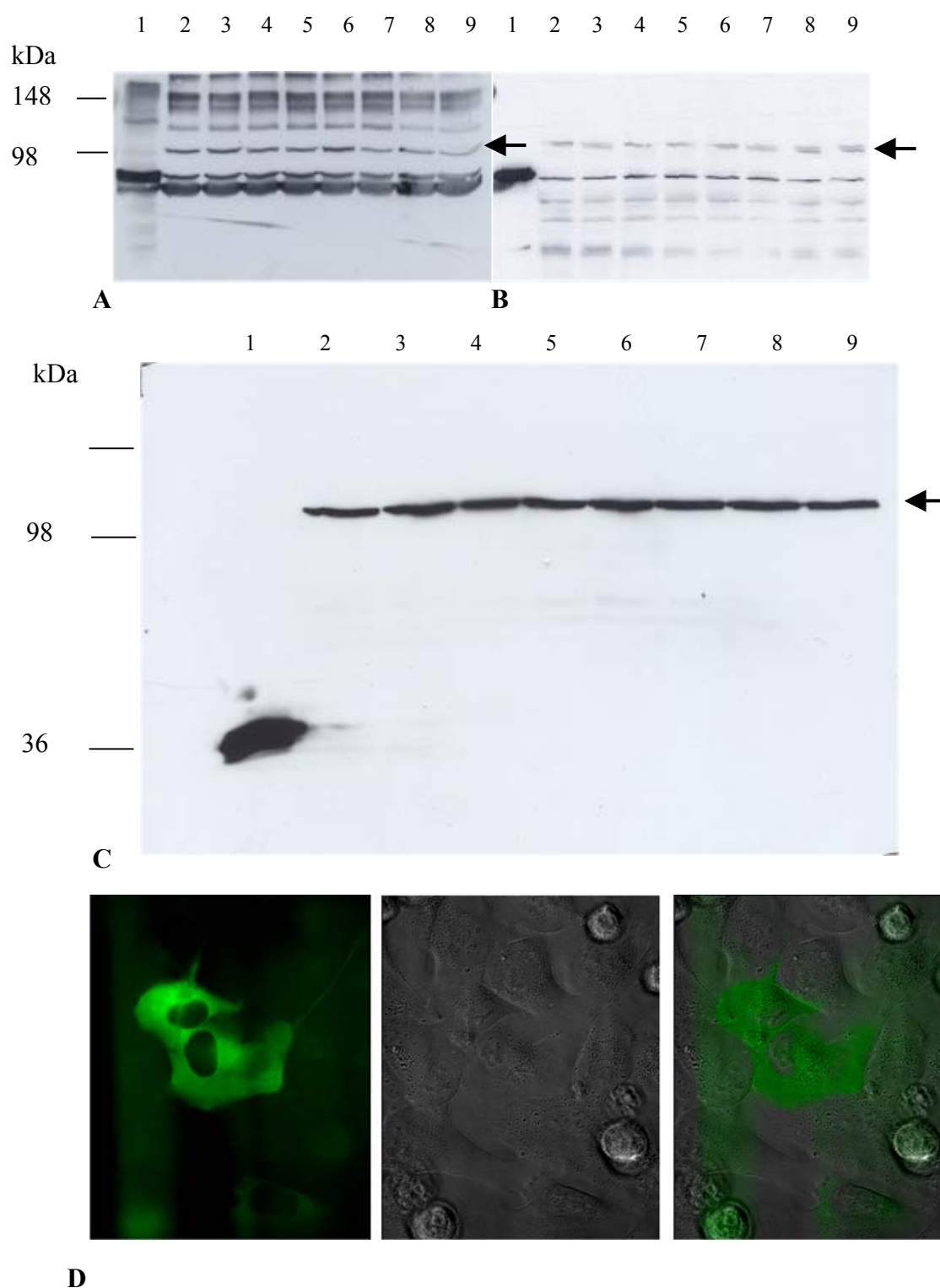
Figure 53. Expression of EYFP-syn80K(C115A)-His$_6$ and domain III acidic loop variants in LCLC 103H cells. Panels A, B and C: Western blot analysis of LCLC 103 H cells transfected with pEYFP-C1-EYFP-syn80K (C115A)-His$_6$.. In all panels: lanes **2** to **9** correspond to EYFP-syn80K (C115A)-His$_6$ and mutants D402A, E403A, D405A, D406A, D408A, D412A, E414A. In panels **A** and **B** the positive control was 1 µg of µ-calpain (C115A) (lane **1**). In panel **C** a lysate from cells transfected with pEYFP-C1 was used as positive control (lane **1**). The antibodies used were polyclonal anti µ-calpain in A, monoclonal anti µ-calpain in B and polyclonal anti GFP in C (see C.2.3.2.7 for details). The arrow points to the 116 kDa band corresponding to the fusion protein. Panel **D** shows a fluorescence image of LCLC 103H cells transiently transfected with pEYFP-

80K (C115A)-His$_6$. From left to right appear the fluorescence image, the phase contrast image and the overlaping of both photos.

D.7.3. Generation and characterization of control cell lines overexpressing EYFP and ECFP-membrane marker

To create these cell lines, *LCLC 103H* cells were stably transfected with the pEYFPC1 plasmid (expressing EYFP alone) and pECFP-Mem plasmid (expressing a ECFP-tagged ubiquitous marker for cellular membranes) from Clontech (C.1.2). The generated cell lines were identified for their fluorescence properties. Cells expressing ECFP-Mem showed a characteristic cyan fluorescence localized at the plasma membrane and other cellular membranes (Figure 54, A). Cells expressing EYFP presented a yellow green fluorescence equally distributed in the cytoplasm (Figure 54, B). Both proteins were detected in cell lysates by a polyclonal anti-GFP antibody (data not shown).
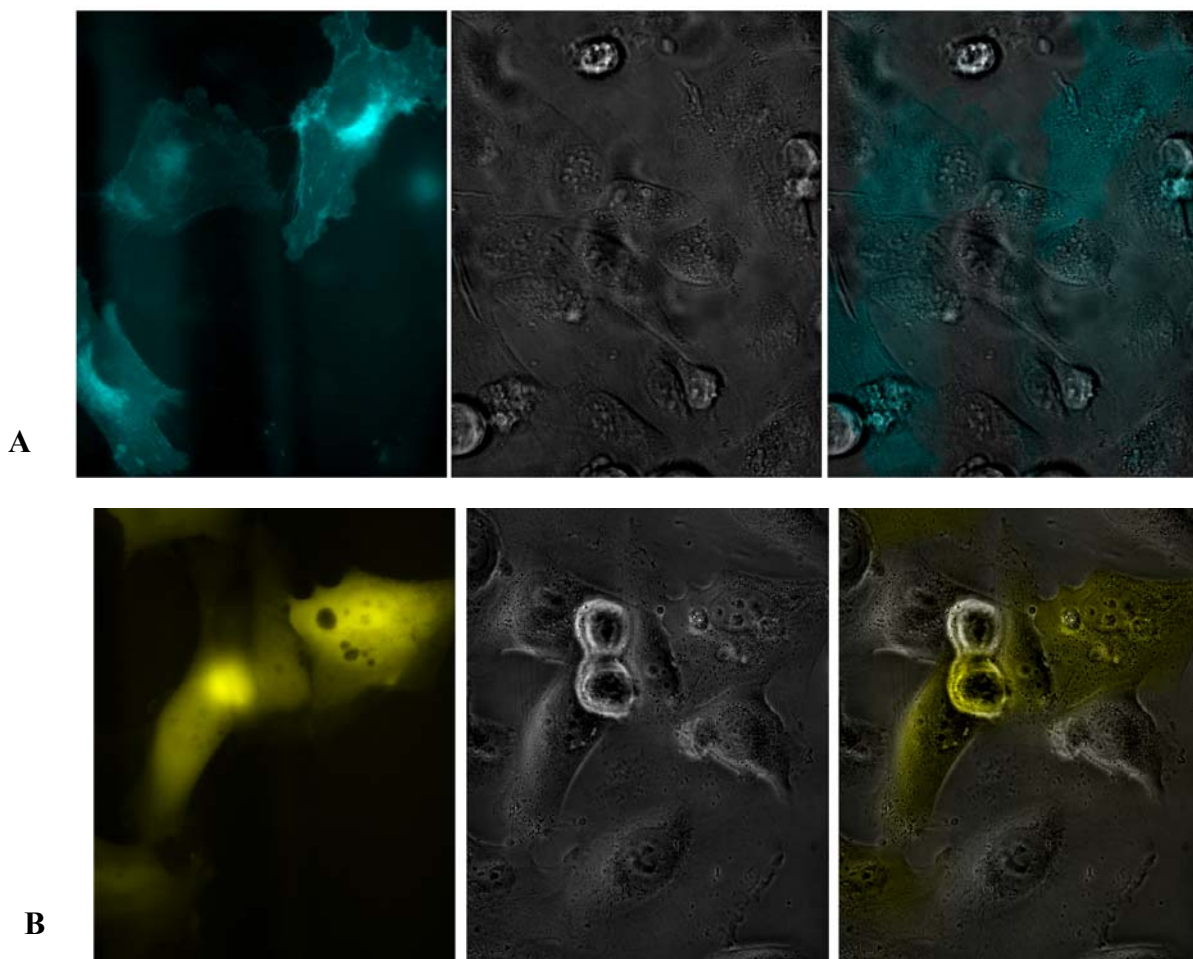
Figure 54. Expression of ECFP-Mem (panel **A**) and EYFP (panel **B**) in LCLC 103H cells transiently transfected with pECFP-Mem and pEYFP-C1 respectively. From left to right appear the fluorescence image, the phase contrast image and the overlapping of both photos.

E. Discussion

The elucidation of the three-dimensional structure of Ca^{2+}-free rat and human m-calpain provided a basis to explain the inactivity of the calpains in the absence of calcium and raised a number of questions concerning functional aspects like the activation of these enzymes by Ca^{2+}, the role of autolysis, subunit dissociation and membrane binding. The experiments described in the previous chapters addressed some of these questions. In the next paragraphs we will discuss the outcome of these studies in the context of data reported by other laboratories.

E.1. Over-expression, purification and characterization of human μ-calpain variants

The group has worked for several years on the establishment of μ-calpain over-expression systems. In 2001 Pfeiler and Gil-Parrado accomplished the expression of μ-calpain in insect and mammalian cell lines. Over-expression in insect cells should serve for the production of high quantites for crystallization studies, whereas expression in mammalian cell lines was intended to investigate the subcellular localization of μ-calpain. The present work is based on the experience acquired in these previous studies and represents the first site-directed mutagenesis study on full-length heterodimeric μ-calpain. In the past, only deletion mutants of human μ-calpain domain III were expressed in *E. coli* (Vilei *et al*., 1997) or *LCLC 103H* and *COS 7* cells (Gil-Parrado *et al.,* 2003). John Elce's laboratory has succesfully expressed rat-μ/m-calpain hybrids in *E. coli* in which domain swaps were intended to provide information about the structural differences responsible for the particular Ca^{2+}-requirement of each isoform (Dutt *et al.,* 2002; Moldoveanu *et al.,* 2002; Moldoveanu *et al.,* 2003). This group has also extensively investigated the protease core of rat μ-calpain expressed in *E. coli* using site-directed mutagenesis. With the exception of active-site mutants reported by Hitomi *et al.* (1998) and Pfeiler (2001), there is no information available about the effect of point mutations on structure and function of human μ-calpain.

In addition to the "Ala scan" in domain III, we have expressed a deletion mutant of the Gly-rich domain V (Figure 55). Contrarily to what has been described in the literature (Elce *et al.,* 1997), this mutation did not improve the expression yields, a result that can be attributed
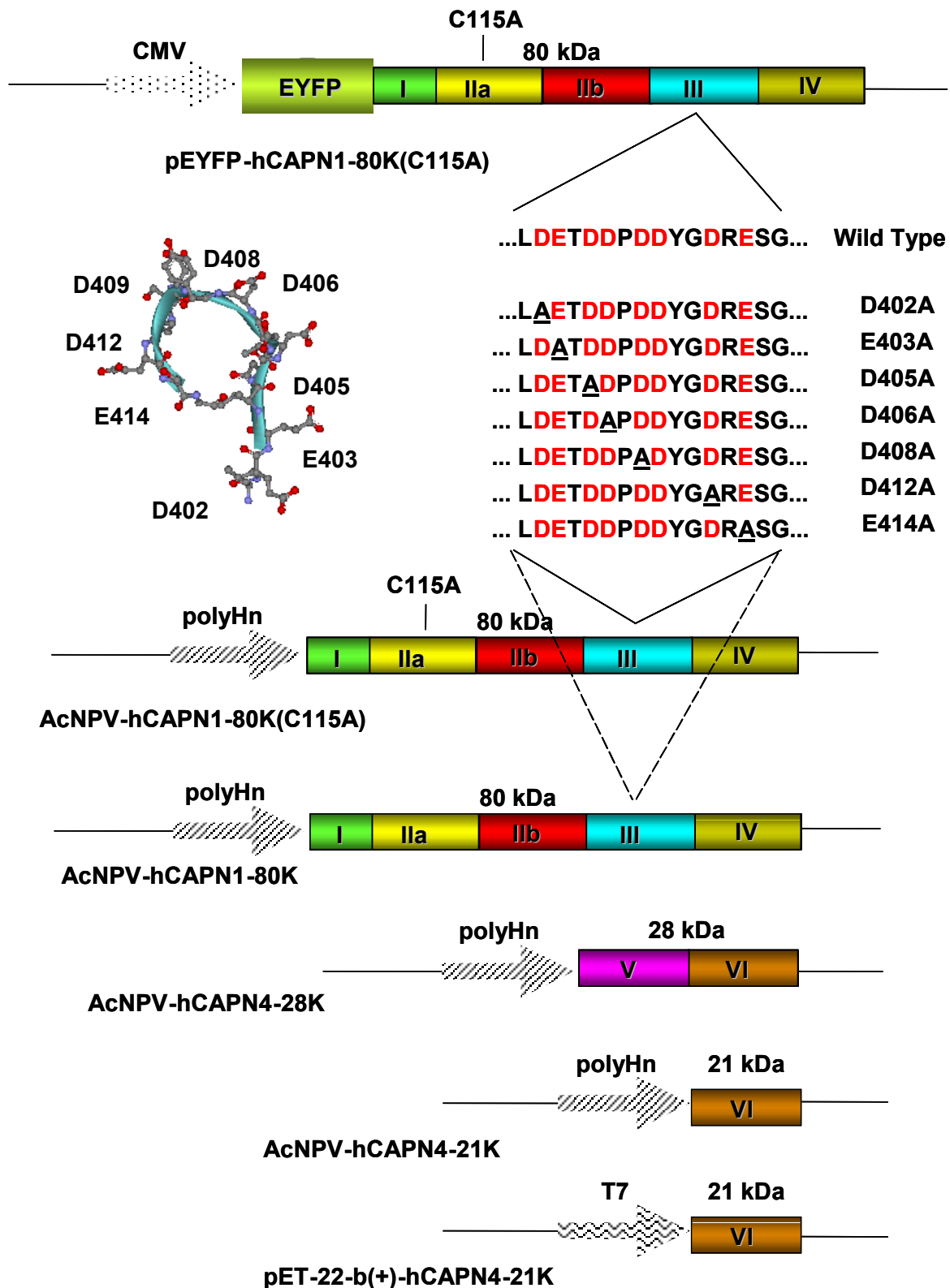
Figure 55. Summary of the plasmid and viral vectors created and/or used in this work for the heterologous expression of human μ-calpain variants in mammalian, insect and bacterial cells. Protein-coding regions are shown as bars in the case of calpain and as an ellipse in the case of EYFP. Arrows represent the promoter regions. The 80 kDa subunit and the 21 kDa variant were C- and N-terminally His$_6$- tagged, respectively.

to differences between bacterial and insect expression systems. With the help of limited proteolysis, fluorescence spectroscopy, and SPR measurements, we have demonstrated that introducing single mutations in the acidic loop of domain III does not affect the structural and (some) functional properties of the C115A active-site mutated human μ-calpain. The same is valid for the domain V deletion mutant, in agreement to what was reported for a 80K/21K m-calpain (Elce *et al.,* 1997).

Concerning the expression of proteolytically active μ-calpain in insect cells, we documented in this work by casein zymography and peptidolytic activity assays the expression of large amounts of active enzyme. The rapid isolation of active μ-calpain on a Ni-NTA column was reported by Pfeiler (2001) and others (Goll *et al.,* 2003) to be associated with autoproteolytic degradation of the enzyme.

Finally, we have expressed inactive EYFP chimeras (Figure 55) of the acidic-loop mutated C115A-80K subunits in human lung carcinoma cells with the aim of analyzing the involvement of the acidic loop in membrane binding of μ-calpain *in situ.* By means of western blot and fluorescence microscopy we detected transient and stable expression of the chimeras. Yet, as reported recently by Larsen (2004), some cleavage of the EYFP fusion protein (probably by endogenous cytosolic proteases, calpain included) might occur during expression, suggesting caution in its use as cell marker.

E.2. Contribution of the acidic loop of domain III to the activation mechanism of μ-calpain

The high conservation of domain III acidic loop throughout the calpain family (Figure 57) suggests an important role of this region in calpain structure and function. In the case of classical C2 domains, the interconnecting loops in the β-sandwich structure serve as Ca^{2+}- and phospholipid-binding units (Figure 62) (Rizo and Sudhoff, 1998). As mentioned in the introductory chapter, recombinantly expressed domains III of rat μ- and m-calpain as well as of *Drosophila* calpain B have been shown to bind Ca^{2+} ions (Tompa *et al.,* 2001; Alexa *et al.,* 2004). Unfortunately, the proteins produced by Tompa were too unstable to initiate any kind of crystallographic study (Tompa, personal communication). Our attempts to express soluble human μ-calpain domain III in *E. coli* were also unsuccesful (data not shown). Thus a crystal structure of domain III in the presence of calcium is not available yet.

In the previous chapters we have described an alternative approach to investigate the putative Ca^{2+} coordination by the acidic loop. By exchanging the acidic residues to Ala we have systematically eliminated the putative Ca^{2+} nucleation sites whithout affecting substantially the electrostatic potential of this region. In this way a discrete weakening of the interactions of these negatively charged residues with basic aminoacids in domain IIb and domain III was achieved. The effect of the mutations was an important reduction of the Ca^{2+} concentration needed for structural rearrangements and activation of the enzyme (see Tables 7, 8, 9 and 13). The relative impact of each mutation on the $[Ca^{2+}]_{0.5}$ was similar for conformational changes and for the cleavage of a peptide substrate, suggesting a distinct relationship between both events. These results strongly support the electrostatic switch activation mechanism proposed by Strobl *et al.*, in which the binding of one to three Ca^{2+} ions to the loop under (partial) charge compensation would create a more compact fold of this loop and reduce its negative potential. Lowering the electrostatic interaction would allow subdomain IIb to turn over to subdomain IIa, eventually leading to the inherent fusion of the catalytic domain. The hydrophobic interface between subdomain IIb and domain III β-strands would easily allow such a rolling motion of subdomain IIb whereas subdomain IIa, clamped through many polar contacts to domain III would remain rigidly oriented with respect to domain III.

In a previous report by Hosfield *et al*. (2000), mutation to Ser of Lys 226 and Lys 230 (note that m-calpain numbering lags 10 aa behind μ-calpain) in the domain IIb helix facing the acidic loop (Figures 14, 54 and 56) altered the specific activity of the enzyme but had no significant effect on the Ca^{2+} requirement for activity. This may be explained by the fact that their activity measurements were performed in a buffer containing 200 mM NaCl. Our TNS fluorescence measurements at the same NaCl concentration and very recent studies concerning subunit dissociation of native bovine calpains (Li *et al.,* 2004) suggest that ionic strengths not far above the physiological ones can largely weaken electrostatic interactions which are very important for the structure and function of the calpain molecule. In Hosfield's study, substitution of Lys-234 and its salt bridge counterpartner Glu-504 to Ser resulted in a ~ 50 % reduction in the $[Ca^{2+}]_{0.5}$. Interestingly, substitution of Glu-504 (Glu-516 in μ-calpain) caused a greater effect than the mutation K234S, suggesting that this acidic residue makes multiple electrostatic contacts. In fact, the D504S mutation abolishes two salt bridges: one with Lys-234 and another with Lys-354 in domain III.

In agreement with these results, we observed in the structure model of μ-calpain (Figures 56, D and 58) that besides interacting with residues Lys-240 and Arg-244 in domain

IIb, the acidic loop is electrostatically "clamped" between residues Arg-400, Arg-413, Arg-486, Arg- 488 and Lys-517 of domain III. The interactions of the acidic loop with these positively charged amino acids might restrain its movement from subdomain IIb in the absence of calcium. Interestingly, the mutations E403A, D405A and D406A had the greatest effect on the Ca^{2+} requirement for conformational changes, membrane binding and enzyme activation. Analysis of the distances between these residues and their surrounding basic residues reveals close contacts to both Lys-240 in subdomain IIb and Lys-517 in domain III. If an exentended linker domain is assumed (Figures 56, E and 58), Lys-517 would form its "root" and could move downwards as a consequence of the small conformational changes produced by Ca^{2+}-binding to domain IV. In this case the Ca^{2+} signal would be effectively transmitted to the acidic loop via Lys 517, resulting in an enhancement of Strobl's electrostatic switch. Our postulates are supported by a similar study published as this thesis was being written (Alexa *et al.,* 2004). Based on site-directed mutagenesis in rat m-calpain and *Drosophila* CALPB these authors hypothesize that -as proposed by Hosfield *et al.* (1999)- the putative transducer acts like a slack rope gaining in tension after being pulled down by the small conformational changes induced by Ca^{2+}-binding to domain IV. Deletion and substitution in rat m-calpain of some of the residues connecting the linker with domain IV via salt bridges (Asp-515, -517 and -522) reduced the Ca^{2+} requirement for activity. In the acidic loop of rat m-calpain, mutation of the pair Glu-396 and Asp-397 (corresponding to Asp-405 and Asp-406 in μ-calpain) to Gln and Asn, respectively, resulted in a 30-fold decrease of the Ca^{2+} requirement for activation. The corresponding mutants in CALPB (D613N, D614N) showed a 7-fold decrease in the $[Ca^{2+}]_{0.5}$. A minor effect (1.5-fold) was observed by changing the pair Glu-399 and Asp-400 to Gln and Asn. These mutants, however, displayed only one fourth of the normal specific activity. In CALPB, the corresponding mutations (D617N and D618N) had no effect on the Ca^{2+} requirement but originated a 1.5-fold decrease in the specific activity. Interestingly, the introduction of repulsive charges (mutation to Lys) effected also a 1.5-fold reduction of the $[Ca^{2+}]_{0.5}$, but reduced 10-20 times the specific activity. Almost complete deletion of the whole loop (Δ395-404) increased 1.8-fold the Ca^{2+} requirement for activation, but led to an unstable, rapidly inactivating enzyme. The authors noticed a possible concerted action of domains III and IV upon Ca^{2+}-binding to both and postulated an "extended transducer activation mechanism" in which the electrostatic switch at the interface of subdomain IIb and domain III as well as the conformational changes in domain IV would equally contribute to calpain activation.

It is not possible to conclude from our study whether the Ca^{2+}-binding and the structural changes measured upon addition of Ca^{2+} take place within domain III. Nonetheless, our results together with Tompa's observations and the structural similarity between the acidic loop of domain III and the Ca^{2+}-binding loops of classic C2 domains support the speculation that at least one calcium ion is complexed by calpain domain III. When our mutants were subjected to limited proteolysis with chymotrypsin, the cleavage sites in domain III were identical, regardless of the incubation with Ca^{2+} or Mg^{2+} and the use of acidic-loop mutated or wild type µ-calpains as substrate. These observations suggest that the putative Ca^{2+}-binding to the loop does not result in major structural rearrangements in domain III but in a modification of the electrostatic potential at the domain interface. The results of our limited proteolysis experiments were similar to the observations made by Moldoveanu (2001) with m-calpain and Thompson (2003) with both µ- and m-calpain. These authors reported a specific tryptic and chymotryptic degradation pattern in the presence of Ca^{2+} in which the protease core of m-calpain was protected from proteolysis in the active conformation, while cleavage sites at positions [255]QKLV and [257]LVKG for trypsin and chymotrypsin, respectively, were present in the -more open- "apo"-conformation. We observed a similar behaviour, with a chymotryptic cleavage site [266]KKLV in domain IIa protected in the presence of Ca^{2+} (Figure 26). The more compact structure of the protease domain in the Ca^{2+}-bound state, due to the assembly of the otherwise disrupted active site, led Moldoveanu and coworkers to speculate that the main conformational changes were not being transmitted from the calmodulin-like domains but generated by direct Ca^{2+}-binding to the papain-like catalytic domain itself. These suppositions were confirmed by the same group when the protease core of rat µ- calpain was expressed in *E. coli* an crystallized in the presence of calcium (Moldoveanu *et al.,* 2002). The X-ray structure of the -so called- mini-µ-calpain revealed Ca^{2+} ions bound to two novel non-EF-hand structures located each in a different subdomain and extremely conserved throughout the calpain family (Figure 57). The Ca^{2+}-bound active site of this mini-calpain was assembled in a papain-like conformation (Figure 56, B). Moldoveanu *et al.,* (2004) were able to elucidate the sequence of steps leading to the formation of the catalytic dyad of mini-µ-calpain and identify the key residues involved in this process. They demonstrated that Ca^{2+}- binding to the first non-EF-hand structure in domain IIa (formed by residues D106 and E185 as nucleation sites and V99, D100, G101, T103, S180, W187 and two water molecules providing coordinations) can be circumvented *in vitro,* but binding of Ca^{2+} to the second site (residues E302, D309 and D331 as nucleation sites, and E302, W303, V327, M329, E333 and two water molecules providing coordinations) and the formation of a salt bridge between R104

and E333 are indispensable for activation. The strong structural and biochemical data provided by Moldoveanu's group, the conservation of the aforementioned key residues in the calpain family (Figure 57) and the fact that some LGMD2A patients show a mutation R118G equivalent to the annihilation of R104 support this mechanism (Richard *et al.,* 1995).
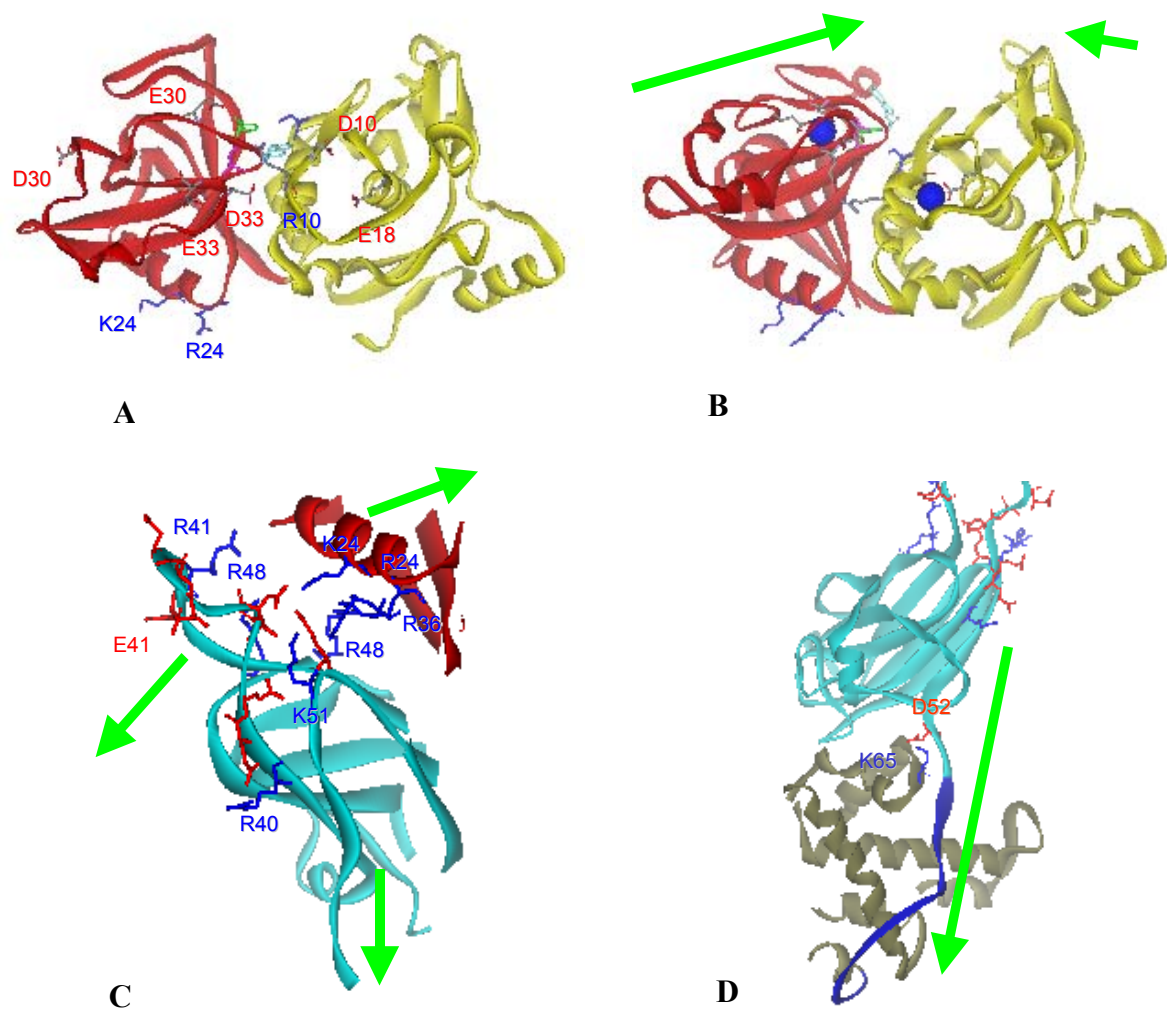
Figure 56. Structural determinants in μ-calpain activation. **A**: Ribbon diagram of the protease core of Ca^{2+}-free human μ-calpain modelled on the coordinates of human m-calpain. Key residues for catalysis were coloured as in Figure 4B. Residues involved in the "Ca^{2+}-switch" are represented in grey and basic and acidic amino acids participating in the electrostatic switch are shown in blue and red respectively. **B**: Conformational changes upon Ca^{2+} binding to the rat μ-calpain protease core (PDB code: 1KXR) take place mostly in subdomain IIb. These changes lead to the assembly of the active site. **C**: The Ca^{2+} switch is supported by an electrostatic switch mechanism at the interface between subdomain IIb and the acidic loop of domain III (model of human μ-calpain based on rat "μ-like" calpain (PDB code: 1QXP). Disruption of attractive electrostatic forces in this region enhances the flexibility of subdomain IIb. **D**: The linker region connects the Ca^{2+} -induced conformational changes in the calmodulin-like domain IV with both the electrostatic and the Ca^{2+} switch in domains III and II. Downward movement of this transducer enhances the effect of charge neutralization at the domain II domain III interface.

Nevertheless, several facts indicate that more than this is required for calpain activation: First, although mini-μ-calpain was active against synthetic and protein substrates, its specific activity was only 1/40 of that of heterodimeric m-calpain, indicating that Ca^{2+}-binding to the protease core is necessary but not sufficient for full activation of the enzyme. This fact became more evident as the same experiments were performed with a mini m-calpain: extremely low activity with SLY-AMC and < 1/100 of the specific activity of heterodimeric m-calpain toward protein substrates were detetected (Moldoveanu *et al.,* 2002; Hata *et al.,* 2001). In the case of rat mini-m-calpain, Moldoveanu *et al.* (2003) determined the crystal structure of the Ca^{2+}-loaded protease core and found a mechanism-based inhibition due to the protrusion of the Trp-106 side chain within the active- site cleft, explaining its low activity. Interestingly, Ca^{2+}-free mini-m-calpain was unstructured, presumably due to the lack of important contacts with domain III. From sequence comparison these authors suggested that the inactivation mechanism described above as well as the requirement for the structural support provided by domain III might be valid for approximately half of all calpain isoforms. In fact, the protease core of maize calpain DEK1, which consists of a membrane-anchoring domain not related to any other calpain in animals and two domains resembling the protease and the C2-like domain of calpain, was recently shown to be inactive when separated from domain III (Wang *et al.,* 2003). Moreover, the $[Ca^{2+}]_{0.5}$ for the cooperative Ca^{2+}-binding of both mini-calpains, as demonstrated by Trp intrinsic fluorescence measurements, and cleavage of the substrate SLY-AMC (in the case of mini-μ-calpain) differ largely from the values measured with the full-length heterodimeric enzyme. This observation points to the existence of important Ca^{2+}-binding sites other than the two in the protease core. Interestingly, both mini-calpains were inhibited by small synthetic inhibitors but not by calpastatin. It is evident that if calpastatin-binding to sites beyond the catalytic domain is required for inhibition of the enzyme, these regions should play an important role in enzyme activity.

In this context, the electrostatic switch activation gains in importance as the probable missing mechanism for complete activation of the calpain molecule. We hypothesize that the movement of the protease domain IIb towards domain IIa is driven by two main forces: (i) the Ca^{2+}-induced disruption of the electrostatic contacts between oppositely charged residues at the interface between domain II and domain III and (ii) the conformational changes in domain II (mainly in subdomain IIb) upon Ca^{2+} nucleation by the binding sites described above (specially the second one, formed by E302, D303 and D331). Our postulate is based on the fact that the heterodimeric D405A mutant has a similar Ca^{2+} requirement for conformational

changes and activity as the mini μ-calpain protease core (~40 μM). Therefore, in a sequential activation mechanism, disruption of electrostatic interactions at the domain IIb-domain III interface might be a prerequisite for the crucial cooperative Ca^{2+}-binding in the papain-like domain.

Comparison of the electrostatic interaction network of the acidic loops in several calpains allows us to speculate about the relationship between the Ca^{2+} requirement for activity of a calpain isoform and the strength of the contacts around the loop. The sequences aligned in Figure 57 correspond to calpain isoforms with different Ca^{2+} requirements from human to plants. Human and rat μ-calpain reportedly require 3-50 μM calcium for half-maximal activity, whereas m-calpains in both species require 0.4 - 0.8 mM (Goll *et al.,* 2003). Chicken μ/m-calpain shows an intermediate Ca^{2+} requirement between μ- and m-calpain (Kawashima *et al.,* 1984). Drosophila CALPB is a fruit fly homologue of m-calpain with a $[Ca^{2+}]_{0.5}$ of 3.3 mM (Jekely and Friedrich, 1999) and lobster CALPM was reported to reach half-maximal activity at concentrations around 0.6 mM (Mykles and Skinner, 1986). *C. elegans* tra 3 has not been purified yet, but there is evidence for its Ca^{2+}-dependent autolytical degradation *in vivo* (Sokol and Kuwabara, 2000). Calpain 3 in turn autolyzes even in the presence of EDTA, indicating that only trace amounts or no Ca^{2+} at all are needed for this process (Kinbara *et al.,* 1998; Branca *et al.,* 1999). Finally, the plant calpain gene DEK1 from maize was recently shown to be constitutively active (no calcium required) although the modelled 3D structure of its protease core matched very well with the one of m-calpain (Wang *et al.,* 2003). A detailed analysis of these sequences reveals that the calcium binding sites in the protease domain are very well conserved throughout the calpain familiy, whereas the residues involved in domain IIb-domain III interactions are more variable. DEK1 for example, lacks the acidic loop and E504 (E516 in μ-calpain) shown by Hosfield (2001) to be a key residue in the interdomain interaction. In *C. elegans* tra 3 the acidic loop is also missing, but E504 is conserved. In this isoform, residues of the protease core involved in the Ca^{2+} switch are better conserved than in DEK1. These two facts could explain why tra 3 requires Ca^{2+} for autolysis whereas DEK1 activity is Ca^{2+}-independent. Lobster CALPM has an extremely large acidic loop. Yet the number of basic interaction partners is the same as in other isoforms, explaining why the Ca^{2+} requirement of this enzyme remains in the low millimolar range. Drosophila CALPB, human and rat m-calpains have similar interdomain contacts and therefore similar calcium requirements for activity. The cluster of basic residues at the C-terminus of domain II (R364 and K365 in μ-calpain) is missing in the case of p94,: a fact that could account for the activation of this isoform at very low Ca^{2+} concentrations.

```
                     1
sp|P07384|CAN1_HUMAN     MSEEIITPVY---CTGVSAQVQKQRARELGLG-----------RHEN----AIKYLG---
sp|P97571|CAN1_RAT       MAEELITPVY---CTGVSAQVQKQRDKELGLG-----------RHEN----AIKYLG---
sp|P00789|CANX_CHICK     -----MMPFG-----GIAARLQRDRLRAEGVG-----------EHNN----AVKYLN---
sp|P17655|CAN2_HUMAN     ------------MAGIAAKLAKDREAAEGLG----------SHER----AIKYLN---
sp|Q07009|CAN2_RAT       ------------MAGIAMKLAKDREAAEGLG----------SHER----AIKYLN---
sp|P20807|CAN3_HUMAN     VAPRTAAEPR---SPGPVPHPAQSKATEAGGGNPSGIYSAIISRNFP----IIGVKE---
tr|Q9VT65|Dm-calpB       HNIGFPALPY-PTAPPPESAPTQEEEPSVGVAEL-SFTSVKVPENQNMFWMGRKATSARQ
tr|Q8MQV0|CALPM_LOBSTER  HCRCYKREGHGHMVDGIESVSLQKSTYYSRVSN--DYTQKRIAKG------GLKIP----
tr|Q22036|Ce-tra3        -------------------------------------MTRSEK----TRHFGN---
tr|Q8RVL1|DEK1_MAIZE     ------------------------------------------------------------

                     40
sp|P07384|CAN1_HUMAN     -----QDYEQLRVRCLQSGTLFRDEAFPPVPQSLGYKDLGPNSSKTYGIKWKRPTELLSN
sp|P97571|CAN1_RAT       -----QDYENLRARCLQNGVLFQDDAFPPVSHSLGFKELGPNSSKTYGIKWKRPTELLSN
sp|P00789|CANX_CHICK     -----QDYEALKQECIESGTLFRDPQFPAGPTALGFKELGPYSSKTRGVEWKRPSELVDD
sp|P17655|CAN2_HUMAN     -----QDYEALRNECLEAGTLFQDPSFPAIPSALGFKELGPYSSKTRGIEWKRPTEICAD
sp|Q07009|CAN2_RAT       -----QDYETLRNECLEAGALFQDPSFPALPSSLGFKELGPYSSKTRGIEWKRPTEICAD
sp|P20807|CAN3_HUMAN     -----KTFEQLHKKCLEKKVLYVDPEFPPDETSLFYSQKFPIQ-----FVWKRPPEICEN
tr|Q9VT65|Dm-calpB       NSVSKGDFQSLRDSCLANGTMFEDPDFPATNASLMYSRRPDRY-----YEWLRPGDIADD
tr|Q8MQV0|CALPM_LOBSTER  ---KKG-FRTLRDECLKSSKLYEDPEFPANDYSINFNGVTRRT-----YVWKRPHEITKN
tr|Q22036|Ce-tra3        -----QNYEKLRKICIKKKQPFVDTLFPPTNQSLFLEQRQSSD-----IVWKRPGELHPD
tr|Q8RVL1|DEK1_MAIZE     ---------------KGERNFTDQEFPPEDRSLFVDPMNPPLKLQVVSEWMRPSDIAKD
                                         : *  **.   ::  .            * ** ::  :

                     94
sp|P07384|CAN1_HUMAN     ------PQFIVDGATRTDICQGALGDCWLLAAIASLTLNDTLLHRVVPHGQS----FQNG
sp|P97571|CAN1_RAT       ------PQFIVDGATRTDICQGALGDCWLLAAIASLTLNETILHRVVPYGQS----FQEG
sp|P00789|CANX_CHICK     ------PQFIVGGATRTDICQGALGDCWLLAAIGSLTLNEELLHRVVPHGQS----FQED
sp|P17655|CAN2_HUMAN     ------PQFIIGGATRTDICQGALGDCWLLAAIASLTLNEEILARVVPLNQS----FQEN
sp|Q07009|CAN2_RAT       ------PQFIIGGATRTDICQGALGDCWLLAAIASLTLNEEILARVVPLDQS----FQEN
sp|P20807|CAN3_HUMAN     ------PRFIIDGANRTDICQGELGDCWFLAAIACLTLNQHLLFRVIPHDQS----FIEN
tr|Q9VT65|Dm-calpB       ------PQFFVEGYSRFDVQQGELGDCWLLAAAANLTQDSTLFFRVIPPDQD----FQEN
tr|Q8MQV0|CALPM_LOBSTER  ------PRFFIDGATRFDIQQGELGDCWLLAAVSNLTLNPQMFHAVVPRDQG----FIDL
tr|Q22036|Ce-tra3        ------PHLFVEGASPNDVTQGIGLGNCWFVSACSALTHNFKLLAQVIPDADDQEWSTKHA
tr|Q8RVL1|DEK1_MAIZE     ISISCQPCLFSGSVNSSDVCQGRLGDCWFLSAVAVLTEMSRISEVIITPEY--------N
                              * ::  .  .  *: ** **:**:::* . **     :    ::.

                     145
sp|P07384|CAN1_HUMAN     YAGIFHFQLWQFGEWVDVVVDDLLPIKD-GKLVFVHSAEGNEFWSALLEKAYAKVNGSYE
sp|P97571|CAN1_RAT       YAGIFHFQLWQFGEWVDVVVDDLLPTKD-GKLVFVHSAQGNEFWSALLEKAYAKVNGSYE
sp|P00789|CANX_CHICK     YAGIFHFQIWQFGEWVDVVVDDLLPTKD-GELLFVHSAECTEFWSALLEKAYAKLNGCYE
sp|P17655|CAN2_HUMAN     YAGIFHFQFWQYGEWVEVVVDDRLPTKD-GELLFVHSAEGSEFWSALLEKAYAKINGCYE
sp|Q07009|CAN2_RAT       YAGIFHFQFWQYGEWVEVVVDDRLPTKD-GELLFVHSAEGSEFWSALLEKAYAKINGCYE
sp|P20807|CAN3_HUMAN     YAGIFHFQFWRYGEWVDVVIDDCLPTYN-NQLVFTKSNHRNEFWSALLEKAYAKLHGSYE
tr|Q9VT65|Dm-calpB       YAGIFHFKFWQYGKWVEVVIDDRLPTYN-GELIYMHSTEKNEFWSALLEKAYAKLHGSYE
tr|Q8MQV0|CALPM_LOBSTER  YAGIFHFKFWQYGKWQEVVVDDRLPTYN-GRLVFMHSKTENEFWCALFEKAYAKLYGGYE
tr|Q22036|Ce-tra3        YAGIFRFRFWRFGKWVEVVIDDLLPTRD-GKLLFARSKTPNEFWSALLEKAFAKLYGCYE
tr|Q8RVL1|DEK1_MAIZE     DEGIYTVRFCIQGEWVAVVVDDWIPCESPGKPAFATSRKQNELWVSILEKAYAKLHGSYE
                         **: .::   *:*  **:** :*  . .. :  *   .*:* :::***:**: * **
```

```
                        268
sp|P07384|CAN1_HUMAN      LVKGHAYSVTGAKQVNYR-------------GQVVSLIRMRNPWG-EVEWTGAWSDSSS
sp|P97571|CAN1_RAT        LVRGHAYSVTDAKQVTYQ-------------GQRVNLIRMRNPWG-EVEWKGPWSDNSY
sp|P00789|CANX_CHICK      LVKGHAYSVTAFKDVNYR-------------GQQEQLIRIRNPWG-QVEWTGAWSDGSS
sp|P17655|CAN2_HUMAN      LVKGHAYSVTGAEEVESN-------------GSLQKLIRIRNPWG-EVEWTGRWNDNCP
sp|Q07009|CAN2_RAT        LVKGHAYSVTGAEEVESS-------------GSLQKLIRIRNPWG-QVEWTGKWNDNCP
sp|P20807|CAN3_HUMAN      LVRGHAYSVTGLDEVPFK-------------GEKVKLVRLRNPWG-QVEWNGSWSDRWK
tr|Q9VT65|Dm-calpB        LIRGHAYSITKVCLMDIS----------TPNRQGKLPMIRMRNPWGNDAEWSGPWSDSSP
tr|Q8MQV0|CALPM_LOBSTER   LIMRHAYSITRVTTVDIKS--------VVPRLQGKAQLIRLHNPWGNEAEWKGSWSDKSP
tr|Q22036|Ce-tra3         LVKGHAYAVSAVCTIDVTNPNERSFTSFIMGSKRKQNLIRLQNPWG-EKEWNGAWSDDSP
tr|Q8RVL1|DEK1_MAIZE      IVQGHAYSILQVREVDGH-----------------KLIQIRNPWANEVEWNGPWSDSSP
                          ::  ***::     :                          :::::***. : **.* *.*

                        313
sp|P07384|CAN1_HUMAN      EWNNVDPYERDQLRVKM-----EDGEFWMSFRDFMREFTRLEICNLTPDALKSRT-----
sp|P97571|CAN1_RAT        EWNKVDPYEREQLRVKM-----EDGEFWMSFRDFIREFTKLEICNLTPDALKSRT-----
sp|P00789|CANX_CHICK      EWDNIDPSDREELQLKM-----EDGEFWMSFRDFMREFSRLEICNLTPDALTKDE-----
sp|P17655|CAN2_HUMAN      SWNTIDPEERERLTRRH-----EDGEFWMSFSDFLRHYSRLEICNLTPDTLTSDT-----
sp|Q07009|CAN2_RAT        SWNTVDPEVRANLTERQ-----EDGEFWMSFSDFLRHYSRLEICNLTPDTLTCDS-----
sp|P20807|CAN3_HUMAN      DWSFVDKDEKARLQHVT----EDGEFWMSYEDFIYHFTKLEICNLTADALQSDK-----
tr|Q9VT65|Dm-calpB        EWRFIPEHTKEEIGLNFD----RDGEFWMSFQDFLNHFDRVEICNLSPDSLTEDQ-----
tr|Q8MQV0|CALPM_LOBSTER   EWNSITPEEKQRLKLNFE----DDGEFWMSFQDFASNFTTVEICDVTPEVFDHDDSDDEN
tr|Q22036|Ce-tra3         EWQNVSASQLSTMGVQPANSDSDDGDFWMPWESFVHYFTDISLCQLFNTSVFSFSR----
tr|Q8RVL1|DEK1_MAIZE      EWTERMKHKLMHVPQSK------NGVFWMSWQDFQIHFRSIYVCRVYPPEMRYSV-----
                          .*           :          :* ***.: .*   :  : :* :    .

                        363
sp|P07384|CAN1_HUMAN      ---------IRKWNTTLYEGTWRRGSTAGGCRNYPATFWVNPQFKIRLDETDDPDDYGDR
sp|P97571|CAN1_RAT        ---------LRNWNTTFYEGTWRRGSTAGGCRNYPATFWVNPQFKIRLEEVDDADDYDSR
sp|P00789|CANX_CHICK      ---------LSRWHTQVFEGTWRRGSTAGGCRNNPATFWINPQFKIKLLEEDDDPGDD
sp|P17655|CAN2_HUMAN      ---------YKKWKLTKMDGNWRRGSTAGGCRNYPNTFWMNPQYLIKLEEEDEDEEDG
sp|Q07009|CAN2_RAT        ---------YKKWKLTKMDGNWRRGSTAGGCRNYPNTFWMNPQYLIKLEEEDE--DDEDG
sp|P20807|CAN3_HUMAN      ---------LQTWTVSVNEGRWVRGCSAGGCRNFPDTFWTNPQYRLKLLEEDD--DPDDS
tr|Q9VT65|Dm-calpB        -----QHSSRRKWEMSMFEGEWTSGVTAGGCRNFLETFWHNPQYIISLEDPDD--EDDD-
tr|Q8MQV0|CALPM_LOBSTER   GNTKMEESAPKRWQMVMYEGAWAAHHSAGGCRNFINTFASNPQFTVQLEDPDD--DDDDD
tr|Q22036|Ce-tra3         --SYDEQIVFSEWTTNG-KKSGAPDDRAGGCHNFKATFCNNPQYIFDIPSPN--------
tr|Q8RVL1|DEK1_MAIZE      -----------------HGQWR-GYNAGGCQDY-DSWHQNPQYRLRVTGRDA-LYPVHV
                          .            ****::   ::  ***: . :    :

                        414
sp|P07384|CAN1_HUMAN      E----------SGCSFVLALMQKHRRRERRFGRDMETIGFAVYEVPPELVGQPAVHLKRD
sp|P97571|CAN1_RAT        E----------SGCSFLLALMQKHRRRERRFGRDMETIGFAVYQVPRELAGQP-VHLKRD
sp|P00789|CANX_CHICK      E----------VACSFLVALMQKHRRRERRVGGDMHTIGFAVYEVPEEAQGSQNVHLKKD
```

Figure 57. Sequence alignment of domains I to III of some members of the calpain family. From top to bottom: human μ-calpain, rat μ-calpain, chicken μ/m-calpain, human m-calpain, rat m-calpain, *Drosophila* CALPB, american lobster CALPM*, C. elegans* tra 3 and the cytosolic tail of maize DEK1. Accession numbers of these isoforms are shown left of each sequence. Amino acid numbering corresponds to human μ-calpain. The identity level between the isoforms is indicated as follows (*) = 100 %, (:) ≥ 75 % and (.) ≥ 50 %. Catalytic amino acids are represented in bold letters and underlined. Key residues in the coordination of Ca^{2+} and initiation of the conformational changes in the protease core are shown in colors. R104 and E333 are underlined. Amino acids involved in the interactions at the interface of domains IIb and III are represented in italic and highlighted with colors. Acidic residues in domain III mutated either in this study or by other groups are underlined Basic residues are coloured in blue and acidic residues in red.

Analysis of the recently published X-ray structure of a μ/m calpain hybrid engineered for efficient expression in *E. coli* that contains 85 % of the rat μ-calpain sequence (Pal *et al.,* 2003) provides further evidence for the influence of electrostatic interactions on the Ca^{2+}-requirements for activity. When compared with the acidic loop region of m-calpain, the acidic loop of μ- calpain has a somewhat more "twisted" structure and the potential electrostatic interactions of the loop with basic residues are partially different (Figure 58). The most obvious difference is that in the μ-calpain loop the role of Asp-400 of m-calpain which interacts with Lys-226 is taken over by a basic residue, Arg-413, interacting with Asp-233 in subdomain IIb. With the exception of Asp-402/Arg-400 (μ-calpain) and Glu-392/Lys-390 (m-calpain) which are separated in sequence by a single residue, the distances of potentially interacting acidic and basic side chains are markedly greater in μ-calpain than in m-calpain and are out of the range (> 4 Å) required for the formation of single stable salt bridges (Kumar and Nussinov, 2002). This difference correlates with a closer positioning of the catalytic Cys-115 Sγ and His-272 Nδ1 (6.3 Å) in the "apo" conformation of μ-like calpain compared to the corresponding atoms of m-calpain (10.5 Å) and might, at least partially, contribute to the lower Ca^{2+}-requirement of μ-calpain.

E.3. Modulation of μ-calpain responsiveness to Ca^{2+} by domain V

In this work we have also analyzed the contribution of domain V of the small subunit (28K) to the primary phase of calpain activation. The first observations concerning this topic were made by DeMartino in 1986, who reported a decrease in the Ca^{2+} requirement for activity of purified bovine m-calpain upon autolytical removal of the NH_2-terminal segment of the 28K subunit. The results of those pioneer experiments were partially ignored for a long time, due to justified concerns about the accuracy of SDS-PAGE to asses the small change of mass produced by autolysis of domain I (Goll *et al.,* 2003) see Figure 7). In addition, several reports defined the removal of the "anchor" as the only event responsible for the reduction of the Ca^{2+} requirement for activity: Imajoh (1986) came to this conclusion by separating rabbit m-calpain subunits and creating hybrids of the autolyzed large subunit with the non-autolyzed small subunit. Brown (1993) proved the same by following the kinetics of bovine m-calpain subunit autolysis and the decrease in the Ca^{2+} requirement for activity. Elce (1997) compared a full-length and a domain V-truncated rat m-calpain expressed in *E. coli*. In all these studies, the effect the autolysis of domain V was found to be not significant when compared to the

	μ-Calpain							m-Calpain					
	D402	E403	D405	D406	D412	R413		E392	E393	D395	E396	D397	D400
D233						4.6	K226						3.2
K240			5.4				K230					2.6	
R364				5.9									
R400	2.9						D390	3.1					
R413					5.8								
K517		5.6	6.0	3.8			K505		5.4	5.2	4.4		
							K506		3.1				
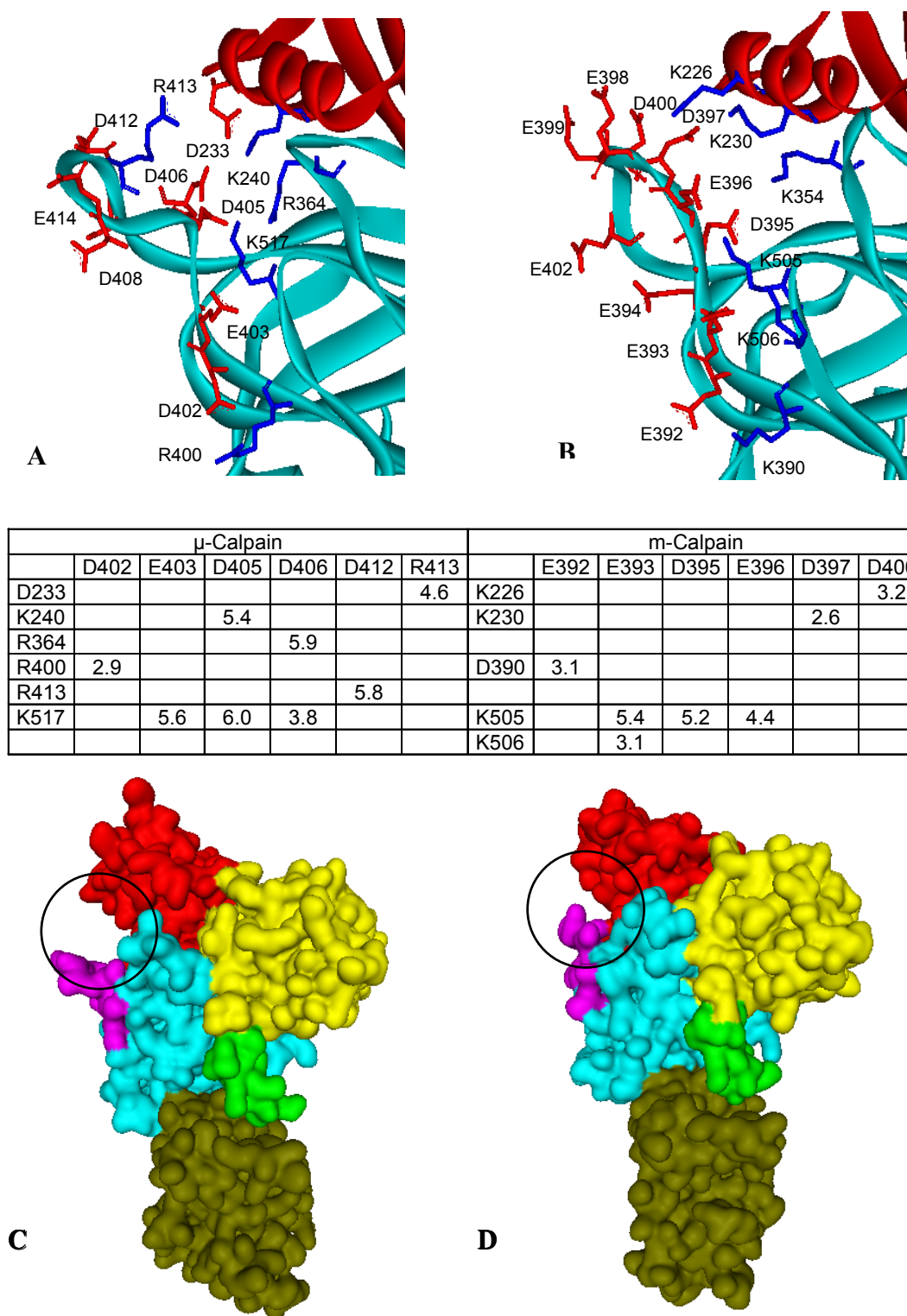
Figure 58. Structural comparison of the acidic loops of μ- and m-calpain. Ribbon plots of (**A**) human μ-calpain modelled using rat "μ-like" calpain (PDB code 1qxp) as template and (**B**) human m-calpain (PDB code 1kfu) showing potential interactions with domain IIb and the root of the domain III-IV linker (transducer). Only side chains with interacting charges separated by < 6 Å are shown and the minimal distances in Å are represented in the table below. The surface structures of both molecules are represented in **C** and **D** (same orientation as in A and B) with the interfaces between domain IIb (red) and domain III acidic loop (magenta) enclosed in circles.

reduction caused by removal of domain I. Of note, in these papers the starting material was already a mixture of full-length and partially degraded small subunit, which is known to lose gradually its first 86 amino acids even when stored at –20 °C and under EDTA (see Figure 7). This would imply that when using purified native and recombinant active calpains the integrity of the small subunit is not guaranteed. The conclusions derived from these experiments with m-calpains do not necessarily apply for μ-calpain. It has been well documented that both enzymes have different kinetics of autolysis, with a faster degradation of the small subunit in the case of m-calpain (Brown and Crawford, 1993) and a parallel cleavage of both NH_2-terminal domains for μ-calpain (Cottin *et al.,* 1991; Zimmerman and Schlaepfer, 1991).

In this work an active-site mutant was used for the first time to test the effect of autolysis of domain V on the increase in Ca^{2+} responsiveness with methods other than the classical activity measurements. Deletion of the first 86 amino acids in domain V resulted in a ~ 4 fold decrease of the Ca^{2+} requirement for conformational changes relative to the full length (C115A) enzyme. These results led us to compare the $[Ca^{2+}]_{0.5}$ for activity of wild type μ-calpain and the Δ1-86 domain V mutant at the very initial stages of enzyme activation (Figure 44). Only freshly prepared lysates were used to avoid premature degradation of the small subunit. The outcome of these experiments was in agreement with the fluorescence spectroscopy measurements, indicating that domain V represents a structural constraint to the activation of calpain, and its autolytical release is as important as the cleavage of the anchor helix. It is difficult to figure out a molecular basis for this function of domain V. If this region would make stable contacts with the protease core or other domains, one would expect to see the corresponding electron density in the crystal structure. However, it has been reported that partial and complete removal of domain V by μ-calpain reduces the Ca^{2+} requirement for the activation of m-calpain (Tompa *et al.,* 1996). In recent studies with μ- and m- calpain the partial removal of domain V by tryptic digestion resulted in an increase of the enzymatic activity (Thompson *et al.,* 2003). We therefore assume that random interactions of this domain with one or more of the Ca^{2+}-binding regions might affect either the exposure of these structures to their ligand or their ability to undergo conformational changes, explaining why removal of domain V enhances the Ca^{2+} sensitivity of the enzyme. The possibility of an alternative cleavage of the NH_2-terminals from either the large or the small subunit as a localization- or process-specific mechanism of calpain activation have been raised by novel observations in tumor cell lines in which increased expression and specific autolysis of the mitochondrial calpain small subunit were tightly associated with calpain activation in an early

stage of apoptosis. (Daniel *et al.*, 2003). Besides the importance of the removal of domain V for the activation mechanism itself, a role of the derived peptides as chemotactic agents on neutrophiles and immunocytes as well as spasmogenic agents has been proposed by the group of Kunimatsu (1989, 1990, 1993, 1995).

E.4. Analysis of the association of μ-calpain with membrane phospholipids

One of the most frequently discussed mechanisms of calpain activation is the putative interaction of these enzymes with biological membranes. This proposed interaction relies on the observation *in vitro* that phospholipids reduce the Ca^{2+} requirement of the calpains for autolysis (Goll *et al.,* 2003). A commonly accepted hypothesis emerging from that observation argues that calpain activation takes place at cellular membranes (Mellgren, 1987; Suzuki *et al.,* 1987). Under resting conditions only small amounts of erythrocyte calpain were detected in the detergent-soluble fraction (Hatanaka *et al.,* 1984) and at the cell membranes *in situ* (Samis and Elce, 1989). This situation is reversed in the presence of a calcium influx: Significant amounts of μ-calpain have been found partially associated with the membrane fraction of lysed cells (Michetti *et al.,* 1996; Zhao *et al.,* 1998) as well as located at the cell pheriphery *in situ* (Saido, Suzuki *et al.,* 1993; Gil-Parrado *et al.,* 2003) upon treatement with Ca^{2+} ionophores. Such observations suggested that a much lower Ca^{2+} requirement for association with phospholipids than for enymatic activity and autolysis could be a prerequisite for calpain activation at cell membranes.

In this work we have determined congruent $[Ca^{2+}]_{0.5}$ values for the binding of μ-calpain to membranes *in vitro* using two distinct biophysical methods. Our data reveal the surprising fact that μ-calpain requires for the association with phospholipid vesicles the same Ca^{2+} concentration as it requires in the absence of phospholipids for activity prior to autolysis (Baki *et al.,* 1996). The Ca^{2+} requirements for vesicle binding were similar to those measured for conformational changes, activation and aggregation, corroborating the existence of a relationship between the structural Ca^{2+} switch and the membrane targeting (Figure 59). These findings suggest that membrane binding might not be a prerequisite for enzyme activation and could even occur as a consequence of the conformational changes accompanying the asembly of the catalytic domain. Recent studies have demonstrated that Ca^{2+}-dependent structural rearrangements of calpain lead to a less soluble conformation with higher tendency to form protein aggregates (Pal *et al.,* 2001; Dainese *et al.,* 2002). We therefore reason that an
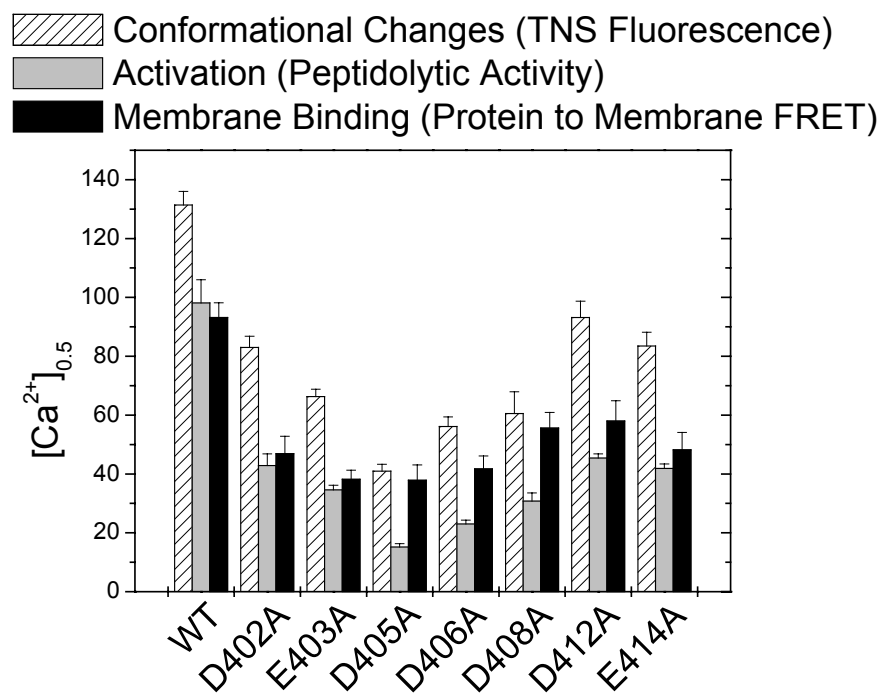
Figure 59. Effect of mutations in the acidic loop of μ-calpain domain III on the Ca^{2+} requirement for conformational changes, activation and membrane binding.

increase in hydrophobicity during transition to the active conformation could be responsible as well for Ca^{2+}-dependent membrane targeting of calpain. Congruently, early work had postulated that a Ca^{2+}-mediated transition from a weakly to a highly hydrophobic conformation accounts for the strong hydrophobic association of calpain with phenyl Sepharose *in vitro* (Gopalakrishna and Head, 1985) or with the insoluble fractions of rat brain homogenates in the order of microsomal > plasma membrane > nuclear fractions (Gopalakrishna and Barsky, 1986).

Our view of membrane binding as a consequence instead of a premise for activation is in agreement with earlier work questioning the influence of phospholipids on calpain activity (Cong, Goll *et al.,* 1989) and demonstrating the inability of inside-out erythrocyte membranes to decrease the Ca^{2+} requirement for calpain autolysis (Goll *et al.,* 2003). In fact, when we incubated 1-5 nM native μ-calpain isolated from human erythrocytes with 40-100 μM of the vesicles listed in Table 4 no significant effects on the $[Ca^{2+}]_{0.5}$ for the hydrolysis of SLY-AMC was observed (data not shown). Probably the reported effects of phospholipid vesicles on the Ca^{2+}-requirement for calpain autolysis *in vitro* can be explained by stabilization of the more hydrophobic active conformation by the aliphatic chains of the phospholipids. Already early studies noticed that all of the phospholipid molecule and not only the headgroup is

required for an effect on calpain autoproteolysis (Coolican and Hathaway, 1984). Thus we postulate that the hydrophobic interaction of calpain with the apolar moiety of phospholipids may increase the effective concentration of activated calpain molecules able to perform autoproteolysis (that lowers the Ca^{2+} requirement for activity) and prevent the formation of inactive large protein aggregates (Pal *et al.,* 2001; Dainese *et al.,* 2002).

Owing to the structural features described in the Introduction, the hydrophobic, Gly-rich domain V (Figure 60) and the C2-like domain III were favorite candidates for being the
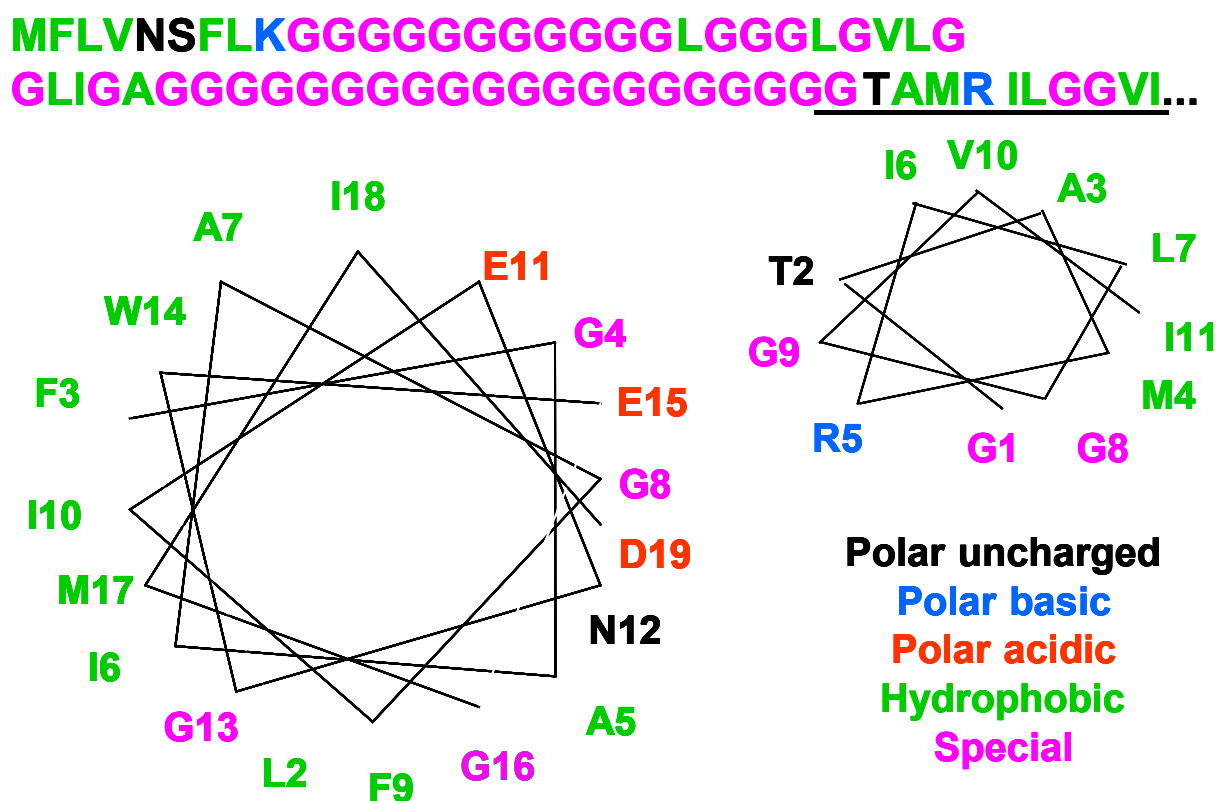
Figure 60. Calpain domain V has the potential to penetrate membranes. The sequence of domain V (top) reveals a hydrophobic region with polyglycine stretches which have been shown to be important for the association with phospholipids (see text for details). A special sequence motif at the C-terminus of the domain (underlined) can potentially form a oblique-oriented α-helix (bottom right) with a highly hydrophobic side (green residues) similar to the one observed in the influenza virus (bottom left).

phospholipid binding sites in calpain. In fact, early studies with intact and autoproteolytically processed calpains as well as with domain V-mimicking synthetic peptides suggested a pivotal role of the N-terminal region of the small subunit in the interaction of calpain with membranes (Imajoh *et al.,* 1986; Crawford *et al.,* 1990; Arthur and Crawford, 1996; Brandenburg *et al.,* 2002).

More recent work has also demonstrated that isolated domain III is able to bind liposome vesicles in a Ca^{2+}-dependent fashion (Tompa *et al.,* 2001, Alexa *et al.,* 2004). Furthermore, domain III-EYFP chimeras translocated in cells from the cytosol to the membranes upon stimulation with the Ca^{2+} ionophore ionomycin (Gil-Parrado *et al.,* 2003). Here we have analyzed for the first time the specific contribution of domain V and domain III in the context of a non-autolyzing active-site mutated heterodimeric μ-calpain. A role of domain V of the small subunit is suggested by the observed distinct reduction of phospholipid affinity of the domain V-truncated (ΔD-V) enzyme (Figure 61).
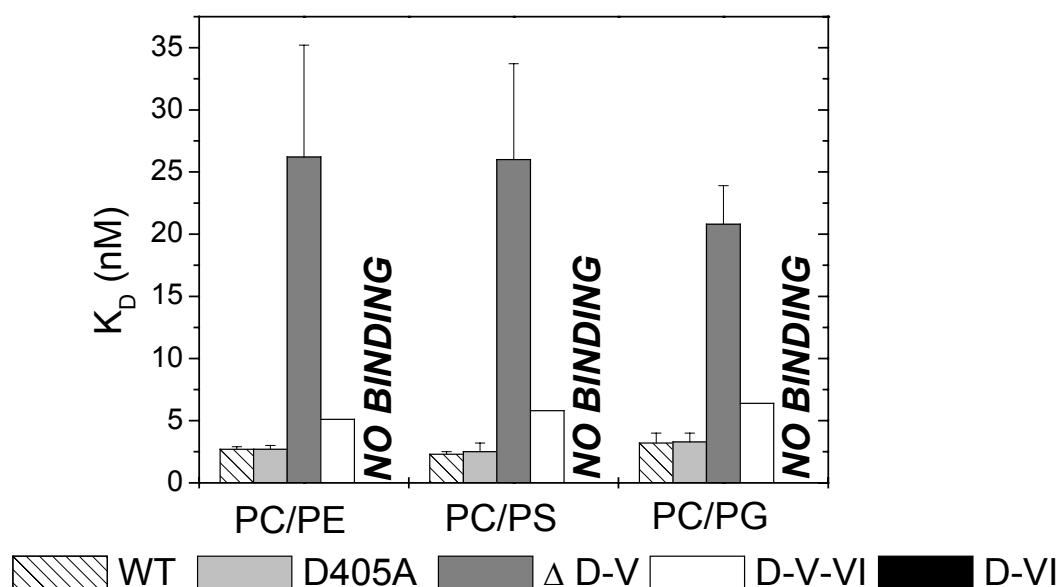
Figure 61. Summary of the binding affinities of calpain variants to immobilized phospholipid vesicles (Biacore)

Further evidence for this provided the Ca^{2+}-dependent phospholipid binding of the isolated full-length small subunit, which was abolished by deletion of domain V. Similar observations had previously been made with grancalcin (Teahan *et al.,* 1992), sorcin (Meyers *et al.,* 1995), DdPEF (Ohkouchi *et al.,* 2001), ALG2 and peflin (Kitaura *et al.,* 2001), which have been grouped in the penta-EF hand protein family together with the small subunit of calpain (Maki *et al.,* 2002). Particularly in the case of peflin deletion of the N-terminal domain resulted in a decreased Ca^{2+} sensitivity of membrane binding. It was discussed that the flexible N-terminal peptide may either (i) enhance a Ca^{2+}-induced conformational

change in the PEF domain that leads to binding to membrane components or (ii) be released from the PEF domain upon binding to Ca^{2+} and directly associate with membranes, in a way similar to the Ca^{2+}-myristoyl switch of recoverin for binding to membranes (Zozulya and Stryer, 1992). The second model suits better to our findings with μ-calpain: the small structural rearrangements caused by Ca^{2+}-binding to the EF-hand structures in domain VI might enhance the transition of domain V from a disordered secondary structure to an oblique-oriented α-helix similar to the membrane-penetrating helix of the influenza virus (Brandenburg *et al.,* 2002) (Figure 60). The importance of the Arg residue in this process has been demonstrated by the abolishment of the binding to radioactively labelled vesicles of a $^{46}G_{10}TAMRILGG^{64}$ synthetic peptide when a R60Q charge-neutralizing mutation was introduced (Arthur and Crawford, 1996). Probably the structural transition involves release of the positive side chain charge of R60 involved in salt bridges or other electrostatic interactions in the "apo" conformation as a consequence of Ca^{2+}-binding to the first EF hand in domain VI. We have discussed in the previous section how transduction of small changes in conformation and/or electrostatic charge around the corresponding EF-hand of domain IV by the flexible ~15 aa D-III/D-IV linker may affect activation events taking place at the interface between domain IIb and domain III in human μ-, rat m- and Drosophila calpain B.

A **B** **C**
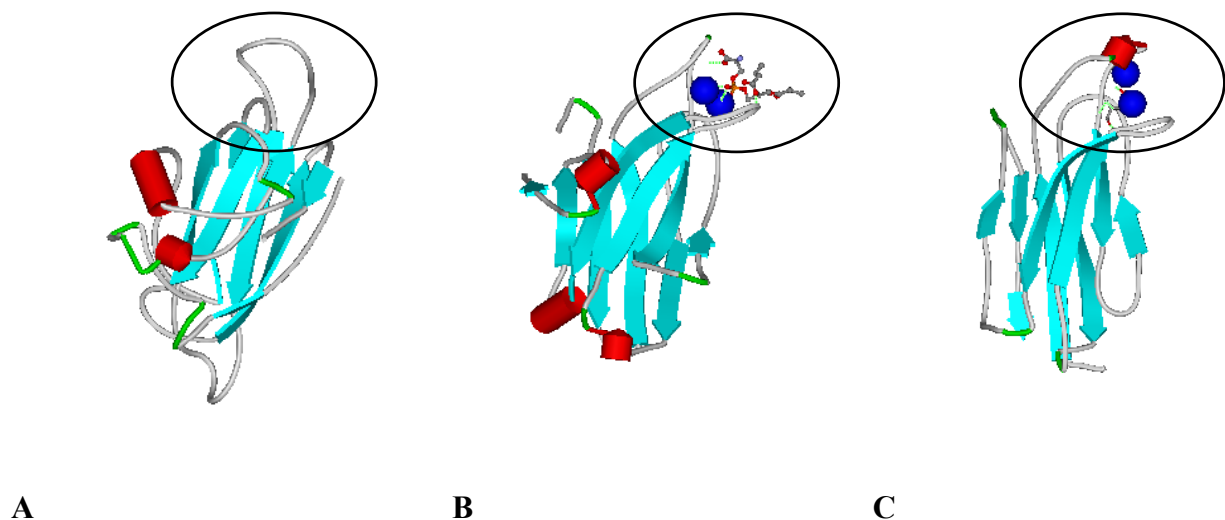
Figure 62. Structural similarities between calpain domain III and the "classical" C2 domains. Schematic representation of the "C2-like" domain III of human m-calpain (**A**), Ca^{2+}-bound C2 domains of PKCα (PDB code 1DSY) (**B**) and cPLA$_2$ (PDB code 1BSI) (**C**). Note in PKCα the electrostatic binding to a phosphatidyl serine molecule (represented here as a ball and stick structure) bridged by the two Ca^{2+} ions. The acidic loop of calpain domain III and the Ca^{2+} binding loop in PKCα and cPLA$_2$ have been encircled for better identification.

A major surprise from our study was the ability of the domain III acidic loop D405A mutant to bind to immobilized phospholipid vesicles with the same affinity as the wild type enzyme did. As anticipated from structure and functional studies, this mutation should disrupt the putatively most important residue in Ca^{2+} nucleation by the C2-like domain III (Figure 62) (Strobl *et al.,* 2000; Alexa *et al.,* 2004). Several site-directed mutagenesis studies with the C2 domains of PKCα (Medkova and Cho, 1998; Corbalan-Garcia *et al.,* 1999), cPLA (Bittova, *et al.,* 1999), Syt (Fernandez-Chacon, *et al.,* 2002) and other C2 domain proteins have shown that mutation of the acidic residues in the Ca^{2+}-binding loops of the isolated domains result in an important decrease of the affinity for membranes. These results do not necessarily mean that domain III plays no role in μ-calpain membrane binding. Our data suggest, however, that either (i) the contribution of Ca^{2+}-mediated electrostatic interactions with membranes via the acidic loop is minimal in the context of a heterodimeric enzyme or (ii) additional sites in domain III are involved in the interactions with membranes. Interestingly, new regions different from the classical Ca^{2+}- and anionic phospholipid-binding loops have been shown in the C2 domain of PKCβ (Sutton and Sprang, 1998) and PKCα (Ochoa, *et al.,* 2002; Rodriguez-Alfaro *et al.,* 2004) to be involved in membrane association. Most surprisingly, μ-calpain showed nor preference for negatively charged headgroups as described for most of Ca^{2+}-dependent membrane-binding C2 domains, neither for neutral/zwitterionic ones as in the case of cPLA (Figure 62) (Cho, 2001; Murray and Honig, 2002). Unlike other C2-domain containing proteins (Das *et al.,* 2003), the binding affinities of calpain to nuclear envelope- and plasma membrane-mimicking bilayers were similar. The latter observations are in agreement with a previous study in which several phospholipids with differently charged headgroups had similar positive effects on calpain autolysis (Arthur and Crawford, 1996). These authors explained the discrepancies in older reports (Coolican and Hathaway, 1984; Pontremoli *et al.,* 1985; Chakrabarti *et al.,* 1990) and the small quantitative differences in headgroup selectivity in their own study by the different ability of the tested phospholipids to form bilayers suitable for interaction. In any case, the lack of headgroup selectivity supports our hydrophobic membrane binding model proposed above. Independent of the headgroup or the vesicle composition evaluated, the dissociation constants measured were within the nanomolar range (see Figure 63) and therefore comparable with those of other Ca^{2+}-dependent membrane binding proteins like anexins V (Tait, Gibson *et al.,* 1989), A1 (Kastl *et al.,* 2002), and A2 (Ross *et al.,* 2003), coagulation factors V (Pusey *et al.,* 1982), VIII (Saenko *et al.,* 1999) and X (Erb *et al.,* 2002) and typical C2-domain containing proteins such
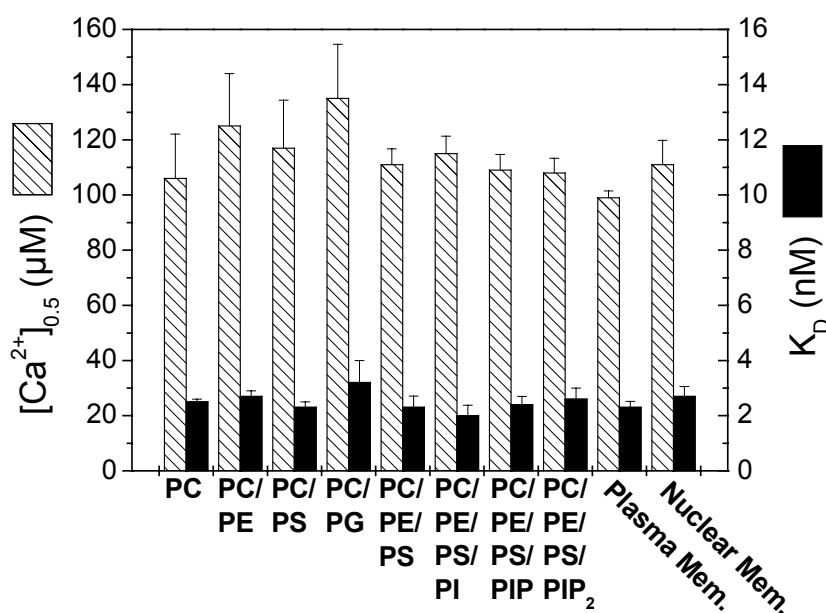
Figure 63. Phospholipid selectivity of heterodimeric human μ-calpain. The Ca^{2+} requirement ($[Ca^{2+}]_{0.5}$) for the binding is plotted on the left Y axis and the affinity (K_D) on the right one.

as PKC (Bazzi and Nelsestuen, 1987) synaptotagmin (Niinobe *et al.,* 1994) and phospholipase A2 (Kim *et al.,* 1997). This observation strongly supports the suitability of phospholipids as interaction partners of calpain at the cell boundaries, a function once attributed exclusively to membrane-associated proteins (Inomata *et al.,* 1990).

E.5. Conclusions and Outlook

The accurate identification of the multiple Ca^{2+}-binding sites in the calpain molecule as well as the elucidation of the conformational changes induced by this cation will be only possible after determination of the crystal structure of a Ca^{2+}-bound calpain. Due to the persistent technical difficulties of this endeavour (Pal *et al.,* 2001), every study addressing the still open questions by methods other than crystallization will help to reveal the mechanisms of calpain activation. In this work the individual contributions of the amino acid residues involved in the previously proposed electrostatic switch activation mechanism have been identified. The fact that an independent research group obtained congruent results with *Drosophila* CALPB and rat m-calpain within the same period enhances the validity of our own results. Both studies, together with the thorough investigation of the Ca^{2+} switch in the protease core by Moldoveanu and colleagues deepen our understanding of the Ca^{2+}-dependent conformational changes leading to calpain activation (Figure 65).

Yet, the central regulatory role of domain III has not been definitively elucidated by the experiments described here. A striking structural feature of the calpains whose function remains to be investigated is the "basic loop" formed by residues K414, R416, R417, R418, R420 and K421 (m-calpain numbering; K414 is K426 in μ-calpain), which is located on the opposite side of the acidic loop (Figures 6, A and 64). Interactions of R417 with E811 and E863 as well as R420 with S788 have been postulated to be structural requirements for the stabilization of domain III by the small subunit (Moldoveanu *et al.,* 2003).
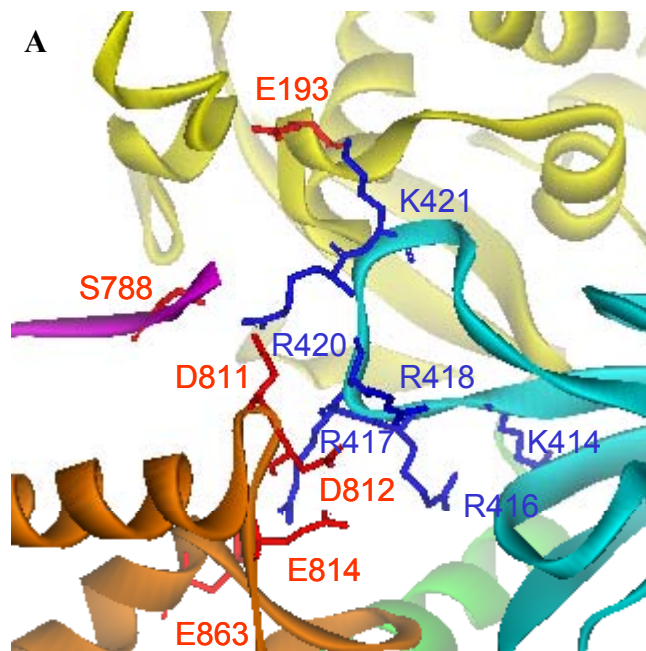
Figure 64. Electrostatic interactions of the basic loop of domain III of human m-calpain.
(**A**) The ribbon plot shows charged residues at the interface between the loop (see also Figure 6, A) and domains VI (brown) and IIa (yellow). Interactions with domain VI are required for heterodimer formation, whereas contacts with subdomain IIb stabilize the protease core.
(**B**) Section of the sequence alignment presented in Figure 57 showing the conservation of the basic loop in the calpain family. Underlined residues represent mutations in CAN3 detected in LGMD2A patients

```
B                                    424          438
sp|P07384|CAN1_HUMAN       MQKHRRRERRFGRDM
sp|P97571|CAN1_RAT         MQKHRRRERRFGRDM
sp|P00789|CANX_CHICK       MQKHRRRERRVGGDM
sp|P17655|CAN2_HUMAN       IQKHRRRQRKMGEDM
sp|Q07009|CAN2_RAT         IQKHRRRQRKMGEDM
sp|P20807|CAN3_HUMAN       MQKNRRKDRKLGASL
tr|Q9VT65|Dm-calpB         MQKNRRSKRNVGIDC
tr|Q8MQV0|CALPM_LOBSTER    MQKNVRQLKRYGVDY
tr|Q22036|Ce-tra3          CSVMFAL IQNDPSE
tr|Q8RVL1|DEK1_MAIZE       ITLTQGVGF SRKTN
```

The fact that deletion of EF-1 from the small subunit affects the stability of the heterodimer demonstrates the importance of these contacts (Elce *et al.,* 1997). Based on our experience with the acidic loop, we believe that further coulombic interactions of the whole basic loop with residues D812, E814 and E862 in EF-hand 1 of domain VI should not be excluded from consideration. Of note, single mutation of one of these acidic residues in domain VI-EF-1 to Ala, together with similar single mutations in EF-2, EF-3 and EF-4, originated a significant increase of the Ca^{2+} requirement for activity of rat m-calpain (Dutt *et al.,* 2000). The most convincing evidence for the importance of this basic loop is provided by the existence of LGMD2A (see B.3) patients harboring the calpain 3 mutations R489W, R490W and R493W which are equivalent to elimination of the charged side chains of R416, R417 and R420 in m-calpain (Jia *et al.,* 2001). Another function of the basic loop noticed by

Moldoveanu (2003) was the stabilization of the protease core through a salt bridge between residues R420 and E193, the coordination of a water molecule by Q419 and Y146 and van der Waals attractive forces between M422 and W106. These interactions should prevent the collapse of W106 described in E.2. Here again LGMD2A patients the mutation E217K (equivalent to E193K in m-calpain) has been observed, providing support for the important role of the basic loop of domain III (Jia *et al.,* 2001).

We therefore postulate that Ca^{2+}-binding to D-VI EF-I causes a disruption of the interactions with the basic loop of D-III which results in overall flexibilization of this domain and favours the previously discussed movement of the acidic loop away from the protease core on the opposite side of the molecule. Additionally, the electrostatic density changes originating by rupture of the contacts of domain III with domain VI might enhance the stabilizing effect on the protease core by reinforcement of the interactions at the interface between the basic loop and the protease domain IIa. In future investigations, the individual role of each residue in the basic loop could be tested with a new Ala scan of this region, followed by a detailed characterization of the generated mutants.

Our experiments concerning domain V reveal a new aspect in calpain activation which needs to be further investigated. Autolytical processing of this domain occurs in several steps. First only 26 residues from the N-terminal are removed, then additional 37 (to Gly-64), and finally 28 more (to Ala-92) to render the Δ91 aa-truncated small subunit. It would be therefore interesting to create deletion mutants simulating the intermediate states in order to find out the minimal cleavage required for the observed reduction of the Ca^{2+} requirement. Alternative expression of these mutants with the full-length large subunit and a domain I deletion mutant would help to clarifiy the individual role of each autolysis step in calpain activation. Of note, some acidic residues at the C-terminus of domain V which have been deleted in our mutant (see appendix G) could be also involved in interactions with the above described basic loop of domain III. Site-directed mutagenesis of these residues would help to clarify this issue.

The data presented in this work concerning the mechanism of membrane binding of calpain contribute to the revision of the calpain activation model which has been taking place in the last couple of years. The fact that a stimulus involving a Ca^{2+} influx is required for the relocation of calpain from the cytosol to the membranes *in vivo* together with a critical
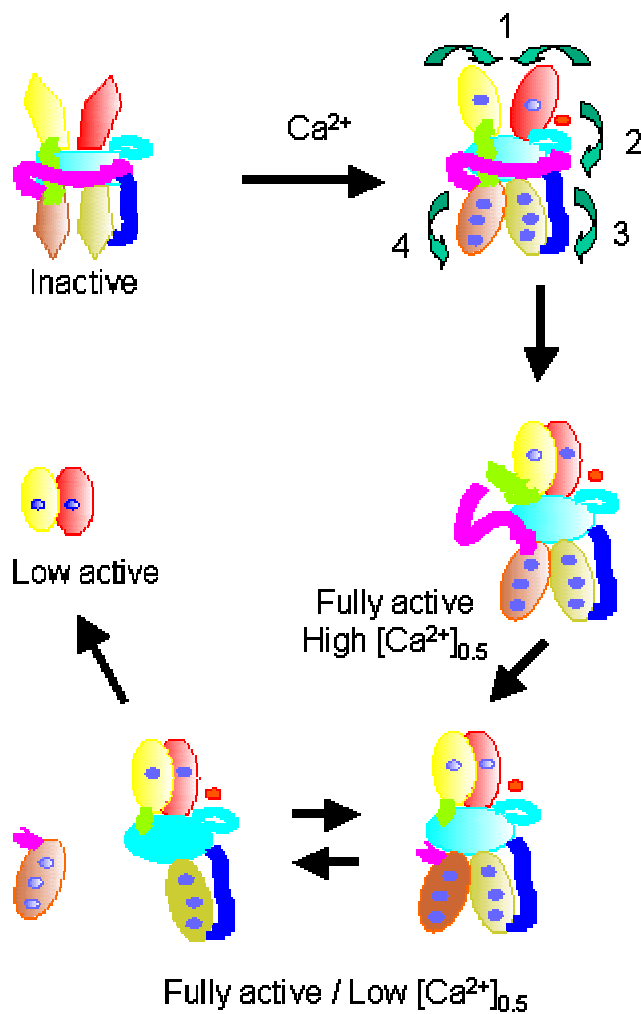
Figure 65. Hypothetical model for the activation of calpain by calcium. Inactive apo-calpain has a rigid conformation stabilized by the anchoring of domain I (green) in domain VI (brown), electrostatic interactions of domain III (cyan) and unspecific wrapping of domain V (magenta) around the molecule. In this conformation, both subdomains of the papain-like core (yellow, red) are too far away to allow substrate processing. Binding of Ca^{2+} to the non-EF-hand sites in the protease domain induces a relative movement of both halves resulting in assembly of the active site (1). This movement is energetically favoured by (2) repulsive forces generated by Ca^{2+} binding at the interface of subdomain IIb (red) and domain III, (3) downward movement of the linker (blue) after small Ca^{2+} induced conformational changes in domain IV (olive-colored), and possibly, (4) flexibilization of domain III upon Ca^{2+}-dependent disruption of contacts to domain VI. Conformational changes throughout the calpain molecule result in exposure of its hydrophobic surfaces, increasing the tendency to form aggregates. Therefore membrane phospholipids might help to stabilize the active conformation. Further constraints are released upon autoproteolytic processing of domains I and V. Such structural rearrangements make subunits more prone to dissociate and reduce the Ca^{2+} requirement of the enzyme. The sequential autolytic degradation of the molecule ends up with the release of a protease core with 1/40 to 1/100 of the activity of full-length calpain which is insensitive to calpastatin inhibition.

evaluation of the experimental design in previous studies have raised concerns about the effectiveness of phospholipids as calpain activators (Goll *et al.,* 2003). Now we see membrane binding as a consequence of the Ca^{2+}-induced conformational changes leading to activation of the calpains. The increasing number of membrane-associated calpain substrates (Goll *et al.,* 2003) might be a reasonable explanation for this specific translocation. Nevertheless, our findings *in vitro* require further confirmation through cell biology experiments. Therefore one of the goals of our work was to prepare a toolkit for the study of membrane association in living cells. Using EYFP-labelled µ-calpain 80K subunits, it will be possible to follow the changes in the localization of the acidic-loop mutants upon addition of a Ca^{2+} ionophore. For instance, a faster movement of the D405A variant to the cell periphery would confirm our results in vitro. Similar studies have already shown a distorted

spatiotemporal localization of classical C2 domains when the Ca^{2+}- and phospholipid-binding loops were mutated (Stahelin *et al.*, 2003, Bolsover *et al.*, 2003, Vallentin *et al.*, 2000). An interesting experiment would be also to compare the mobilities of our C115A inactive mutant and the wild type 80K-EYFP variant created by Gil-Parrado *et al.* (2003). During the reported association of calpains with cytoskeletal proteins and subcellular organelles (Kumamoto *et al.*, 1992; Lane *et al.*, 1992; Hood *et al.*, 2003) the cleavage of some unknown interaction partner(s) might be required prior to membrane translocation.

The effectiveness of several calpain activator proteins and molecules reported in the past decades (Takeyama *et al.*, 1986; Melloni *et al.*, 1998) as factors helping to activate calpains at intracellular Ca^{2+} concentrations has been questioned by our group (Pfeiler, 2001) and others (Goll *et al.*, 2003). Now, by demonstrating that phospholipids might not be the additional activating factor as well, we provide further hints for the existence of a hitherto unknown additional activation mechanism. In this direction some groups have already started to analyze more carefully the role of phosphorylation in calpain activation. Although the calpains are reportedly non-phosphorylated *in vivo* (Adaci *et al.*, 1986), recent studies with improved proteomics technology claim that bovine μ- and m- calpains are phosphorylated at multiple sites *in situ* (Goll *et al.*, 2003). Phosphorylated calpains show an important increase in their specific activity (Goll, personal communication). In fact, it has been very recently demonstrated that phosphorylation of m-calpain at position Ser-50 by the extracellular signal-regulated kinase (ERK) activates the enzyme even in the absence of cytosolic calcium fluxes (Glading *et al.*, 2004). Once again, there are contradictory reports concerning this topic: Glu substitutions of the consensus phosphorylation sites Ser-50, Ser-67 and Thr-70 had no effect on the Ca^{2+} requirement or specific activity *in vitro* of bacterially expressed m-calpain, and the effect of Glu substitutions of Ser-369 and Thr-370 was rather inactivating (Smith *et al.*, 2003). Other posttranslational modifications such as acylation or nitrosylation remain to be investigated.

In the next future experiments which help to conciliate the information obtained *in vitro* with the *in vivo* observations must be designed in order to gain more insight in the biology of the calpains. At this point the novel proteomics technologies seem to become the most promising methodology to pursue such endeavor. A clear understanding of the activation mechanism of the calpains will provide the fundament for the design and synthesis of highly specific pharmacologically relevant calpain inhibitors.

F. Abbreviations

A_λ	absorption at the wavelength λ
ACE	angiotensin converting enzyme
AcNPV	*Autographa californica* nuclear polyhedrosis virus
AMC	7-amino-4-methylcoumarin
APS	ammonium peroxydisulfat
ATP	adenosine-5'-triphosphate
BCA	bicinchoninic acid
BIA	biomolecular interaction analysis
β-ME (2-ME)	β-mercaptoethanol
bp	base pair
BSA	bovine serum albumin
$[Ca^{2+}]_{0.5}$	Half-maximal calcium concentration
CaBP	Ca^{2+} binding protein
CD1	calpastatin domain 1
cDNA	complementary DNA
CIP	calf intestinal phosphatase
d	2'-deoxy-
D	calpain domain (DI, DIIa, DIIb, DIII, DIV, DV, DVI)
DAG	diacylglycerol
Dansyl	N-(5-dimethylaminonaphtalene-1-sulfonyl)
DHPE	1,2-dihexadecanoyl-*sn*-glycero-3-phosphoethanolamine
DMSO	dimethyl sulfoxide
ds	double-stranded
DTT	1,4 dithiothreitol
dYT	double yeast/tryptone growth medium
E-64	L-trans-epoxysuccinyl-leucylamido-(4-guanidino)-butan
EC	enzyme commission classification system numbers
ECFP	enhanced cyan fluorescent protein
ECM	extracellular matrix
EDTA	ethylendiamintetraacetic acid
EGFP	enhanced green fluorescent protein

EGTA	ethylenglycol-bis-(2-aminoethylether)-tetraacetic acid
ERK	extracellular signal regulated kinase
EYFP	enhanced yellow fluorescent protein
FPLC	fast-performance liquid chromatography
FRET	fluorescence resonance energy transfer
g	gravity acceleration
GFP	green fluorescent protein
His_6-	hexahistidine
HIV	human immunodeficiency virus
HPLC	high-performance liquid chromatography
IAP	inhibitor of apoptosis protein
ICE	interleukin converting enzyme
IPTG	isopropylthiogalactoside
K_d	equilibrium dissociation constant
K_i	equilibrium dissociation constant of a enzyme-inhibitor complex
LGMD2A	limb girdle muscular dystrophy type 2a
MHC	major histocompability complex
MOI	multiplicity of infection
n.d.	not determined
NHS	N-hydroxysuccinimide
Ni-NTA	nickel-nitrilacetic acid
NTP	nucleoside 5'-triphosphate
OD_λ	optical density at the wavelength λ
p94	calpain 3
p.a.	pro analysi (analytical grade)
PAGE	polyacrylamide gel electrophoresis
PCR	polymerase chain reaction
PC	1-palmitoyl-2-oleoyl-sn-glycero-3-phosphocholine
PE	1-palmitoyl-2-oleoyl-sn-glycero-3-phosphoethanolamine
PEF	penta EF-hand
PEG	polyethylenglycol
PelB	pectylase from *Erwinia carotovora*
pfu	plaque-forming unit
PG	1-palmitoyl-2-oleoyl-sn-glycero-3-[phospho-rac-(1-glycerol)]

PI	L-a-phosphatidylinositol
PIP	L-a-phosphatidylinositol-4-phosphate
PIP_2	L-a-phosphatidylinositol-4,5-biphosphate
PS	1-palmitoyl-2-oleoyl-sn-glycero-3-[phospho-L-serine]
PVDF	polyvinylidene difluoride
RNase	ribonuclease
RP	reverse phase
rpm	revolutions per minute
RT	room temperature
RU	resonance unit
SDS	sodium dodecyl sulfate
SPR	surface plasmon resonance
Suc-	succinyl-
TEMED	N, N, N', N'-tetramethylethylendiamine
Tris	trishydroxymethylamonium
UV	ultraviolet
v/v	volume/volume
w/v	weight/volume
80K	calpain 80 kDa large catalytic subunit
28K	calpain 28 kDa small regulatory subunit
21K	truncated (ΔDV) calpain small regulatory subunit

G. References

Adachi, Y., N. Kobayashi, et al. (1986). "Ca2+-dependent cysteine proteinase, calpains I and II are not phosphorylated in vivo." Biochem Biophys Res Commun **136**(3): 1090-6.

Alexa, A., Z. Bozoky, et al. (2004). "Contribution of distinct structural elements to activation of calpain by Ca2+ ions." J Biol Chem.

Anagli, J., E. M. Vilei, et al. (1996). "Purification of active calpain by affinity chromatography on an immobilized peptide inhibitor." Eur J Biochem **241**(3): 948-54.

Ansorge, W., A. Rosenthal, et al. (1988). "Non-radioactive automated sequencing of oligonucleotides by chemical degradation." Nucleic Acids Res **16**(5): 2203-6.

Aoki, K., S. Imajoh, et al. (1986). "Complete amino acid sequence of the large subunit of the low-Ca2+-requiring form of human Ca2+-activated neutral protease (muCANP) deduced from its cDNA sequence." FEBS Lett **205**(2): 313-7.

Arthur, J. S. and C. Crawford (1996). "Investigation of the interaction of m-calpain with phospholipids: calpain-phospholipid interactions." Biochim Biophys Acta **1293**(2): 201-6.

Arthur, J. S. and J. S. Elce (2000). "Fluorescence measurements of Ca2+ binding to domain VI of calpain." Methods Mol Biol **144**: 121-7.

Arthur, J. S., J. S. Elce, et al. (2000). "Disruption of the murine calpain small subunit gene, Capn4: calpain is essential for embryonic development but not for cell growth and division." Mol Cell Biol **20**(12): 4474-81.

Azam, M., S. S. Andrabi, et al. (2001). "Disruption of the mouse mu-calpain gene reveals an essential role in platelet function." Mol Cell Biol **21**(6): 2213-20.

Baki, A., P. Tompa, et al. (1996). "Autolysis parallels activation of mu-calpain." Biochem J **318 (Pt 3)**: 897-901.

Barrett, A. J. (1979). "Protein degradation in health and disease. Introduction: the classification of proteinases." Ciba Found Symp(75): 1-13.

Barrett, A. J. and N. D. Rawlings (2001). "Evolutionary lines of cysteine peptidases." Biol Chem **382**(5): 727-33.

Barrett, A. J., N. D. Rawlings, et al. (1998). Handbook of Proteolytic Enzymes. San Diego, Academic Press.

Barth, R. and J. S. Elce (1981). "Immunofluorescent localization of a Ca2+-dependent neutral protease in hamster muscle." Am J Physiol **240**(5): E493-8.

Bazzi, M. D. and G. L. Nelsestuen (1987). "Association of protein kinase C with phospholipid vesicles." Biochemistry **26**(1): 115-22.

Bepler, G., A. Koehler, et al. (1988). "Characterization of the state of differentiation of six newly established human non-small-cell lung cancer cell lines." Differentiation **37**(2): 158-71.

Berridge, M. J., P. Lipp, et al. (2000). "The versatility and universality of calcium signalling." Nat Rev Mol Cell Biol **1**(1): 11-21.

Birnboim, H. C. and J. Doly (1979). "A rapid alkaline extraction procedure for screening recombinant plasmid DNA." Nucleic Acids Res **7**(6): 1513-23.

Bittova, L., M. Sumandea, et al. (1999). "A structure-function study of the C2 domain of cytosolic phospholipase A2. Identification of essential calcium ligands and hydrophobic membrane binding residues." J Biol Chem **274**(14): 9665-72.

Blanchard, H., P. Grochulski, et al. (1997). "Structure of a calpain Ca(2+)-binding domain reveals a novel EF-hand and Ca(2+)-induced conformational changes." Nat Struct Biol **4**(7): 532-8.

Blanchard, H., Y. Li, et al. (1996). "Ca(2+)-binding domain VI of rat calpain is a homodimer in solution: hydrodynamic, crystallization and preliminary X-ray diffraction studies." Protein Sci **5**(3): 535-7.

Boatright, K. M. and G. S. Salvesen (2003). "Caspase activation." Biochem Soc Symp(70): 233-42.

Bolsover, S. R., J. C. Gomez-Fernandez, et al. (2003). "Role of the Ca2+/phosphatidylserine binding region of the C2 domain in the translocation of protein kinase Calpha to the plasma membrane." J Biol Chem **278**(12): 10282-90.

Branca, D., A. Gugliucci, et al. (1999). "Expression, partial purification and functional properties of themuscle-specific calpain isoform p94." Eur J Biochem **265**(2): 839-46.

Brandenburg, K., F. Harris, et al. (2002). "Domain V of m-calpain shows the potential to form an oblique-orientated alpha-helix, which may modulate the enzyme's activity via interactions with anionic lipid." Eur J Biochem **269**(22): 5414-22.

Brown, N. and C. Crawford (1993). "Structural modifications associated with the change in Ca2+ sensitivity on activation of m-calpain." FEBS Lett **322**(1): 65-8.

Busch, W. A., M. H. Stromer, et al. (1972). "Ca 2+ -specific removal of Z lines from rabbit skeletal muscle." J Cell Biol **52**(2): 367-81.

Celis, J. E. (1998). Cell Biology: A Laboratory Handbook. Toronto, Academic Press.

Chakrabarti, A. K., S. Dasgupta, et al. (1990). "Regulation of the calcium-activated neutral proteinase (CANP) of bovine brain by myelin lipids." Biochim Biophys Acta **1038**(2): 195-8.

Chakrabarti, A. K., S. Dasgupta, et al. (1996). "Regulation of brain m calpain Ca2+ sensitivity by mixtures of membrane lipids: activation at intracellular Ca2+ level." J Neurosci Res **44**(4): 374-80.

Cho, W. (2001). "Membrane targeting by C1 and C2 domains." J Biol Chem **276**(35): 32407-10.

Cho, W., L. Bittova, et al. (2001). "Membrane binding assays for peripheral proteins." Anal Biochem **296**(2): 153-61.

Cong, J., D. E. Goll, et al. (1989). "The role of autolysis in activity of the Ca2+-dependent proteinases (mu-calpain and m-calpain)." J Biol Chem **264**(17): 10096-103.

Coolican, S. A. and D. R. Hathaway (1984). "Effect of L-alpha-phosphatidylinositol on a vascular smooth muscle Ca2+-dependent protease. Reduction of the Ca2+ requirement for autolysis." J Biol Chem **259**(19): 11627-30.

Corbalan-Garcia, S., J. A. Rodriguez-Alfaro, et al. (1999). "Determination of the calcium-binding sites of the C2 domain of protein kinase Calpha that are critical for its translocation to the plasma membrane." Biochem J **337 (Pt 3)**: 513-21.

Cormack, B. P., R. H. Valdivia, et al. (1996). "FACS-optimized mutants of the green fluorescent protein (GFP)." Gene **173**(1 Spec No): 33-8.

Cottin, P., S. Poussard, et al. (1991). "Free calcium and calpain I activity." Biochim Biophys Acta **1079**(2): 139-45.

Crawford, C., N. R. Brown, et al. (1990). "Investigation of the structural basis of the interaction of calpain II with phospholipid and with carbohydrate." Biochem J **265**(2): 575-9.

Croall, D. E. and G. N. DeMartino (1991). "Calcium-activated neutral protease (calpain) system: structure, function, and regulation." Physiol Rev **71**(3): 813-47.

Dainese, E., R. Minafra, et al. (2002). "Conformational changes of calpain from human erythrocytes in the presence of Ca2+." J Biol Chem **277**(43): 40296-301.

Daman, A., F. Harris, et al. (2001). "A theoretical investigation into the lipid interactions of m-calpain." Mol Cell Biochem **223**(1-2): 159-63.

Danial, N. N. and S. J. Korsmeyer (2004). "Cell death: critical control points." Cell **116**(2): 205-19.

Daniel, K. G., J. S. Anderson, et al. (2003). "Association of mitochondrial calpain activation with increased expression and autolysis of calpain small subunit in an early stage of apoptosis." Int J Mol Med **12**(2): 247-52.

Das, S., J. E. Dixon, et al. (2003). "Membrane-binding and activation mechanism of PTEN." Proc Natl Acad Sci U S A **100**(13): 7491-6.

Davletov, B., O. Perisic, et al. (1998). "Calcium-dependent membrane penetration is a hallmark of the C2 domain of cytosolic phospholipase A2 whereas the C2A domain of synaptotagmin binds membranes electrostatically." J Biol Chem **273**(30): 19093-6.

Dayton, W. R., D. E. Goll, et al. (1976). "A Ca2+-activated protease possibly involved in myofibrillar protein turnover. Purification from porcine muscle." Biochemistry **15**(10): 2150-8.

Dear, T. N. and T. Boehm (2001). "Identification and characterization of two novel calpain large subunit genes." Gene **274**(1-2): 245-52.

DeMartino, G. N. and D. K. Blumenthal (1982). "Identification and partial purification of a factor that stimulates calcium-dependent proteases." Biochemistry **21**(18): 4297-303.

DeMartino, G. N., C. A. Huff, et al. (1986). "Autoproteolysis of the small subunit of calcium-dependent protease II activates and regulates protease activity." J Biol Chem **261**(26): 12047-52.

Diaz, B. G., S. Gross, et al. (2001). "Cystatins as calpain inhibitors: engineered chicken cystatin- and stefin B-kininogen domain 2 hybrids support a cystatin-like mode of interaction with the catalytic subunit of mu-calpain." Biol Chem **382**(1): 97-107.

Dutt, P., J. S. Arthur, et al. (2000). "Roles of individual EF-hands in the activation of m-calpain by calcium." Biochem J **348 Pt 1**: 37-43.

Dutt, P., C. N. Spriggs, et al. (2002). "Origins of the difference in Ca2+ requirement for activation of mu- and m-calpain." Biochem J **367**(Pt 1): 263-9.

Eaves, G. N. and C. D. Jeffries (1963). "Effect of Ph on the Formation of Exocellular Nuclease in Aging Broth Cultures of Serratia Marcescens." J Bacteriol **85**: 1194-6.

Edman, P. and G. Begg (1967). "A protein sequenator." Eur J Biochem **1**(1): 80-91.

Edmunds, T., P. A. Nagainis, et al. (1991). "Comparison of the autolyzed and unautolyzed forms of mu- and m-calpain from bovine skeletal muscle." Biochim Biophys Acta **1077**(2): 197-208.

Elce, J. S. (1999). Expression of calpain in bacteria and insect cells. Calpain: Pharmacology and Toxicology of Calcium-Dependent Protease. K. K. Wang and P. W. Yuen. Philadelphia, PA, Taylor and Francis**:** 51-62.

Elce, J. S., P. L. Davies, et al. (1997). "The effects of truncations of the small subunit on m-calpain activity and heterodimer formation." Biochem J **326 (Pt 1)**: 31-8.

Elce, J. S., C. Hegadorn, et al. (1997). "Autolysis, Ca2+ requirement, and heterodimer stability in m-calpain." J Biol Chem **272**(17): 11268-75.

Ellis, H. M. and H. R. Horvitz (1986). "Genetic control of programmed cell death in the nematode C. elegans." Cell **44**(6): 817-29.

Erb, E. M., J. Stenflo, et al. (2002). "Interaction of bovine coagulation factor X and its glutamic-acid-containing fragments with phospholipid membranes. A surface plasmon resonance study." Eur J Biochem **269**(12): 3041-6.

Farkas, A., P. Tompa, et al. (2003). "Revisiting ubiquity and tissue specificity of human calpains." Biol Chem **384**(6): 945-9.

Farkas, A., P. Tompa, et al. (2004). "Autolytic activation and localization in Schneider cells (S2) of calpain B from Drosophila." Biochem J **378**(Pt 2): 299-305.

Fernandez-Chacon, R., O. H. Shin, et al. (2002). "Structure/function analysis of Ca2+ binding to the C2A domain of synaptotagmin 1." J Neurosci **22**(19): 8438-46.

Fuentes-Prior, P., K. Fujikawa, et al. (2002). "New insights into binding interfaces of coagulation factors V and VIII and their homologues lessons from high resolution crystal structures." Curr Protein Pept Sci **3**(3): 313-39.

Fukuda, M., E. Katayama, et al. (2002). "The calcium-binding loops of the tandem C2 domains of synaptotagmin VII cooperatively mediate calcium-dependent oligomerization." J Biol Chem **277**(32): 29315-20.

Gabrijelcic-Geiger, D., R. Mentele, et al. (2001). "Human micro-calpain: simple isolation from erythrocytes and characterization of autolysis fragments." Biol Chem **382**(12): 1733-7.

Gasteiger, E., A. Gattiker, et al. (2003). "ExPASy: The proteomics server for in-depth protein knowledge and analysis." Nucleic Acids Res **31**(13): 3784-8.

Gerke, V. and S. E. Moss (2002). "Annexins: from structure to function." Physiol Rev **82**(2): 331-71.

Gershoni, J. M. and G. E. Palade (1983). "Protein blotting: principles and applications." Anal Biochem **131**(1): 1-15.

Gil-Parrado, S. (2001). Ubiquitous Human Calpains: Cellular Localization, Subunit Interactions and Apoptosis Involvement. Institut für Organische Chemie und Biochemie. München, Technische Universität München.

Gil-Parrado, S., I. Assfalg-Machleidt, et al. (2003). "Calpastatin exon 1B-derived peptide, a selective inhibitor of calpain: enhancing cell permeability by conjugation with penetratin." Biol Chem **384**(3): 395-402.

Gil-Parrado, S., O. Popp, et al. (2003). "Subcellular localization and in vivo subunit interactions of ubiquitous mu-calpain." J Biol Chem **278**(18): 16336-46.

Glading, A., R. J. Bodnar, et al. (2004). "Epidermal growth factor activates m-calpain (calpain II), at least in part, by extracellular signal-regulated kinase-mediated phosphorylation." Mol Cell Biol **24**(6): 2499-512.

Glading, A., D. A. Lauffenburger, et al. (2002). "Cutting to the chase: calpain proteases in cell motility." Trends Cell Biol **12**(1): 46-54.

Goll, D. E., V. F. Thompson, et al. (2003). "The calpain system." Physiol Rev **83**(3): 731-801.

Goll, D. E., V. F. Thompson, et al. (1992). "Is calpain activity regulated by membranes and autolysis or by calcium and calpastatin?" Bioessays **14**(8): 549-56.

Gollmitzer, N. (1999). Gentechnische Herstellung von μ-Calpain mit dem Baculovirus-Expressionssystem und Charakterisierung der rekombinanten Domäne VI. Adolf Butenandt Institut für Physiologische Chemie, Physikalische Biochemie und Zellbiologie. München, Ludwig-Maximilians-Universität**:** 73.

Gopalakrishna, R. and S. H. Barsky (1986). "Hydrophobic association of calpains with subcellular organelles. Compartmentalization of calpains and the endogenous inhibitor calpastatin in tissues." J Biol Chem **261**(30): 13936-42.

Gopalakrishna, R. and J. F. Head (1985). "Rapid purification of calcium-activated protease by calcium-dependent hydrophobic-interaction chromatography." FEBS Lett **186**(2): 246-50.

Graham-Siegenthaler, K., S. Gauthier, et al. (1994). "Active recombinant rat calpain II. Bacterially produced large and small subunits associate both in vivo and in vitro." J Biol Chem **269**(48): 30457-60.

Guroff, G. (1964). "A Neutral, Calcium-Activated Proteinase from the Soluble Fraction of Rat Brain." J Biol Chem **239**: 149-55.

Haas, J., E. C. Park, et al. (1996). "Codon usage limitation in the expression of HIV-1 envelope glycoprotein." Curr Biol **6**(3): 315-24.

Haeseleer, F., Y. Imanishi, et al. (2002). "Calcium-binding proteins: intracellular sensors from the calmodulin superfamily." Biochem Biophys Res Commun **290**(2): 615-23.

Hanahan, D. (1983). "Studies on transformation of Escherichia coli with plasmids." J Mol Biol **166**(4): 557-80.

Harris, A. L., G. J. S., et al. (1995). Bioorg Med Chem Lett **5**: 393-398.

Hartley, B. S. (1960). "Proteolytic enzymes." Annu Rev Biochem **29**: 45-72.

Hata, S., H. Sorimachi, et al. (2001). "Domain II of m-calpain is a Ca(2+)-dependent cysteine protease." FEBS Lett **501**(2-3): 111-4.

Hatanaka, M., N. Yoshimura, et al. (1984). "Evidence for membrane-associated calpain I in human erythrocytes. Detection by an immunoelectrophoretic blotting method using monospecific antibody." Biochemistry **23**(14): 3272-6.

Hathaway, D. R., D. K. Werth, et al. (1982). "Limited autolysis reduces the Ca2+ requirement of a smooth muscle Ca2+-activated protease." J Biol Chem **257**(15): 9072-7.

Heim, R., A. B. Cubitt, et al. (1995). "Improved green fluorescence." Nature **373**(6516): 663-4.

Heim, R., D. C. Prasher, et al. (1994). "Wavelength mutations and posttranslational autoxidation of green fluorescent protein." Proc Natl Acad Sci U S A **91**(26): 12501-4.

Heim, R. and R. Y. Tsien (1996). "Engineering green fluorescent protein for improved brightness, longer wavelengths and fluorescence resonance energy transfer." Curr Biol **6**(2): 178-82.

Hengartner, M. O. (2000). "The biochemistry of apoptosis." Nature **407**(6805): 770-6.

Hewick, R. M., M. W. Hunkapiller, et al. (1981). "A gas-liquid solid phase peptide and protein sequenator." J Biol Chem **256**(15): 7990-7.

Hitomi, K., Y. Uchiyama, et al. (1998). "Purification and characterization of the active-site-mutated recombinant human mu-calpain expressed in baculovirus-infected insect cells." Biochem Biophys Res Commun **246**(3): 681-5.

Hong, H., S. C. el-Saleh, et al. (1990). "Fluorescence spectroscopic analysis of calpain II interactions with calcium and calmodulin antagonists." Int J Biochem **22**(4): 399-404.

Hood, J. L., B. B. Logan, et al. (2003). "Association of the calpain/calpastatin network with subcellular organelles." Biochem Biophys Res Commun **310**(4): 1200-12.

Horikawa, Y., N. Oda, et al. (2000). "Genetic variation in the gene encoding calpain-10 is associated with type 2 diabetes mellitus." Nat Genet **26**(2): 163-75.

Hosfield, C. M., J. S. Elce, et al. (1999). "Crystal structure of calpain reveals the structural basis for Ca(2+)-dependent protease activity and a novel mode of enzyme activation." Embo J **18**(24): 6880-9.

Hosfield, C. M., T. Moldoveanu, et al. (2001). "Calpain mutants with increased Ca2+ sensitivity and implications for the role of the C(2)-like domain." J Biol Chem **276**(10): 7404-7.

Huang, Y. and K. K. Wang (2001). "The calpain family and human disease." Trends Mol Med **7**(8): 355-62.

Huston, R. B. and E. G. Krebs (1968). "Activation of skeletal muscle phosphorylase kinase by Ca2+. II. Identification of the kinase activating factor as a proteolytic enzyme." Biochemistry **7**(6): 2116-22.

Imajoh, S., H. Kawasaki, et al. (1986). "The amino-terminal hydrophobic region of the small subunit of calcium-activated neutral protease (CANP) is essential for its activation by phosphatidylinositol." J Biochem (Tokyo) **99**(4): 1281-4.

Imajoh, S., H. Kawasaki, et al. (1986). "Limited autolysis of calcium-activated neutral protease (CANP): reduction of the Ca2+-requirement is due to the NH2-terminal processing of the large subunit." J Biochem (Tokyo) **100**(3): 633-42.

Inomata, M., Y. Saito, et al. (1990). "Binding sites for calcium-activated neutral protease on erythrocyte membranes are not membrane phospholipids." Biochem Biophys Res Commun **171**(2): 625-32.

Ishiura, S., H. Murofushi, et al. (1978). "Studies of a calcium-activated neutral protease from chicken skeletal muscle. I. Purification and characterization." J Biochem (Tokyo) **84**(1): 225-30.

Jekely, G. and P. Friedrich (1999). "Characterization of two recombinant Drosophila calpains. CALPA and a novel homolog, CALPB." J Biol Chem **274**(34): 23893-900.

Jia, Z., V. Petrounevitch, et al. (2001). "Mutations in calpain 3 associated with limb girdle muscular dystrophy: analysis by molecular modeling and by mutation in m-calpain." Biophys J **80**(6): 2590-6.

Jimenez, J. L., G. R. Smith, et al. (2003). "Functional recycling of C2 domains throughout evolution: a comparative study of synaptotagmin, protein kinase C and phospholipase C by sequence, structural and modelling approaches." J Mol Biol **333**(3): 621-39.

Johnson, G. V. and R. P. Guttmann (1997). "Calpains: intact and active?" Bioessays **19**(11): 1011-8.

Johnson, J. D., Z. Han, et al. (2004). "RyR2 and Calpain-10 Delineate a Novel Apoptosis Pathway in Pancreatic Islets." J Biol Chem **279**(23): 24794-802.

Kamita, S. G. and S. Maeda (1997). "Sequencing of the putative DNA helicase-encoding gene of the Bombyx mori nuclear polyhedrosis virus and fine-mapping of a region involved in host range expansion." Gene **190**(1): 173-9.

Kamphuis, I. G., K. H. Kalk, et al. (1984). "Structure of papain refined at 1.65 A resolution." J Mol Biol **179**(2): 233-56.

Kastl, K., M. Ross, et al. (2002). "Kinetics and thermodynamics of annexin A1 binding to solid-supported membranes: a QCM study." Biochemistry **41**(31): 10087-94.

Kawasaki, H. and S. Kawashima (1996). "Regulation of the calpain-calpastatin system by membranes (review)." Mol Membr Biol **13**(4): 217-24.

Kawashima, S., M. Nomoto, et al. (1984). "Comparison of calcium-activated neutral proteases from skeletal muscle of rabbit and chicken." J Biochem (Tokyo) **95**(1): 95-101.

Kim, Y., L. Lichtenbergova, et al. (1997). "A phospholipase A2 kinetic and binding assay using phospholipid-coated hydrophobic beads." Anal Biochem **250**(1): 109-16.

Kinbara, K., S. Ishiura, et al. (1998). "Purification of native p94, a muscle-specific calpain, and characterization of its autolysis." Biochem J **335 (Pt 3)**: 589-96.

Kitaura, Y., S. Matsumoto, et al. (2001). "Peflin and ALG-2, members of the penta-EF-hand protein family, form a heterodimer that dissociates in a Ca2+-dependent manner." J Biol Chem **276**(17): 14053-8.

Kozak, M. (1987). "At least six nucleotides preceding the AUG initiator codon enhance translation in mammalian cells." J Mol Biol **196**(4): 947-50.

Kretsinger, R. H. and C. E. Nockolds (1973). "Carp muscle calcium-binding protein. II. Structure determination and general description." J Biol Chem **248**(9): 3313-26.

Kühne, W. (1876). "Ueber das Sekret des Pankreas." Verhandlungen des naturhistorisch-medicinischen Vereins zu Heidelberg **1**(4): 233-235.

Kumamoto, T., W. C. Kleese, et al. (1992). "Localization of the Ca(2+)-dependent proteinases and their inhibitor in normal, fasted, and denervated rat skeletal muscle." Anat Rec **232**(1): 60-77.

Kumar, S. and R. Nussinov (2002). "Relationship between ion pair geometries and electrostatic strengths in proteins." Biophys J **83**(3): 1595-612.

Kunimatsu, M., S. Higashiyama, et al. (1989). "Calcium dependent cysteine proteinase is a precursor of a chemotactic factor for neutrophils." Biochem Biophys Res Commun **164**(2): 875-82.

Kunimatsu, M., X. J. Ma, et al. (1990). "Neutrophil chemotactic activity of N-terminal peptides from the calpain small subunit." Biochem Biophys Res Commun **169**(3): 1242-7.

Kunimatsu, M., X. J. Ma, et al. (1995). "Neutrophil chemotactic N-acetyl peptides from the calpain small subunit are also chemotactic for immunocytes." Biochem Mol Biol Int **35**(2): 247-54.

Kunimatsu, M., X. J. Ma, et al. (1993). "Neutrophil responses induced by formyl and acetyl peptides with the N-terminal sequence of the calpain small subunit." Biochem Mol Biol Int **31**(3): 477-84.

Lackowicz, J. R. (1983). Principles of Fluorescence Spectroscopy. New York, Plenum Press.

Laemmli, U. K. (1970). "Cleavage of structural proteins during the assembly of the head of bacteriophage T4." Nature **227**(259): 680-5.

Lane, R. D., D. M. Allan, et al. (1992). "A comparison of the intracellular distribution of mu-calpain, m-calpain, and calpastatin in proliferating human A431 cells." Exp Cell Res **203**(1): 5-16.

Larsen, A. K., T. De Veyra, et al. (2004). "Expression of human, mouse, and rat m-calpains in Escherichia coli and in murine fibroblasts." Protein Expr Purif **33**(2): 246-55.

Lewit-Bentley, A. and S. Rety (2000). "EF-hand calcium-binding proteins." Curr Opin Struct Biol **10**(6): 637-43.

Li, H., V. F. Thompson, et al. (2004). "Effects of autolysis on properties of micro- and m-calpain." Biochim Biophys Acta **1691**(2-3): 91-103.

Lin, G. D., D. Chattopadhyay, et al. (1997). "Crystal structure of calcium bound domain VI of calpain at 1.9 A resolution and its role in enzyme assembly, regulation, and inhibitor binding." Nat Struct Biol **4**(7): 539-47.

Liu, K., L. Li, et al. (2000). "Antisense RNA-mediated deficiency of the calpain protease, nCL-4, in NIH3T3 cells is associated with neoplastic transformation and tumorigenesis." J Biol Chem **275**(40): 31093-8.

Lomasney, J. W., H. F. Cheng, et al. (1999). "Activation of phospholipase C delta1 through C2 domain by a Ca(2+)-enzyme-phosphatidylserine ternary complex." J Biol Chem **274**(31): 21995-2001.

Luckow, V. A. and M. D. Summers (1989). "High level expression of nonfused foreign genes with Autographa californica nuclear polyhedrosis virus expression vectors." Virology **170**(1): 31-9.

Machleidt, W., I. Assfalg-Machleidt, et al. (1993). Kinetics and molecular mechanism of inhibition of cysteine proteinases by their protein inhibitors. Innovations in Proteases and their Inhibitors. F. X. Aviles. Berlin, Germany, Walter de Gruyter**:** 179-196.

Maki, M., Y. Kitaura, et al. (2002). "Structures, functions and molecular evolution of the penta-EF-hand Ca2+-binding proteins." Biochim Biophys Acta **1600**(1-2): 51-60.

Maki, M., E. Takano, et al. (1987). "All four internally repetitive domains of pig calpastatin possess inhibitory activities against calpains I and II." FEBS Lett **223**(1): 174-80.

Malitschek, B. and M. Schartl (1991). "Rapid identification of recombinant baculoviruses using PCR." Biotechniques **11**(2): 177-8.

Medkova, M. and W. Cho (1998). "Mutagenesis of the C2 domain of protein kinase C-alpha. Differential roles of Ca2+ ligands and membrane binding residues." J Biol Chem **273**(28): 17544-52.

Medkova, M. and W. Cho (1999). "Interplay of C1 and C2 domains of protein kinase C-alpha in its membrane binding and activation." J Biol Chem **274**(28): 19852-61.

Mellgren, R. L. (1987). "Calcium-dependent proteases: an enzyme system active at cellular membranes?" Faseb J **1**(2): 110-5.

Melloni, E., M. Michetti, et al. (1998). "Molecular and functional properties of a calpain activator protein specific for mu-isoforms." J Biol Chem **273**(21): 12827-31.

Melloni, E., M. Michetti, et al. (1998). "Mechanism of action of a new component of the Ca(2+)-dependent proteolytic system in rat brain: the calpain activator." Biochem Biophys Res Commun **249**(3): 583-8.

Meyer, S. L., D. Bozyczko-Coyne, et al. (1996). "Biologically active monomeric and heterodimeric recombinant human calpain I produced using the baculovirus expression system." Biochem J **314 (Pt 2)**: 511-9.

Meyer, W. L., E. H. Fischer, et al. (1964). "Activation of Skeletal Muscle Phosphorylase B Kinase by Ca." Biochemistry **28**: 1033-9.

Meyers, M. B., C. Zamparelli, et al. (1995). "Calcium-dependent translocation of sorcin to membranes: functional relevance in contractile tissue." FEBS Lett **357**(3): 230-4.

Michetti, M., F. Salamino, et al. (1996). "Autolysis of human erythrocyte calpain produces two active enzyme forms with different cell localization." FEBS Lett **392**(1): 11-5.

Minami, Y., Y. Emori, et al. (1987). "E-F hand structure-domain of calcium-activated neutral protease (CANP) can bind Ca2+ ions." J Biochem (Tokyo) **101**(4): 889-95.

Missiaen, L., W. Robberecht, et al. (2000). "Abnormal intracellular ca(2+)homeostasis and disease." Cell Calcium **28**(1): 1-21.

Moldoveanu, T., C. M. Hosfield, et al. (2001). "Ca(2+)-induced structural changes in rat m-calpain revealed by partial proteolysis." Biochim Biophys Acta **1545**(1-2): 245-54.

Moldoveanu, T., C. M. Hosfield, et al. (2002). "A Ca(2+) switch aligns the active site of calpain." Cell **108**(5): 649-60.

Moldoveanu, T., C. M. Hosfield, et al. (2003). "Calpain silencing by a reversible intrinsic mechanism." Nat Struct Biol **10**(5): 371-8.

Moldoveanu, T., Z. Jia, et al. (2004). "Calpain activation by cooperative Ca2+ binding at two non-EF-hand sites." J Biol Chem **279**(7): 6106-14.

Molinari, M. and E. Carafoli (1997). "Calpain: a cytosolic proteinase active at the membranes." J Membr Biol **156**(1): 1-8.

Murachi, T., K. Tanaka, et al. (1980). "Intracellular Ca2+-dependent protease (calpain) and its high-molecular-weight endogenous inhibitor (calpastatin)." Adv Enzyme Regul **19**: 407-24.

Murray, D. and B. Honig (2002). "Electrostatic control of the membrane targeting of C2 domains." Mol Cell **9**(1): 145-54.

Mykles, D. L. and D. M. Skinner (1986). "Four Ca2+-dependent proteinase activities isolated from crustacean muscle differ in size, net charge, and sensitivity to Ca2+ and inhibitors." J Biol Chem **261**(21): 9865-71.

Nakagawa, K., H. Masumoto, et al. (2001). "Dissociation of m-calpain subunits occurs after autolysis of the N-terminus of the catalytic subunit, and is not required for activation." J Biochem (Tokyo) **130**(5): 605-11.

Nalefski, E. A. and J. J. Falke (1996). "The C2 domain calcium-binding motif: structural and functional diversity." Protein Sci **5**(12): 2375-90.

Nalefski, E. A. and J. J. Falke (1998). "Location of the membrane-docking face on the Ca2+-activated C2 domain of cytosolic phospholipase A2." Biochemistry **37**(51): 17642-50.

Nalefski, E. A. and J. J. Falke (2002). "Use of fluorescence resonance energy transfer to monitor Ca(2+)-triggered membrane docking of C2 domains." Methods Mol Biol **172**: 295-303.

Nalefski, E. A. and A. C. Newton (2001). "Membrane binding kinetics of protein kinase C betaII mediated by the C2 domain." Biochemistry **40**(44): 13216-29.

Nalefski, E. A., M. A. Wisner, et al. (2001). "C2 domains from different Ca2+ signaling pathways display functional and mechanistic diversity." Biochemistry **40**(10): 3089-100.

Nestle, M. and W. K. Roberts (1969). "An extracellular nuclease from Serratia marcescens. I. Purification and some properties of the enzyme." J Biol Chem **244**(19): 5213-8.

Niinobe, M., Y. Yamaguchi, et al. (1994). "Synaptotagmin is an inositol polyphosphate binding protein: isolation and characterization as an Ins 1,3,4,5-P4 binding protein." Biochem Biophys Res Commun **205**(2): 1036-42.

Ochoa, W. F., S. Corbalan-Garcia, et al. (2002). "Additional binding sites for anionic phospholipids and calcium ions in the crystal structures of complexes of the C2 domain of protein kinase calpha." J Mol Biol **320**(2): 277-91.

Ohkouchi, S., K. Nishio, et al. (2001). "Identification and characterization of two penta-EF-hand Ca(2+)-binding proteins in Dictyostelium discoideum." J Biochem (Tokyo) **130**(2): 207-15.

Ohno, S., Y. Emori, et al. (1984). "Evolutionary origin of a calcium-dependent protease by fusion of genes for a thiol protease and a calcium-binding protein?" Nature **312**(5994): 566-70.

Ohno, S., Y. Emori, et al. (1986). "Nucleotide sequence of a cDNA coding for the small subunit of human calcium-dependent protease." Nucleic Acids Res **14**(13): 5559.

Ono, Y., K. Kakinuma, et al. (2004). "Possible regulation of the conventional calpain system by skeletal muscle-specific calpain, p94/calpain 3." J Biol Chem **279**(4): 2761-71.

Ormo, M., A. B. Cubitt, et al. (1996). "Crystal structure of the Aequorea victoria green fluorescent protein." Science **273**(5280): 1392-5.

Pace, C. N., F. Vajdos, et al. (1995). "How to measure and predict the molar absorption coefficient of a protein." Protein Sci **4**(11): 2411-23.

Pal, G. P., T. De Veyra, et al. (2003). "Crystal structure of a micro-like calpain reveals a partially activated conformation with low Ca2+ requirement." Structure (Camb) **11**(12): 1521-6.

Pal, G. P., J. S. Elce, et al. (2001). "Dissociation and aggregation of calpain in the presence of calcium." J Biol Chem **276**(50): 47233-8.

Perisic, O., H. F. Paterson, et al. (1999). "Mapping the phospholipid-binding surface and translocation determinants of the C2 domain from cytosolic phospholipase A2." J Biol Chem **274**(21): 14979-87.

Pfeiler, D. (2001). Gentechnische Herstellung und Charakterisierung von rekombinanten Proteinen zur Bestimmung der molekularen Eigenschaften des humanes μ-Calpains. Fakultät für Chemie. München, Technische Universität München**:** 231.

Pontremoli, S., E. Melloni, et al. (1988). "An endogenous activator of the Ca2+-dependent proteinase of human neutrophils that increases its affinity for Ca2+." Proc Natl Acad Sci U S A **85**(6): 1740-3.

Pontremoli, S., E. Melloni, et al. (1987). "Isovalerylcarnitine is a specific activator of calpain of human neutrophils." Biochem Biophys Res Commun **148**(3): 1189-95.

Pontremoli, S., E. Melloni, et al. (1985). "Binding to erythrocyte membrane is the physiological mechanism for activation of Ca2+-dependent neutral proteinase." Biochem Biophys Res Commun **128**(1): 331-8.

Pontremoli, S., E. Melloni, et al. (1985). "Role of phospholipids in the activation of the Ca2+-dependent neutral proteinase of human erythrocytes." Biochem Biophys Res Commun **129**(2): 389-95.

Pontremoli, S., E. Melloni, et al. (1990). "Isovalerylcarnitine is a specific activator of the high calcium requiring calpain forms." Biochem Biophys Res Commun **167**(1): 373-80.

Pontremoli, S., P. L. Viotti, et al. (1990). "Identification of an endogenous activator of calpain in rat skeletal muscle." Biochem Biophys Res Commun **171**(2): 569-74.

Pusey, M. L., L. D. Mayer, et al. (1982). "Kinetic and hydrodynamic analysis of blood clotting factor V-membrane binding." Biochemistry **21**(21): 5262-9.

Raser, K. J., A. Posner, et al. (1995). "Casein zymography: a method to study mu-calpain, m-calpain, and their inhibitory agents." Arch Biochem Biophys **319**(1): 211-6.

Rawlings, N. D. and A. J. Barrett (1993). "Evolutionary families of peptidases." Biochem J **290 (Pt 1)**: 205-18.

Reverter, D., H. Sorimachi, et al. (2001). "The structure of calcium-free human m-calpain: implications for calcium activation and function." Trends Cardiovasc Med **11**(6): 222-9.

Reverter, D., S. Strobl, et al. (2001). "Structural basis for possible calcium-induced activation mechanisms of calpains." Biol Chem **382**(5): 753-66.

Richard, I., O. Broux, et al. (1995). "Mutations in the proteolytic enzyme calpain 3 cause limb-girdle muscular dystrophy type 2A." Cell **81**(1): 27-40.

Richard, I., C. Roudaut, et al. (2000). "Loss of calpain 3 proteolytic activity leads to muscular dystrophy and to apoptosis-associated IkappaBalpha/nuclear factor kappaB pathway perturbation in mice." J Cell Biol **151**(7): 1583-90.

Richardson, C. D. (1995). Baculovirus Expression Protocols. Totowa, New Jersey, Humana Press.

Rizo, J. and T. C. Sudhof (1998). "C2-domains, structure and function of a universal Ca2+-binding domain." J Biol Chem **273**(26): 15879-82.

Rodriguez-Alfaro, J. A., J. C. Gomez-Fernandez, et al. (2004). "Role of the lysine-rich cluster of the C2 domain in the phosphatidylserine-dependent activation of PKCalpha." J Mol Biol **335**(4): 1117-29.

Ross, M., V. Gerke, et al. (2003). "Membrane composition affects the reversibility of annexin A2t binding to solid supported membranes: a QCM study." Biochemistry **42**(10): 3131-41.

Saenko, E., A. Sarafanov, et al. (1999). "Use of surface plasmon resonance for studies of protein-protein and protein-phospholipid membrane interactions. Application to the binding of factor VIII to von Willebrand factor and to phosphatidylserine-containing membranes." J Chromatogr A **852**(1): 59-71.

Saido, T. C., M. Shibata, et al. (1992). "Positive regulation of mu-calpain action by polyphosphoinositides." J Biol Chem **267**(34): 24585-90.

Saido, T. C., H. Suzuki, et al. (1993). "In situ capture of mu-calpain activation in platelets." J Biol Chem **268**(10): 7422-6.

Saklatvala, J., H. Nagase, et al. (2003). "A tribute to Alan J. Barrett." Biochem Soc Symp(70): ix-x.

Sambrook, J., E. F. Fritsch, et al. (1989). Molecular Cloning: A Laboratory Manual. Cold Spring Harbor, New York, Cold Spring Harbor Laboratory Press.

Samis, J. A. and J. S. Elce (1989). "Immunogold electron-microscopic localization of calpain I in human erythrocytes." Thromb Haemost **61**(2): 250-3.

Sanger, F., S. Nicklen, et al. (1977). "DNA sequencing with chain-terminating inhibitors." Proc Natl Acad Sci U S A **74**(12): 5463-7.

Santella, L., K. Kyozuka, et al. (1998). "Calcium, protease action, and the regulation of the cell cycle." Cell Calcium **23**(2-3): 123-30.

Sato, K. and S. Kawashima (2001). "Calpain function in the modulation of signal transduction molecules." Biol Chem **382**(5): 743-51.

Schagger, H. and G. von Jagow (1987). "Tricine-sodium dodecyl sulfate-polyacrylamide gel electrophoresis for the separation of proteins in the range from 1 to 100 kDa." Anal Biochem **166**(2): 368-79.

Schwede, T., J. Kopp, et al. (2003). "SWISS-MODEL: An automated protein homology-modeling server." Nucleic Acids Res **31**(13): 3381-5.

Sealey, P. G. and E. M. Southern (1982). Gel electrophoresis of DNA. Gel electrophoresis of nucleic acids. A practical approach. D. Rickwood and B. D. Hames. Oxford, IRL Press**:** 39-76.

Shiba, E., H. Ariyoshi, et al. (1992). "Purification and characterization of a calpain activator from human platelets." Biochem Biophys Res Commun **182**(2): 461-5.

Skene, J. H. and I. Virag (1989). "Posttranslational membrane attachment and dynamic fatty acylation of a neuronal growth cone protein, GAP-43." J Cell Biol **108**(2): 613-24.

Smith, P. K., R. I. Krohn, et al. (1985). "Measurement of protein using bicinchoninic acid." Anal Biochem **150**(1): 76-85.

Smith, S. D., Z. Jia, et al. (2003). "Glutamate substitutions at a PKA consensus site are consistent with inactivation of calpain by phosphorylation." FEBS Lett **542**(1-3): 115-8.

Sokol, S. B. and P. E. Kuwabara (2000). "Proteolysis in Caenorhabditis elegans sex determination: cleavage of TRA-2A by TRA-3." Genes Dev **14**(8): 901-6.

Sorimachi, H., T. C. Saido, et al. (1994). "New era of calpain research. Discovery of tissue-specific calpains." FEBS Lett **343**(1): 1-5.

Sorimachi, H. and K. Suzuki (2001). "The structure of calpain." J Biochem (Tokyo) **129**(5): 653-64.

Spencer, M. J., J. R. Guyon, et al. (2002). "Stable expression of calpain 3 from a muscle transgene in vivo: immature muscle in transgenic mice suggests a role for calpain 3 in muscle maturation." Proc Natl Acad Sci U S A **99**(13): 8874-9.

Stahelin, R. V., J. D. Rafter, et al. (2003). "The molecular basis of differential subcellular localization of C2 domains of protein kinase C-alpha and group IVa cytosolic phospholipase A2." J Biol Chem **278**(14): 12452-60.

Strobl, S., C. Fernandez-Catalan, et al. (2000). "The crystal structure of calcium-free human m-calpain suggests an electrostatic switch mechanism for activation by calcium." Proc Natl Acad Sci U S A **97**(2): 588-92.

Sutton, R. B. and S. R. Sprang (1998). "Structure of the protein kinase Cbeta phospholipid-binding C2 domain complexed with Ca2+." Structure **6**(11): 1395-405.

Suzuki, K. (1991). "Nomenclature of calcium dependent proteinase." Biomed Biochim Acta **50**(4-6): 483-4.

Suzuki, K., S. Imajoh, et al. (1987). "Calcium-activated neutral protease and its endogenous inhibitor. Activation at the cell membrane and biological function." FEBS Lett **220**(2): 271-7.

Suzuki, K. and H. Sorimachi (1998). "A novel aspect of calpain activation." FEBS Lett **433**(1-2): 1-4.

Suzuki, K., S. Tsuji, et al. (1981). "Limited autolysis of Ca2+-activated neutral protease (CANP) changes its sensitivity to Ca2+ ions." J Biochem (Tokyo) **90**(1): 275-8.

Tagawa, K., C. Taya, et al. (2000). "Myopathy phenotype of transgenic mice expressing active site-mutated inactive p94 skeletal muscle-specific calpain, the gene product responsible for limb girdle muscular dystrophy type 2A." Hum Mol Genet **9**(9): 1393-402.

Tait, J. F., D. Gibson, et al. (1989). "Phospholipid binding properties of human placental anticoagulant protein-I, a member of the lipocortin family." J Biol Chem **264**(14): 7944-9.

Takai, Y., M. Yamamoto, et al. (1977). "A proenzyme of cyclic nucleotide-independent protein kinase and its activation by calcium-dependent neutral protease from rat liver." Biochem Biophys Res Commun **77**(2): 542-50.

Takeyama, Y., H. Nakanishi, et al. (1986). "A calcium-protease activator associated with brain microsomal-insoluble elements." FEBS Lett **194**(1): 110-4.

Tanaka, T. and H. Hidaka (1980). "Hydrophobic regions function in calmodulin-enzyme(s) interactions." J Biol Chem **255**(23): 11078-80.

Teahan, C. G., N. F. Totty, et al. (1992). "Isolation and characterization of grancalcin, a novel 28 kDa EF-hand calcium-binding protein from human neutrophils." Biochem J **286 (Pt 2)**: 549-54.

Thompson, V. F., K. Lawson, et al. (2000). "Effect of mu-calpain on m-calpain." Biochem Biophys Res Commun **267**(2): 495-9.

Thompson, V. F., K. R. Lawson, et al. (2003). "Digestion of mu- and m-calpain by trypsin and chymotrypsin." Biochim Biophys Acta **1648**(1-2): 140-53.

Todd, B., D. Moore, et al. (2003). "A Structural Model for the Inhibition of Calpain by Calpastatin: Crystal Structures of the Native Domain VI of Calpain and its Complexes with Calpastatin Peptide and a Small Molecule Inhibitor." J Mol Biol **328**(1): 131-46.

Tomimatsu, Y., S. Idemoto, et al. (2002). "Proteases involved in long-term potentiation." Life Sci **72**(4-5): 355-61.

Tompa, P., A. Baki, et al. (1996). "The calpain cascade. Mu-calpain activates m-calpain." J Biol Chem **271**(52): 33161-4.

Tompa, P., Y. Emori, et al. (2001). "Domain III of calpain is a ca2+-regulated phospholipid-binding domain." Biochem Biophys Res Commun **280**(5): 1333-9.

Travis, J., A. Banbula, et al. (2000). "The role of bacterial and host proteinases in periodontal disease." Adv Exp Med Biol **477**: 455-65.

Turk, D., B. Turk, et al. (2003). "Papain-like lysosomal cysteine proteases and their inhibitors: drug discovery targets?" Biochem Soc Symp(70): 15-30.

Uhlmann, F. (2003). "Separase regulation during mitosis." Biochem Soc Symp(70): 243-51.

Vallentin, A., C. Prevostel, et al. (2000). "Membrane targeting and cytoplasmic sequestration in the spatiotemporal localization of human protein kinase C alpha." J Biol Chem **275**(8): 6014-21.

Verdaguer, N., S. Corbalan-Garcia, et al. (1999). "Ca(2+) bridges the C2 membrane-binding domain of protein kinase Calpha directly to phosphatidylserine." Embo J **18**(22): 6329-38.

Vieira, J. and J. Messing (1991). "New pUC-derived cloning vectors with different selectable markers and DNA replication origins." Gene **100**: 189-94.

Vilei, E. M., S. Calderara, et al. (1997). "Functional properties of recombinant calpain I and of mutants lacking domains III and IV of the catalytic subunit." J Biol Chem **272**(41): 25802-8.

Wang, C., J. K. Barry, et al. (2003). "The calpain domain of the maize DEK1 protein contains the conserved catalytic triad and functions as a cysteine proteinase." J Biol Chem **278**(36): 34467-74.

Wang, K. K. (2000). "Calpain and caspase: can you tell the difference?" Trends Neurosci **23**(1): 20-6.

Weiss, J. (1997). "The Hill equation revisited: uses and misuses." FASEB J. **11**(11): 835-841.

Wells, J., M. Vasser, et al. (1985). Gene **34**: 315-323.

Wilson, K. P., J. A. Black, et al. (1994). "Structure and mechanism of interleukin-1 beta converting enzyme." Nature **370**(6487): 270-5.

Wu, P. and L. Brand (1994). "Resonance energy transfer: methods and applications." Anal Biochem **218**(1): 1-13.

Yajima, Y. and S. Kawashima (2002). "Calpain function in the differentiation of mesenchymal stem cells." Biol Chem **383**(5): 757-64.

Yang, T. T., L. Cheng, et al. (1996). "Optimized codon usage and chromophore mutations provide enhanced sensitivity with the green fluorescent protein." Nucleic Acids Res **24**(22): 4592-3.

Yoshikawa, Y., H. Mukai, et al. (2000). "Isolation of two novel genes, down-regulated in gastric cancer." Jpn J Cancer Res **91**(5): 459-63.

Yoshizawa, T., H. Sorimachi, et al. (1995). "Calpain dissociates into subunits in the presence of calcium ions." Biochem Biophys Res Commun **208**(1): 376-83.

Zhang, X., J. Rizo, et al. (1998). "Mechanism of phospholipid binding by the C2A-domain of synaptotagmin I." Biochemistry **37**(36): 12395-403.

Zhao, X., R. Posmantur, et al. (1998). "Subcellular localization and duration of mu-calpain and m-calpain activity after traumatic brain injury in the rat: a casein zymography study." J Cereb Blood Flow Metab **18**(2): 161-7.

Zheng, T. S. and R. A. Flavell (2000). "Divinations and surprises: genetic analysis of caspase function in mice." Exp Cell Res **256**(1): 67-73.

Zimmerman, U. J., L. Boring, et al. (2000). "The calpain small subunit gene is essential: its inactivation results in embryonic lethality." IUBMB Life **50**(1): 63-8.

Zimmerman, U. J. and W. W. Schlaepfer (1988). "Activation of calpain I and calpain II: a comparative study using terbium as a fluorescent probe for calcium-binding sites." Arch Biochem Biophys **266**(2): 462-9.

Zimmerman, U. J. and W. W. Schlaepfer (1991). "Two-stage autolysis of the catalytic subunit initiates activation of calpain I." Biochim Biophys Acta **1080**(3): 275.

Zozulya, S. and L. Stryer (1992). "Calcium-myristoyl protein switch." Proc Natl Acad Sci U S A **89**(23): 11569-73.

H. Appendix

The cDNA sequences of human μ-calpain 80 kDa subunit (CAPN1) and 28 kDa subunit (CAPN4) are listed in this appendix. The amino acid sequences (according to the one letter code) and stop codons (*) are shown under the coding DNA sequences.

Sequence of human μ-calpain (80 kDa) large subunit (Aoki, Imajoh et al 1986):

```
      ATGTCGGAGGAGATCATCACGCCGGTGTACTGCACTGGGGTGTCAGCCCAAGTGCAGAAG
  1   ---------+---------+---------+---------+---------+---------+ 60
      TACAGCCTCCTCTAGTAGTGCGGCCACATGACGTGACCCCACAGTCGGGTTCACGTCTTC
      M   S   E   E   I   I   T   P   V   Y   C   T   G   V   S   A   Q   V   Q   K   -

      CAGCGGGCCAGGGAGCTGGGCCTGGGCCGCCATGAGAATGCCATCAAGTACCTGGGCCAG
 61   ---------+---------+---------+---------+---------+---------+ 120
      GTCGCCCGGTCCCTCGACCCGGACCCGGCGGTACTCTTACGGTAGTTCATGGACCCGGTC
      Q   R   A   R   E   L   G   L   G   R   H   E   N   A   I   K   Y   L   G   Q   -

      GATTATGAGCAGCTGCGGGTGCGATGCCTGCAGAGTGGGACCCTCTTCCGTGATGAGGCC
121   ---------+---------+---------+---------+---------+---------+ 180
      CTAATACTCGTCGACGCCCACGCTACGGACGTCTCACCCTGGGAGAAGGCACTACTCCGG
      D   Y   E   Q   L   R   V   R   C   L   Q   S   G   T   L   F   R   D   E   A   -

      TTCCCCCCGGTACCCCAGAGCCTGGGTTACAAGGACCTGGGTCCCAATTCCTCCAAGACC
181   ---------+---------+---------+---------+---------+---------+ 240
      AAGGGGGGCCATGGGGTCTCGGACCCAATGTTCCTGGACCCAGGGTTAAGGAGGTTCTGG
      F   P   P   V   P   Q   S   L   G   Y   K   D   L   G   P   N   S   S   K   T   -

      TATGGCATCAAGTGGAAGCGTCCCACGGAACTGCTGTCAAACCCCCAGTTCATTGTGGAT
241   ---------+---------+---------+---------+---------+---------+ 300
      ATACCGTAGTTCACCTTCGCAGGGTGCCTTGACGACAGTTTGGGGGTCAAGTAACACCTA
      Y   G   I   K   W   K   R   P   T   E   L   L   S   N   P   Q   F   I   V   D   -

      GGAGCTACCCGCACAGACATCTGCCAGGGAGCACTGGGGGACTGCTGGCTCTTGGCGGCC
301   ---------+---------+---------+---------+---------+---------+ 360
      CCTCGATGGGCGTGTCTGTAGACGGTCCCTCGTGACCCCCTGACGACCGAGAACCGCCGG
      G   A   T   R   T   D   I   C   Q   G   A   L   G   D   C   W   L   L   A   A   -

      ATTGCCTCCCTCACTCTCAACGACACCCTCCTGCACCGAGTGGTTCCGCACGGCCAGAGC
361   ---------+---------+---------+---------+---------+---------+ 420
      TAACGGAGGGAGTGAGAGTTGCTGTGGGAGGACGTGGCTCACCAAGGCGTGCCGGTCTCG
      I   A   S   L   T   L   N   D   T   L   L   H   R   V   V   P   H   G   Q   S   -

      TTCCAGAATGGCTATGCCGGCATCTTCCATTTCCAGCTGTGGCAATTTGGGGAGTGGGTG
421   ---------+---------+---------+---------+---------+---------+ 480
      AAGGTCTTACCGATACGGCCGTAGAAGGTAAAGGTCGACACCGTTAAACCCCTCACCCAC
      F   Q   N   G   Y   A   G   I   F   H   F   Q   L   W   Q   F   G   E   W   V   -

      GACGTGGTCGTGGATGACCTGCTGCCCATCAAGGACGGGAAGCTAGTGTTCGTGCACTCT
481   ---------+---------+---------+---------+---------+---------+ 540
      CTGCACCAGCACCTACTGGACGACGGGTAGTTCCTGCCCTTCGATCACAAGCACGTGAGA
      D   V   V   V   D   D   L   L   P   I   K   D   G   K   L   V   F   V   H   S   -
```

```
      GCCGAAGGCAACGAGTTCTGGAGCGCCCTGCTTGAGAAGGCCTATGCCAAGGTAAATGGC
 541  ---------+---------+---------+---------+---------+---------+ 600
      CGGCTTCCGTTGCTCAAGACCTCGCGGGACGAACTCTTCCGGATACGGTTCCATTTACCG
       A  E  G  N  E  F  W  S  A  L  L  E  K  A  Y  A  K  V  N  G   -

      AGCTACGAGGCCCTGTCAGGGGGCAGCACCTCAGAGGGCTTTGAGGACTTCACAGGCGGG
 601  ---------+---------+---------+---------+---------+---------+ 660
      TCGATGCTCCGGGACAGTCCCCCGTCGTGGAGTCTCCCGAAACTCCTGAAGTGTCCGCCC
       S  Y  E  A  L  S  G  G  S  T  S  E  G  F  E  D  F  T  G  G   -

      GTTACCGAGTGGTACGAGTTGCGCAAGGCTCCCAGTGACCTCTACCAGATCATCCTCAAG
 661  ---------+---------+---------+---------+---------+---------+ 720
      CAATGGCTCACCATGCTCAACGCGTTCCGAGGGTCACTGGAGATGGTCTAGTAGGAGTTC
       V  T  E  W  Y  E  L  R  K  A  P  S  D  L  Y  Q  I  I  L  K   -

      GCGCTGGAGCGGGGCTCCCTGCTGGGCTGCTCCATAGACATCTCCAGCGTTCTAGACATG
 721  ---------+---------+---------+---------+---------+---------+ 780
      CGCGACCTCGCCCCGAGGGACGACCCGACGAGGTATCTGTAGAGGTCGCAAGATCTGTAC
       A  L  E  R  G  S  L  L  G  C  S  I  D  I  S  S  V  L  D  M   -

      GAGGCCATCACTTTCAAGAAGTTGGTGAAGGGCCATGCCTACTCTGTGACCGGGGCCAAG
 781  ---------+---------+---------+---------+---------+---------+ 840
      CTCCGGTAGTGAAAGTTCTTCAACCACTTCCCGGTACGGATGAGACACTGGCCCCGGTTC
       E  A  I  T  F  K  K  L  V  K  G  H  A  Y  S  V  T  G  A  K   -

      CAGGTGAACTACCGAGGCCAGGTGGTGAGCCTGATCCGGATGCGGAACCCCTGGGGCGAG
 841  ---------+---------+---------+---------+---------+---------+ 900
      GTCCACTTGATGGCTCCGGTCCACCACTCGGACTAGGCCTACGCCTTGGGGACCCCGCTC
       Q  V  N  Y  R  G  Q  V  V  S  L  I  R  M  R  N  P  W  G  E   -

      GTGGAGTGGACGGGAGCCTGGAGCGACAGCTCCTCAGAGTGGAACAACGTGGACCCATAT
 901  ---------+---------+---------+---------+---------+---------+ 960
      CACCTCACCTGCCCTCGGACCTCGCTGTCGAGGAGTCTCACCTTGTTGCACCTGGGTATA
       V  E  W  T  G  A  W  S  D  S  S  S  E  W  N  N  V  D  P  Y   -

      GAACGGGACCAGCTCCGGGTCAAGATGGAGGACGGGGAGTTCTGGATGTCATTCCGAGAC
 961  ---------+---------+---------+---------+---------+---------+ 1020
      CTTGCCCTGGTCGAGGCCCAGTTCTACCTCCTGCCCCTCAAGACCTACAGTAAGGCTCTG
       E  R  D  Q  L  R  V  K  M  E  D  G  E  F  W  M  S  F  R  D   -

      TTCATGCGGGAGTTCACCCGCCTGGAGATCTGCAACCTCACACCCGACGCCCTCAAGAGC
1021  ---------+---------+---------+---------+---------+---------+ 1080
      AAGTACGCCCTCAAGTGGGCGGACCTCTAGACGTTGGAGTGTGGGCTGCGGGAGTTCTCG
       F  M  R  E  F  T  R  L  E  I  C  N  L  T  P  D  A  L  K  S   -
```

```
      CGGACCATCCGCAAATGGAACACCACACTCTACGAAGGCACCTGGCGGCGGGGGAGCACC
1081  ---------+---------+---------+---------+---------+---------+ 1140
      GCCTGGTAGGCGTTTACCTTGTGGTGTGAGATGCTTCCGTGGACCGCCGCCCCCTCGTGG
       R  T  I  R  K  W  N  T  T  L  Y  E  G  T  W  R  R  G  S  T   -

      GCGGGGGGCTGCCGAAACTACCCAGCCACCTTCTGGGTGAACCCTCAGTTCAAGATCCGG
1141  ---------+---------+---------+---------+---------+---------+ 1200
      CGCCCCCCGACGGCTTTGATGGGTCGGTGGAAGACCCACTTGGGAGTCAAGTTCTAGGCC
       A  G  G  C  R  N  Y  P  A  T  F  W  V  N  P  Q  F  K  I  R   -

      CTGGATGAGACGGATGACCCGGACGACTACGGGGACCGCGAGTCAGGCTGCAGCTTCGTG
1201  ---------+---------+---------+---------+---------+---------+ 1260
      GACCTACTCTGCCTACTGGGCCTGCTGATGCCCCTGGCGCTCAGTCCGACGTCGAAGCAC
       L  D  E  T  D  D  P  D  D  Y  G  D  R  E  S  G  C  S  F  V   -

      CTCGCCCTTATGCAGAAGCACCGTCGCCGCGAGCGCCGCTTCGGCCGCGACATGGAGACT
1261  ---------+---------+---------+---------+---------+---------+ 1320
      GAGCGGGAATACGTCTTCGTGGCAGCGGCGCTCGCGGCGAAGCCGGCGCTGTACCTCTGA
       L  A  L  M  Q  K  H  R  R  R  E  R  R  F  G  R  D  M  E  T   -

      ATTGGCTTCGCGGTCTACGAGGTCCCTCCGGAGCTGGTGGGCCAGCCGGCCGTACACTTG
1321  ---------+---------+---------+---------+---------+---------+ 1380
      TAACCGAAGCGCCAGATGCTCCAGGGAGGCCTCGACCACCCGGTCGGCCGGCATGTGAAC
       I  G  F  A  V  Y  E  V  P  P  E  L  V  G  Q  P  A  V  H  L   -

      AAGCGTGACTTCTTCCTGGCCAATGCGTCTCGGGCGCGCTCAGAGCAGTTCATCAACCTG
1381  ---------+---------+---------+---------+---------+---------+ 1440
      TTCGCACTGAAGAAGGACCGGTTACGCAGAGCCCGCGCGAGTCTCGTCAAGTAGTTGGAC
       K  R  D  F  F  L  A  N  A  S  R  A  R  S  E  Q  F  I  N  L   -

      CGAGAGGTCAGCACCCGCTTCCGCCTGCCACCCGGGGAGTATGTGGTGGTGCCCTCCACC
1441  ---------+---------+---------+---------+---------+---------+ 1500
      GCTCTCCAGTCGTGGGCGAAGGCGGACGGTGGGCCCCTCATACACCACCACGGGAGGTGG
       R  E  V  S  T  R  F  R  L  P  P  G  E  Y  V  V  V  P  S  T   -

      TTCGAGCCCAACAAGGAGGGCGACTTCGTGCTGCGCTTCTTCTCAGAGAAGAGTGCTGGG
1501  ---------+---------+---------+---------+---------+---------+ 1560
      AAGCTCGGGTTGTTCCTCCCGCTGAAGCACGACGCGAAGAAGAGTCTCTTCTCACGACCC
       F  E  P  N  K  E  G  D  F  V  L  R  F  F  S  E  K  S  A  G   -

      ACTGTGGAGCTGGATGACCAGATCCAGGCCAATCTCCCCGATGAGCAAGTGCTCTCAGAA
1561  ---------+---------+---------+---------+---------+---------+ 1620
      TGACACCTCGACCTACTGGTCTAGGTCCGGTTAGAGGGGCTACTCGTTCACGAGAGTCTT
       T  V  E  L  D  D  Q  I  Q  A  N  L  P  D  E  Q  V  L  S  E   -

      GAGGAGATTGACGAGAACTTCAAGGCCCTCTTCAGGCAGCTGGCAGGGGAGGACATGGAG
1621  ---------+---------+---------+---------+---------+---------+ 1680
      CTCCTCTAACTGCTCTTGAAGTTCCGGGAGAAGTCCGTCGACCGTCCCCTCCTGTACCTC
       E  E  I  D  E  N  F  K  A  L  F  R  Q  L  A  G  E  D  M  E   -
```

```
      ATCAGCGTGAAGGAGTTGCGGACAATCCTCAATAGGATCATCAGCAAACACAAAGACCTG
1681  ---------+---------+---------+---------+---------+---------+ 1740
      TAGTCGCACTTCCTCAACGCCTGTTAGGAGTTATCCTAGTAGTCGTTTGTGTTTCTGGAC
       I  S  V  K  E  L  R  T  I  L  N  R  I  I  S  K  H  K  D  L   -

      CGGACCAAGGGCTTCAGCCTAGAGTCGTGCCGCAGCATGGTGAACCTCATGGATCGTGAT
1741  ---------+---------+---------+---------+---------+---------+ 1800
      GCCTGGTTCCCGAAGTCGGATCTCAGCACGGCGTCGTACCACTTGGAGTACCTAGCACTA
       R  T  K  G  F  S  L  E  S  C  R  S  M  V  N  L  M  D  R  D   -

      GGCAATGGGAAGCTGGGCCTGGTGGAGTTCAACATCCTGTGGAACCGCATCCGGAATTAC
1801  ---------+---------+---------+---------+---------+---------+ 1860
      CCGTTACCCTTCGACCCGGACCACCTCAAGTTGTAGGACACCTTGGCGTAGGCCTTAATG
       G  N  G  K  L  G  L  V  E  F  N  I  L  W  N  R  I  R  N  Y   -

      CTGTCCATCTTCCGGAAGTTTGACCTGGACAAGTCGGGCAGCATGAGTGCCTACGAGATG
1861  ---------+---------+---------+---------+---------+---------+ 1920
      GACAGGTAGAAGGCCTTCAAACTGGACCTGTTCAGCCCGTCGTACTCACGGATGCTCTAC
       L  S  I  F  R  K  F  D  L  D  K  S  G  S  M  S  A  Y  E  M   -

      CGGATGGCCATTGAGTCGGCAGGCTTCAAGCTCAACAAGAAGCTGTACGAGCTCATCATC
1921  ---------+---------+---------+---------+---------+---------+ 1980
      GCCTACCGGTAACTCAGCCGTCCGAAGTTCGAGTTGTTCTTCGACATGCTCGAGTAGTAG
       R  M  A  I  E  S  A  G  F  K  L  N  K  K  L  Y  E  L  I  I   -

      ACCCGCTACTCGGAGCCCGACCTGGCGGTCGACTTTGACAATTTCGTTTGCTGCCTGGTG
1981  ---------+---------+---------+---------+---------+---------+ 2040
      TGGGCGATGAGCCTCGGGCTGGACCGCCAGCTGAAACTGTTAAAGCAAACGACGGACCAC
       T  R  Y  S  E  P  D  L  A  V  D  F  D  N  F  V  C  C  L  V   -

      CGGCTAGAGACCATGTTCCGATTTTTTCAAAAACTCTGGACACAGATCTGGATGGAGTTGTG
2041  ---------+---------+---------+---------+---------+---------+ 2100
      GCCGATCTCTGGTACAAGGCTAAAAAGTTTTGAGACCTGTGTCTAGACCTACCTCAACAC
       R  L  E  T  M  F  R  F  F  K  T  L  D  T  D  L  D  G  V  V   -

      ACCTTTGACTTGTTTAAGTGGTTGCAGCTGACCATGTTTGCATGA
2101  ---------+---------+---------+---------+----- 2145
      TGGAAACTGAACAAATTCACCAACGTCGACTGGTACAAACGTACT
       T  F  D  L  F  K  W  L  Q  L  T  M  F  A  *
```

Sequence of human calpain (28 kDa) small subunit (Ohno, Emori et al 1986):

```
   ATGTTCCTGGTTAACTCGTTCTTGAAGGGCGGCGGCGGCGGCGGCGGGGGGAGGCGGGGGC
1  ---------+---------+---------+---------+---------+---------+ 60
   TACAAGGACCAATTGAGCAAGAACTTCCCGCCGCCGCCGCCGCCGCCCCCTCCGCCCCCG
    M  F  L  V  N  S  F  L  K  G  G  G  G  G  G  G  G  G  G  G   -
```

```
       CTGGGTGGGGGCCTGGGAAATGTGCTTGGAGGCCTGATCAGCGGGGCCGGGGGCGGCGGC
  61   ---------+---------+---------+---------+---------+---------+ 120
       GACCCACCCCCGGACCCTTTACACGAACCTCCGGACTAGTCGCCCCGGCCCCCGCCGCCG
       L   G   G   G   L   G   N   V   L   G   G   L   I   S   G   A   G   G   G   G   -

       GGCGGCGGCGGCGGCGGCGGCGGTGGTGGAGGCGGCGGTGGCGGTGGAACGGCCATGCGC
 121   ---------+---------+---------+---------+---------+---------+ 180
       CCGCCGCCGCCGCCGCCGCCGCCACCACCTCCGCCGCCACCGCCACCTTGCCGGTACGCG
       G   G   G   G   G   G   G   G   G   G   G   G   G   G   T   A   M   R   -

       ATCCTAGGCGGAGTCATCAGCGCCATCAGCGAGGCGGCTGCGCAGTACAACCCGGAGCCC
 181   ---------+---------+---------+---------+---------+---------+ 240
       TAGGATCCGCCTCAGTAGTCGCGGTAGTCGCTCCGCCGACGCGTCATGTTGGGCCTCGGG
       I   L   G   G   V   I   S   A   I   S   E   A   A   A   Q   Y   N   P   E   P   -

       CCGCCCCCACGCACACATTACTCCAACATTGAGGCCAACGAGAGTGAGGAGGTCCGGCAG
 241   ---------+---------+---------+---------+---------+---------+ 300
       GGCGGGGGTGCGTGTGTAATGAGGTTGTAACTCCGGTTGCTCTCACTCCTCCAGGCCGTC
       P   P   P   R   T   H   Y   S   N   I   E   A   N   E   S   E   E   V   R   Q   -

       ATGAACATTCTCAATAAGGTTGTGACACGACACCCTGATCTGAAGACTGATGGTTTTGGC
 361   ---------+---------+---------+---------+---------+---------+ 420
       TACTTGTAAGAGTTATTCCAACACTGTGCTGTGGGACTAGACTTCTGACTACCAAAACCG
       M   N   I   L   N   K   V   V   T   R   H   P   D   L   K   T   D   G   F   G   -

       ATTGACACATGTCGCAGCATGGTGGCCGTGATGGATAGCGACACCACAGGCAAGCTGGGC
 421   ---------+---------+---------+---------+---------+---------+ 480
       TAACTGTGTACAGCGTCGTACCACCGGCACTACCTATCGCTGTGGTGTCCGTTCGACCCG
       I   D   T   C   R   S   M   V   A   V   M   D   S   D   T   T   G   K   L   G   -

       TTTGAGGAATTCAAGTACTTGTGGAACAACATCAAAAGGTGGCAGGCCATATACAAACAG
 481   ---------+---------+---------+---------+---------+---------+ 540
       AAACTCCTTAAGTTCATGAACACCTTGTTGTAGTTTTCCACCGTCCGGTATATGTTTGTC
       F   E   E   F   K   Y   L   W   N   N   I   K   R   W   Q   A   I   Y   K   Q   -

       TTCGACACTGACCGATCAGGGACCATTTGCAGTAGTGAACTCCCAGGTGCCTTTGAGGCA
 541   ---------+---------+---------+---------+---------+---------+ 600
       AAGCTGTGACTGGCTAGTCCCTGGTAAACGTCATCACTTGAGGGTCCACGGAAACTCCGT
       F   D   T   D   R   S   G   T   I   C   S   S   E   L   P   G   A   F   E   A   -

       GCAGGGTTCCACCTGAATGAGCATCTCTATAACATGATCATCCGACGCTACTCAGATGAA
 601   ---------+---------+---------+---------+---------+---------+ 660
       CGTCCCAAGGTGGACTTACTCGTAGAGATATTGTACTAGTAGGCTGCGATGAGTCTACTT
       A   G   F   H   L   N   E   H   L   Y   N   M   I   I   R   R   Y   S   D   E   -

       AGTGGGAACATGGATTTTGACAACTTCATCAGCTGCTTGGTCAGGCTGGACGCCATGTTC
 661   ---------+---------+---------+---------+---------+---------+ 720
       TCACCCTTGTACCTAAAACTGTTGAAGTAGTCGACGAACCAGTCCGACCTGCGGTACAAG
       S   G   N   M   D   F   D   N   F   I   S   C   L   V   R   L   D   A   M   F   -
```

```
     CGTGCCTTCAAATCTCTTGACAAAGATGGCACTGGACAAATCCAGGTGAACATCCAGGAG
721  ---------+---------+---------+---------+---------+---------+ 780
     GCACGGAAGTTTAGAGAACTGTTTCTACCGTGACCTGTTTAGGTCCACTTGTAGGTCCTC
     R   A   F   K   S   L   D   K   D   G   T   G   Q   I   Q   V   N   I   Q   E   -


     TGGCTGCAGCTGACTATGTATTCCTGA
781  ---------+---------+------- 807
     ACCGACGTCGACTGATACATAAGGACT
     W   L   Q   L   T   M   Y   S   *   -
```

I. Curriculum Vitae

1. Personal Data

Name: Amaury Ernesto Fernández-Montalván

Date of birth: 18/10/1974

Place of birth: Havana, Cuba

2. Preuniversity schooling

Sept. 1980-Jul. 1982:   Elementary School "Lidia Doce", Havana

Sept. 1982-Jul. 1983:   Elementary School "Mariana Grajales", Havana

Sept. 1983-Jul. 1986:   Elementary School "Fabricio Ojeda", Havana

Sept. 1986-Jul. 1989:   Junior High School "Otto Barroso", Havana

Sept. 1989-Jul. 1992:   Senior High School "Vladimir I. Lenin", Havana

3. University studies

Sept. 1992-Dec. 1996:   Biochemistry studies at the Faculty of Biology, University of Havana

1997:   Diploma thesis at the Enzymology Group, Departement of Biochemistry, Faculty of Biology, University of Havana.
Graduation as Master of Biochemistry (MSc)

4. Postgraduate studies and professional career

Sept. 1997-Apr. 1999:   Junior scientist at the Department of Biochemistry of the Cuban Research Institute of Sugar Cane Derivatives (ICIDCA).

Apr.-Oct. 1999:   Guest researcher at the Department of Toxicology, Faculty of Medicine of the Christian Albrechts University of Kiel, Germany

Oct. 1999-May 2000:   Guest researcher at the Department of Clinical Chemistry and Biochemistry, Faculty of Medicine of the Ludwig-Maximiliams University, Munich, Germany

May 2000-Jun. 2004:   PhD studies at the Department of Clinical Chemistry and Biochemistry and the Adolf-Butenandt Institute of the Faculty of Medicine of the Ludwig-Maximiliams University, Munich, Germany